

METHODS FOR MULTILOOP COMPUTATIONS AND THEIR APPLICATION TO VECTOR BOSON PAIR PRODUCTION IN NNLO QCD

DISSERTATION

zur

Erlangung der naturwissenschaftlichen Doktorwürde
(Dr. sc. nat.)

vorgelegt der

Mathematisch-naturwissenschaftlichen Fakultät
der

Universität Zürich

von

LORENZO TANCREDI

aus

Italien

Promotionskomitee

PROF. DR. THOMAS GEHRMANN (VORSITZ)

PD. DR. MASSIMILIANO GRAZZINI

PROF. DR. BENJAMIN KILMINSTER

PROF. DR. STEFANO POZZORINI

Zürich, 2014

Abstract

In the last decades particle physics went through an impressive number of discoveries and developments, both from the theoretical and from the experimental point of view. In particular in the few years which went by after the beginning of the LHC era, not only a new particle has been discovered, whose properties strongly indicate this should be the long hunted Higgs boson, but also many precision measurements within the Standard Model are becoming available. This is challenging theoretical physicists to keep pace with the experiments and produce theoretical predictions which are as accurate as the experimental results. The Standard Model relies on the mathematical framework of quantum field theory and the complexity of this theory makes any exact computation within it a formidable task, forcing us to almost entirely resort to perturbative expansions in Feynman diagrams. In this thesis we will present a detailed overview of techniques for the calculation of multiloop Feynman integrals, both in massless and in massive theories. The natural application of these methods is to high precision calculations of observables relevant for LHC physics. Among these an important role is played by the production of pairs of electroweak vector bosons. Large part of this thesis will be thus dedicated to the calculation of second order corrections to such processes. At the same time we will also elaborate on some recent developments in the computation of massive Feynman integrals and specifically we will study in detail the two-loop massive sunrise graph.

Zusammenfassung

In den letzten Jahrzehnten geschahen in Teilchenphysik unzählige Entwicklungen, sowohl in Theorie als auch im Experiment. Mit der Inbetriebnahme des LHC hat eine neue Epoche begonnen: Es wurde einerseits ein neues Elementarteilchen entdeckt, dessen Eigenschaften mit denen des lange gesuchten Higgs Boson übereinstimmen, andererseits stehen mehr und mehr Präzisionsmessungen zur Verfügung. Die Herausforderung für theoretische Physiker ist deshalb, mit den Experimenten Schritt zu halten und gleichfalls Berechnungen zu hoher Genauigkeit auszuführen. Das Standardmodell der Elementarteilchenphysik ist auf der Quantenfeldtheorie aufgebaut, welche quantitative Vorhersagen nur im Rahmen einer perturbativen Entwicklung in Feynman-Diagrammen erlaubt. In dieser Dissertation werden die Methoden zur Berechnung von Feynman-Diagrammen ausführlich beschrieben, sowohl in masselosen als auch in massiven Theorien. Die natürliche Anwendung dieser Methoden ist zur Präzisionsberechnung von Prozessen, die wichtig für LHC-Physik sind. Dabei spielt die Produktion zweier Eichbosonen eine sehr bedeutende Rolle. In einem grossen Teil dieser Dissertation werden wir uns daher dem Problem widmen, diese Prozesse in zweiter Ordnung der Störungstheorie zu beschreiben. Desweiteren dokumentieren wir neue Methoden zur Berechnung massiver Feynman-Diagramme, und wenden diese auf das sogenannte Sunrise-Diagramm an.

Contents

Prologue	v
I Review	1
1 Perturbative calculations in the Standard Model	3
1.1 A brief introduction	3
1.1.1 Scattering amplitudes	6
1.2 QCD - Quantum Chromo-Dynamics	8
1.2.1 The QCD Feynman Rules	9
1.2.2 Perturbative calculations in QCD	12
1.2.3 NNLO computations in QCD	14
2 A diagrammatic approach to multiloop computations	19
2.1 Tensor decomposition for scattering amplitudes	20
2.1.1 The case of $q\bar{q} \rightarrow Z\gamma$	22
2.2 Reduction to Master Integrals	24
2.2.1 Integration by parts identities (IBPs)	26
2.2.2 Lorentz invariance identities (LIs)	26
2.2.3 Symmetry relations	28
2.2.4 The Laporta Algorithm	28
2.2.5 Schouten pseudo-identities (SIs)	29
3 Master Integrals	33
3.1 Preliminaries	33
3.2 Special Functions in Particle Physics	34
3.2.1 Special functions 1. Multiple Polylogarithms - MPLs	35
3.2.2 Special functions 2. Elliptic integrals in particle physics	40
3.3 Analytical computation of Master Integrals	44
3.3.1 Differential Equations for MIs	45
3.3.2 Solution as iterated integrals and the canonical form	50
3.3.3 Building up the basis bottom-up	52
3.3.4 The boundary conditions	58
3.3.5 A toy example: the one-loop massive sunrise	58

3.4	Outlook	63
II	Results	65
4	The MIs for $q\bar{q} \rightarrow VV$ production	67
4.1	Introduction	67
4.2	Notation and reduction to master integrals	68
4.3	The basis	70
4.3.1	Differential equations	74
4.4	Integration and boundary conditions	74
4.5	Solutions and checks	76
4.6	Real valued functions and expansions	77
4.7	Conclusions	78
5	The MIs of the two-loop massive sunrise graph	79
5.1	Introduction	79
5.2	The Schouten Identities for the Sunrise graph	81
5.3	A New Set of Master Integrals	85
5.3.1	The expansion of the Equations around $d = 2$	89
5.4	Second-order Differential Equation for $S(d; p^2)$	90
5.5	Shifting relations from $d = 2$ to $d = 4$ dimensions	92
5.6	The imaginary parts of the Master Integrals.	95
5.7	Conclusions	102
6	Two-loop QCD Amplitudes for $q\bar{q} \rightarrow Z\gamma/W\gamma$	105
6.1	Introduction	105
6.2	Kinematics and basic helicity structure	107
6.3	Outline of the calculation	112
6.4	Two-loop helicity amplitudes	116
6.5	Checks on the result	119
6.6	Conclusions and Outlook	120
7	ZZ production at hadron colliders in NNLO QCD	121
	Conclusions	127
	Acknowledgements	131
	Appendices	
	Appendix A The canonical basis for $q\bar{q} \rightarrow VV$	135

Appendix B The two-loop massive sunrise	139
B.1 The first-order differential equations	139
B.2 The second-order differential equation	141
B.3 Tarasov's shift	143

Prologue

It would probably be impossible to precisely identify the birth of that branch of physics that we refer today to as *Particle Physics*. Beyond the shadow of a doubt, anyway, two moments of this long journey have a special significance, not only for having been a breakthrough in knowledge, but also because of their symbolic importance. On the one hand, the discovery of the *electron* in 1897 by J.J. Thompson opened the way, both theoretically and technologically, to a century of apparently endless discoveries. On the other hand, the discovery of the Higgs boson in the summer of 2012 by thousands of researchers at CERN in Geneva, appears like the natural conclusion of that century of discoveries, since the Higgs boson was the last missing building block of the so called *Standard Model of Particle Physics*.

The 115 years that went by from the discovery of the electron by a handful of physicists studying cathode rays in a small laboratory to the discovery of the Higgs boson by two independent collaborations of around three thousands physicists each in the largest physics laboratory ever built by mankind, tell an exciting tale, made of many successes but also of many failures, and where every single step combined to make the next one possible.

If the discovery of the Higgs boson can be seen as one of the most important achievements of human knowledge, it must also be recognised as an unavoidable turning point. As it is the celebration of the great construction of the standard model, it will also force us to confront the limits of it, in order to be able to find a possible way to go further and beyond it. Although the successes of the standard model are indisputably impressive, its lacks are as striking. On the one hand, it allows us to describe with an astonishing degree of precision almost any phenomenon which can occur on Earth and which can be reproduced and studied in a physics laboratory. On the other hand, though, countless evidence from cosmology and astrophysics show that, if our understanding of the universe is correct, then what we are able to describe and understand is only a mere 8% of its total content of matter and energy. The fact that all phenomena that escape a description through the known laws of physics are beyond the reach of experiments, and therefore cannot be studied in a laboratory, has put physicists in an awkward situation for a long time. It is clear to everyone that our description of the world is incomplete, but at the same time it turns out to be enough to describe any phenomenon we can study with very high precision, so that no one knows precisely in which direction to look, in order to find a hint of what might be the missing piece.

It is mainly for this reason that particle physicists have only two instruments to further our present limited understanding of the world: *very high precision* and *very high energy* experiments. Testing the present theory to very high precision is in fact the only way we can hope to find something which does not work as well as expected. Moreover, the higher the energy the larger is the spectrum of possible new theories we can investigate. Extensions of the standard model, in fact, typically require the existence of new states (i.e. new particles) which have not yet been observed. One possible explanation for it is that these new states, if they exist, may have very large invariant masses or very short life-times, and as such we can only hope to produce them in a particle collider if we study collisions with enough energy. In the last 50/60 years this has generated a tireless competition between states first and continents later to build larger and larger particle colliders, which ultimately led to the construction of the LHC, the *Large Hadron Collider*, in Geneva. Since 2010 the LHC has been operating at the unprecedented energy of 7 TeV in the center of mass frame, which has been increased up to 8 TeV in 2012. Moreover this value is planned to be almost doubled to around 14 TeV by 2015. The LHC is not only the largest but also the most expensive experiment ever built to study fundamental physics, and countries from all over the world participated in its construction.

The discovery of the *Higgs Boson* at the LHC in July 2012 will be, hopefully, the first of a long series. As theoretical particle physicists, our role is *also* that of providing the experiments with as many as possible precise theoretical predictions within the standard model and its extensions, to be confronted with the new experimental results. For the time being, the only way we have available to do that is using perturbation theory (in particular within *QCD*, the theory of strong interactions, which plays a fundamental role in the description of hadronic collisions). This thesis will be therefore devoted to studying some aspects of perturbative calculations in the standard model, and in particular in *QCD*, describing how these ultimately allowed us to produce very precise predictions for a class of processes of fundamental importance for LHC physics: *vector boson pair production*. We will start reviewing some of the core aspects of perturbative calculations in Quantum Field Theory (QFT), discussing in details the newest developments which took place in the last decades, until the most recent ones, which are deeply transforming this field at the very moment this thesis is being written. All these new developments have brought us very close to what will probably be the *NNLO Revolution*, which is finally making it possible to compute second order corrections in perturbation theory to most $2 \rightarrow 2$ processes relevant not only for the LHC physics, but also in general for a deeper understanding of the underlying structures of perturbative calculations in quantum field theory.

Part I

Review

Chapter 1

Perturbative calculations in the Standard Model

1.1 A brief introduction

The Standard Model of Particle Physics (SM) is the currently accepted fundamental theory which governs the elementary constituents of matter and their interactions. Its “discovery” is undoubtedly one of the greatest achievements of human knowledge and it is ultimately the result of the joint efforts of thinkers from all over the world over a period of thousands of years¹. The basis of the SM rests on two fundamental pillars: *Special Relativity* (SR) and *Quantum Mechanics* (QM). At the beginning of the 20th century SR and QM had brought two colossal revolutions in theoretical physics, opening scenarios that had never even been contemplated before. Nevertheless, it soon became clear that unifying these two systems under the same framework was all but a straightforward task.

SR is in fact based on the fundamental assumption that *space* and *time* cannot exist as distinct entities but must be necessarily treated on equal footing as coordinates of a four-dimensional space-time manifold. On the other hand, by its very construction, QM relies on quite the opposite assumption. In QM space (the *position*) is the eigenvalue of an *hermitian operator*, and as such is *quantised*, while *time* is instead a mere label needed for parametrising the evolution of operators and their eigenvalues, and in particular to label the evolution of the position eigenstate itself. And it is precisely this asymmetry that makes its unification with SR so difficult.

From this perspective, two approaches may be attempted in order to restore this symmetry. One could think to *promote* time to be an operator, or alternatively one could *downgrade* space to be only a parameter. Promoting time to be an operator is a viable option and a consistent relativistic quantum mechanics can be developed along these lines, even though this turns out to be considerably more complicated,

¹For a thorough review and discussion of the subject we refer to standard textbooks, see for example [1–3] and references therein.

and we won't elaborate further on this².

On the other hand, following the idea of downgrading the position to be “just” a label is the starting point for the development of *Quantum Field Theory* (QFT), which is the mathematical language needed to formulate the Standard Model of Particle Physics. In QFT space and time are both labels needed to parametrise the *fields*, which become the *fundamental operators* of the theory.

Let us consider assigning to each point \vec{x} in space an operator $\phi(\vec{x})$. The infinite set of operators obtained in this way is called a *quantum field*. In order to make the symmetry between space and time entirely evident, it is convenient to work in the Heisenberg picture, where the time-dependence is carried by the operators, i.e.

$$\phi(\vec{x}, t) = e^{iHt/\hbar} \phi(\vec{x}) e^{-iHt/\hbar}, \quad (1.1)$$

where H is the Hamiltonian of the system. In the Heisenberg picture position and time are treated on the same footing, which makes it easier to explicitly maintain the Lorentz covariance of the formalism.

Once fields are promoted to be operators, one immediately realises that their quantisation naturally leads to the concept of an *elementary particle*, namely the quanta of a quantised field can be identified with the elementary particles which we see in our experiments. In particular, given a field $\phi(\vec{x}, t)$ and its momentum conjugate $\pi(\vec{x}, t)$, the quantisation of the theory is obtained by imposing the analogues of the non-relativistic commutation relations, which for fields are translated into the usual *equal-time* commutation relations:

$$\begin{aligned} [\phi(\vec{x}, t_0), \phi(\vec{y}, t_0)] &= 0, \\ [\pi(\vec{x}, t_0), \pi(\vec{y}, t_0)] &= 0, \\ [\phi(\vec{x}, t_0), \pi(\vec{y}, t_0)] &= i \delta^3(\vec{x} - \vec{y}). \end{aligned}$$

Upon doing this, one obtains *bosonic field quanta*, such as in the case of photons and the electromagnetic field.

In order to obtain *fermionic quanta* one must instead substitute the quantum commutator conditions by anticommutator ones:

$$\begin{aligned} \{\phi(\vec{x}, t_0), \phi(\vec{y}, t_0)\} &= 0, \\ \{\pi(\vec{x}, t_0), \pi(\vec{y}, t_0)\} &= 0, \\ \{\phi(\vec{x}, t_0), \pi(\vec{y}, t_0)\} &= i \delta^3(\vec{x} - \vec{y}). \end{aligned}$$

Note that the fact that all fields and their conjugates (anti)commute whenever $\vec{x} \neq \vec{y}$ (at equal times) reflects the requirement of microcausality.

²The main problem in following this path is that, once time is promoted to be an operator, one must choose which variables to use in order to parametrise the evolution of the operators. A natural choice can be the proper time τ of the particle, but any other monotonic function of τ would work equally well and this infinite redundancy must be accounted for.

In this form, one might still argue that a preferred role is assigned by the statement of (anti)commutation relations at a given fixed time t_0 , to the non-covariant surface $t = t_0$, breaking in this way the explicit Lorentz covariance of the formalism. Nevertheless, one can prove that such (anti)commutation relations are explicitly Lorentz covariant, or equivalently, the surface $t = t_0$ can be substituted by the covariant notion of *space-like* surface on which to specify the commutation relations (see for example [1]). We will not elaborate further on this. Recall anyway, that starting from the assumption of equal-time (anti)commutation relations, one can calculate in QFT the corresponding relations for different times. In this way one finds that in general such (anti)commutators involve the propagator specific to the type of fields being considered.

In its current formulation the SM content can be organised into two large families. The first contains fermionic fields, whose quanta are the elementary particles which constitute the matter content of the theory. The quanta of the bosonic fields, which constitute the second family, are the force carriers, i.e. the mediators of the fundamental interactions. In this picture, a very special place is that held by the *Higgs field*. In its minimal realisation, the Higgs field is the *only scalar field* in the SM and its quantum, the *Higgs Boson*, recently observed at the LHC [4, 5], is the only known scalar particle in the theory.

As we shortly discussed, the SM is based on the two fundamental pillars of SR and QM. Neither of the two, nevertheless, is enough to predict what the nature of particles and forces must be; only the experimental evidence can tell what the matter content of the theory must be, and what are the properties of the interactions among them. It is widely accepted that what we know about the physical world can be described in terms of fermionic fields which interact through *four fundamental forces*, namely: electromagnetism, the weak force, the strong force and the gravitational force. The modern approach to incorporate such interactions in the framework of QFT is that of *gauge theories*, i.e. each of these interactions is the manifestation of an underlying *gauge symmetry* of the theory. Note that once more the interaction with the Higgs field is a notable exception to this, insofar as it does not derive from a gauge symmetry. From this point of view the electromagnetic interactions are characterised by an U(1) gauge symmetry, the weak interactions by an SU(2) gauge symmetry and the strong interactions by an SU(3) one. Finally, if the group of transformations is taken to be as that of all coordinate transformations, one is naturally led to a gauge theory for gravity.

The SM allows for a consistent description of the electromagnetic, weak and strong forces and their quantisation. One of the most revolutionary discoveries of the last century has been that electromagnetism and the weak forces are actually unified in the so called *electro-weak interactions*, whose structure is based on a spontaneously broken $SU(2)_L \times U(1)_Y$ gauge group. Such a gauge symmetry in fact, if not broken, would not allow for the existence of any massive particles. The observed masses of fermions and of (some) vector bosons are instead generated *dynamically* by the inter-

action with the Higgs field which breaks the symmetry group $SU(2)_L \times U(1)_Y$ down to the $U(1)_{em}$ electromagnetic gauge group, leaving one single massless vector boson, the *photon*. The other three mediators of the electro-weak force, the Z, W^+, W^- bosons acquire instead a mass, which is proportional to their coupling with the Higgs boson. Finally the theory of strong interactions, *Quantum Chromo-Dynamics (QCD)*, is based on an $SU(3)$ unbroken gauge group, whose force carriers, the *gluons*, remain massless. A tentative unification of the strong and the electro-weak interaction has been attempted in different ways, but no real experimental evidence for such unification exists.

Unfortunately the same formalism cannot be trivially extended to gravity, which would in this way give rise to a *non-renormalisable* theory, and as such useless for providing any meaningful physical predictions. Different ways have been attempted to construct a theory which would consistently account for the presence of gravity together with the other fundamental interactions, the most notable example of which is *string theory*. Nevertheless, at the moment there is no way to verify these theories experimentally and at the same time there is in practise no physical phenomenon which we can reproduce in a laboratory and which cannot be explained to high accuracy by the Standard Model in its original formulation, making it difficult for any other theory to replace it.

From now on we will be focussing on quantum field theory only, and specifically on the standard model as the theory of fundamental interactions. We will in particular elaborate on how one can extract numerical predictions from it using perturbation theory through the pictorial expansion in *Feynman diagrams*.

1.1.1 Scattering amplitudes

The starting point for building up any quantum field theory is a *Lagrangian density* $\mathcal{L}[\phi_i(x)]$, which is a functional of the fundamental fields $\phi_i(x)$ and encodes all symmetries of the theory. Given the Lagrangian, the *action* for the theory is obtained by integrating it over the four-dimensional space-time

$$\mathcal{S} = \int d^4x \mathcal{L}[\phi_i(x)].$$

In QFT elementary particles are point-like objects which interact (or *scatter*) with each other through the exchange of quanta of the force fields. Moreover, being QFT based on Quantum Mechanics, the theory is by its very construction non-deterministic and the fundamental *observables* which we can aim to compute are therefore typically *probability distributions*. A “classical” observable is the *total cross-section* σ , which measures the total probability of an event to happen.

Let us consider a scattering process where an initial free state $|i\rangle$ of total 4-momentum p_i evolves into the final free state $|f\rangle$ of total 4-momentum p_f through local interactions only, $|i\rangle \longrightarrow |f\rangle$. In total generality initial and final states will

be characterised by their quantum numbers (for example the *spin* or the *polarisation* of fermions and vector bosons). For the sake of simplicity we will neglect here these internal degrees of freedom, since keeping track of them would not add anything conceptually to what follows.

The total cross-section σ for this process can be written in terms of the so-called *Scattering-matrix* (or *S-matrix*), which relates initial to final states and describes the evolution of the system during the interaction. Given the asymptotic states above, the S-matrix elements are defined as

$$\langle f | S | i \rangle = \delta_{fi} + i (2\pi)^4 \delta(p_f - p_i) \mathcal{M}_{fi}, \quad (1.2)$$

where the δ_{fi} term is related to the unscattered forward propagating state, while \mathcal{M}_{fi} parametrises the “actual” interaction. One finds that, in terms of \mathcal{M}_{fi} , the total cross-section for the process can be written, up to an overall constant which depends only the kinematics of the process and is referred to as *flux factor*, as

$$\sigma \propto \int d\phi_f |\mathcal{M}_{fi}|^2, \quad (1.3)$$

where $|\mathcal{M}_{fi}|^2$ is the modulus squared of the scattering matrix elements, \mathcal{M}_{fi} , and $d\phi_f$ represents the phase-space of the final state $|f\rangle$ ³.

Unfortunately the analytical computation of the S-matrix (and consequently of the matrix elements \mathcal{M}_{fi}) from general principles is an almost impossible task to achieve in general, even in the easiest scalar field theories, and the only viable approach is through *perturbation theory*.

The S-matrix can be expanded as a power series in the *number of exchanges of virtual particles* among the external fields. In particular each of these “exchanges” takes place through *local interactions* between external and internal states. Every local interaction is in turn associated with an intrinsic strength, measured by the so-called *coupling constants*. In electromagnetism such coupling is nothing but the fine structure constant

$$\alpha_{em} = \frac{e^2}{4\pi}, \quad \text{with } e = \text{electron charge}. \quad (1.4)$$

If the coupling is small enough, we can then safely limit ourselves to the very first terms of the series and this often provides a very good approximation of the full result. Nonetheless, it is very well known that in quantum field theory the strength of the couplings is not really constant, but instead depends on (or equivalently it “runs” with) the energy scale at which the interaction takes place. In the case of the quantum relativistic theory of electromagnetism, *Quantum Electro-Dynamics*

³Let us note here that, for comparing the results with actual experiments, in some cases it can be convenient to sum and/or average over spins and polarisation of the initial and final states, and considering therefore the *unpolarised* total cross-section.

(QED), the value of the coupling constant α_{em} becomes larger with the increase of the momentum transfer, for example

$$\alpha_{em}(Q^2 \approx 0) \approx \frac{1}{137}, \quad \text{and} \quad \alpha_{em}(Q^2 \approx m_W^2) \approx \frac{1}{128},$$

where $m_W \approx 80$ GeV is the W boson invariant mass. The smallness of α_{em} at all typical energies which can be probed in most experiments guarantees fast convergence of the perturbative series to what we expect to be the “real”, *non-perturbative*, result. In the next section we will briefly discuss how this picture changes drastically in the case of strong interactions.

Assuming in any case that the coupling constant is small enough (so that the perturbative expansion is valid), the different orders of the series can be computed using the pictorial representation provided by *Feynman diagrams*. Through a straightforward procedure, given the *Lagrangian density* of the theory, one can obtain the so-called *Feynman rules*, i.e. a set of rules which associate a mathematical meaning to every part of a diagram. In practice, given an initial and a final state, one has to draw all possible configurations of propagating particles which connect the latter through all interactions allowed by the Lagrangian. Depending on the number of external and internal propagating particles every diagram will belong to a specific order in the perturbative expansion, so that, at every order in the approximation, only a well-defined subset of diagrams must be considered. Needless to say, as the perturbative order increases, the number of possible configurations in the diagrams also increases as a result of simple combinatorial arguments, so that the number of diagrams to be drawn (and consequently *evaluated*) quickly becomes prohibitively large.

In what follows we will focus on the explicit case of Quantum Chromo-Dynamics. We will briefly summarise the main properties of the theory, starting from the Lagrangian up to the Feynman rules. We will also elaborate on the problem of UV and IR divergences which affect virtually any computations in QCD and discuss how these can be consistently *regularised* and accounted for to produce finite numerical predictions.

1.2 QCD - Quantum Chromo-Dynamics

Quantum Chromo-Dynamics, or QCD, is the theory that describes the dynamics of *quarks*, the elementary particles which constitute hadrons. Initially it was a common belief that hadrons, which are observed both in bosonic (*mesons*) and fermionic (*baryons*) states, had to be fundamental particles. The typical example is that of protons and neutrons, which were for a long time thought to be the elementary constituents of atomic nuclei. Nevertheless, from the 1950s on a larger and larger number of apparently different hadrons were observed in different experiments, suggesting that such particles could not be really elementary but had to be instead composite objects. The *quark model* explains the nature of baryons and mesons as

respectively *bound states* of three quarks and of a quark-antiquark pair. Quarks are spin-1/2 particles and experimentally we know that they exist in at least six different kinds (or flavours), namely up (u), down (d), strange (s), charm (c), bottom (b) and top (t). The experimental evidence of baryonic states made of 3 apparently identical quarks required the introduction of a new quantum number in order to accommodate the spin statistics theorem. This new degree of freedom, which was given the name of *colour*, had to exist in at least three different values (red, blue and green), in order to explain the existence of the observed Δ^{++} baryon, which is a bound state of three (otherwise identical) u quarks. All observed hadronic states are colourless, i.e. in the baryonic case they are a combination of red-blue-green coloured quarks, while in the mesonic case always a colour-anticolour combination (red-antired, blue-antiblue, green-antigreen). This experimental fact, which is usually referred to as *colour confinement*, is believed to be a non-perturbative property of QCD, but a rigorous proof of this is not yet known. The quark model doesn't contain any information on the dynamics of quarks, but is instead primarily a classification scheme which can explain the existence of hadrons and their quantum numbers to a good extent.

Starting from the experimental findings described above and from the successes of the quark model, QCD was built as a quantum field theory where quarks are the point-like elementary particles carrying the strong (colour) charge. As in electrodynamics, quarks interact through the exchange of bosonic force carriers, the *gluons*. QCD is a gauge theory and assumes invariance under the gauge group $SU(3)$. Quarks transform according to the fundamental representation of $SU(3)$ and as such carry three possible colour-charges. Gluons on the contrary transform according to the adjoint representation and can exist in 8 different colour states.

1.2.1 The QCD Feynman Rules

The QCD Feynman rules can be directly read off from the QCD Lagrangian density. The latter can be written as a sum of three terms:

$$\mathcal{L}_{QCD} = \mathcal{L}_{classic} + \mathcal{L}_{gauge-fix} + \mathcal{L}_{ghost}. \quad (1.5)$$

The dynamics of quarks is generated by the first piece, $\mathcal{L}_{classic}$, while the last two terms are needed in order to allow for a consistent quantisation of the theory. The full QCD Lagrangian and its covariant quantisation are extensively discussed in many textbooks, which we refer to for further details (see for example [2, 6, 7]). The first term reads:

$$\mathcal{L}_{classic} = \sum_f \bar{\psi}_{f,i} (i \not{D}_{ij} - m_f \delta_{ij}) \psi_{f,j} - \frac{1}{4} F_{\mu\nu}^a F^{\mu\nu,a}, \quad (1.6)$$

where f is the flavour index, i, j, \dots are the colour indices in the fundamental representation and a, b, \dots are the ones in the adjoint representation. The $\psi_{f,i}$ are the quark fields, and the covariant derivative reads

$$D_{ij}^\mu = \partial_{ij}^\mu \delta_{ij} - ig_s A_a^{ij} t_{ij}^a,$$

where A_a^μ are the gluon fields and the matrices t_{ij}^a are the generators of the fundamental representation of $SU(N)$, with $N = 3$ the number of colours. The t_{ij}^a fulfil the algebra

$$[t^a, t^b] = i f^{abc} t^c, \quad (1.7)$$

where f^{abc} are the structure constants. The constant g_s is the coupling strength of quarks to gluons. Finally the gluonic field tensor reads

$$F_{\mu\nu}^a = \partial_\mu A_\nu^a - \partial_\nu A_\mu^a + g_s f_{abc} A_\mu^b A_\nu^c. \quad (1.8)$$

The gauge invariance of $\mathcal{L}_{classic}$ is reflected in the freedom of the gluon fields to change by a total derivative and leave the latter invariant. In other words, if one tries to quantise naively $\mathcal{L}_{classic}$, one finds that it is not possible to define an unambiguous expression for the gluon propagator. This in turn translates, in terms of path integral quantisation, into an infinite contribution of each gluonic field to the path integral over the exponential of the action. In order to proceed further one needs therefore to force the gluons on a specific gauge, and this can be achieved by the *Faddeev-Popov method*. The latter allows to quantise the theory in an explicitly covariant way, at the expenses of introducing new *unphysical* degrees of freedom, the so-called *Faddeev-Popov ghosts*.

Applying this procedure on the $\mathcal{L}_{classic}$ produces the last two terms of the Lagrangian (1.6). The first of the two, $\mathcal{L}_{gauge-fix}$, can be written as

$$\mathcal{L}_{gauge-fix} = \frac{1}{2\xi} (\partial_\mu A_a^\mu)^2 \quad (1.9)$$

where the parameter ξ is arbitrary and it is needed in order to specify the gauge in a covariant way. The gauges obtained in this way are also called R_ξ gauges. A typical choice is $\xi = 1$, the so-called Feynman gauge, which we will be using throughout this thesis, unless otherwise specified. Obviously, physical results cannot depend on the explicit value of the parameter ξ .

Upon specifying the gauge by (1.9) one is left, at the level of the path integral, with an overall determinant which multiplies the exponential of the action and still depends on the gluon fields A^μ . Because of its dependence on A^μ this determinant cannot be factored out as an overall normalisation factor, but instead its contribution to the action can be represented as another term in the Lagrangian which involves a new set of *anti-commuting fields*, the Faddeev-Popov ghosts⁴:

$$\mathcal{L}_{ghost} = (\partial_\mu \chi_a^*) (\partial^\mu \delta_{ab} - g_s f_{abc} A_c^\mu) \chi_b. \quad (1.10)$$

⁴We note here that this pattern is typical of non-abelian gauge theories. Indeed the same Faddeev-Popov method can be applied in the case of an abelian theory, like QED. Nevertheless, in this case one finds that the determinant which gives rise to the unphysical ghost fields is *independent* of the photon field and can be therefore factored out from the path integral and treated as a contribution to the overall normalisation factor.

The *ghost* fields χ_a are scalar fields, which nevertheless fulfil fermionic anticommutation relations.

From (1.6, 1.9, 1.10) one can read off at once all *QCD Feynman Rules*. We will use straight lines for quarks, curly lines for gluons and dashed lines for ghosts. Moreover we will employ the usual Feynman *slash-notation* $\not{p} = p^\mu \gamma_\mu$, where γ^μ are the Dirac gamma matrices.

- The propagators for internal quarks, gluons and ghosts read (in the R_ξ gauges) respectively:

$$\begin{array}{ccc}
 i & & j \\
 \longrightarrow & & \\
 & & i \delta_{ij} / (\not{p} - m + i\epsilon)
 \end{array}$$

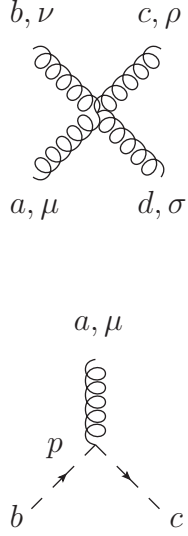
$$\begin{array}{ccc}
 a, \mu & & b, \nu \\
 \text{oooooo} & & \\
 & & \delta_{ab} \left[-g_{\mu\nu} + (1 - \xi) \frac{p_\mu p_\nu}{p^2 + i\epsilon} \right] i / (p^2 + i\epsilon)
 \end{array}$$

$$\begin{array}{ccc}
 a & & b \\
 \text{---} \longrightarrow \text{---} & & \\
 & & i \delta_{ab} / (p^2 + i\epsilon)
 \end{array}$$

- The interaction vertices are:

$$\begin{array}{ccc}
 & a, \mu & \\
 & \text{oooo} & \\
 & \swarrow \searrow & \\
 i & & j
 \end{array}
 \quad -i g_s t_{ij}^a \gamma^\mu$$

$$\begin{array}{ccc}
 & b, \nu & \\
 & \text{oooo} & \\
 & \swarrow \searrow & \\
 p_1 & & p_3 \\
 \text{oooo} & & \text{oooo} \\
 a, \mu & & c, \rho
 \end{array}
 \quad -g_s f_{abc} [(p_1 - p_2)^\rho g^{\mu\nu} + (p_2 - p_3)^\mu g^{\nu\rho} + (p_3 - p_1)^\nu g^{\rho\mu}]$$



The image shows two Feynman diagrams. The top diagram is a four-point vertex where two gluons (curly lines) enter from the top and two exit from the bottom. The top-left gluon is labeled b, ν , the top-right c, ρ , the bottom-left a, μ , and the bottom-right d, σ . To its right are three terms in square brackets, each preceded by a minus sign and a coupling constant $-g_s^2$. The first term is $f_{eac}f_{ebd}[g^{\mu\nu}g^{\rho\sigma} - g^{\mu\sigma}g^{\nu\rho}]$, the second is $f_{ead}f_{ebc}[g^{\mu\nu}g^{\rho\sigma} - g^{\mu\rho}g^{\nu\sigma}]$, and the third is $f_{eab}f_{ecd}[g^{\mu\rho}g^{\nu\sigma} - g^{\mu\sigma}g^{\nu\rho}]$. The bottom diagram is a three-point vertex where a gluon (curly line) enters from the top and two quarks (dashed lines) exit from the bottom. The top gluon is labeled a, μ , the bottom-left quark b , and the bottom-right quark c . The momentum of the quark b is labeled p . To the right of this diagram is the expression $g_s f_{abc} p^\mu$.

Note that all momenta have to be taken as ingoing. In addition to these rules one has the following:

1. For each internal loop of momentum k we must integrate over the loop momentum with the integration measure $\int d^d k / (2\pi)^d$, where d is the number of space-time dimensions.
2. Every fermionic loop (i.e. quark- and ghost-loops) comes with a factor (-1) .
3. Finally one must also multiply by an overall symmetry factor which accounts for all equivalent permutations of internal or external legs in each diagram.

Note that every vertex comes with its own power of the coupling g_s , so that the Feynman diagrams which can be built with these Feynman rules can be classified in terms of the total number of powers of the coupling which they contain. In particular, with the increase of this number, diagrams containing one or more *closed loops* can be drawn. The main difficulty in the evaluation of the latter lies then in the computation of the loop integrals. These often diverge in $d = 4$ space-time dimensions, both in the UV and in the IR (i.e. respectively for very large and very small or collinear loop momenta, as we will discuss more precisely in the following), and we will use everywhere *dimensional regularisation* [8–10] in order to regularise and collect both kinds of divergences.

1.2.2 Perturbative calculations in QCD

As briefly discussed above, in QFT the only way we can extract predictions from the theory is through the S -matrix, which can be, at least formally, perturbatively expanded as a Dyson series in Feynman diagrams. Starting from the Feynman rules one can then give a mathematical meaning to this pictorial expansion. Such “formal”

perturbative series becomes an actual tool for providing precise phenomenological predictions if, at the energies under consideration, the coupling constant of the theory is small enough. We mentioned earlier that as far as QED is concerned this is always the case in practise.

The situation is instead quite different in QCD. The most important breakthrough which led to the formulation of QCD was indisputably the discovery that non-abelian gauge theories possess the crucial property of *asymptotic freedom* [11–15]. Due to asymptotic freedom one finds that the strong coupling constant

$$\alpha_S = \frac{g_s^2}{4\pi}, \quad \text{with } g_s = \text{the quark-gluon coupling},$$

has the opposite behaviour with respect to that of QED, namely instead of increasing with the increase of the energy scale, it decreases.

The running of the coupling constant with the energy scale is a direct consequence of the renormalisation group equations. As briefly mentioned above, quantum field theories, and in particular QCD, suffer from two kinds of “infinities” (or divergences), UV and IR. We will discuss in more detail the role of IR divergences in the next paragraph and elaborate on how they are expected to cancel when computing any physical quantity. On the other hand UV divergences do not cancel but have instead to be *renormalised*. QCD turns out to be a renormalisable theory, in the sense that one can successfully reabsorb all UV divergences, at every order in perturbation theory, into redefinitions of all fields and parameters of the theory.

This renormalisation procedure has however a twofold degree of arbitrariness. On the one hand, in subtracting a divergent quantity, one can always add to it any arbitrary finite part; this choice defines the so-called *renormalisation scheme*. Moreover, this procedure naturally introduces the dependence on a spurious scale (the *renormalisation scale* μ_R), which physically represents the energy scale at which the renormalised quantities are defined. Self-consistency requires that these different arbitrary choices cannot affect the values of any physical quantities, and this in turn imposes strong constraints on the behaviour of renormalised quantities when changing the renormalisation scheme or varying the renormalisation scale. Such requirements are mathematically expressed by a set of differential equations called the *renormalisation group equations*. By deriving and solving these equations for the renormalised coupling constant α_S in *massless* QCD one finds precisely that for up to sixteen massless quark flavours the value of α_S becomes smaller as the scale μ_R increases.

Equivalently one finds that, upon lowering the energy scale, the value of the coupling constant increases, soon spoiling the validity of perturbation theory. As a typical example, at the energy scale corresponding to the proton mass $m_p \approx 938$ MeV one has

$$\alpha_S(m_p^2) \approx 0.55,$$

which is far from being a “very small number”. On the contrary at energies of the order of the Z -boson invariant mass, $m_Z \approx 90$ GeV, one has

$$\alpha_S(m_Z^2) \approx 0.1.$$

It is obviously a very non-trivial problem that of giving a precise estimate of the energy scale where perturbation theory in QCD would break down, requiring therefore a completely different non-perturbative approach. Nevertheless, one can reasonably expect that for the energy range of modern colliders like LEP, Tevatron or LHC, which spans from hundreds of GeV to tens of TeV, perturbation theory should be safely applicable. The impressive number of calculations performed in the past years have indeed demonstrated the predictive power of perturbative QCD for a large spectrum of observables, both in hadronic and leptonic collisions. Moreover one more important point should be mentioned here. The property of colour confinement tells us that quarks can not be observed as free states, but instead they must always “cluster” into hadronic bound states. This complicates enormously the picture when we try to compare predictions from perturbative QCD with the actual experiments. The expansion in Feynman diagrams allows us in fact to describe only the so-called *hard scattering* among the elementary constituents. On the other hand in a real experiment we cannot scatter partons but only hadrons, and the QCD particles produced in the collision will in turn immediately recombine into hadronic bound states, which will then constitute the final observable products in the detectors. This phenomenon is usually referred to as *hadronisation*.

The problem of comparing QCD perturbative calculations with the experiments is a very complex one, and we will not consider it further, referring instead to the literature for a more complete discussion [6,7]. We recall however that this is possible mainly thanks to the *factorisation theorem*, which allows one to split the problem in two different phases: the *hard scattering*, described within perturbative QCD, and the *hadronisation*, which must be addressed with some different methods.

1.2.3 NNLO computations in QCD

As seen above, asymptotic freedom together with the factorisation theorem, allow us to use perturbation theory in QCD to perform precise computations in QCD for high energy hadron colliders, ignoring *de facto* all complications related to strong-coupling non-perturbative effects. We discussed how, starting from the Feynman rules of the theory, one can compute the S-matrix elements for a scattering process by decomposing them into Feynman diagrams. Finally, given the S-matrix one can virtually compute any observable (for example the total cross-section σ) by integrating the modulus squared of these matrix elements on the relevant phase-space.

This apparently straightforward procedure is actually highly non-trivial in practice, in particular for higher perturbative orders. To clarify this point, let us consider a generic QCD process where a final state X is produced through quark-antiquark annihilation

$$q(p_1) + \bar{q}(p_2) \rightarrow X(q), \quad (1.11)$$

with $q = p_1 + p_2$ and for simplicity $p_1^2 = p_2^2 = 0$ while $q^2 \neq 0$. In what follows we will focus only on the general properties of high order corrections; therefore we will neglect overall normalisation factors which are not relevant for the general discussion.

The total cross section for the production of the final state X in perturbative QCD, $\sigma^{(X)}$, can be expanded in powers of α_S . Normalising to the number of powers of α_S of the born cross-section we can write

$$\sigma^{(X)} = \sigma_{LO}^{(X)} + \left(\frac{\alpha_S}{2\pi}\right) \sigma_{NLO}^{(X)} + \left(\frac{\alpha_S}{2\pi}\right)^2 \sigma_{NNLO}^{(X)} + \dots, \quad (1.12)$$

where LO stands for *Leading Order*, NLO for *Next-to-Leading Order*, NNLO for *Next-to-Next-to-Leading Order*, etc.

The computation of the *born* is, at least in principle, entirely straightforward. We can in fact safely write down and evaluate all tree-level Feynman diagrams contributing to the amplitude and square them (in case summing and averaging over spins and polarisations of the external states). The amplitude obtained in this way can then be integrated over the phase-space of the final state X such that the leading order contribution to the total cross-section can be written as:

$$\sigma_{LO}^{(X)} \propto \int d\phi_X |\mathcal{M}_X^{(0)}|^2.$$

Note that, as far as the LO is concerned, in many cases this integral can be even computed analytically in closed form.

Let us consider now the next order of the expansion, i.e. $\sigma_{NLO}^{(X)}$. Two different classes of diagrams contribute to this order in α_S . First of all one has to include all the so-called *virtual diagrams*, i.e. those diagrams containing an internal loop, which are suppressed in the perturbative expansion by one power of α_S with respect to the tree-level. These diagrams, as shortly discussed above, are in general divergent as the number of space-time dimensions approaches $d = 4$. These divergences can be of two different natures, UV and IR, and they can be regularised and isolated using dimensional regularisation. The UV divergences, which are associated with the loop momentum being allowed to assume arbitrarily large values, are then consistently removed by *renormalisation*, leaving a virtual amplitude which still contains *explicit* IR divergences. The latter, which are instead associated with the loop momenta becoming arbitrarily small (*soft divergences*), or arbitrarily collinear to any massless external particle (*collinear divergences*), are *non-physical* and are due to the fact that, in building up $\sigma_{NLO}^{(X)}$, we neglected a second class of diagrams which contributes to the same order in powers of α_S . These diagrams, the so-called *real corrections*, are those where the final state X is produced in association with an additional *very soft* or *very collinear* parton, for example:

$$q(p_1) + q(p_2) \rightarrow X(q) + g(p_3). \quad (1.13)$$

It is clear that from the experimental point of view there is no way to distinguish such soft or collinear partons in any “realistic” detector, and consequently they are naturally part of the measured cross-section for the production of the final state X alone.

Taking these contributions into account the NLO total cross-section can be schematically written as the sum of two terms

$$\sigma_{NLO}^{(X)} \propto \int d\phi_X 2 \operatorname{Re} \left(\mathcal{M}_X^{(0)*} \mathcal{M}_X^{(1)} \right) + \int d\phi_{Xj} |\mathcal{M}_{Xj}^{(0)}|^2, \quad (1.14)$$

where $\mathcal{M}_X^{(1)}$ is the one-loop amplitude, while $\mathcal{M}_{Xj}^{(0)}$ is the tree-level amplitude for the production of the final state X with an additional parton j .

Note that in (1.14) the first piece contains all virtual corrections coming from the one-loop diagrams (contracted with the tree-level), while the second contains the real corrections. The two terms are separately IR divergent, but once added together their sum is IR finite. This result, known as the KLN theorem [16, 17], is of crucial importance and ensures that physical quantities are free of IR divergences⁵.

At this point it is important to stress that, while in the virtual piece all IR divergences are explicit, since they come directly from the one-loop amplitude $\mathcal{M}_X^{(1)}$, the same is not true for the real corrections, where the IR poles are generated only after the integration over their specific phase-space $d\phi_{Xj}$ ⁶. Obviously if one is able to perform the two phase-space integrations analytically the cancellation of the poles is straightforward and can be seen explicitly. Unfortunately in the general case the phase-space integrals cannot be solved analytically, in particular when considering more *exclusive observables* than the total cross-section, where the integration is not extended to the whole phase-space. In these cases one can only resort to a fully numerical approach, which is rendered highly non-trivial by the presence of the IR divergences themselves. In order to achieve that, one needs a so-called *subtraction scheme*, which allows one to subtract these divergences at the level of the integrand, so that one is left with convergent integrals which can be more easily evaluated numerically. Different schemes have been developed for the subtraction of IR singularities at NLO, like the FKS scheme [18] and the Catani-Seymour dipole subtraction [19]. These schemes are completely general and, at least in principle, they enable one to compute NLO corrections to any infrared safe inclusive or exclusive observable.

The cancellation structure, which at NLO is quite simple, becomes obviously much more involved at NNLO or beyond, where more interference terms have to be taken into account. Let us consider the NNLO corrections to the cross-section for the production of the final state X through $q\bar{q}$ annihilation, $\sigma_{NNLO}^{(X)}$. Here three different classes of contributions have to be taken into account. First of all one must compute all virtual diagrams, namely the two-loop Feynman diagrams where X is produced as the final state. As a second piece, one has also to include the so-called

⁵We note here that while this is always true for the total cross-section, one has in general to be careful in defining the observables to compute. Those observables which are free of IR singularities, and as such can be safely computed in perturbative QCD, are said to be *infrared safe*.

⁶Note that the two phase-spaces are different and therefore one cannot simply sum the two *integrand*s in order to achieve the cancellation of the IR poles *before integrating*.

real-virtual contributions, i.e. the interference of the one-loop virtual amplitude with the tree-level amplitude, where one additional external parton is produced in the final state. Finally, similarly to the NLO case, one has the double-real contributions, where two additional external partons are produced in the final state. Schematically the cross-section can be written as:

$$\begin{aligned} \sigma_{NNLO}^{(X)} \propto & \int d\phi_X 2 \operatorname{Re} \left(\mathcal{M}_X^{(0)*} \mathcal{M}_X^{(2)} \right) \\ & + \int d\phi_{Xj} 2 \operatorname{Re} \left(\mathcal{M}_{Xj}^{(0)*} \mathcal{M}_{Xj}^{(1)} \right) + \int d\phi_{Xij} |\mathcal{M}_{Xij}^{(0)}|^2, \end{aligned} \quad (1.15)$$

where $d\phi_{Xij}$ is the phase-space with two additional external partons, and as before $d\phi_{Xj}$ is the phase-space with one additional external parton.

Again, as in the easier NLO case, each term is individually IR divergent, and in particular, while in the double-virtual piece all IR divergences are already explicit at the level of the amplitude, in the real-virtual and in the double-virtual parts the divergences become explicit only after the integration over their different phase-spaces. Obviously in this case, even more than in the NLO case, the phase-space integrals are typically extremely difficult to be computed analytically and the only possibility is that of resorting to numerical integration. Therefore, also at NNLO a subtraction scheme is needed in order to subtract all divergences at the level of the integrands and render the numerical integration possible. Due to the interplay of these three different pieces, building up subtraction schemes at NNLO which are at the same time *efficient* (fast) and *flexible* (easily extended to different processes) required a considerable amount of work, mainly in the understanding of the structure of IR singularities in QCD. Only recently different fast and reliable methods have become available, among which Sector Decomposition [20–24], q_T -Subtraction [25] and Antenna Subtraction [26–28] have been successfully applied for NNLO computations.

Obviously, thinking of going one order higher, namely to NNNLO (or N³LO), is even a more formidable task, and will require an even more thorough understanding of the underlying structure of IR singularities in QCD amplitudes. Some very promising first steps in this direction have recently been taken in the computation of the N³LO corrections to Higgs production in gluon fusion [29, 30].

In conclusion we discussed how, in order to extract precise numerical predictions from QCD using perturbation theory, one needs typically to consider different contributions. After UV renormalisation the latter are still separately IR divergent. These singularities cancel in all physical quantities only when all ingredients are combined together. When applying this to the case of the NNLO there are two main difficulties that must be overcome. The first is the computation of the *virtual* (two-loop) corrections to the amplitude. The second is the establishment of a subtraction method which allows the numerical integration of the virtual contributions together with the double-real and the real-virtual ones. In what follows we will not elaborate further on the nature of these subtraction methods, focussing instead on the problem of

computing two-loop virtual corrections. The methods that will be presented below are quite general and can be, at least in principle, applied to any QFT, both in the massless and in the massive case, and up to any number of loops. In practise, such methods have been extremely successful as far as two- (and sometimes three-) loop computations are concerned, for problems which depend on up to three independent scales⁷. In particular, as we will see in the following, as long as the solution can be expressed in terms of particular classes of functions, the *Chen iterated integrals* [31], the computation of the virtual corrections can be made almost completely algorithmic.

⁷The first four-scale problems are currently under study with the same methods and it will be interesting to follow developments in this direction.

Chapter 2

A diagrammatic approach to multiloop computations

In the previous section we discussed some very general features of precision calculations in the standard model and in particular in QCD, where the contribution of the latter is of primary importance when considering high energy physics experiments at hadron colliders like the Tevatron or the LHC. As we saw, in order to carry out successfully a typical NNLO computation in fixed order perturbation theory three different ingredients are needed. The two-loop virtual matrix elements, the one-loop single-real matrix elements and the tree-level double-real matrix elements. These three pieces have to be correctly combined together in order to provide a finite numerical prediction for a physical observable. This pattern, as expected, increases in complexity when we try and go higher in the perturbative expansion, where more and more different pieces interfere with each other contributing to the final, physical result.

In what follows we will focus only on the virtual contributions, whose computation can proceed through at least two different but equivalent approaches.

1. **A diagrammatic approach**, based on the direct computation of the Feynman diagrams which contribute to the process at the perturbative order under consideration.
2. **A unitarity-based approach**, where, whenever possible, the unitarity properties of the scattering amplitudes are employed in order to avoid the direct computation of all Feynman diagrams.

In spite of the unquestionable beauty and elegance of the unitarity-based techniques, their applicability remains still today usually confined either to one-loop computations or to very specific two- and multi-loop problems, since a complete multi-loop generalisation of such techniques is not yet at disposal. In these more complicated cases a “direct” diagrammatic approach is still usually more effective and is therefore more often pursued.

2.1 Tensor decomposition for scattering amplitudes

For the sake of simplicity let us start considering a generic QCD process with N external particles of momenta p_1, \dots, p_N , even though the present discussion could be easily generalised to any other renormalisable quantum field theory. Let the first b momenta represent bosonic states, while the remaining $f = N - b$ are fermionic states:

$$\begin{aligned} \{p_1, \dots, p_b\} & \quad b \text{ bosonic states,} \\ \{p_{b+1}, \dots, p_N\} & \quad f \text{ fermionic states.} \end{aligned}$$

The scattering amplitude for this process can be schematically written as $\mathcal{S}(p_1, \dots, p_N)$, where, for the sake of simplicity, we suppress all dependence on the quantum numbers of the external particles. In QCD we can expand any amplitude as a Laurent series in the coupling constant α_S as follows:

$$\begin{aligned} \mathcal{S}(p_1, \dots, p_N) &= \mathcal{S}^{(0)}(p_1, \dots, p_N) + \left(\frac{\alpha_S}{2\pi}\right) \mathcal{S}^{(1)}(p_1, \dots, p_N) \\ &+ \left(\frac{\alpha_S}{2\pi}\right)^2 \mathcal{S}^{(2)}(p_1, \dots, p_N) + \dots \end{aligned} \quad (2.1)$$

Suppose now that we want to compute the l -th order of this expansion, namely the l -loop virtual corrections to the QCD process under consideration $\mathcal{S}^{(l)}(p_1, \dots, p_N)$. In a direct diagrammatic approach we start off by generating all Feynman diagrams which contribute to that perturbative order. Every l -loop diagram $\mathcal{F}^{(l)}(p_1, \dots, p_N)$ can be seen as an integral over all loop momenta of a tensor in Minkowski space, where every free Lorentz index must be contracted with an external on-shell *bosonic* state:

$$\mathcal{F}^{(l)}(p_1, \dots, p_N) = \epsilon_{\mu_1}(p_1) \dots \epsilon_{\mu_b}(p_b) \int \prod_{j=1}^l \mathfrak{D}k_j F^{\mu_1 \dots \mu_b}(k_1, \dots, k_l; p_1, \dots, p_N). \quad (2.2)$$

Note that in this expression we factored out explicitly the wave functions of the external bosonic particles, while those of the external fermions are still contained in the tensor $F^{\mu_1 \dots \mu_b}(k_1, \dots, p_N)$.

We can then perform *tensor reduction* in order to project out all Lorentz indices from the loop momenta to the external momenta. In this way we end up with a tensorial object where the entire dependence on the loop integrals is enclosed in scalar coefficients, which can be factored out from the Lorentz tensor structure of the amplitude:

$$\mathcal{F}^{(l)}(p_1, \dots, p_N) = \epsilon_{\mu_1}(p_1) \dots \epsilon_{\mu_b}(p_b) \sum_{k=1}^m f_k^{(l)}(p_1, \dots, p_N) t_k^{\mu_1 \dots \mu_b}(p_1, \dots, p_N). \quad (2.3)$$

Notice that the m tensor structures $t_k^{\mu_1 \dots \mu_b}(p_1, \dots, p_N)$ do not depend on the loop integration variables, whose dependence is instead entirely enclosed in the coefficients $f_k^{(l)}(p_1, \dots, p_N)$.

The fact that a decomposition as in (2.3) exists is a general feature and is a direct consequence of Lorentz and Gauge invariance of scattering amplitudes. In particular, we can turn this argument inside out and employ symmetry considerations from the very beginning in order to predict the most general tensor decomposition allowed for the scattering amplitude $\mathcal{S}(p_1, \dots, p_N)$, and consequently also for the Feynman diagrams in which it is decomposed.

Considering the generic process described above, employing Lorentz and Gauge invariance we decompose its scattering amplitude as follows:

$$\mathcal{S}(p_1, \dots, p_N) = \epsilon_{\mu_1}(p_1) \dots \epsilon_{\mu_b}(p_b) \sum_{k=1}^n C_k(p_1, \dots, p_N) T_k^{\mu_1 \dots \mu_b}(p_1, \dots, p_N), \quad (2.4)$$

where now the n linearly independent tensor structures $T_k^{\mu_1 \dots \mu_b}(p_1, \dots, p_N)$ are completely general and independent of the perturbative order (and so on the number of loops l), but are instead determined only by the nature of the external particles and of the interactions allowed among them. From (2.1) it is obvious that also the coefficients $C_k(p_1, \dots, p_N)$, which can be considered as generalised *form factors* of the problem, can be expanded as a power series in α_S :

$$\begin{aligned} C_k(p_1, \dots, p_N) &= C_k^{(0)}(p_1, \dots, p_N) + \left(\frac{\alpha_S}{2\pi}\right) C_k^{(1)}(p_1, \dots, p_N) \\ &+ \left(\frac{\alpha_S}{2\pi}\right)^2 C_k^{(2)}(p_1, \dots, p_N) + \dots \end{aligned} \quad (2.5)$$

where obviously the l -th coefficient $C_k^{(l)}(p_1, \dots, p_N)$ receives contribution from all l -loop QCD Feynman diagrams.

In order to extract the contribution to the coefficients $C_k^{(l)}(p_1, \dots, p_N)$ from a Feynman diagrammatic representation of the scattering amplitude we can build up n projection operators $P_k(p_1, \dots, p_N)$ which, once applied on the amplitude $\mathcal{S}(p_1, \dots, p_N)$, single out the contribution of that given graph to the coefficient $C_k(p_1, \dots, p_N)$; in other words we require that:

$$\sum_{spins} P_k(p_1, \dots, p_N) \epsilon_{\mu_1}(p_1)^* \dots \epsilon_{\mu_b}(p_b)^* \mathcal{S}(p_1, \dots, p_N) = C_k(p_1, \dots, p_N), \quad (2.6)$$

where the sum runs on all spins and polarisations of the external particles.

Starting from the assumption that the tensor structure in (2.4) is the most general allowed by Lorentz and Gauge symmetry, we can decompose the projectors as well in the same basis of tensors:

$$P_k(p_1, \dots, p_N) = \sum_{j=1}^n A_j(p_1, \dots, p_N) [T_k^{\mu_1 \dots \mu_b}(p_1, \dots, p_N)]^\dagger, \quad (2.7)$$

where the A_k are in turn scalar coefficients, whose explicit form can be determined applying eq. (2.7) on eq. (2.4) and requiring that eq. (2.6) is fulfilled.

Once the exact form of the coefficients A_k is given, it is straightforward to apply the P_k on the Feynman diagrammatic decomposition of the amplitude in order to compute the contribution of every diagram to the value of the coefficients $C_k^{(l)}(p_1, \dots, p_N)$.

Applying any of the n projectors on a Feynman diagram and summing over spins and polarizations of the external particles, one ends up in total generality with a linear combination of a large number of l -loop *scalar* Feynman integrals (note that all Lorentz indices are contracted in (2.6)). In particular, any integral produced in this way can be schematically written as:

$$\mathcal{I}(p_1, \dots, p_N) = \int \prod_{j=1}^l \mathfrak{D}k_j \frac{(S_1)^{a_1} \dots (S_\rho)^{a_\rho}}{D_1^{b_1} \dots D_\tau^{b_\tau}}, \quad (2.8)$$

where the S_j are scalar products among any of the external and the internal momenta, while the D_j are loop propagators, respectively raised to integer powers a_j and b_j .

Applying this procedure to a $2 \rightarrow 2$ QCD process at two loops one ends up typically with an order of magnitude of *thousands* of distinct scalar integrals of the form (2.8). Computing all these integrals separately appears clearly as a formidable task, even more if we imagine of going higher in either the number of loops or the number of external legs.

2.1.1 The case of $q\bar{q} \rightarrow Z\gamma$

In order to exemplify the ideas described above, let us consider the case of the two-loop corrections to the production of two electroweak vector bosons in massless QCD. In particular, let us focus on the case where one of the vector bosons is massive (say a Z boson) and the other is an on-shell (massless) photon γ .

The main partonic subprocess which contributes to this reaction is the quark-antiquark annihilation channel, namely we consider the following process:

$$q(p_1) + \bar{q}(p_2) \rightarrow \gamma(-p_3) + Z(p_4), \quad (2.9)$$

with $p_j^2 = 0$ for $j = 1, 2, 3$ and $p_4^2 = m_Z^2$ is the mass of the Z -boson. Moreover we can introduce the Mandelstam invariants defined as:

$$\begin{aligned} s_{12} &= (p_1 + p_2)^2 > 0, & s_{13} &= (p_1 + p_3)^2 < 0, \\ s_{23} &= (p_2 + p_3)^2 < 0, & \text{with } s_{12} + s_{13} + s_{23} &= m_Z^2. \end{aligned} \quad (2.10)$$

This process has been studied in [32] and a detailed account can be found in Chapter 6, while here we will limit ourselves to considering the tensor structure. In particular, the scattering amplitude for this process can be written as:

$$\mathcal{S}_{Z\gamma}(p_1; p_3; p_2) = S_\mu(p_1; p_3; p_2) \epsilon_4^\mu(p_4) \quad (2.11)$$

where $S_\mu(p_1; p_3; p_2)$ represents the partonic current and $\epsilon_4(p_4)$ is the polarization vector of the Z -boson.

Using Lorentz and Gauge invariance we can easily show that the latter can be decomposed in 7 independent tensor structures as follows:

$$\begin{aligned} S_\mu(p_1; p_3; p_2) = & A_{11} T_{11\mu} + A_{12} T_{12\mu} + A_{13} T_{13\mu} \\ & + A_{21} T_{21\mu} + A_{22} T_{22\mu} + A_{23} T_{23\mu} \\ & + B T_\mu, \end{aligned} \quad (2.12)$$

where $T_{ij\mu}$ and T_μ are defined as:

$$\begin{aligned} T_{1j\mu} &= \bar{v}(p_1) \left[\not{p}_3 \epsilon_3 \cdot p_1 p_{j\mu} - \frac{s_{13}}{2} \epsilon_3 p_{j\mu} + \frac{s_{j4}}{4} \epsilon_3 \not{p}_3 \gamma_\mu \right] u(p_2), \\ T_{2j\mu} &= \bar{v}(p_1) \left[\not{p}_3 \epsilon_3 \cdot p_2 p_{j\mu} - \frac{s_{23}}{2} \epsilon_3 p_{j\mu} + \frac{s_{j4}}{4} \gamma_\mu \not{p}_3 \epsilon_3 \right] u(p_2), \\ T_\mu &= \bar{v}(p_1) \left[s_{23} \left(\gamma_\mu \epsilon_3 \cdot p_1 + \frac{1}{2} \epsilon_3 \not{p}_3 \gamma_\mu \right) - s_{13} \left(\gamma_\mu \epsilon_3 \cdot p_2 + \frac{1}{2} \gamma_\mu \not{p}_3 \epsilon_3 \right) \right] u(p_2), \end{aligned} \quad (2.13)$$

and used the notation:

$$s_{14} = s_{12} + s_{13}, \quad s_{24} = s_{12} + s_{23}, \quad s_{34} = s_{13} + s_{23}.$$

On the other hand the A_{ij} and B are scalar coefficients. Following the discussion in [33] we can derive 7 projection operators which, once applied on the partonic amplitude (2.12) single out these coefficients:

$$\begin{aligned} \sum_{spins} P_\mu(A_{ij}) (\epsilon_4^\mu(p_4) \epsilon_4^\nu(p_4)^*) S_\nu(p_1; p_3; p_2) &= A_{ij} \\ \sum_{spins} P_\mu(B) (\epsilon_4^\mu(p_4) \epsilon_4^\nu(p_4)^*) S_\nu(p_1; p_3; p_2) &= B. \end{aligned} \quad (2.14)$$

We prefer not to give here the explicit form of these projectors and refer to [33] for further details. Note anyway that, as already discussed above, the decomposition in (2.12) is completely general and does not depend on the perturbative features of the theory. Obviously, being true at non-perturbative level, it must as well be true once the scattering amplitude is perturbatively expanded in Feynman diagrams. We can then proceed and generate, for example with QGRAF [34], all Feynman diagrams which contribute to the tree-level, the one-loop and the two-loop massless QCD corrections to the process above, and apply the projectors on the Feynman diagrams in order to single out the different perturbative contributions to the coefficients A_{ij} and B . There are 2 diagrams at tree level, 10 diagrams at one loop and 143 diagrams at two loops. While the tree-level and the one-loop corrections do not present any particular difficulties, much more interesting is the computation of the two-loop diagrams. Upon contracting all two-loop diagrams with the projectors above we can express the entire two-loop contribution to the partonic amplitude in terms of around 2000 scalar integrals of the form (2.8). It is then clear that attempting a direct computation of

all the integrals separately could easily become a formidable (and probably hopeless!) enterprise.

In the following section we will describe how, using **Integration by parts identities**, **Lorentz invariance identities** and **Symmetry relations** one can find a large number of relations among all these integral, and in this way drastically reduce the number of independent integrals which must ultimately be computed. The result of the use of these techniques for the computation of the two-loop corrections to $q\bar{q} \rightarrow Z\gamma/W\gamma$ [32] are described in Chapters 6.

2.2 Reduction to Master Integrals

Following the steps outlined above one can cast a generic multi-loop scattering amplitude as a linear combination of tensor structures, whose form is only dictated by Lorentz invariance and symmetry considerations, multiplied by scalar coefficients, which contain the full dependence on the loop integrals. As we have seen in the previous section for $Z\gamma$ production, already when studying two-loop corrections to such coefficients, we are faced with the problem of computing hundreds or thousands of loop integrals. As it is well known, nevertheless, such task can be enormously simplified once one realises that dimensionally regularised Feynman Integrals do satisfy a large number of relations, which allow one to express most of those integrals in terms of a much smaller subset of *independent integrals* (where “independent” is to be understood in the sense of the identities introduced below), which are now commonly referred to as *Master Integrals* (MIs). For a detailed review on the argument see for example [35, 36], which we will be referring to in what follows.

Before being able to describe the different classes of identities fulfilled by dimensionally regularised Feynman Integrals, let us start off with some notation. Let us consider again the l -loop corrections to a generic process in QFT with N external particles of momenta p_1, \dots, p_N . As we discussed, any Feynman diagram contributing to such process can be decomposed in scalar integrals, as in (2.8):

$$\mathcal{I}(p_1, \dots, p_N) = \int \prod_{j=1}^l \mathfrak{D}k_j \frac{(S_1)^{a_1} \dots (S_\rho)^{a_\rho}}{D_1^{b_1} \dots D_\tau^{b_\tau}}. \quad (2.15)$$

Working in the Euclidean metric every propagators will be $D_j = q_j^2 + m_j^2$, where q_j is in general a combination of internal and external momenta, while the masses m_j can be equal or different from zero.

It is very useful to organise these integrals in terms of so-called *topologies*. The topology of an integral is defined solely by its propagators, regardless of the powers they are raised to, or of the different scalar products that contain. Given a certain topology, we can define its *sub-topologies* as all topologies that can be obtained from the original one removing one or more denominators *in all possible ways*. The set of all sub-topologies constitutes the so-called *sub-topology tree*.

Consider now an integral belonging to a certain topology, and so characterised by a fixed set of denominators. It is clear that not all possible scalar products among external and internal momenta can be linearly independent from the denominators. In particular, given the N external momenta and the l loop momenta, one can build up

$$\rho = l \left(N + \frac{l}{2} - \frac{1}{2} \right)$$

independent scalar products among them (which contain *at least* one loop momentum!). Moreover, given the τ different propagators as in (2.8), all but $\sigma = (\rho - \tau)$ scalar products can be re-expressed as linear combination of these denominators, while the σ remaining scalar products will be called *irreducible*. After tensor reduction the most general scalar Feynman integral will then be of the form:

$$\mathcal{I}(p_1, \dots, p_N) = \int \prod_{j=1}^l \mathfrak{D}k_j \frac{(S_1)^{a_1} \dots (S_\sigma)^{a_\sigma}}{D_1^{b_1} \dots D_\tau^{b_\tau}}. \quad (2.16)$$

where the $a_j, b_j \geq 0$.

We denote with $I_{t,r,s}$ the class of integrals with t different denominators (raised to any positive power), $r = \sum_j (b_j - 1)$ powers of denominators, and $s = \sum_j a_j$ powers of irreducible scalar products. One can show that the total number of different integrals belonging to the class $I_{t,r,s}$ is:

$$N(I_{t,r,s}) = \binom{r+t-1}{t-1} \binom{s+\sigma-1}{\sigma-1}. \quad (2.17)$$

With the definition of topology above, it is obvious that t is the only parameter that determines the topology of an integral (even though there will be in general different topologies with the same value of t !). On the other hand, increasing or decreasing the values of r, s for fixed values of t will not change the topology of the integral, but will typically produce integrals which belong to the same topology or to its sub-topology tree.

Topic of the next paragraphs will be that of deriving identities which relate the different integrals in these classes, for increasing or decreasing values of $\{t, r, s\}$. We can start off by dividing these identities into two large groups:

1. The first is made up by those identities which are valid for any value of the dimensions d (where d can be treated as a continuous parameter in dimensional regularisation). As we will discuss, these identities are based on symmetry properties of the dimensionally regularised Feynman integrals and can be divided in: **Integration by parts identities**, **Lorentz invariance identities** and **Symmetry relations**. This class of identities is also the most important one inasmuch as it constitutes the bulk of identities needed to reduce all integrals in a given topology to a small number of MIs.

2. The second group is made up instead by identities which are exactly valid only for fixed, integer values of the dimensions d , and that for this reason can be considered as *pseudo-identities* for continuous values of d . An example of such identities is given by the recently introduced **Schouten pseudo-identities** [37]. The latter, as they are not valid for arbitrary values of d , cannot reduce the number of independent MIs as generic functions of d . On the other hand, though, being valid for fixed values of d (say $d = n$, with $n \in \mathbb{N}$) they can be used in order to determine particularly convenient choices of MIs as far as their series expansion for $d \approx n$ in $(d - n)$ is concerned.

2.2.1 Integration by parts identities (IBPs)

The so-called *integration by parts identities* [38–40] are by far the most important class of identities that can be established among dimensionally regularised Feynman integrals. They can be seen as a generalisation of Gauss’ theorem in d -dimension and are based on the consideration that, given a Feynman integral as a function of the dimensions d , there always exists a value of d in the complex plane where the integral is well defined and therefore convergent¹. Necessary condition for the convergence of an integral is the integrand be zero at the boundaries. Given an integral as in (2.16), such condition can be rephrased as:

$$\int \prod_{j=1}^l \mathfrak{D}k_j \frac{\partial}{\partial k_n^\mu} \left(v_m^\mu \frac{(S_1)^{a_1} \dots (S_\sigma)^{a_\sigma}}{D_1^{b_1} \dots D_\tau^{b_\tau}} \right) = 0, \quad (2.18)$$

where the v_m^μ are any of the internal or external momenta $v_m^\mu = \{k_1^\mu, \dots, k_l^\mu; p_1^\mu, \dots, p_N^\mu\}$.

The latter are needed in order to deal only with scalar quantities. In this way $l(l + N - 1)$ IBPs can be established for each integrand. Upon explicitly evaluating the derivatives and contracting with the momenta v_m^μ new integrals belonging to the same topology (or to its sub-topologies) are generated. In particular, each IBP identity can relate integrals with $(s - 1)$, s and $(s + 1)$ powers of scalar products, and $(t + r)$ or $(t + r + 1)$ powers of propagators. Notice that by contracting with v_m^μ new reducible scalar products can be generated, which could then simplify some of the denominators producing integrals belonging to any of the $(t - 1)$ -sub-topologies of the original topology. Finally it should be clear that, in realistic applications to multi-loop or multi-leg processes, one can encounter cases where hundreds of thousands (or even millions) of IBPs can be derived for complicated topologies.

2.2.2 Lorentz invariance identities (LIs)

The Lorentz invariance of scalar Feynman integrals (2.16) can be exploited in order to derive more identities among the integrals [35]. In particular, consider an

¹Note that all scaleless integrals in dimensional regularisation are zero for consistency.

infinitesimal Lorentz transformation on the external momenta

$$p_i^\mu \rightarrow p_i^\mu + \delta p_i^\mu = p_i^\mu + \omega^{\mu\nu} p_{i,\nu},$$

where $\omega_{\mu\nu}$ is a *totally antisymmetric tensor*. Since the integrals are Lorentz scalars we find on the one hand:

$$\mathcal{I}(p_i + \delta p_i) = \mathcal{I}(p_i). \quad (2.19)$$

On the other hand, since any infinitesimal transformation can be written as:

$$\mathcal{I}(p_i + \delta p_i) = \mathcal{I}(p_i) + \omega^{\mu\nu} \sum_j p_{j,\nu} \frac{\partial}{\partial p_j^\mu} \mathcal{I}(p_i), \quad (2.20)$$

using (2.19) together with the antisymmetry of the tensor $\omega_{\mu\nu}$, we find that:

$$\sum_j \left(p_{j,\mu} \frac{\partial}{\partial p_j^\nu} - p_{j,\nu} \frac{\partial}{\partial p_j^\mu} \right) \mathcal{I}(p_i) = 0. \quad (2.21)$$

In order to build up scalar relations eq. (2.21) can be multiplied with any antisymmetric combination of the external momenta $p_n^\mu p_m^\nu$.

As exemplification let us consider the two cases of the three- and four-point functions. The former depend on two independent external momenta, say p_1 and p_2 , so that only one LI can be build up, namely:

$$(p_1^\mu p_2^\nu - p_1^\nu p_2^\mu) \sum_{j=1}^2 \left(p_{j,\mu} \frac{\partial}{\partial p_j^\nu} - p_{j,\nu} \frac{\partial}{\partial p_j^\mu} \right) \mathcal{I}(p_1, p_2) = 0. \quad (2.22)$$

Four-point functions can depend instead on three independent momenta, p_1 , p_2 and p_3 , so that three different LIs can be established:

$$(p_1^\mu p_2^\nu - p_1^\nu p_2^\mu) \sum_{j=1}^3 \left(p_{j,\mu} \frac{\partial}{\partial p_j^\nu} - p_{j,\nu} \frac{\partial}{\partial p_j^\mu} \right) \mathcal{I}(p_1, p_2, p_3) = 0, \quad (2.23)$$

$$(p_1^\mu p_3^\nu - p_1^\nu p_3^\mu) \sum_{j=1}^3 \left(p_{j,\mu} \frac{\partial}{\partial p_j^\nu} - p_{j,\nu} \frac{\partial}{\partial p_j^\mu} \right) \mathcal{I}(p_1, p_2, p_3) = 0, \quad (2.24)$$

$$(p_2^\mu p_3^\nu - p_2^\nu p_3^\mu) \sum_{j=1}^3 \left(p_{j,\mu} \frac{\partial}{\partial p_j^\nu} - p_{j,\nu} \frac{\partial}{\partial p_j^\mu} \right) \mathcal{I}(p_1, p_2, p_3) = 0. \quad (2.25)$$

It has been recently proven [41] that LIs are not linear independent from IBPs, as they can be reproduced generating and solving larger systems of IBPs. If this implies that, in order to ensure a complete reduction to a minimal set of MIs, LIs are not strictly required, one finds that reproducing them with the IBPs would be computationally much more expensive. LIs are therefore still extensively used in all public and private codes for automated reduction to MIs in order to speed up the solution of the system of IBPs.

2.2.3 Symmetry relations

Often one further class of relations, valid for any value of the dimensions d , must be taken into account in order to ensure a complete reduction to a minimal set of MIs, the so-called *symmetry relations*. The latter can be established among integrals inside the same topology or even among integrals belonging to different topologies, whenever it is possible to perform a shift of the loop momenta which does not change the value of the *integral* (i.e. which has Jacobian equal to 1), while it transforms the *integrand* into a linear combination of *different integrands*.

We refer to those symmetry relations which map a sector onto itself as *sector symmetries*. These are particularly important in order to ensure that a *minimal* number of MIs for a given sector is identified. Implementing symmetry relations in a fully automated way is a very non-trivial task and only recently this has been successfully accomplished in the public code Reduze 2 [42]. The code uses a mixed approach between a combinatorial matcher and graph and matroid theory in order to find all possible shifts among integrals in the same or in different sectors.

2.2.4 The Laporta Algorithm

In the sections above we showed how, mainly exploiting the properties of dimensionally regularised Feynman integrals, large sets of identities can be derived among the latter. As a result not all integrals are independent from each other and by inverting these relations most of them can be ultimately re-expressed as linear combinations of a small subset of basic integrals.

The identities discussed above are by definition linear identities among the integrals with rational coefficients which can depend only on the dimensions d and on the external invariants of the problem. At a first glance, therefore, their solution should not present any conceptual difficulties. In practical application, nevertheless, the number of such equations can grow up to tens or hundreds of thousands (sometimes even millions), requiring the use of computer algebra in order to handle the complexity of the resulting expressions. Moreover, even using computer algebra, the inversion of such huge linear systems can be very cumbersome due to the largeness of the intermediate expressions. In this respect two subtle points deserve to be discussed:

1. First of all, as it is well known, while the number of MIs is fixed, we are still free to choose as masters any subset of integrals which are linearly independent in the sense of IBPs, LIs and SRs. Changing the basis of integrals can influence substantially the largeness of the reduction identities. A “good choice” of MIs is then very desirable in order to make as simple as possible the final result. We will come on the issue of finding a good basis in Section 3.3.2.
2. Assuming to neglect the (not entirely well defined) problem of selecting a good basis, we are left with the more practical problem of solving the system of

IBPs, LIs and SRs. The system contains typically many more equations than unknown, and therefore a lot of redundancy. This means that, typically, more equations, apparently different from each other, are linear dependent from each other. Moreover, once the basis has been determined, the order in which the equations are chosen and solved in order to express all integrals in terms of this basis is not unique. It is indeed well known that, while every ordering must produce the same final result, the complexity of the intermediate expressions is strongly dependent on this choice. Whenever dealing with problems with a large number of independent scales, where the intermediate expressions can very easily blow up, it is thus extremely important to find a set of criteria which might help select an ordering for the solution of the equations in the system.

The **Laporta Algorithm** [40, 43] suggests a series of criteria which should be used in order to choose at each step of the solution which equation should be inverted first and in this way try and limit the growth of the intermediate expressions. The algorithm is straightforward to implement in a computer algebra system, and in the last years many public and private implementation have become available, making the reduction to MIs a conceptually solved issue [42–46], provided obviously that enough computational resources are at disposal.

2.2.5 Schouten pseudo-identities (SIs)

Very recently [37] a new class of identities among integrals in a given sector has been proposed. These identities have been dubbed *Schouten pseudo-identities*. The name *pseudo-identities* was introduced in order to stress the fact that these identities are strictly true only in a fixed, integer number of dimensions, in contrast to IBPs, LIs and sector symmetries, which are true for continuous d .

As it is well known, in any integer number of dimensions $d = n$ one cannot have more than n linearly independent vectors. In order to see how this piece of information can be used in connection to the reduction to MIs, let us start off considering some explicit cases. Let us consider 2 linearly independent vectors a_μ, b_μ in $d = 2$ dimensions. Consider now the quantity

$$\epsilon(a, b) = \epsilon_{\mu\nu} a^\mu b^\nu, \quad (2.26)$$

where $\epsilon_{\mu\nu}$ is the Levi-Civita tensor with two indices, with $\epsilon_{11} = \epsilon_{22} = 0$ and $\epsilon_{12} = -\epsilon_{21} = 1$. By squaring eq.(2.26) we get at once

$$\epsilon^2(a, b) = a^2 b^2 - (a \cdot b)^2. \quad (2.27)$$

So far all quantities are defined strictly in $d = 2$ dimensions. As it is obvious by its very definition, if the dimension d takes any *non-vanishing* integer value smaller than 2, the r.h.s of equation (2.26) vanishes, and so does the r.h.s of (2.27). We proceed then defining the *Schouten polynomial* $P_2(d; a, b)$ as

$$P_2(d; a, b) = a^2 b^2 - (a \cdot b)^2, \quad (2.28)$$

where now all quantities are assumed to be defined in d -continuous dimensions. By its very definition the Schouten polynomial P_2 vanishes for $d < 2$:

$$P_2(1; a, b) = 0.$$

Following the very same procedure, given any triplet of vectors a^μ, b^μ, c^μ defined in $d = 3$ dimensions, we consider the quantity

$$\epsilon(a, b, c) = \epsilon_{\mu\nu\rho} a^\mu b^\nu c^\rho, \quad \text{with } \epsilon_{123} = 1, \quad (2.29)$$

and evaluate its square as

$$\epsilon(a, b, c)^2 = a^2 b^2 c^2 - a^2 (b \cdot c)^2 - b^2 (a \cdot c)^2 - c^2 (a \cdot b)^2 + 2(a \cdot b)(b \cdot c)(a \cdot c), \quad (2.30)$$

where, again, all quantities are to be thought for the moment strictly in $d = 3$ dimensions. We proceed then by defining the Schouten polynomial $P_3(d; a, b, c)$ as:

$$P_3(d; a, b, c) = a^2 b^2 c^2 - a^2 (b \cdot c)^2 - b^2 (a \cdot c)^2 - c^2 (a \cdot b)^2 + 2(a \cdot b)(b \cdot c)(a \cdot c), \quad (2.31)$$

where now the three vectors a^μ, b^μ, c^μ are to be interpreted as d -dimensional vectors. By construction, $P_3(d; a, b, c)$ vanishes at $d = 1$ and $d = 2$ dimensions

$$P_3(1; a, b, c) = P_3(2; a, b, c) = 0. \quad (2.32)$$

Needless to say, the procedure can be easily iterated in any integer number of dimensions n , generating Schouten polynomials vanishing in $d = 1, \dots, n - 1$ dimensions, provided that one has n independent vectors to start with. We note, in passing, that the Schouten polynomial generated by a given set of vectors is nothing by their *Gram determinant*.

Obviously in physical applications we are interested mainly in the $d \rightarrow 4$ limit. In this sense one would naively expect that the only relevant Schouten polynomials are those which vanish in $d = 1, 2, 3, 4$ dimensions, and so built up starting from 5 different vectors. This would indeed limit the range of applicability of such identities to only those Feynman diagrams which depend on 5 or more vectors. Nevertheless, by means of the so-called Tarasov-Lee shifting relations [47, 48], one can reach $d = 4$ from any different, even value of d , as they relate the values of Feynman graphs for numbers of dimensions d differing by *two units*. In this sense the $d = 1$ Schouten polynomials (2.28), easily established for any Feynman amplitude in which at least 2 vectors occur, are of no practical use. The next simplest example are the Schouten polynomials in $d = 2$ (2.31), which can in turn be built up for any Feynman amplitude with at least 3 independent vectors.

Once the Schouten-polynomials have been built, they can be at least in principle used in order to determine the number of independent MIs in a given number of

integer dimensions. Let us consider a given topology with n propagators, so that any integral belonging to such topology will be written as:

$$\mathcal{I}(b_1, \dots, b_n) = \int \prod_{j=1}^l \mathfrak{D}^{k_j} \frac{1}{D_1^{b_1} \dots D_n^{b_n}}.$$

Let us consider now the following quantity

$$Z(d; b_1, \dots, b_n) = \int \prod_{j=1}^l \mathfrak{D}^{k_j} \frac{P_a(k_1, \dots, k_l; p_1, \dots, p_{N-1})}{D_1^{b_1} \dots D_n^{b_n}}, \quad (2.33)$$

where $P_a(k_1, \dots, k_l; p_1, \dots, p_{N-1})$ is a Schouten-polynomial built out of some of the loop momenta and the external momenta of the graph that we are considering, such that

$$\lim_{d \rightarrow m} P_a(k_1, \dots, k_l; p_1, \dots, p_{N-1}) \rightarrow 0, \quad \text{for any } m \in \mathbb{N}, \quad m < a.$$

Note that in (2.33) we wrote explicitly the dependence on the number of dimensions d . Assuming now that there exists one or more choices of powers of the denominators b_1, \dots, b_n such that the integral in (2.33) is convergent as $d \rightarrow m$, we get at once

$$\lim_{d \rightarrow m} Z(d; b_1, \dots, b_n) \rightarrow 0. \quad (2.34)$$

On the other hand, from its very definition (2.33), keeping the full dependence from the dimensions d , the Schouten polynomial at the numerator of $Z(d; b_1, \dots, b_n)$ can be expanded and the resulting integrals can be reduced to the *conventional* MIs through the use of the Laporta Algorithm described above. Assuming that the graph under consideration can be reduced to N MIs $M_j(d; x_k)$, one gets in general:

$$Z(d; b_1, \dots, b_n) = \sum_{j=1}^N C_j(d; x_k) M_j(d; x_k), \quad (2.35)$$

where the x_k are the external invariants on which the integrals depend, and the coefficients $C_j(d; x_k)$ are rational functions of the dimensional parameter d and of the x_k . If no divergences are present in the limit $d \rightarrow m$, using (2.34) and (2.35) we get at once

$$0 = \lim_{d \rightarrow m} \left(\sum_{j=1}^N C_j(d; x_k) M_j(d; x_k) \right), \quad (2.36)$$

which gives precisely a relation among the MIs as $d \rightarrow m$. We stress here once more that the whole procedure is well defined as long as all quantities in the equations

above are finite as $d \rightarrow m$. This can always be straightforwardly achieved if only UV divergences are present by raising suitably the powers of the denominators. A generalisation of this procedure to the case of presence of IR divergences is presently under study. The applications of the Schouten pseudo-identities to the specific case of the two-loop massive sunrise will be discussed in Chapter 5.

Chapter 3

Master Integrals

3.1 Preliminaries

In the previous chapter we saw how, following a by now standard procedure, given a scattering amplitude at a certain order in perturbation theory, this can be reduced to a linear combination of a small sub-set of scalar integrals dubbed *Master Integrals*. The (*quite non-trivial*) issue that remains to be faced is their computation.

Two different (and in some sense *complementary*) approaches have been extensively pursued in the context of Feynman integrals evaluation, namely on one side a “standard” *analytical* approach, and on the other a fully *numerical* one. Clearly, since integration is a very non-trivial operation, developing a fully numerical approach might look very appealing. Nevertheless, given the fact that Feynman integrals are often divergent as the number of dimensions d approaches the physical value $d = 4$, in order to have flexible and reliable numerical algorithms these divergences have to be automatically and consistently taken into account and regularised, before the actual integration can be performed. Such procedure is not impossible in principle (see for example the *Sector Decomposition algorithm* [49–51]) and promising results have already been achieved in this direction [52]. In any case this remains far from trivial and moreover it is very difficult to get *fast* and *precise* results on the whole phase-space, especially when considering *very exclusive observables*. Particularly non-trivial is also the numerical treatment of endpoint singularities, which in the case of non-planar massless Feynman Integrals can become so serious to make a numerical approach, even via sector decomposition, not applicable¹.

An analytical approach has instead the advantage of giving much stronger control on the final result. In regard to this it is worth mentioning that the very definition of “*analytic result*” implies that, in principle, one can evaluate it numerically with high precision in a negligible amount of time. Multiloop integrals typically cannot

¹See for example the case of the massless crossed double-box with all on-shell massless legs [53,54]. The sector decomposition algorithm succeeds in isolating all UV and IR poles but the presence of endpoint singularities due to the on-shell constraint $s + t + u = 0$ makes the numerical integration of the coefficients highly unstable.

be expressed as combinations of so-called elementary functions (rational functions, logarithms, trigonometric functions and their inverse); therefore computing them analytically means expressing them in terms of *special functions* whose analytical and algebraic properties are well understood and which can be numerically evaluated by fast-converging series expansions. And it is precisely in the study and classification of these special functions that the last 20 years saw very promising developments.

In what follows we will first focus on introducing the properties of some of the special functions which appear more often in the computation of Feynman Integrals, switching afterwards our attention to the methods that have been simultaneously developed in order to carry out explicitly such integrals. We will see how the effectiveness of such methods (in particular of the differential equations method) relies mainly on the simple algebraic properties of a class of special functions, the Multiple Polylogarithms, which can be used to represent analytically a wide set of multiloop Feynman Integrals.

3.2 Special Functions in Particle Physics

Since the dawning of particle physics it became soon clear that a particular class of functions has a special role in the evaluation of Feynman diagrams, the *Polylogarithms* and their recent generalisations, which we will refer generally to as *Multiple Polylogarithms* (MPLs). The latter are defined as repeated integrations over *linear* rational functions and can in principle depend on an arbitrary number of additional independent variables. The first appearance of functions of this type in the mathematical literature can be traced back to a series of articles published by E.E. Kummer in 1840 [55]. Similar functions have been studied later on under the name of *Hyperlogarithms* by Poincaré, who generalised them allowing dependence on different variables. Recently they have been receiving renewed interest in the mathematical literature, see for example [56], where they are by now commonly referred to as *Multiple Polylogarithms*.

From the viewpoint of particle physicists, it has been known for a long time that the evaluation of the finite piece in $d = 4$ of one-loop Feynman Integrals requires the introduction of the *Euler dilogarithm* $\text{Li}_2(x)$ and of its generalisation, the *Nielsen Polylogarithms* [57]. When going higher with the perturbative order, nevertheless, Nielsen polylogarithms are not sufficient and a further generalisation has to be considered. It was in fact precisely in the context of two- and three-loop calculations in QFT that a sub-class of the Hyperlogarithms, depending on one single variable, was “re-discovered” by particle physicists and dubbed *Harmonic Polylogarithms* (HPLs) [58]. The “discovery” of the HPLs, and their subsequent generalisation to multiscale problems under the name of *2-dimensional HPLs* (2d-HPLs) first [59], and *Generalised Harmonic Polylogarithms* (GHPLs) afterwards, was the beginning of an epoch of almost 20 years of explosive development in the understanding of multiloop computations. In particular it was the unveiling of the algebraic properties satisfied by these

functions [56, 58–65], together with the development of very precise routines for their numerical evaluation on the whole complex plane [66–71], which worked as a boost in the computation of multiloop virtual corrections to multiscale problems. This, together with the almost contemporary establishment of fast and reliable subtraction methods for the numerical evaluation of differential distributions (see Section 1.2.3), contributed to bring effectively NNLO QCD corrections for $2 \rightarrow 2$ processes finally within reach. We will summarise the definitions and some of the most relevant properties of these functions in the next Section 3.2.1, referring to the literature on the subject for a more complete introduction.

In spite of the (in some sense even *surprisingly*) wide range of applicability of multiple-polylogarithmic functions in the computation of multiloop and multiscale Feynman Integrals, it is well known that already at the two-loop level these functions are not sufficient and new mathematical structures appear, in particular when considering Feynman graphs with internal masses. The first (and probably most famous) example studied in the literature is that of the two-loop massive sunrise graph, whose analytical structure is known to contain *integrals over elliptic integrals* [37, 72–80]. Very recently it has been shown that the finite piece of the sunrise graph in $d = 2$ can be written in terms of the newly introduced *elliptic dilogarithms* [80, 81]. While for the case of the two-loop massive sunrise the appearance of these functions is well understood in terms of the presence of a massive three-particle cut (see Section 3.2.2), this is not always the case. For example, the two-loop crossed ladder vertex diagram with two massive exchanges [82] does not have any massive three-particle cut, but is nevertheless known to evaluate to integrals over elliptic integrals. The nature of the specific combinations of elliptic functions relevant in Feynman diagrams computation is still largely unknown and matter of research. For this reason we will only briefly comment in Section 3.2.2 on a specific sub-class of such functions, the *complete elliptic integrals*, elucidating their connection with the computation of the massive three-body phase space. We will discuss later on in detail how this can be connected to the imaginary part of the two-loop massive sunrise graph, see Chapter 5.

3.2.1 Special functions 1. Multiple Polylogarithms - MPLs

In the present section we will give a very elementary introduction to Multiple Polylogarithms, trying to stress how they are very naturally defined as repeated integrals over *linear rational functions*. The literature on the subject is extremely vast, and we do not aim here to completeness. MPLs can be equivalently defined as infinite series, as well as iterated integrals, and many slightly different notations are adopted both in the mathematics and physics literature. For a thorough account of all aspects and properties of Multiple Polylogarithms we refer to the review by Vollinga and Weinzierl [68].

MPLs are a particular case of *Chen Iterated integrals* [31] and as such can be defined consistently from their integral representation. In order to elucidate this

structure let us start off by considering the definition of the logarithm:

$$\ln(x) = \int_1^x \frac{dt}{t}, \quad \ln\left(1 - \frac{x}{a}\right) = \int_0^x \frac{dt}{t-a}, \quad \text{with } x < a, a \neq 0, \quad (3.1)$$

where in particular we can define for $a = 1$

$$\ln(1-x) = \int_0^x \frac{dt}{t-1}, \quad \text{with } x < 1.$$

As a first generalisation of the logarithm let us consider now the *Euler Dilogarithm* (or Spence's function) $\text{Li}_2(x)$:

$$\text{Li}_2(x) = - \int_0^x \frac{dt}{t} \log(1-t) = \sum_{n=1}^{\infty} \frac{x^n}{n^2}, \quad \forall x \in \mathbb{C} \setminus [1, \infty). \quad (3.2)$$

From its very integral representation it is clear that the $\text{Li}_2(x)$ is nothing but an iterated integral over two rational kernels:

$$\text{Li}_2(x) = - \int_0^x \frac{dt}{t} \int_0^t \frac{du}{u-1}.$$

Iterating this definition an arbitrary number of times we obtain to the so-called *classical-polylogarithms* [83]:

$$\begin{aligned} \text{Li}_{n+1}(x) &= \int_0^x \frac{dt}{t} \text{Li}_n(t), \quad \forall x \in \mathbb{C} \setminus [1, \infty) \\ \text{Li}_1(x) &= -\log(1-x). \end{aligned} \quad (3.3)$$

To summarise, the Li_n are defined through a first integration over the kernel $1/(t-1)$, followed by repeated integrations over the same kernel $1/t$. The index n is called *weight* of the polylogarithm and its value corresponds to the number of integrations needed to define the corresponding function. This apparently “harmless” definition has nevertheless the property of breaking the (to some extent) *natural* symmetry among the two kernels, namely the kernel $1/(t-1)$ contributes only to the first integration, while the second kernel $1/t$ participates in all the subsequent ones. The natural way to restore (and actually enlarge) this symmetry is by extending this definition and allowing the symmetrical integration over all three possible kernels $1/t$, $1/(t-1)$ and $1/(t+1)$.

We can start off by defining the three functions of *weight* 1:

$$G(0; x) = \ln(x), \quad G(1; x) = \int_0^x \frac{dt}{t-1}, \quad G(-1; x) = \int_0^x \frac{dt}{t+1}, \quad (3.4)$$

where obviously

$$G(1; x) = \ln(1-x), \quad G(-1, x) = \ln(1+x).$$

We can then define iteratively the functions of higher weights as:

$$G(\vec{0}_n; x) = \frac{1}{n!} \ln(x)^n, \quad \text{with} \quad \vec{0}_n = \underbrace{\{0, \dots, 0\}}_n, \quad (3.5)$$

and

$$G(a, \vec{n}; x) = \int_0^x \frac{dt}{t-a} G(\vec{n}; t), \quad \text{with} \quad a = \{0, 1, -1\}, \quad (3.6)$$

where the vector \vec{n} has entries also drawn from the set $\{0, 1, -1\}$. Equations (3.4, 3.6) define the *Harmonic Polylogarithms* (HPLs).

We note here, in passing, the the HPLs defined above, due to the symmetrical choice of the integration kernels, form a closed set under the transformations [58]:

$$x \rightarrow -x, \quad x \rightarrow \frac{1}{x}, \quad x \rightarrow \frac{1-x}{1+x}. \quad (3.7)$$

From their very definition the HPLs depend on one single variable x and as such they are very well suited to describe two-scale Feynman integrals. These are in fact *homogeneous functions* of the external invariants and therefore can only depend on one dimensionless ratio between the two. Examples of such Feynman integrals are, among the others, the one-loop massive sunrise with equal masses, the QED one- and two-loop form factor, the two-loop massless 4-point functions with all external legs on-shell, and many others.

When considering multiscale problems, nevertheless, we cannot expect HPLs to be enough, since such integrals depend in general on two or more genuinely independent dimensionless ratios. It was in particular in the context of the computation of the two-loop master integrals for 3-jet production at LEP that such generalisation was for the first time taken into account with the introduction of the so-called 2d-HPLs [59, 84]. These functions have been further generalised allowing the dependence on, at least in principle, an arbitrary number of different scales, and are equivalent to the MPLs already known in the mathematical literature. Their definition can be given iteratively in the same way as for the HPLs starting at weight 1 with:

$$G(0; x) = \ln(x), \quad G(a; x) = \int_0^x \frac{dt}{t-a} = \ln\left(1 - \frac{x}{a}\right), \quad \text{with} \quad a \neq 0, \quad (3.8)$$

and then for higher weights:

$$G(\vec{0}_n; x) = \frac{1}{n!} \ln(x)^n, \quad \text{with} \quad \vec{0}_n = \underbrace{\{0, \dots, 0\}}_n, \quad (3.9)$$

$$G(a, \vec{n}; x) = \int_0^x \frac{dt}{t-a} G(\vec{n}; t), \quad (3.10)$$

with no restriction on the values of a , which can in turn be functions of the other external invariants.

Main properties of the MPLs

The MPLs defined in (3.8) and (3.10) fulfil different fundamental properties, which we briefly summarise here.

- Iterated integrals form a *shuffle algebra*. This allows one to express the product of two MPLs of weight n and m as a linear combination of MPLs of weight $n+m$. In particular given 2 MPLs of weight respectively n and m , one finds:

$$G(a_1, \dots, a_n; x) G(a_{n+1}, \dots, a_{n+m}; x) = \sum_{\sigma \in \Sigma(n, m)} G(a_{\sigma(1)}, \dots, a_{\sigma(n+m)}; x), \quad (3.11)$$

where $\Sigma(n, m)$ denotes the set of all *riffle shuffles* of the two sets of n and m indices, i.e. all shuffles which preserve the relative order of the elements in the two sets.

- Given any $G(\vec{a}; x) = G(a_1, \dots, a_n; x)$, if its rightmost index $a_n \neq 0$ then it is invariant under a rescaling of all its arguments, i.e. given any $z \in \mathbb{C}^*$:

$$G(a_1, \dots, a_n; x) = G(z a_1, \dots, z a_n; z x). \quad (3.12)$$

- Moreover, given $G(\vec{a}; x) = G(a_1, \dots, a_n; x)$ with $a_1 \neq 0$ and $a_n \neq 0$, it also satisfies the so-called *Hölder convolution*, i.e. given any $p \in \mathbb{C}^*$

$$G(a_1, \dots, a_n; 1) = \sum_{k=0}^n (-1)^k G\left(1 - a_k, \dots, 1 - a_1; 1 - \frac{1}{p}\right) G\left(a_{k+1}, \dots, a_n; \frac{1}{p}\right), \quad (3.13)$$

which in the limit $p \rightarrow \infty$ becomes:

$$G(a_1, \dots, a_n; 1) = (-1)^n G(1 - a_n, \dots, 1 - a_1; 1). \quad (3.14)$$

- As a last comment, it is useful to notice that the cut structure of the MPLs is entirely contained in their indices, in particular the function $G(\vec{a}; x) = G(a_1, \dots, a_n; x)$ can develop an imaginary part if and only if the argument x becomes larger than any of the indices a_j , i.e. if $\exists j$ such that $x > a_j$.

One point deserves to be stressed here. As already discussed, MPLs are defined as repeated integrals over linear rational functions. This fundamental property allows one to systematically derive functional identities among polylogarithms (for example *transformations of arguments, limiting values, series expansions* and so on) by simple repeated integrations by parts on their integral representations. Polylogarithms, in fact, by construction, have a very simple behaviour under differentiation with respect to their argument; namely, given an MPL of weight $n > 0$, with one differentiation one obtains a combination of MPLs of weight $n - 1$. Iterating this operation a sufficient number of times one can reduce any MPL to rational functions, whose transformation relations can be obtained algebraically in a straightforward manner.

The symbol-map and the coproduct for MPLs

This in principle simple procedure has been recently systematised by the use of the so-called *symbol-map*, a linear map which associates to every multiple polylogarithm of weight n an element in the n -fold tensor power of a given vector space of one-forms (for further details see [64] and references therein). The symbol-map can be defined recursively by considering iterated differentials of multiple polylogarithms, but can also be directly read off from all possible “triangulations” of particular decorated polygons associated to the MPLs. We refer again in particular to [64] for more details on this derivation.

The main advantage of the symbol-map is that, while still being a very simple linear map, it captures many of the analytical properties of MPLs. It is conjectured in particular that all functional relations among MPLs correspond to relations among their symbols, so that necessary condition for two expressions written in terms of MPLs to be equal, is that their symbols must be equal. On the other hand much more difficult is the so-called *inverse problem* (often also referred to as the issue of the *integration of a symbol*); namely given a tensor in this vector space of one-forms, how to find a function whose symbol matches it. A possible construction of such functions is described in detail in [64].

Even more recently a further step in this direction has been made with the introduction of the *coproduct formalism* [65]. Multiple polylogarithms equipped with the shuffle product form in fact a *Hopf algebra* graded by weight. Given such an algebra, a concept of coproduct can be defined, which has been proven to be compatible with the algebra structure of the multiple polylogarithms [62]. The coproduct has the advantage, with respect to the symbol formalism, to retain information about the ζ values, allowing to simplify substantially the *inverse problem* quoted above. We will not elaborate further on this, referring to the literature and in particular to [85, 86] for a detailed description of how such formalism can be used in order to simplify the computation of Feynman diagrams. It is nevertheless important to stress that the use of a coproduct augmented symbol formalism, in association with the numerical routines provided in [68], has allowed to handle in the last years (in an almost completely automated way) the computation of large numbers of Feynman diagrams which evaluate to multiple polylogarithms only, see for example [86–91].

3.2.2 Special functions 2. Elliptic integrals in particle physics

Unfortunately not all multiloop Feynman integrals can be expressed in terms of MPLs only. It is very well known that whenever a (at least two-scale) Feynman integral contains a massive three-particle cut, then its imaginary part will possibly contain *complete elliptic integrals*. Elliptic integrals and their inverse, i.e. the *Jacobi elliptic functions*, have been studied thoroughly in the mathematical literature and many results have been known for a long time. Nevertheless, at the present day, it is not yet clear which role elliptic functions play in the calculation of Feynman

diagrams. For this reason we will not embark here on a comprehensive review on elliptic functions and their properties, which would anyway be outside the scope of this thesis. On the other hand, since some of the properties of (in particular) complete elliptic integrals will be used extensively in what follows when studying the imaginary part of the two-loop massive sunrise graph, we will anyway include here some basic definitions and properties which will be useful later on.

One the first places where elliptic integrals make their appearance in physics is in the computation of the three-particle massive phase space, which, as we will see in Chapter 5, is equivalent to the computation of the imaginary part of the two-loop massive sunrise. Let us start off considering a system of three massive particles with masses m_1 , m_2 and m_3 , and total energy $\sqrt{s} = W$. The three-body phase-space in d space-time dimensions factors into two two-body phase spaces and if $W > (m_1 + m_2 + m_3)$ (i.e. above threshold) it can be written as follows:

$$\begin{aligned}\Phi_3(d; s, m_1^2, m_2^2, m_3^2) &= \int_{(m_2+m_3)^2}^{(\sqrt{s}-m_1)^2} db \Phi_2(d; s, b, m_1^2) \Phi_2(d; b, m_2^2, m_3^2) \\ &= C^2(d) \int_{(m_2+m_3)^2}^{(\sqrt{s}-m_1)^2} db \frac{1}{\sqrt{R_2(s, b, m_1^2)} \sqrt{R_2(b, m_2^2, m_3^2)}} \\ &\quad \times \left(\frac{R_2(s, b, m_1^2)}{s} \frac{R_2(b, m_2^2, m_3^2)}{b} \right)^{(d-2)/2},\end{aligned}\quad (3.15)$$

where we introduced the usual Källen function:

$$R_2(a, b, c) = a^2 + b^2 + c^2 - 2ab - 2ac - 2bc,$$

and $C(d)$ is a constant which depends only on the dimensions d and whose explicit value is not important in what follows.

Evaluating now the phase-space in $d = 4$ space-time dimensions we find (up to an overall normalisation)

$$\Phi_3(4; s, m_1^2, m_2^2, m_3^2) \propto \int_{b_2}^{b_3} db \frac{\sqrt{R_4(b; b_1, b_2, b_3, b_4)}}{b},$$

where

$$\begin{aligned}R_4(b; b_1, b_2, b_3, b_4) &= (b - b_1)(b - b_2)(b_3 - b)(b_4 - b) \\ &= R_2(s, b, m_1^2) R_2(b, m_2^2, m_3^2)\end{aligned}$$

and we introduced the notation:

$$(m_2 - m_3)^2 = b_1 \leq (m_2 + m_3)^2 = b_2 \leq (W - m_1)^2 = b_3 \leq (W + m_1)^2 = b_4. \quad (3.16)$$

Let us define now the following integrals

$$I(n, W) = \int_{b_2}^{b_3} db \frac{b^n}{\sqrt{R_4(b; b_1, b_2, b_3, b_4)}}. \quad (3.17)$$

One has obviously that

$$\int_{b_2}^{b_3} db \frac{d}{db} \left[b^n \sqrt{R_4(b; b_1, b_2, b_3, b_4)} \right] = 0 .$$

By working out the derivative, one gets an identity involving up to five integrals of the type $I(n, W)$ with different values of n :

$$\begin{aligned} 0 = & 2(n+2) I(n+3, W) - (2n+3)(b_1 + b_2 + b_3 + b_4) I(n+2, W) \\ & + 2(n+1) [b_1(b_2 + b_3 + b_4) + b_2(b_3 + b_4) + b_3 b_4] I(n+1, W) \\ & - (2n+1) [b_1 b_2(b_3 + b_4) + b_3 b_4(b_1 + b_2)] I(n, W) \\ & + (2n) b_1 b_2 b_3 b_4 I(n-1, W). \end{aligned}$$

In this way all integrals needed for the evaluation of the three-body massive phase-space can be expressed as combination of only four *master integrals*, which can be chosen to be:

$$\begin{aligned} I(-1, W) &= \int_{b_2}^{b_3} \frac{db}{b \sqrt{R_4(b; b_1, b_2, b_3, b_4)}}, \\ I(0, W) &= \int_{b_2}^{b_3} \frac{db}{\sqrt{R_4(b; b_1, b_2, b_3, b_4)}}, \\ I(1, W) &= \int_{b_2}^{b_3} \frac{db b}{\sqrt{R_4(b; b_1, b_2, b_3, b_4)}}, \\ I(2, W) &= \int_{b_2}^{b_3} \frac{db b^2}{\sqrt{R_4(b; b_1, b_2, b_3, b_4)}}. \end{aligned} \tag{3.18}$$

In the same way, starting for instance from

$$\int_{b_2}^{b_3} db \frac{d}{db} \left[\frac{1}{b-b_1} \sqrt{R_4(b; b_1, b_2, b_3, b_4)} \right] = 0 ,$$

one finds

$$\begin{aligned} \int_{b_2}^{b_3} \frac{db}{(b-b_1) \sqrt{R_4(b; b_1, b_2, b_3, b_4)}} &= \frac{1}{(b_2-b_1)(b_3-b_1)(b_4-b_1)} \\ &\times [b_1(b_1-b_2-b_3-b_4)I(0, W) + (b_1+b_2+b_3+b_4)I(1, W) - 2I(2, W)] . \end{aligned} \tag{3.19}$$

The four integrals above $I(n, W)$, with $n = -1, 0, 1, 2$, are an equivalent representation of the usual *complete elliptic integrals* $K(w^2)$, $E(w^2)$, $\Pi(a; w^2)$ of first, second and third kind, namely:

$$K(w^2) = \int_0^1 \frac{dx}{\sqrt{(1-x^2)(1-w^2 x^2)}}, \quad 0 < w^2 < 1, \tag{3.20}$$

$$E(w^2) = \int_0^1 dx \sqrt{\frac{1-w^2x^2}{1-x^2}}, \quad 0 < w^2 < 1, \quad (3.21)$$

$$\Pi(a; w^2) = \int_0^1 \frac{dx}{\sqrt{(1-x^2)(1-w^2x^2)}(1-ax^2)}, \quad 0 < w^2, a < 1. \quad (3.22)$$

Indeed, the standard change of variables

$$b = \frac{b_1(b_3 - b_2)x^2 - b_2(b_3 - b_1)}{(b_3 - b_2)x^2 - (b_3 - b_1)}, \quad x^2 = \frac{(b_3 - b_1)(b - b_2)}{(b_3 - b_2)(b - b_1)}, \quad (3.23)$$

gives

$$\begin{aligned} I(-1, W) &= \frac{2}{\sqrt{(b_3 - b_1)(b_4 - b_2)}} \frac{1}{b_1 b_2} [b_2 K(w^2) - (b_2 - b_1) \Pi(a_2, w^2)], \\ I(0, W) &= \frac{2}{\sqrt{(b_3 - b_1)(b_4 - b_2)}} K(w^2), \\ I(1, W) &= \frac{2}{\sqrt{(b_3 - b_1)(b_4 - b_2)}} [b_1 K(w^2) + (b_2 - b_1) \Pi(a_1, w^2)], \\ I(2, W) &= \frac{2}{\sqrt{(b_3 - b_1)(b_4 - b_2)}} [(b_1^2 + b_1(b_2 + b_3) - b_2 b_3) K(w^2) \\ &\quad - (b_3 - b_1)(b_4 - b_2) E(w^2) \\ &\quad + (b_2 - b_1)(b_1 + b_2 + b_3 + b_4) \Pi(a_1, w^2)], \end{aligned} \quad (3.24)$$

where

$$\begin{aligned} w^2 &= \frac{(b_4 - b_1)(b_3 - b_2)}{(b_4 - b_2)(b_3 - b_1)}, \\ a_1 &= \frac{(b_3 - b_2)}{(b_3 - b_1)}, \\ a_2 &= \frac{b_1(b_3 - b_2)}{b_2(b_3 - b_1)}. \end{aligned}$$

A standard result of the theory of complete elliptic integrals states that any integral of the form

$$\Pi(l_1, l_2, l_3; a; w^2) = \int_0^1 \frac{dx}{\sqrt{(1-x^2)^{l_1}(1-w^2x^2)^{l_2}(1-ax^2)^{l_3}}},$$

can, for any value of l_1, l_2, l_3 , be either completely reduced to elementary functions, or to a combination of elementary functions and of the three complete elliptic integrals $K(w^2)$, $E(w^2)$ and $\Pi(a, w^2)$. In this sense, in order to express the three-body phase space above, one can either use $I(-1, W)$, $I(0, W)$, $I(1, W)$, $I(2, W)$, or equivalently $E(w^2)$, $K(w^2)$, $\Pi(a_1, w^2)$, $\Pi(a_2, w^2)$.

Depending on the situation, it might be convenient to switch between these two representations, for example in order to derive functional relations among these functions in particular kinematical limits. As a first example, let us consider the case when one of the three masses becomes zero, for example $m_3 \rightarrow 0$. In this case one immediately sees that

$$b_1 = b_2 \rightarrow m_2^2, \quad \text{and} \quad w^2 = \frac{(b_4 - b_1)(b_3 - b_2)}{(b_4 - b_2)(b_3 - b_1)} \rightarrow 1,$$

and the complete elliptic integrals (3.20, 3.21, 3.22) become trivially logarithms and rational functions.

As a second example, let us discuss also the limit of equal masses $m_1 = m_2 = m_3 = m$. In this case it is more convenient to use the representation for the elliptic integrals through the $I(n, W)$. In terms of the previously introduced b_j in fact this limit gives

$$b_1 \rightarrow 0, \quad b_2 \rightarrow 4m^2, \quad b_3 \rightarrow (W - m)^2, \quad b_4 \rightarrow (W + m)^2.$$

Using these relations the variables on which the complete elliptic integrals depend become:

$$w^2 \rightarrow \frac{(W - 3m)(W + m)^3}{(W + 3m)(W - m)^3}, \quad a_1 \rightarrow 1 - \frac{4m^2}{(W - m)^2}, \quad a_2 \rightarrow 0,$$

which show that the function $\Pi(a_2, w^2)$ reduces to $K(w^2)$, leaving us with three independent functions. On the other hand, it is well known that in this limit only two functions are independent, and that in particular $\Pi(a_1, w^2)$ must reduce to a linear combination of $K(w^2)$ and $E(w^2)$.

In order to see this, let us go back to the integrals $I(n, W)$. In this limit, thanks to $b_1 = 0$ we can read equation (3.19) as an identity expressing $I(-1, W)$ in terms of $I(1, W)$, $I(2, W)$, reducing in this way the number of independent integrals to 3. Furthermore, in the equal-mass limit one finds [92]:

$$\int_{4m^2}^{(W-m)^2} db \frac{d}{db} \ln \left(\frac{b(W^2 + 3m^2 - b) + \sqrt{R_2(b, m^2, m^2)} \sqrt{R_2(s, b, m^2)}}{b(W^2 + 3m^2 - b) - \sqrt{R_2(b, m^2, m^2)} \sqrt{R_2(s, b, m^2)}} \right) = 0.$$

Working out the derivatives and expressing them in terms of the $I(n, W)$ one finds:

$$I(1, W) = \frac{1}{3}(W^2 + 3m^2) I(0, W), \quad (3.25)$$

showing, as expected, that in the equal-mass limit the three-body phase space can be expressed in terms of two independent functions only.

Rewriting this identity in terms of the standard elliptic integrals we find in particular the following identity:

$$\Pi(a_1, w^2) = \frac{(W^2 + 3m^2)}{12m^2} K(w^2). \quad (3.26)$$

Recalling that in this limit:

$$w^2 = \frac{(W - 3m)(W + m)^3}{(W + 3m)(W - m)^3} \quad a_1 = 1 - \frac{4m^2}{(W - m)^2},$$

and expressing W/m and w^2 in terms of a_1 one finds

$$\frac{W}{m} = 1 + \frac{2}{\sqrt{1 - a_1}}, \quad w^2 = \frac{a_1(1 + \sqrt{1 - a_1})}{1 + 2\sqrt{1 - a_1}}.$$

In this way (3.26) can be rewritten as:

$$\Pi \left(a_1, \frac{a_1(1 + \sqrt{1 - a_1})}{1 + 2\sqrt{1 - a_1}} \right) = \frac{2 - a_1 + \sqrt{1 - a_1}}{3(1 - a_1)} K \left(\frac{a_1(1 + \sqrt{1 - a_1})}{1 + 2\sqrt{1 - a_1}} \right), \quad (3.27)$$

which we could not find in this form in the literature.

3.3 Analytical computation of Master Integrals

After dimensional regularisation has been established as the preferred regularisation technique for Feynman diagrams computation, many diverse methods have been developed in order to attempt a direct, analytical calculation of dimensionally regularised Feynman Integrals. Most of these methods rely on the possibility of finding a suitable parametrisation of the integrand which allows to compute the integral by direct integration, for example using *Feynman parameters* or *Mellin-Barnes* representations. These methods have proven to be very powerful for one-loop integrals and even for various multiloop one- and two-scale problems (see for example the planar and some non-planar massless double-boxes with all external legs on-shell [53, 93]). Nevertheless, as the number of scales increases, attempting a direct integration via Feynman parametrisation (or Mellin Barnes) becomes more and more prohibitive. Very recently, nevertheless, promising developements in this direction have been achieved by exploiting Feynman parametrisation together with the criterion of *linear reducibility* [94], see for example [85]. These ideas have moreover been recently implemented into an open-source Maple code [95].

A particularly interesting alternative to a direct integration of Feynman integrals is the use of a mixed approach based on hyperspherical variables and dispersion relations [96, 97], which ultimately allowed the analytical computation of the 3-loop correction to the $g - 2$ of the electron in QED [40]. The idea is to make use of the unitarity properties of the S-matrix in order to write a dispersion relation for a given Feynman graph in terms of its imaginary part, whose computation is usually easier than that of the entire Feynman graph and can be attempted using Cutkosky-Veltman rule [98, 99].

In spite of the many successes of these methods, their main limitation relies in the difficulty of computing higher orders in the expansions of the Feynman graphs in

the dimensional regulator $\epsilon = (4 - d)/2$. As we shortly discussed previously, in fact, it often happens that, at every order in ϵ , a given Feynman integral can be expressed as particularly simple classes of functions, the previously introduced *MPLs*. This structure, nevertheless, when attempting a direct integration, remains often “hidden” under an apparently much more complicated multifold Mellin-Barnes representation or by many integrals over a large number of Feynman parameters. The breakthrough in this sense came with the method of the *differential equations for MIs* [35, 100, 101]. The method consists in using IBPs in order to derive *linear first order* differential equations in the external invariants satisfied by the master integrals.

As we will describe in the following sections, this method has two main advantages, which could be summarised as follows:

1. First of all the integration over the different d -dimensional loop momenta can be entirely by-passed and reduced to a one-dimensional integration in one variable (typically a dimensionless ratio of the external invariants), provided that we can somehow triangularise the system of differential equations.
2. The Laurent expansion in ϵ becomes completely trivial, since it can be carried out already at the level of the differential equations producing as a result a set of *chained differential equations* which can be easily studied in a bottom-up approach order by order in ϵ .

3.3.1 Differential Equations for MIs

The idea of approaching the computation of MIs by deriving and solving differential equations for the latter was first introduced by Kotikov [100], who nevertheless considered only the case of differential equations with respect to the internal masses. Later on the method was extended and generalised to differential equations in all external invariants by Remiddi [101], and by Gehrmann and Remiddi [35], effectively making it applicable to all MIs with only massless internal propagators. And it is precisely in the computation of MIs in massless theories that the method of differential equations showed its highest potential, making *de facto* possible the computation of (*massless*) two-loop QCD corrections to many $2 \rightarrow 2$ processes of wide phenomenological interest, like for example 3-jet production at LEP or vector-boson pair production at LHC.

To see how the method works let us consider a process with n external legs with momenta p_1, \dots, p_n . Obviously due to momentum conservation only $(n - 1)$ are really independent. At any loop-order, given Lorentz invariance, the scattering amplitude for such process can depend only on the $n(n - 1)/2$ different external invariants, i.e. the scalar products among the external momenta $s_{ij} = p_i \cdot p_j$. For the sake of simplicity let us introduce the following notation for the external invariants:

$$\vec{x} = (x_1, \dots, x_{n(n-1)/2}) = (s_{11}, \dots, s_{1(n-1)}, \dots, s_{(n-1)(n-1)}).$$

By using the chain-rule we can express the derivatives with respect to any of the external momenta as linear combinations of the derivatives with respect to the external invariants:

$$\frac{\partial}{\partial p_i^\mu} = \sum_j \frac{\partial x_j}{\partial p_i^\mu} \frac{\partial}{\partial x_j}. \quad (3.28)$$

The $(n-1)$ relations in (3.28) can be further contracted with any of the external momenta in order to get $(n-1)^2$ scalar equations:

$$p_l^\mu \frac{\partial}{\partial p_i^\mu} = p_l^\mu \sum_j \frac{\partial x_j}{\partial p_i^\mu} \frac{\partial}{\partial x_j}. \quad (3.29)$$

We can then invert the relations (3.29) in order to re-express the $n(n-1)/2$ derivatives in the external invariants as linear combinations of the derivatives in the external momenta. Obviously since

$$(n-1)^2 - \frac{n(n-1)}{2} = \frac{(n-1)(n-2)}{2} \geq 0, \quad \forall n \geq 2,$$

the system (3.29) is often over-constraint (i.e. there are more equations than unknowns) so that we can in principle express the derivatives in the external invariants as different (and apparently inconsistent) linear combinations of the derivatives in the external momenta. However the Lorentz Invariance identities, Section 2.2.2, provide us precisely with $(n-1)(n-2)/2$ relations among the derivatives with respect to the external momenta, once applied on scalar Feynman integrals. Using the LIs one can prove that these apparently different representation are indeed all equivalent to each other. Note that all these considerations are completely independent from the loop order we are considering, but only depend on the Lorentz invariance properties of the process. Once a choice has been made we end up with:

$$\frac{\partial}{\partial x_j} = \sum_{ik} A_{ik}^{(j)}(\vec{x}; \epsilon) p_l^\mu \frac{\partial}{\partial p_i^\mu}, \quad (3.30)$$

where the $A_{ik}^{(j)}(\vec{x}; \epsilon)$ are rational functions of the dimensional regulator ϵ and of the $n(n-1)/2$ external invariants \vec{x}

Let us consider now the same process but this time at a given loop-order l . As described in the previous sections we can, at least in principle, write down all Feynman diagrams contributing to the latter, identify all scalar integrals and generate and solve all IBPs, LIs and SRs in order to reduce them to MIs.

Let us focus our attention on a specific sector, say with m different propagators and which is reduced to $n > 0$ MIs. As exemplification let us assume we choose as masters Feynman integrals with no residual scalar products at the numerator. In this way any MI will have in general the form:

$$M_a(\vec{x}; \epsilon) = \int \prod_{j=1}^l \mathfrak{D}k_j \frac{1}{D_1^{\tau_1} \dots D_m^{\tau_m}}, \quad \text{with} \quad \tau_1, \dots, \tau_m > 0. \quad (3.31)$$

We can then apply the differential operators in (5.5.2) directly on the integral representations (3.31). Upon explicitly performing the derivatives with respect to the external momenta we will produce a linear combination of integrals belonging to the same sector (and obviously to its sub-sectors!), with rational coefficients. The resulting integrals can therefore be in turn reduced again to the MIs of the sector plus their sub-topologies. In doing so we end up with a system of *linear first-order differential equations* with rational coefficients for the n MIs:

$$\frac{\partial}{\partial x_j} M_a(\vec{x}; \epsilon) = C_{ab}^{(j)}(\vec{x}; \epsilon) M_b(\vec{x}; \epsilon) + D_{al}^{(j)}(\vec{x}; \epsilon) m_l(\vec{x}; \epsilon), \quad (3.32)$$

where the $C_{ab}^{(j)}(\vec{x}; \epsilon)$ and the $D_{al}^{(j)}(\vec{x}; \epsilon)$ are at most rational functions of \vec{x} and ϵ , while the $m_l(\vec{x}; \epsilon)$ are the sub-topologies of the sector under consideration. It is useful to discuss separately the two cases where 1 or more MIs are present.

The case of one single Master Integral

Let us consider the case where $n = 1$ and so only one MI is present. The system (3.40) reduces in this case to a *single linear first-order differential equation* with *rational coefficients* for every external invariant:

$$\frac{\partial}{\partial x_j} M(\vec{x}; \epsilon) = C^{(j)}(\vec{x}; \epsilon) M(\vec{x}; \epsilon) + D_l^{(j)}(\vec{x}; \epsilon) m_l(\vec{x}; \epsilon). \quad (3.33)$$

It is now clear that, provided that a suitable boundary condition is known, any of the differential equations in the external invariants can always be, at least formally, solved by quadrature, giving a solution in closed form for the MI in terms of a single one dimensional integral in any of the external invariants. The problem is then simplified from that of solving l loop integrals in d dimensions, to the solution of a single, one-dimensional integral. In particular, given the differential equation in one of the external invariants (say x_j) and defining the corresponding integrating factor

$$H_j(\vec{x}; \epsilon) = \exp \left(\int^{x_j} dx_j C^{(j)}(\vec{x}; \epsilon) \right),$$

the solution can be formally written as

$$M(\vec{x}; \epsilon) = H_j(\vec{x}; \epsilon) \int^{x_j} \left(\frac{D_l^{(j)}(\vec{x}; \epsilon) m_l(\vec{x}; \epsilon)}{H_j(\vec{x}; \epsilon)} \right) dx_j + C_j, \quad (3.34)$$

where C_j is a constant with respect to x_j (but will still depend in general on ϵ and on the other external invariants). Plugging (3.34) into any of the remaining

differential equations in the other external invariants (say x_k) on which the master $M(\vec{x}; \epsilon)$ depends, and imposing the latter to be satisfied, one can obtain a new linear first order differential equation for C_j in the invariant x_k , which fixes its value up to a function which does not depend neither on x_j nor on x_k . Repeating this procedure for all differential equations in all external invariants one can, at least in principle, fix the solution of the master integral up to a constant C , which depends only on the dimensional regularisation parameter ϵ .

This last constant could be fixed, for example, evaluating the integral for a particular choice of the external invariants, which is typically an easier task. We will discuss more in detail in what follows how even this last explicit integration can be most of the times avoided exploiting the knowledge of the cut structure of the integral, i.e. imposing regularity of the solution (3.34) in some specific kinematical limits (see Section 3.3.4).

Following the steps outlined above one can, at least in principle, obtain the solution for the master integral $M(\vec{x}; \epsilon)$ retaining *full dependence* on the dimensional regularisation parameter ϵ . In practical applications nonetheless, one is usually interested in the solution expanded as Laurent series in ϵ for $\epsilon \approx 0$. This can be very easily done already at the level of the differential equations. One can in fact expand as series in ϵ all terms in (3.33), where the master integral itself is given by a Laurent series:

$$M(\vec{x}; \epsilon) = \sum_{i=a}^{\infty} M^{(i)}(\vec{x}) \epsilon^i, \quad (3.35)$$

and a is typically a *negative* integer and represents the power of the deepest pole in ϵ . Plugging this expansion into (3.33) and collecting for ϵ one is left with a *chained system of differential equations* for the different coefficients of the expansion $M^{(i)}(\vec{x})$, which can be solved bottom up, starting from the deepest pole.

This approach has two main advantages. On the one hand, upon expanding in ϵ , one is left with an easier set of differential equations, where the dependence on one of the parameters, e.g. ϵ , is completely factorised. On the other, expanding first the differential equations and only as a second step integrating them, one obtains at once the coefficients of the expansion in ϵ , which are those of physical relevance. It is in fact very well known that, in many practical cases, even if the differential equations (3.33) are solvable in closed form in terms of special function (typically complicated hypergeometric functions), one is then left with the problem of expanding these functions in powers of ϵ , task which is very often prohibitive due to their complexity.

The case of more Master Integrals

Those cases where the sector is reduced to more than $n > 1$ MI are much more involved, and consequently much more interesting. Given a system of n coupled

differential equations, no general method is known for finding its solution, even in the case of linear, first-order differential equations with rational coefficients. The problem of solving a system of n coupled differential equations for n Master Integrals is in fact equivalent to that of solving an n -th order differential equation for one of the masters.

The system of differential equation (3.40) can be written in matrix form as

$$\begin{aligned} \frac{\partial}{\partial x_j} \begin{pmatrix} M_1(\vec{x}; \epsilon) \\ \dots \\ M_n(\vec{x}; \epsilon) \end{pmatrix} &= \begin{pmatrix} C_{11}^{(j)}(\vec{x}; \epsilon) & \dots & C_{1n}^{(j)}(\vec{x}; \epsilon) \\ \dots & \dots & \dots \\ C_{n1}^{(j)}(\vec{x}; \epsilon) & \dots & C_{nn}^{(j)}(\vec{x}; \epsilon) \end{pmatrix} \begin{pmatrix} M_1(\vec{x}; \epsilon) \\ \dots \\ M_n(\vec{x}; \epsilon) \end{pmatrix} + \text{Sub-topologies} \\ \rightarrow \quad \frac{\partial}{\partial x_j} \vec{M}(\vec{x}; \epsilon) &= C(\vec{x}; \epsilon) \vec{M}(\vec{x}; \epsilon) + \text{Sub-topologies}. \end{aligned} \quad (3.36)$$

The problem would be however substantially simplified and reduced to the previous case, if one could find a way to triangularise the matrix $C(\vec{x}; \epsilon)$. In this case one could solve, again at least formally, all equations by quadrature, one after the other.

Obviously the problem of finding a rotation in the space of the master integrals which triangularises the matrix $C(\vec{x}; \epsilon)$ is equivalent to that of solving an n -th order differential equation and it usually turns out to be a formidable task, at least as long as the full dependence on ϵ is kept.

However as for the case of one single MI treated above, it is well known that in many practical applications the problem becomes much easier if the system of differential equations is expanded as Laurent series in ϵ around $\epsilon \approx 0$. In particular it has been seen that, very often, a triangular form as $\epsilon = 0$ can be reached by a suitable rotation in the space of MIs using only IBPs, LIs and SRs. This is equivalent to say that, considering all possible integrals in a given topology, and all possible IBPs, LIs and SRs which relate these integrals to each other, it is possible to bring the system of differential equations in triangular form as $\epsilon = 0$ by simply making a suitable choice of the masters selected by the Laporta Algorithm.

Even if no general principles are known in order to select the right basis of MIs and achieve such triangularisation, in most applications a simple trial and error approach has proven to be very effective and such a basis could often be found quite easily (see, among the others, [59, 84, 86, 87, 102–104]). Once the system of differential equations is in triangular form, upon expanding everything as Laurent series in ϵ , the problem is reduced to the previous case and the solution can always be written in closed form, order by order in ϵ , by repeated quadrature.

3.3.2 Solution as iterated integrals and the canonical form

Until now we discussed the structure of differential equations for Master Integrals and elucidated how, provided that the system can be put in triangular form, one can, at least formally, find a solution to it by quadrature, order by order in ϵ .

A different, but equally important problem, is that of being able to solve these integrals analytically in closed form in terms of known special functions. The method of differential equations, in particular when applied to ϵ -expanded Feynman integrals, suggests by its very construction a particularly suitable class of functions as natural tool for representing the latter, namely the so called *Chen iterated integrals* [31]. As we saw in the previous sections in fact, upon expanding the differential equations (and the MIs themselves) as Laurent series in ϵ , one is left with a system of *chained* differential equations, which can be solved bottom-up starting from the deepest pole. Since given the differential equations for the j -th order, all previous orders of the expansion will appear as inhomogeneous terms, one has that, order by order in ϵ , the solution is defined as a one-dimensional integral over the previous terms in the expansion. This structure is by definition *iterative*, and in this sense it suggests that a convenient representation of the solution should be in terms of iterated integrals, a special case of which is constituted by the MPLs.

This structure becomes obviously more transparent if one manages to put the differential equations in triangular form. We can nevertheless do even better than that. It has been recently suggested [105] that in many cases the differential equations can be put in an even more convenient form where the dependence on ϵ is completely factorised from the kinematics, and the differential equations take the form:

$$\frac{\partial}{\partial x_j} \begin{pmatrix} m_1(\vec{x}; \epsilon) \\ \dots \\ m_n(\vec{x}; \epsilon) \end{pmatrix} = \epsilon \begin{pmatrix} c_{11}^{(j)}(\vec{x}) & \dots & c_{1n}^{(j)}(\vec{x}) \\ \dots & \dots & \dots \\ c_{n1}^{(j)}(\vec{x}) & \dots & c_{nn}^{(j)}(\vec{x}) \end{pmatrix} \begin{pmatrix} m_1(\vec{x}; \epsilon) \\ \dots \\ m_n(\vec{x}; \epsilon) \end{pmatrix}, \quad (3.37)$$

where the new basis of master integrals $m_j(\vec{x}; \epsilon)$ can be reached from the original basis $M(\vec{x}; \epsilon)$ through IBPs. In particular if the coefficients $c_{nk}^{(j)}(\vec{x})$ are in $d\text{-log}$ form² for every external invariant x_j , then the system of differential equations can be further rephrased as:

$$d \vec{m}(\vec{x}; \epsilon) = \epsilon d A(\vec{x}) \vec{m}(\vec{x}; \epsilon), \quad (3.38)$$

where the differential d acts on all external invariants and the matrix $A(\vec{x})$ can be rewritten as:

$$A(\vec{x}) = \sum_{\alpha=1}^a A_\alpha \ln(r_\alpha), \quad (3.39)$$

where finally the r_α are just rational functions of the external invariants.

If this is the case, then all equations are *completely decoupled* as $\epsilon \rightarrow 0$ (or equivalently as $d \rightarrow 4$), and can be integrated trivially in terms of the previously introduced multiple polylogarithms. While casting the differential equations in the canonical form (3.38) is not strictly necessary for their integration, it is still very

²I.e. if they can be rewritten as the differential of a logarithm of a suitable argument.

desirable for different reasons. In particular the MIs computed in the canonical basis \vec{m} , once expanded as Laurent series in ϵ , end up having a particularly compact representation in terms of *pure functions of uniform transcendental weight* [105]. Having a result in this form, in particular in the case of multiscale or multiloop problems, helps to handle the largeness of the intermediate expressions and also the complexity of the final result.

The issue of the existence of such a basis for any multiloop problem remains, in particular for those cases which cannot be expressed in terms of MPLs. Moreover, even in those cases where it is known that the final result contains only MPLs, no algorithm for finding such basis is known. On the other hand, it is normally much easier to find a basis of MIs in terms of which the differential equations are in triangular form as $\epsilon \rightarrow 0$. As we will show in the following, having a system of differential equations which fulfils this criterium [90] is a good starting point and in some cases it allows to build up a canonical basis in an almost completely algorithmic way. Moreover it has been realised that the further requirement of linearity in ϵ of the homogeneous system of differential equations plays an important role in making this possible. In particular in [106] it has been shown that, if the *entire system* has only linear dependence ϵ , then the rotation to a canonical basis can be rephrased in terms of the *Magnus series*.

In what follows we will describe in detail the algorithmic procedure that we used in order to build up a canonical basis for the set of master integrals needed for the QCD two-loop corrections to the production of two massive vector bosons with the same mass [90], see Chapter 4. This algorithm has been developed in [90, 106].

While we claim no generality in this approach and no proof can be given that it would work in more involved cases, we found it particularly elementary and algorithmically straightforward to implement, so that its extension to more difficult cases should not present particular conceptual difficulties³.

3.3.3 Building up the basis bottom-up

Before describing in detail the method we used to find a canonical basis, let us recall some notation and definitions which will be useful in the following. We start off by considering a *topology* (or *sector*) given by a set of t different propagators (matching the loop integrals of some Feynman diagram). Its *sub-topologies* (or *sub-sectors*) are defined as the set of all possible arrangements of propagators obtained from the original topology by removing one or more propagators in all possible ways. In the case of two-loop corrections to vector boson pair production in massless QCD, for example, where all tadpoles are identically zero, the first non-zero sectors will be those with $t = 3$ (corresponding to the *sunrise topologies*), while the highest sectors

³Note that, as already mentioned, the algorithm assumes to have an initial basis of master integrals which fulfils some precise requirements. While normally finding such a basis is not difficult with a simple *trial and error* procedure, the criteria proposed in [105] can be used precisely to tentatively guess this starting point.

will contain at most $t = 7$ different propagators.

As discussed in the previous sections, by generating and solving all IBPs, LIs and SRs for a given integral family, some sectors will be reduced to one or more MIs while some other, the so-called *reducible sectors*, will be completely reduced to their sub-topologies. In what follows we can completely neglect these reducible sectors.

Let us consider now a sector with a given value of t and which is reduced to $n \geq 1$ MIs. As it is well known, the differential equations for the latter will in general contain all their sub-topologies as inhomogeneous terms. Therefore, it is natural to try and follow a bottom-up approach in t , such that, when studying the differential equations for the MIs of a given sector with a given value of t , we can assume that all its sub-topologies fulfil differential equations already in canonical form. For the MIs of the sector under consideration we use the notation: $f_a(x_k; \epsilon)$ with $a = 1, \dots, n$. The differential equations for the n MIs read in total generality:

$$\frac{\partial}{\partial x_j} f_a(x_k; \epsilon) = C_{ab}^{(j)}(x_k; \epsilon) f_b(x_k; \epsilon) + D_{al}^{(j)}(x_k; \epsilon) m_l(x_k; \epsilon), \quad (3.40)$$

where the $C_{ab}^{(j)}(x_k; \epsilon)$ and the $D_{al}^{(j)}(x_k; \epsilon)$ are at most rational functions of x_k and ϵ , while the $m_l(x_k; \epsilon)$ are the sub-topologies, whose differential equations are, by construction, already in the canonical form:

$$\frac{\partial}{\partial x_j} m_l(x_k; \epsilon) = \epsilon A_{lr}^{(j)}(x_k) m_r(x_k; \epsilon). \quad (3.41)$$

Let us consider now the $n \times n$ matrix of the coefficients of the homogeneous equation $\mathbb{C}(x_k; \epsilon) = \{C_{ab}^{(j)}(x_k; \epsilon)\}_{ab}$. Our method relies on the assumption that we can find a starting basis of MIs $f_a(x_k; \epsilon)$ such that:

1. The matrix $\mathbb{C}(x_k, \epsilon)$ has only *linear dependence*⁴ on ϵ , i.e

$$\mathbb{C}(x_k, \epsilon) = \mathbb{C}^{(0)}(x_k) + \epsilon \mathbb{C}^{(1)}(x_k). \quad (3.42)$$

2. The matrix $\mathbb{C}^{(0)}(x_k)$ is *triangular*.

Obviously in the case where $n = 1$ the matrix $\mathbb{C}(x_k; \epsilon)$ reduces to a *scalar* and the condition 2. is always trivially satisfied. On the other hand there is no real restriction on the dependence on ϵ of the functions $D_{al}^{(j)}(x_k; \epsilon)$. As an exemplification we can assume a typical situation where they contain terms of the following form:

$$D_{al}^{(j)}(x_k; \epsilon) = \alpha_{al}^{(j)}(x_k) + \beta_{al}^{(j)}(x_k) \epsilon + \frac{\gamma_{al}^{(j)}(x_k)}{1 - 2\epsilon}, \quad (3.43)$$

⁴Note that this same requirement was assumed in [106], but for the *entire* system of differential equations for *all* MIs, including all sub-topologies, while here we require it, for every value of t , only for the homogeneous part of the system.

where the functions $\alpha_{al}^{(j)}$, $\beta_{al}^{(j)}$, $\gamma_{al}^{(j)}$ depend only on the external invariants x_k . Note that if the factor $1/(1-2\epsilon)$ were substituted by any other linear factor $1/(u+v\epsilon)$, with $u, v \in \mathbb{Z}$, the argument would proceed in the exact same way. Moreover, as it will become clear in what follows, a more complicated dependence on ϵ in the inhomogeneous terms (for example polynomial in ϵ) can be, at least in principle, treated with a suitable extension of the method described below.

For every sector at a given t we proceed as follows:

1. Starting from (3.40), and using the assumption (3.42), we first attempt to solve the homogeneous system for $\epsilon = 0$

$$\frac{\partial}{\partial x_j} \vec{f}(x_k) = C^{(0)}(x_k) \vec{f}(x_k), \quad \forall j, \quad (3.44)$$

in terms of *rational functions only*. While there is obviously *a priori* no guarantee that this can be done in general (without introducing, for example, logarithms of the external invariants x_k), we found that, in all cases we worked with, this was always the case. If this is possible, then it is equivalent to finding a rotation $f_a(x_k; \epsilon) \rightarrow g_a(x_k; \epsilon)$ such that the system (3.40) becomes:

$$\frac{\partial g_a(x_k; \epsilon)}{\partial x_j} = \epsilon \tilde{C}_{ab}^{(j)}(x_k) g_b(x_k; \epsilon) + \tilde{D}_{al}^{(j)}(x_k; \epsilon) m_l(x_k; \epsilon), \quad (3.45)$$

where the functions $\tilde{C}_{ab}^{(j)}(x_k)$ are simple rational functions of the external invariants only, while the $\tilde{D}_{al}^{(j)}(x_k; \epsilon)$ will have in general the same decomposition as in (3.43):

$$\tilde{D}_{al}^{(j)}(x_k; \epsilon) = \tilde{\alpha}_{al}^{(j)}(x_k) + \tilde{\beta}_{al}^{(j)}(x_k) \epsilon + \frac{\tilde{\gamma}_{al}^{(j)}(x_k)}{1-2\epsilon}. \quad (3.46)$$

2. Once the differential equations are in form (3.45), only the sub-topologies need to be fixed in order to achieve a complete canonical form. Assuming an ϵ -dependence as in eq.(3.46), we start removing *first* all subtopologies proportional to the coefficients $\gamma_{al}^{(j)}$. This can be attempted performing a shift in the MIs basis as follows:

$$g_a(x_k; \epsilon) \rightarrow h_a(x_k; \epsilon) = g_a(x_k; \epsilon) + \frac{\Gamma_{al}(x_k)}{1-2\epsilon} m_l(x_k, \epsilon), \quad (3.47)$$

where the $\Gamma_{al}(x_k)$ are rational functions of the external invariants and whose explicit form will be determined in the following. Note that, since the differential equations for the sub-topologies are already in canonical form (3.41), this ensures that upon performing this shift and partial-fractioning in ϵ we will only

produce terms proportional ϵ^0 , ϵ , or $1/(1-2\epsilon)$. Upon performing the shifts in (3.47), in fact, we are left with:

$$\begin{aligned}
\frac{\partial h_a(x_k; \epsilon)}{\partial x_j} &= \epsilon \tilde{C}_{ab}^{(j)}(x_k) h_b(x_k; \epsilon) + \epsilon \tilde{\beta}_{al}^{(j)}(x_k) m_l(x_k; \epsilon) \\
&+ \left[\tilde{\alpha}_{al}^{(j)}(x_k) + \frac{\Gamma_{bl}(x_k)}{2} \tilde{C}_{ab}^{(j)}(x_k) \right] m_l(x_k; \epsilon) \\
&- \frac{1}{2} \Gamma_{al}(x_k) A_{lr}^{(j)}(x_k) m_r(x_k; \epsilon) \\
&+ \frac{1}{1-2\epsilon} \left\{ \left[\frac{\partial \Gamma_{al}(x_k)}{\partial x_j} + \tilde{\gamma}_{al}^{(j)}(x_k) - \frac{1}{2} \tilde{C}_{ab}^{(j)}(x_k) \Gamma_{bl}(x_k) \right] m_l(x_k; \epsilon) \right. \\
&\quad \left. + \frac{1}{2} \Gamma_{al}(x_k) A_{lr}^{(j)}(x_k) m_r(x_k; \epsilon) \right\}. \tag{3.48}
\end{aligned}$$

The explicit form of the functions $\Gamma_{al}(x_k)$ can be, at least in principle, determined by imposing that all terms proportional to $1/(1-2\epsilon)$ are cancelled, in other words that:

$$\begin{aligned}
&\left[\frac{\partial \Gamma_{al}(x_k)}{\partial x_j} + \tilde{\gamma}_{al}^{(j)}(x_k) - \frac{1}{2} \tilde{C}_{ab}^{(j)}(x_k) \Gamma_{bl}(x_k) \right] m_l(x_k; \epsilon) \\
&+ \frac{1}{2} \Gamma_{al}(x_k) A_{lr}^{(j)}(x_k) m_r(x_k; \epsilon) = 0. \tag{3.49}
\end{aligned}$$

Eq. (3.49) is a linear system of first-order coupled differential equations for the unknown $\Gamma_{al}(x_k)$ whose solution can be, at least in principle, as difficult as the solution of the original system (3.40). Nevertheless, in all cases that we encountered, the system could be easily solved with an *Ansatz*. In particular, assuming that a basis which realises the canonical form (3.38) exists and assuming that such basis can be reached through a rotation which only involves *rational functions*⁵, we can write the most general *Ansatz* for the functions $\Gamma_{al}(x_k)$ as linear combination of all possible linearly independent rational functions⁶ which appear in the original differential equations (3.45). Collecting for the independent rational functions, and requiring their coefficients to be zero,

⁵Note that this requirement is perfectly sensible as long as we assume that such basis can be reached from any other basis through IBPs, LIs and symmetry relations only and potential roots coming from the solution of the homogeneous equations can be rationalised, similar like in our case where the Landau variable x absorbs the root $\sqrt{s(s-4m^2)}$.

⁶Where here “linearly independent” has to be intended in the sense of a complete partial fractioning in all external invariants x_k .

we are left with a large system of linear equations with numerical coefficients whose solution is now, at least in principle, completely straightforward.

Note that, in a typical case, there will be more equations than unknowns and the system will be over-constrained with many equations being linearly dependent from each other. For the same reason, it is in no way guaranteed that a solution to such a system exists. Nevertheless, once more, for all cases that we worked with, a solution could always be found.

3. Once this step has been performed, we are left with a new system of equations for the new MIs $h_a(x_k; \epsilon)$ which reads:

$$\frac{\partial}{\partial x_j} h_a(x_k; \epsilon) = \epsilon \left[\tilde{C}_{ab}^{(j)}(x_k) h_b(x_k; \epsilon) + E_{al}^{(j)}(x_k) m_l(x_k; \epsilon) \right] + F_{al}^{(j)}(x_k) m_l(x_k; \epsilon), \quad (3.50)$$

where the $E_{al}^{(j)}(x_k)$ and the $F_{al}^{(j)}(x_k)$ are again simple rational functions of the external invariants x_k . We can now proceed removing the remaining terms which are not proportional to ϵ . This can be achieved in the same way as before by performing the shift:

$$h_a(x_k; \epsilon) \rightarrow m_a(x_k; \epsilon) = h_a(x_k; \epsilon) + G_{al}(x_k) m_l(x_k; \epsilon), \quad (3.51)$$

where again the $G_{al}(x_k)$ are rational functions of the external invariants.

Note that, since the MIs depend in general on many external invariants x_j , for every a, l fixed, there has to exist a single function $G_{al}(x_k)$, such that the terms not proportional to ϵ in (3.50) cancel under the shift (3.51) for all differential equations in all external invariants x_j . This condition can be rephrased as:

$$\frac{\partial}{\partial x_j} G_{al}(x_k) + F_{al}^{(j)}(x_k) = 0, \quad \forall j. \quad (3.52)$$

With the same assumptions as before we can solve these equations with an *Ansatz* imposing that the solution must be a linear combination of rational functions in the external invariants only. Again, in all cases where we applied this method, a solution could always be found.

4. After the final shift (3.51) is performed the canonical form is reached:

$$\frac{\partial m_a(x_k; \epsilon)}{\partial x_j} = \epsilon H_{ab}^{(j)}(x_k) m_b(x_k; \epsilon), \quad (3.53)$$

where the $H_{ab}^{(j)}(x_k)$ are only rational functions and the indices $\{a, b\}$ run on the MIs of the given sectors plus on all their sub-topologies.

We would like to emphasise that there is no guarantee that, given any sets of MIs to start with, all steps described above can be always successfully carried out. These require in each instance to find a shift which only involves rational functions and which eliminates at every step the un-wanted terms in the differential equations. It should also be noted that the two steps 2. and 3. must be performed in this order. It is clear in fact from (3.48) that the first step will produce in general terms in the equations which are proportional to ϵ^0 , and which will be removed only during the following step.

Extension to polynomial dependence on ϵ

In the very same way as discussed above we can treat the more general case where the differential equations (3.45) admit a polynomial dependence on ϵ in the sub-topologies and/or higher powers of factors $1/(u + v\epsilon)$.

Let us consider for simplicity a sector with only one master integral $f(x; \epsilon)$, which depends on one single external invariant x and which has only one sub-topology $m(x; \epsilon)$. Let us assume again that the differential equation for the sub-topology is in canonical form

$$\frac{d}{dx}m(x; \epsilon) = \epsilon A(x) m(x; \epsilon). \quad (3.54)$$

Moreover, let us suppose that the differential equation for the MI $f(x; \epsilon)$ is *almost* in canonical form except for a term proportional to ϵ^n ,

$$\frac{d}{dx}f(x; \epsilon) = \epsilon (C_1(x)f(x; \epsilon) + C_2(x)m(x; \epsilon)) + \epsilon^n C_3(x)m(x; \epsilon), \quad (3.55)$$

where the $C_j(x)$ are all rational functions of the external invariant x .

Using again (3.54), we can perform the shift:

$$f(x; \epsilon) \rightarrow g(x; \epsilon) = f(x; \epsilon) + \epsilon^{n-1} G(x) m(x; \epsilon). \quad (3.56)$$

Inserting this expression in (3.55) and using the fact that the differential equations for the sub-topology $m(x; \epsilon)$ are in canonical form, it is clear that we will produce terms proportional to ϵ^n and ϵ^{n-1} only. We can then fix the function $G(x)$ imposing that the shift (3.56) removes all terms proportional to ϵ^n , being in this way left only with terms proportional to ϵ^{n-1} . Proceeding in this way, starting from the highest power of ϵ , we can tentatively remove all undesirable terms from the differential equations and bring them to the canonical form (3.38).

The very same idea applies to higher powers of factors $1/(u + v\epsilon)$ which multiply any subtopology whose equations are already in canonical form. Starting from the highest powers we can tentatively remove all terms one after the other until we are reduced to the case treated in the section above.

Comments on the basis change

Following the construction of the canonical basis as described in the previous section, it becomes clear that the issue of finding a canonical basis for a set of master integrals is somehow connected to that of being able to integrate out the homogeneous part of the system in $\epsilon = 0$ in terms of rational functions only. In this sense, having a basis of MIs whose differential equations are in canonical form is, for *practical purposes*, almost equivalent to having a basis whose differential equations are triangular for $\epsilon = 0$, and whose homogeneous parts can be integrated in terms of rational functions only. From this point of view, casting the system of differential equations into canonical form consists in separating into two different steps the two conceptually different issues of: (a) integrating the homogeneous parts of the equations (which provide the somehow “*trivial*” rational prefactors of the MIs), and (b) integrating the “*non-trivial*” dependence of the master integrals on *transcendental functions*. It looks reasonable to think that such a “factorisation” can be achievable as long as the master integrals are expressed in terms of MPLs only. On the other hand, it is not yet clear how and if this structure could be preserved or generalised in the case of more complicated functional behaviours.

It is also important to stress that, both if the equations are in canonical form, and if the equations are triangular for $\epsilon = 0$ (*with the homogeneous part solvable in terms of rational functions only*), their integration becomes straightforward. A task which remains is the determination of the boundary terms, which is non-trivial in particular in the case of non-planar integrals. In this regard, having the equations in canonical form does not solve any conceptual difficulties by itself. In either case, the canonical basis gives not only a clearer view on the structure of the problem, it also has great practical advantages due to the simpler and more compact expressions which need to be handled in this approach.

3.3.4 The boundary conditions

Having the differential equations in normal form renders their integration completely algebraic. It remains anyway the issue of fixing the boundary conditions. In order to determine completely the solution of a system of n differential equations, n boundary conditions must be specified. This can be done, for example, by explicitly calculating the integrals in a specific kinematical point, either attempting a direct integration or using for example asymptotic expansions [107–109].

In most applications, nevertheless, this is not required. Very often in fact such boundary values can be inferred directly from the system of differential equations, without having to resort to any explicit separate calculations. Let us consider again the general form of the system in (3.36). The coefficients $C_{nk}^{(j)}(\vec{x}; \epsilon)$ are, as already discussed, rational functions of the external invariants and of ϵ . Typically these coefficients will contain poles in the external invariants which correspond to the different *thresholds* and *pseudo-thresholds* of the problem. A solution of this system

of equations is then expected to show a singular behaviour in all these kinematical points, while it is well known that the MIs must be regular when the kinematical invariants approach the *pseudo-thresholds*. It turns out that in many case of physical interest⁷ imposing regularity in these kinematical limits is sufficient for determining *quantitatively* all boundary terms needed for the determination of the MIs.

3.3.5 A toy example: the one-loop massive sunrise

In order to exemplify all techniques described in the last two chapters it is useful to work out a toy example like the massive one-loop sunrise. For the sake of simplicity let us assume to work in Euclidean kinematics, so that the integrals belonging to the sunrise topology can be written as:

$$\mathcal{I}(n_1, n_2) = \text{---} \overset{p^2}{\circlearrowleft} \text{---} = \int \frac{\mathfrak{D}^d k}{(k^2 + m^2)^{n_1} ((k - p)^2 + m^2)^{n_2}}, \quad (3.57)$$

where we use the integration measure

$$\int \mathfrak{D}^d k = \frac{1}{C(d)} \int \frac{d^d k}{(2\pi)^{d-2}}, \quad (3.58)$$

with

$$C(d) = (4\pi)^{(4-d)/2} \Gamma\left(3 - \frac{d}{2}\right). \quad (3.59)$$

The only sub-topology of the sunrise is the massive tadpole:

$$\mathcal{I}(n_1, 0) = \mathcal{I}(0, n_2) = \int \frac{\mathfrak{D}^d k}{(k^2 + m^2)^{n_1}}. \quad (3.60)$$

As a first step one needs to perform a full reduction to MIs of the whole sub-topology tree, which in this case is constituted by the Tadpoles $\mathcal{I}(n_1, 0)$ and the sunrise integrals $\mathcal{I}(n_1, n_2)$ only. Deriving and solving the IBPs one finds that all integrals can be reduced to 2 MIs only, one for the tadpole and one for the sunrise. Choosing naively as masters:

$$M_1 = \mathcal{I}(1, 0) = \int \frac{\mathfrak{D}^d k}{(k^2 + m^2)}, \quad M_2 = \mathcal{I}(1, 1) = \int \frac{\mathfrak{D}^d k}{(k^2 + m^2)((k - p)^2 + m^2)}, \quad (3.61)$$

we find for example the following reduction equations:

⁷A counter example to this is given by the massless non-planar double-boxes with all on-shell external legs. These integrals have cuts in all three Mandelstam variables s, t, u , and the only denominators appearing in the differential equations are the three cuts in these variables, so that no regularity condition can be imposed in any of those points, see for example [53, 54, 106].

$$\mathcal{I}(2, 0) = \mathcal{I}(0, 2) = -\frac{(d-2)}{2m^2} M_1, \quad (3.62)$$

$$\mathcal{I}(2, 1) = \mathcal{I}(1, 2) = -\frac{(d-2)}{2m^2(p^2 + 4m^2)} M_1 - \frac{(d-3)}{p^2 + 4m^2} M_2, \quad (3.63)$$

and similar equations hold for higher powers of the internal propagators. Once the MIs have been identified we can use the differential equation method in order to compute them. We will assume from now on that the analytical expression for the Tadpole is known:

$$M_1 = \mathcal{I}(1, 0) = \frac{m^{d-2}}{(d-2)(d-4)},$$

and proceed bottom-up deriving a differential equation for $M_2 = \mathcal{I}(1, 1)$ in the only external invariant p^2 .

Let us start off by noticing that using $p^2 = p^\mu p_\mu$ and the chain rule, we obtain

$$\frac{\partial p^2}{\partial p_\mu} = 2p^\mu,$$

and consequently the derivative with respect to p^2 can be written as:

$$p_\mu \frac{\partial}{\partial p_\mu} = p_\mu \frac{\partial p^2}{\partial p_\mu} \frac{\partial}{\partial p^2} \longrightarrow \frac{\partial}{\partial p^2} = \frac{1}{2p^2} \left(p_\mu \frac{\partial}{\partial p_\mu} \right).$$

Applying this differential operator on the master integral $\mathcal{I}(1, 1) = M_2$ and acting with it on its integral representation we get at once:

$$\begin{aligned} \frac{d}{dp^2} M_1 &= \frac{1}{2p^2} \left(p_\mu \frac{\partial}{\partial p_\mu} \right) \int \mathcal{D}^d k \frac{1}{(k^2 + m^2)((k-p)^2 + m^2)} \\ &= \frac{1}{2p^2} (\mathcal{I}(0, 2) - \mathcal{I}(1, 1)) - \frac{1}{2} \mathcal{I}(1, 2), \end{aligned}$$

which, using the IBPs in order to reduce the *r.h.s* to MIs, becomes:

$$\frac{d}{dp^2} M_2 = \frac{1}{2} \left(\frac{(d-3)}{p^2 + 4m^2} - \frac{1}{p^2} \right) M_2 - \frac{(d-2)}{p^2(p^2 + 4m^2)} M_1. \quad (3.64)$$

This is an inhomogeneous linear first-order differential equation for M_2 and can be easily solved through Euler's method of the variation of the constants. We are

interested in particular in its solution expanded as Laurent series in $(d-4)$. Putting $d=4$ in the homogenous part of this equation one sees immediately that its solution contains a square-root, namely

$$\begin{aligned} \frac{d}{dp^2} H_2 &= \frac{1}{2} \left(\frac{1}{p^2 + 4m^2} - \frac{1}{p^2} \right) H_2 \\ \longrightarrow H_2 &= \sqrt{\frac{p^2 + 4m^2}{p^2}}. \end{aligned}$$

Before proceeding with the expansion and the subsequent integration order by order in $(d-4)$ it is therefore convenient to switch to the so-called Landau variable x :

$$p^2 = m^2 \frac{(1-x)^2}{x}, \quad (3.65)$$

so that the root is rationalised and becomes

$$H_2 = \sqrt{\frac{p^2 + 4m^2}{p^2}} \rightarrow \frac{1+x}{1-x}.$$

Deriving a new differential equation in x instead that in p^2 we find:

$$\frac{d}{dx} M_2 = \left[\frac{2}{(1+x)(1-x)} - (d-4) \frac{(1-x)}{2x(1+x)} \right] M_2 + \frac{(d-2)}{m^2 (1+x)(1-x)} M_1. \quad (3.66)$$

Upon substituting the known value for the tadpole M_1 and expanding everything in $(d-4)$ we get order by order the following set of chained differential equations:

$$\frac{d}{dx} M_2^{(-1)} = \left(\frac{1}{1+x} + \frac{1}{1-x} \right) M_2^{(-1)} + \frac{1}{2} \left(\frac{1}{1+x} + \frac{1}{1-x} \right),$$

$$\frac{d}{dx} M_2^{(0)} = \left(\frac{1}{1+x} + \frac{1}{1-x} \right) M_2^{(0)} + \left(\frac{1}{1+x} - \frac{1}{2x} \right) M_2^{(-1)},$$

...

$$\frac{d}{dx} M_2^{(n)} = \left(\frac{1}{1+x} + \frac{1}{1-x} \right) M_2^{(n)} + \left(\frac{1}{1+x} - \frac{1}{2x} \right) M_2^{(n-1)},$$

where we put

$$M_2 = m^{(d-4)} \left(\frac{M_2^{(-1)}}{(d-4)} + M_2^{(0)} + (d-4) M_2^{(1)} + \mathcal{O}((d-4)^2) \right).$$

Note that the homogeneous equation is the same at every order, and that all equations are actually functionally identical, except for the first order. Given the structure above one way to proceed is, first of all, to integrate out the homogeneous part at every order in $(d-4)$:

$$\frac{d}{dx} f(x) = \left(\frac{1}{1+x} + \frac{1}{1-x} \right) f(x) \quad \rightarrow \quad f(x) = \frac{1+x}{1-x}.$$

Defining then the new functions $\widetilde{M}^{(n)}$ as:

$$M_2^{(n)} = f(x) \widetilde{M}^{(n)}, \quad (3.67)$$

we obtain the new set of equations:

$$\frac{d}{dx} \widetilde{M}^{(-1)}(x) = \frac{1}{(1+x)^2},$$

$$\frac{d}{dx} \widetilde{M}^{(n)}(x) = \left(\frac{1}{1+x} - \frac{1}{2x} \right) \widetilde{M}^{(n-1)}(x), \quad \forall n \geq 1.$$

It is now clear that at every order in $(d-4)$ the solution will only contain HPLs of indices $\{0, -1\}$. Integrating the first two orders we get:

$$\widetilde{M}^{(-1)} = -\frac{1}{1+x} + C^{(-1)},$$

$$\widetilde{M}^{(0)} = +\frac{1}{1+x} + \frac{1}{2} (G(0, x) - G(-1, x)) + C^{(-1)} \left(G(-1, x) - \frac{1}{2} G(0, x) \right) + C^{(0)},$$

where $C^{(-1)}$ and $C^{(0)}$ are the two integration constants which still need to be fixed. In order to do it we need a boundary condition for the integral. As already anticipated, this does not require any additional calculations. We can use indeed the fact that as $p^2 \rightarrow 0$ (or equivalently $x \rightarrow 1$) the integral must be regular, while in the differential equation (3.66) explicit denominators $1/(1-x)$ appear. Multiplying (3.66) by $(1-x)$ and taking the limit $x \rightarrow 1$, imposing that

$$\lim_{x \rightarrow 1} \left[(1-x) \frac{d}{dx} M_2 \right] = 0,$$

we find the relation:

$$\lim_{x \rightarrow 1} M_2 = -\frac{(d-2)}{2m^2} M_1 = m^{(d-4)} \left(-\frac{1}{2} \frac{1}{(d-4)} \right), \quad (3.68)$$

which, once substituted into (3.67), fixes completely the solution of (3.66). In particular for the first three orders we find:

$$\begin{aligned} M_2^{(-1)} &= -\frac{1}{2}, \\ M_2^{(0)} &= +\frac{1}{2} - \frac{1}{2} \left(\frac{1}{2} - \frac{1}{1-x} \right) G(0, x), \\ M_2^{(1)} &= -\frac{1}{2} + \frac{1}{2} \left(\frac{1}{2} - \frac{1}{1-x} \right) \left(\frac{\zeta_2}{2} - G(0, x) - \frac{1}{2} G(0, 0, x) + G(-1, 0, x) \right). \end{aligned}$$

As a last remark, it is worth noting that if we had chosen a different basis of MIs, the differential equations could have been cast from the beginning in canonical form, see Section 3.3.2. Picking as new basis of master integrals:

$$\begin{aligned} m_1 &= \mathcal{I}(2, 0) \\ m_2 &= \frac{(1-x)(1+x)}{x} \mathcal{I}(2, 1), \end{aligned}$$

we find at once

$$\frac{d}{dx} m_2 = (d-4) \left[\frac{(x-1)}{2x(1+x)} m_2 + \frac{1}{2x} m_1 \right],$$

which can be now trivially integrated as series expansion in $(d-4)$ in the same way as before. As illustration of the simpler structure of the results, the first three orders of the expansion in this new basis fit on one single line:

$$m_2^{(-1)} = 0, \quad m_2^{(0)} = -\frac{1}{4} G(0, x), \quad m_2^{(1)} = -\frac{1}{8} [\zeta_2 + 2 G(-1, 0, x) - G(0, 0, x)]. \quad (3.69)$$

Note moreover that the result in (3.69) is as expected of uniform transcendental weight.

3.4 Outlook

In the previous chapters we provided a detailed account of some of the methods which are nowadays employed in order to carry out a typical multiloop computation in analytical form. In what remains of this thesis we will elaborate on some of the original results which we have obtained employing these techniques.

In Chapter 4 we will start presenting the results recently obtained in the computation of the two-loop master integrals relevant for the production of two massive vector bosons with the same mass in hadronic collisions [86, 90]. We will show how after employing IBPs, LIs and SRs all integrals relevant for this process can be reduced to a subset of 75 MIs. The latter can be computed by means of the differential equations method. In particular, given a starting basis of master integrals whose differential equations are already triangular as $d \rightarrow 4$, we will show how using the algorithm described above the differential equations can be cast in canonical form, see Section 3.3.2.

In Chapter 5, as a second application of the differential equations method, we will present a thorough study of the master integrals emerging from the reduction of the two-loop massive sunrise graph [37]. As it is well known, this is the first example of a Feynman graph which does not evaluate to simple multiple polylogarithms. We will show how a naive reduction to MIs would produce 4 independent master integrals which fulfil 4 coupled first order differential equations. Using the newly introduced Schouten identities (see Section 2.2.5) we will prove that *at most* 2 out of the 4 differential equations can be decoupled in the limit for $d \rightarrow 2$ (or equivalently $d \rightarrow 4$), while the remaining 2 equations stay coupled and admit solutions which cannot be expressed through multiple polylogarithms, but instead involve *integrals over elliptic integrals*.

In Chapters 6 and 7 finally, we will use some of the results obtained in Chapter 4 together with other results known for a longer time in the literature, in order to study more in detail vector boson pair production at hadron colliders. We will start off describing the computation of the two-loop QCD helicity amplitudes for the production of a massive and a massless vector boson in the $q\bar{q}$ [32] channel, and conclude describing the first NNLO computation of the fully inclusive cross section for the production of two on-shell Z -bosons at the LHC [110].

Part II

Results

Chapter 4

The MIs for $q\bar{q} \rightarrow VV$ production

The material presented in this chapter is the result of an original research done in collaboration with T. Gehrmann, A. von Manteuffel and E. Weihs, and it is entirely based on the two papers [86, 90].

4.1 Introduction

Precision studies of the electroweak interaction at the LHC are based on a wealth of observables derived from vector boson pair production, $\gamma\gamma$, $Z\gamma$, $W\gamma$, ZZ , WW , WZ , which allow to test the $SU(2)_L \times U(1)_Y$ gauge structure and the field content of the Standard Model. Anomalous contributions to these interactions can probe physics beyond the Standard Model at energy scales well beyond direct searches. To fully exploit these observables, precise theoretical predictions are of crucial importance, including especially higher order perturbative corrections. To reach an accuracy in the per-cent range, thus matching the experimental precision at the LHC, corrections to next-to-leading order (NLO) in the electroweak theory and to next-to-next-to-leading order (NNLO) in QCD are to be included.

The full set of NLO QCD corrections [111–114] and large parts of the NLO electroweak corrections [115–120] have been derived for vector boson pair production. NNLO QCD corrections were calculated up to now for $\gamma\gamma$ [121] and $Z\gamma$ [122] production. Moreover very recently, based on the results presented in this chapter, the NNLO QCD corrections for on-shell ZZ production have become available [110]. Key ingredient to this NNLO calculations are the two-loop matrix elements for $q\bar{q} \rightarrow V_1 V_2$, which were known up to now for $\gamma\gamma$ [123, 124] and $V\gamma$ [32, 125] production, and for $q\bar{q} \rightarrow WW$ in the high energy approximation [126]. The full calculation of two-loop matrix elements for the production of two massive vector bosons requires the derivation of a new class of two-loop Feynman integrals: two-loop four-point functions with internal massless propagators and two massive external legs. First results on these were obtained already with the derivation of the full set of planar two-loop integrals for vector boson pairs with equal mass [86] and two different masses [89]. In the present chapter we describe the calculation of the full set of two-loop four point

functions relevant to vector boson pair production with two equal masses. A subset of these, the three-point functions with three massive external legs and all massless internal propagators, has already been known for some time in the literature [85, 127]. Very recently also the full set of master integrals with two different external masses have become available [91].

The problem kinematics and notation are described in Section 4.2. Working in dimensional regularisation with $d = 4 - 2\epsilon$ space-time dimensions, we identify the relevant master integrals (MI) and derive differential equations for them employing integration-by-parts (IBP) [38, 39] and Lorentz-invariance (LI) [35] reductions through the Laporta algorithm [43] implemented in the Reduze code [42, 46]. The master integrals are then determined by solving these differential equations [35, 100, 101, 128] and matching generic solutions to appropriate boundary values obtained in special kinematical limits. Improving upon our earlier results [86], we are now transforming the differential equations to a canonical form [105] which renders their integration trivial after an expansion in ϵ . The algorithm applied for this transformation is described in detail in Section 3.3.3, similar procedures have been put forward most recently in [106, 129]. With this, the remaining non-trivial step in the calculation of the master integrals is the determination of the boundary terms, which we describe in Section 4.4. We use a similar setup for our parametrisation and treatment of functions as in the first calculation [87] of non-planar double boxes with this type of external kinematics. In particular, our solutions are described in terms of multiple polylogarithms. We fix the boundary terms of all complicated integrals by imposing a simple set of regularity conditions. The implementation of these conditions and further processing of the multiple polylogarithms relies on computer-algebra implementations of the coproduct augmented symbol formalism [63, 65, 94, 130] and other techniques, which we described in [86, 131]. Section 6.5 contains a discussion of our solutions and the checks we performed on them. In section 4.6 we describe the final form of our analytical results in terms of a particular set of real valued $\text{Li}_{2,2}$, Li_n ($n = 2, 3, 4$) and \ln functions, optimised for fast and stable numerical evaluations. We complement our exact results by expanding them at the production threshold and in the high-energy region. We conclude in Section 6.6 and specify the exact definition of our canonical basis in appendix A. For all algebraic manipulations we made extensive use of FORM [132] and Mathematica [133].

4.2 Notation and reduction to master integrals

We consider the production of two vector bosons V of mass m in the scattering kinematics:

$$q(p_1) + \bar{q}(p_2) \rightarrow V(q_1) + V(q_2), \quad (4.1)$$

where $p_1^2 = p_2^2 = 0$ and $q_1^2 = q_2^2 = m^2$. The Mandelstam invariants are

$$s = (p_1 + p_2)^2, \quad t = (p_1 - q_1)^2, \quad u = (p_2 - q_1)^2, \quad \text{with} \quad s + t + u = 2m^2, \quad (4.2)$$

so that in the physical region relevant for vector-boson pair production we have:

$$s > 4m^2, \quad t < 0, \quad u < 0, \quad \text{with} \quad m^2 > 0. \quad (4.3)$$

We choose to work with dimensionless variables x , y and z defined by

$$s = m^2 \frac{(1+x)^2}{x}, \quad t = -m^2 y, \quad u = -m^2 z, \quad \text{with} \quad \frac{(1+x)^2}{x} - y - z = 2 \quad (4.4)$$

The Landau variable x absorbs a square root $\sqrt{s(s-4m^2)}$ in the differential equations which is associated with the two massive particle threshold.

We organise all Feynman integrals required for the computation of $q\bar{q} \rightarrow VV$ into three different integral families named *Topo A*, *Topo B* and *Topo C*, where the first two topologies are needed to represent respectively the double-boxes with adjacent and non-adjacent massive legs, while the third contains all non-planar integrals. We choose the propagators of the three topologies as listed in Table 4.1.

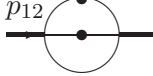
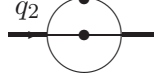

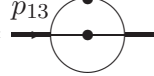
<i>Topo A</i>	<i>Topo B</i>	<i>Topo C</i>
k^2	k^2	k^2
l^2	l^2	l^2
$(k-l)^2$	$(k-l)^2$	$(k-l)^2$
$(k-p_1)^2$	$(k-p_1)^2$	$(k-p_1)^2$
$(l-p_1)^2$	$(l-p_1)^2$	$(l-p_1)^2$
$(k-p_1-p_2)^2$	$(k-p_1+q_1)^2$	$(k-p_1-p_2)^2$
$(l-p_1-p_2)^2$	$(l-p_1+q_1)^2$	$(k-l-q_1)^2$
$(k-p_1-p_2+q_1)^2$	$(k-p_1-p_2+q_1)^2$	$(l-p_1-p_2+q_1)^2$
$(l-p_1-p_2+q_1)^2$	$(l-p_1-p_2+q_1)^2$	$(k-l-p_1-p_2)^2$


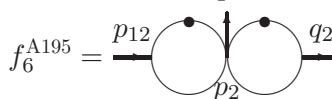
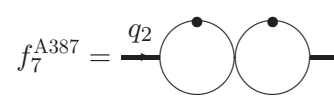
Table 4.1: Propagators in the three different integral families used to represent all two-loop 4-point integrals with two massless and two massive legs with the same mass.

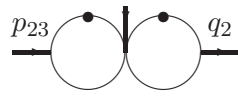
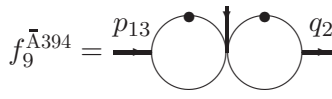
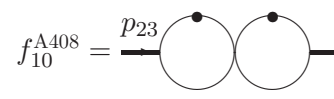
As it is well known, using IBPs, LIs and symmetry relations all Feynman integrals described by these three integral families can be reduced to a small subset, the master integrals. We performed this reduction for all integrals relevant for our process using the automated codes Reduze 1 and Reduze 2 [42, 46, 134, 135]. After the reduction we find that all integrals can be expressed in terms of 75 MIs, some of which are actually not genuinely independent, but can instead be related to each other through a permutation of the external legs $p_1 \leftrightarrow p_2$.


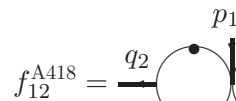
In [86], we described the computation of the MIs embedded in *Topo A* and *Topo B*. In the present work we conclude the computation of all non-planar MIs in *Topo C*.




Applying the algorithm described in Section 3.3.3 we could find a canonical basis for all MIs contributing to both planar and non-planar corrections to $q\bar{q} \rightarrow VV$. In total there are 75 MIs, some of which are not truly independent but instead are related by a permutation of the external legs $p_1 \leftrightarrow p_2$ (or equivalently $q_1 \leftrightarrow q_2$).

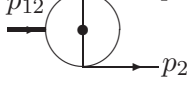
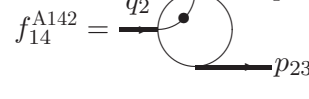
$f_1^{A38} =$ 
 $f_2^{A134} =$ 
 $f_3^{A148} =$ 
 $f_4^{\bar{A}148} =$ 

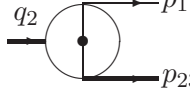
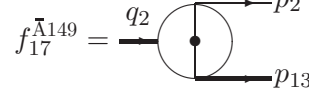

$f_5^{A99} =$ 
 $f_6^{A195} =$ 
 $f_7^{A387} =$ 


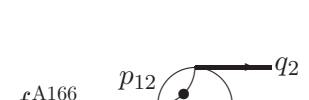
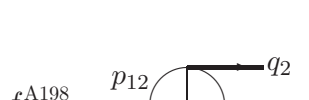
$f_8^{A394} =$ 
 $f_9^{\bar{A}394} =$ 
 $f_{10}^{A408} =$ 

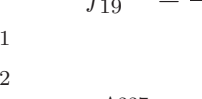
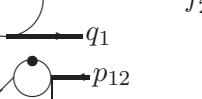
$f_{11}^{\bar{A}408} =$ 
 $f_{12}^{A418} =$ 

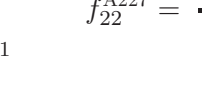
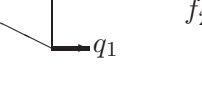
$f_{13}^{A53} =$ 
 $f_{14}^{A142} =$ 
 $f_{15}^{\bar{A}142} =$ 

$f_{16}^{A149} =$ 
 $f_{17}^{\bar{A}149} =$ 

$f_{18}^{A166} =$ 
 $f_{19}^{A166} =$ 
 $f_{20}^{A198} =$ 

$f_{21}^{A198} =$ 
 $f_{22}^{A227} =$ 
 $f_{23}^{A419} =$ 

$f_{24}^{A199} =$ 
 $f_{25}^{A398} =$ 

$f_{26}^{\bar{A}398} =$ 
 $f_{27}^{A422} =$ 

$$\begin{aligned}
f_{28}^{A174} &= \text{Diagram 1} & f_{29}^{A181} &= \text{Diagram 2} & f_{30}^{A181} &= \text{Diagram 3} \\
f_{31}^{\bar{A}181} &= \text{Diagram 4} & f_{32}^{\bar{A}181} &= \text{Diagram 5} & f_{33}^{A182} &= \text{Diagram 6} \\
f_{34}^{A182} &= \text{Diagram 7} & f_{35}^{\bar{A}182} &= \text{Diagram 8} & f_{36}^{\bar{A}182} &= \text{Diagram 9} \\
f_{37}^{A214} &= \text{Diagram 10} & f_{38}^{\bar{A}214} &= \text{Diagram 11} & f_{39}^{A427} &= \text{Diagram 12} \\
f_{40}^{A215} &= \text{Diagram 13} & f_{41}^{\bar{A}215} &= \text{Diagram 14} & f_{42}^{A430} &= \text{Diagram 15} \\
f_{43}^{A247} &= \text{Diagram 16} & f_{44}^{A247} &= \text{Diagram 17} & f_{45}^{A247} &= \text{Diagram 18} \\
f_{46}^{A446} &= \text{Diagram 19} & f_{47}^{A446} &= \text{Diagram 20} \\
f_{48}^{B174} &= \text{Diagram 21} & f_{49}^{\bar{B}174} &= \text{Diagram 22} & f_{50}^{B182} &= \text{Diagram 23} \\
f_{51}^{B213} &= \text{Diagram 24} & f_{52}^{B213} &= \text{Diagram 25} & f_{53}^{B213} &= \text{Diagram 26} \\
f_{54}^{B213} &= \text{Diagram 27} & f_{55}^{B249} &= \text{Diagram 28} & f_{56}^{B215} &= \text{Diagram 29} \\
f_{57}^{\bar{B}215} &= \text{Diagram 30} & f_{58}^{B247} &= \text{Diagram 31} & f_{59}^{B247} &= \text{Diagram 32} \\
f_{60}^{C231} &= \text{Diagram 33} & f_{61}^{C252} &= \text{Diagram 34} & f_{62}^{C318} &= \text{Diagram 35}
\end{aligned}$$

The diagrams represent various Feynman-like structures with external lines labeled p_1, p_2, q_1, q_2 and internal lines with dots or loops. Some diagrams include labels like $(l-p_{123})^2$, $(k)^2$, and $(k-p_1)^2$.

The image displays 15 Feynman diagrams arranged in three rows, each representing a different integral family f_{ij}^C . Thick lines represent massive external particles, and dots indicate additional powers of the corresponding propagator. The diagrams are as follows:

- Row 1:
 - f_{63}^{C126} : A box diagram with external lines p_2, p_1, q_2, q_1 . Internal lines are k and l . Numerator $(k)^2$.
 - f_{64}^{C126} : A box diagram with external lines p_2, p_1, q_2, q_1 . Internal lines are k and l . Numerator $(k)^2$.
 - f_{65}^{C207} : A box diagram with external lines p_1, p_2, q_2, q_1 . Internal lines are k and l . Numerator $(k-l-p_{12})^2$.
- Row 2:
 - f_{66}^{C207} : A box diagram with external lines p_1, p_2, q_2, q_1 . Internal lines are k and l . Numerator $(k-l-p_{12})^2$.
 - f_{67}^{C207} : A box diagram with external lines p_1, p_2, q_2, q_1 . Internal lines are k and l . Numerator $(k-p_{12})^2$.
 - f_{68}^{C207} : A box diagram with external lines p_1, p_2, q_2, q_1 . Internal lines are k and l . Numerator $(l-p_1)^2$.
- Row 3:
 - f_{69}^{C239} : A box diagram with external lines p_1, p_2, q_2, q_1 . Internal lines are k and l . Numerator $(k)^2$.
 - f_{70}^{C239} : A box diagram with external lines p_1, p_2, q_2, q_1 . Internal lines are k and l . Numerator $(l-p_1)^2$.
 - f_{71}^{C254} : A box diagram with external lines p_1, p_2, q_2, q_1 . Internal lines are k and l . Numerator $(k)^2$.
 - f_{72}^{C254} : A box diagram with external lines p_1, p_2, q_2, q_1 . Internal lines are k and l . Numerator $(k)^2$.
 - f_{73}^{C382} : A box diagram with external lines p_1, p_2, q_2, q_1 . Internal lines are k and l . Numerator $(k)^2$.
 - f_{74}^{C382} : A box diagram with external lines p_1, p_2, q_2, q_1 . Internal lines are k and l . Numerator $(k)^2$.
 - f_{75}^{C382} : A box diagram with external lines p_1, p_2, q_2, q_1 . Internal lines are k and l . Numerator $(k)^2$.

Thick lines denote the massive external particles, dots additional powers of the corresponding propagator. We introduced the short-hand notations $p_{ij} = p_i + p_j$ and $p_{ijk} = p_i + p_j + p_k$, where $p_3 = -q_1$. In some cases we denote additional numerators of the integrand, where the definition of the loop momenta k, l is implicitly given by the corresponding integral family in table 4.1. The families \bar{A} and \bar{B} emerge from A and B by swapping the two incoming momenta p_1 and p_2 .

Given any of the integral families $T = A, B, C$ (and the crossed variants), every integral is defined with the integration measure:

$$f_n^T = \left(\frac{S_\epsilon}{16\pi^2} \right)^{-2} (m^2)^{2\epsilon} \int \frac{d^d k}{(2\pi)^d} \frac{d^d l}{(2\pi)^d} \frac{1}{D_{T_1}^{n_1} \dots D_{T_9}^{n_9}}, \quad (4.5)$$

where the indices T_j run over the propagators in the different integral families, $d = 4 - 2\epsilon$ and

$$S_\epsilon = (4\pi)^\epsilon \frac{\Gamma(1+\epsilon) \Gamma^2(1-\epsilon)}{\Gamma(1-2\epsilon)}. \quad (4.6)$$

The transition between $\Re(m^2) > 0$ and $\Re(m^2) < 0$ is understood to be taken with $\Im(m^2) > 0$.

Let us note here that, as already discussed above, the main point of our bottom-up construction of the canonical basis is that we do not need to look at the global properties of the 75×75 matrix, but we can move step by step for increasing values of t , treating separately the differential equations for different sectors which are topologically disentangled from each other. In this sense we need to verify *separately for every topology* that the two requirements of (1) triangularity as $\epsilon \rightarrow 0$, and (2)

linearity in ϵ , are satisfied only for the homogeneous part of the sub-system¹.

Deriving the differential equations for the basis above one immediately sees that:

1. All sub-systems of differential equations, topology by topology, have the property that their homogeneous part is triangular (or even decouples) in the limit $\epsilon \rightarrow 0$.
2. On the other hand *almost* all sub-systems fulfil the property of linearity in ϵ , except six, which are:

$$\begin{aligned} &\{f_{18}^{A166}, f_{19}^{A166}\}, \quad \{f_{20}^{A198}, f_{21}^{A198}\}, \quad \{f_{29}^{A181}, f_{30}^{A181}\}, \\ &\{f_{31}^{\bar{A}181}, f_{32}^{\bar{A}181}\}, \quad \{f_{33}^{A182}, f_{34}^{A182}\}, \quad \{f_{35}^{\bar{A}182}, f_{36}^{\bar{A}182}\}. \end{aligned}$$

In particular the homogeneous systems contain terms proportional to ϵ^2 and $1/(1 - 2\epsilon)$.

In order to put these sub-systems in the right form (note that four of them are equal two-by-two under a permutation of the external momenta) one can proceed in different ways. Since the systems are very simple (in all cases 2×2 systems) one can study directly the homogeneous parts of the latter and, one-by-one, look for appropriate linear combinations of the two MIs which remove the terms in ϵ^2 and $1/(1 - 2\epsilon)$. In particular in the case of sectors 181 and 182 (and their crossing) it is easy to see that these unwanted terms are removed by a simple rescaling of the two masters.

For the first two sectors ($A166$ and $A198$), this is not enough and a proper linear combination of the two MIs in the sector is needed. Nevertheless, having the exact solution for all planar MIs at hand [86] it is clear that, for both sectors, the second MI (the one with a dotted propagator f_{19}^{A166} , f_{21}^{A198}) is already in the right form (i.e. it is a function of uniform transcendentality multiplied by a single rational factor), and therefore must not be changed. This implies that only the scalar MI must be substituted by a linear combination of the two, which can be easily found imposing that also the latter becomes a function of uniform transcendentality multiplied by a single rational factor (or, equivalently, that the homogeneous part of the system contains only a linear dependence on ϵ).

Once the differential equations for these four sectors have been put in the right form we can easily apply our algorithm to all remaining MIs. As a result we get a new basis $\vec{m} = \{m_j\}$ with $j = 1, \dots, 75$ whose differential equations with respect to both external invariants (x, z) are in canonical form. We enclose the explicit definition of the basis expressed in terms of the initial choice of MIs depicted above in Appendix A.

¹Note that, while this is enough to ensure that the property of triangularity is true for the whole system, the same is in general not true for the linearity in ϵ .

4.3.1 Differential equations

Given the basis in Appendix A we can derive differential equations in both independent variables (x, z) . As already anticipated the equations take the canonical form (3.38):

$$d\vec{m}(\epsilon; x, z) = \epsilon dA(x, z) \vec{m}(\epsilon; x, z) \quad (4.7)$$

where the differential d acts on the two variables x, z . The matrix $A(x, z)$ does not depend on ϵ and it can be decomposed as

$$A(x, z) = \sum_{k=1}^{10} A_k \ln(r_k), \quad (4.8)$$

where the A_k are *constant matrices*, whose entries are in particular just *rational numbers*, and the r_k are polynomial functions of (x, z) and constitute the so-called alphabet of the GHPLs which will be needed in order to integrate the equations:

$$r_k = \{ x, 1-x, 1+x, z, 1+z, x-z, 1-xz, \\ 1+x^2-xz, 1+x+x^2-xz, z(1+x+x^2)-x \}. \quad (4.9)$$

Expanding in ϵ , the canonical form ensures full decoupling of the differential equations (4.7) order by order in ϵ . The integration *up to a boundary term* becomes trivial and can be carried out entirely algebraically.

4.4 Integration and boundary conditions

We consider the full system of differential equations for all 75 master integrals in a uniform manner. Our normalisation is such that the solutions for our master integrals have a Taylor expansion,

$$\vec{m}(\epsilon; x, z) = \sum_{i=0}^{\infty} \vec{m}^{(i)}(x, z) \epsilon^i, \quad (4.10)$$

where the weight 0 contributions start at ϵ^0 . We solve the full vector of coefficient functions $\vec{m}^{(i)}$ order by order in ϵ up to and including weight 4.

For master integrals depending on z we choose to integrate the partial differential equation in z for fixed x implied by (4.7). This gives us the solution up to a function of x , which needs to be fixed by additional constraints discussed below. For master integrals independent on z we integrate the partial differential equation in x , which determines the solution up to a constant. It is obvious that this procedure naturally leads to iterated integrals. The $d \ln$ form of the differential equations ensures that the iterated integrals can be expressed in terms of Goncharov's multiple polylogarithms

$$G(w_1, w_2, \dots, w_n; z) \equiv \int_0^z dt \frac{1}{t - w_1} G(w_2, \dots, w_n; t), \quad (4.11)$$

$$G(\underbrace{0, \dots, 0}_n; z) \equiv \frac{1}{n!} \ln^n z. \quad (4.12)$$

Here, the w_i are complex rational functions of the indeterminants. To handle non-linear letters we also employ generalised weights [136].

$$G([f(o)], w_2, \dots, w_n; z) = \int_0^z dt \frac{f'(t)}{f(t)} G(w_2, \dots, w_n; t), \quad (4.13)$$

where $f(o)$ is an irreducible rational polynomial and o is a dummy variable.

In order to fix the boundary terms we use two ingredients. For some of the simplest integrals, namely a small number of tadpole, bubble and triangle integrals, we use their known analytic solutions from the literature [86, 137]. For all other integrals we require the absence of logarithmic divergencies for the solutions in certain kinematical limits. This requires the linear combinations of master integrals multiplying the corresponding $d \ln$ terms in the differential equations to vanish in the respective limit. This completely fixes the remaining boundary terms, i.e. the unknown functions of x respectively the constants.

Since we consider also non-planar integrals it is unavoidable to deal with cuts in s , t and u at the same time, i.e. we have to handle uncrossed and crossed kinematics. From the Feynman parameter representation it is clear that there is a Euclidean region with s , t , u , m^2 all less than zero, such that the integrals are real. From the on-shell relation (4.4) one sees, however, that it is not possible to parametrise this region employing real valued parameters x , z and m^2 . Note that in the scheme [87] employed here, the solutions develop explicit and implicit imaginary parts already during the iterative integration procedure.

We require regularity of each integral in some of the following collinear and, depending on its cut structure, threshold limits:

$$z \rightarrow x, \quad z \rightarrow 1/x, \quad z \rightarrow -1, \quad z \rightarrow (1 + x + x^2)/x, \quad x \rightarrow 1. \quad (4.14)$$

We emphasise that we impose these conditions for points in the unphysical region, the algebraically equivalent limits in the physical region may actually be divergent due to branch cuts. The difference between the two cases lies in the way the signs of the imaginary parts of the parameters needs to be chosen when approaching the respective point, as dictated by the Feynman propagator $i0$ prescription.

We assign a small positive imaginary part to s , t , u and m^2 to fix branch cut ambiguities. While the m^2 dependence is not explicit in our dimensionless master integrals $\vec{m}(\epsilon; x, z)$ anymore, we anticipate its former presence with $\Re(m^2) < 0$. This translates to (small) imaginary parts $\Im(x) > 0$, $\Im(z) < 0$ and $\Im(y) = \Im((1 + x^2 - xz)/x) > 0$. The limits were computed using in-house Mathematica packages for multiple polylogarithms [138, 139], where we employed both, coproduct based and non-coproduct based limit algorithms. In practice we employ small but finite imaginary parts, such that the complex parameters fulfil the on-shell relation (4.4). We match the constants appearing in the limit computations by a numerical fitting procedure. This step utilises the numerical evaluation of multiple polylogarithms [68] in GiNaC [134].

4.5 Solutions and checks

We obtain the solutions in terms of GHPLs of argument z and x with weights respectively

$$G(f(x); z), \quad \text{with} \quad f(x) = \left\{ 0, -1, x, \frac{1}{x}, \frac{(1+x^2)}{x}, \frac{x}{(1+x+x^2)}, \frac{(1+x+x^2)}{x} \right\},$$

and

$$G(n; x), \quad \text{with} \quad n = \{0, -1, 1, [1+o^2], [1+o+o^2]\}.$$

The explicit expressions are rather lengthy and therefore we do not write them here explicitly but refer to the ancillary files of the arXiv submission of [90].

We performed several checks on the results. First of all, we integrated the whole 75×75 system of differential equations at once, fixing consistently all boundary conditions using the limits described above. We explicitly verified that our solutions fulfil the partial differential equations both in x and in z . This is a non-trivial check for integrals depending on both variables, for which we fixed x -dependent boundary terms by regularity conditions.

As a subset of the integrals considered here, we re-calculated all non-trivial planar master integrals presented in [86]. Taking $z' \rightarrow z' + i0$ and swapping masters 3 and 4 of sector B213 in the result of that reference, we translate these expressions to our new functional basis and find perfect agreement at the analytical level.

For the previously unknown non-planar master integrals we compared our results against numerical samples obtained with the sector decomposition program SecDec2 [51, 140]. We found the program particularly useful since it allowed us to perform checks of our results both in the Euclidean and in the physical region. In the Euclidean region we set x to a truly complex number. Note that to obtain a real number at all consists already in a very non-trivial check of our solution. In particular, we could verify all our master integrals in the Euclidean region with a typical precision of at least 4 digits for the weight 4 coefficients. On the other hand, the numerical evaluation by sector decomposition in the Minkowski region was much more cumbersome. Using SecDec2 we could evaluate all *scalar integrals* (integrals with no dots nor scalar products) up to weight 4, finding good agreement with our result. For sectors involving more than one master integral we additionally considered integrals with dots and/or scalar products. For them we could check at least the weight 3 contributions, in some cases also the weight 4 parts. The combination of these checks in the Euclidean and in the Minkowski region provides stringent evidence for the correctness of our results.

4.6 Real valued functions and expansions

For the purpose of numerical evaluation in the physical region the primary form of our solutions is not optimal yet, e.g. because the multiple polylogarithms are not single valued and their numerical evaluation is not straightforward. We follow the procedure described in [64] and project onto a new functional basis which consists of $\text{Li}_{2,2}$, classical polylogarithms Li_n ($n = 2, 3, 4$) and logarithms. The Li-functions are related to the G -functions via

$$\text{Li}_n(x_1) = -G(\underbrace{0, \dots, 0}_n, 1; x_1), \quad \text{Li}_{2,2}(x_1, x_2) = G\left(0, \frac{1}{x_1}, 0, \frac{1}{x_1 x_2}; 1\right). \quad (4.15)$$

In our new functional basis we allow for rather complicated rational functions of x and z . We choose them such that the functions are real valued and the imaginary parts of the solutions are explicit over the entire physical domain.

In [131] it was demonstrated that this method works also in the presence of generalised weights, which could in fact be eliminated at the level of the amplitude. In the present case we work at the level of the master integrals. Also here, we successfully apply this projection onto real valued functions and eliminate all generalised weights $\{[1 + o^2], [1 + o + o^2]\}$ using a coproduct based algorithm.

We can actually go one step further and restrict the target function space even more. For the functions $\text{Li}_n(x_1)$, $\text{Li}_{2,2}(x_1, x_2)$ we select real arguments with

$$|x_1| < 1, \quad |x_1 x_2| < 1. \quad (4.16)$$

In this way, the multiple polylogarithms are not only real valued but correspond directly to a convergent power series expansion

$$\text{Li}_n(x_1) = - \sum_{j_1=1}^{\infty} \frac{x_1^{j_1}}{j_1^n}, \quad (4.17)$$

$$\text{Li}_{2,2}(x_1, x_2) = \sum_{j_1=1}^{\infty} \sum_{j_2=1}^{\infty} \frac{x_1^{j_1}}{(j_1 + j_2)^2} \frac{(x_1 x_2)^{j_2}}{j_2^2} \quad (4.18)$$

see e.g. eq. (20) of [68]. While it is not a priori obvious that such a restricted set of functions is sufficient to represent our master integrals, we find that this is indeed the case. Our choice of functions drastically improves the numerical evaluation time, since it avoids additional transformations which would be required otherwise to map to an appropriate expansion. Evaluating all master integrals discussed here takes only fractions of a second in a generic phase space point on a single core.

For completeness, we also expand our solutions both at the production threshold and in the small mass region. The threshold region is characterised by $\beta \rightarrow 0$ for fixed $\cos \theta$, where $\beta = \sqrt{1 - 4m^2/s}$ is the velocity of each vector boson and θ the scattering angle in the center-of-mass frame, such that $z = 1 + 2\beta(\beta + \cos \theta)/(1 - \beta^2)$.

We find it convenient to directly expand our full solutions in the real-valued function representation, rather than the individual G -functions. The expansion contains β , $\ln \beta$, GHPLs of argument $\cos \theta$ and weights $\{-1, 1\}$ as well as the constants $\ln(2)$ and $\text{Li}_4(1/2)$. Similarly, we consider the small mass limit $m^2/s \rightarrow 0$ for fixed $\phi = -(t - m^2)/s$. The expansion contains m^2/s , $\ln(m^2/s)$ and GHPLs of argument ϕ and weights $\{0, 1\}$. The first couple of orders for both expansions as well as our results in terms of real-valued functions are provided via ancillary files on the arXiv, see [90].

4.7 Conclusions

We computed the full set of master integrals relevant to the two-loop QCD corrections to the production of two vector bosons of equal mass in the collision of massless partons. These two-loop four-point functions are computed using the differential equation method [35, 100, 101, 128]. Having cast the differential equations in canonical basis, they can be solved in an elegant and compact manner in terms of iterated integrals. These general solutions are then matched onto appropriate boundary values, requiring non-trivial transformations of the iterated integrals. Our analytical results for all master integrals are expressed in terms of multiple polylogarithms, they are provided with the arXiv submission of [90]. We find that it is possible to employ a restricted set of multiple polylogarithms, which allows for a particularly fast and precise numerical evaluation. We validated our solutions against numerical samples obtained using sector decomposition.

With the full set of master integrals derived here, it is now possible to derive the two-loop corrections to the amplitudes for $q\bar{q} \rightarrow W^+W^-$ and $q\bar{q} \rightarrow ZZ$, and to compute the NNLO corrections to the pair production of massive vector bosons. In particular we have recently completed the computation of the NNLO QCD corrections to total cross section for on-shell ZZ production, see [110] and Chapter 7. The case of WW production is currently under study. Combined with precision measurements of these observables at the LHC, these results will allow for a multitude of tests of the electroweak theory at unprecedented precision.

Chapter 5

The MIs of the two-loop massive sunrise graph

The results presented in this chapter are entirely based on a collaboration with E. Remiddi and appeared for the first time in [37].

5.1 Introduction

The Feynman integrals associated to the two-loop loop self-mass Feynman graph of Fig.(5.1), usually referred to as *sunrise*, have been widely studied in the literature within the framework of the integration by parts identities [38, 39], and it is by now well known that they can be expressed in terms of four Master Integrals (MIs), [141], which satisfy a system of four first-order coupled differential equations, [128] (equivalent to a single fourth-order differential equation for any of the Master Integrals). Several numerical approaches to the numerical solution of the equations with satisfactory degree of precision have been worked out, (see for instance [142]), but a complete treatment of the general case with three different masses in $d = 4$ dimensions is still missing.

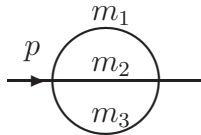


Figure 5.1: The two-loop sunrise.

In the equal mass case the number of independent Master Integrals reduces to two, so that the two by two first-order system of differential equations can be rewritten as a single second-order differential equation for one of the Master Integrals, say the full scalar amplitude (see below). In Ref. [77] it is shown how to build the analytic solution of that equation in terms of elliptic integrals, both for $d = 2$ and $d = 4$; the two cases,

related by the Tarasov's shifting relations [47], are very similar, with the $d = 2$ case just marginally simpler than the $d = 4$ case. The analytic solution provides with the necessary information for writing out very precise and fast converging expansions for the accurate numerical evaluation of the two MIs [143].

More recently, an interesting paper [144] has shown, by using algebraic geometry arguments, that in $d = 2$ dimensions the full scalar amplitude satisfies a second-order differential equation also in the different mass case. The equation was then solved in [79] by suitably extending the method of [77]; let us observe here that the analytic solution of the second-order differential equation is equivalent to the analytic knowledge of two (of the four) Master Integrals of the sunrise with different masses.

The problem of extending the approach to $d = 4$, which is the physically relevant case, remains, as the straightforward use of the Tarasov's dimension-shifting relations is unfortunately not sufficient. Indeed, as will be shown in this chapter, by explicitly working out the shifting relations one finds that any of the four Master Integrals at $d \approx 4$ dimensions can be expressed as a combination of *all* the four Master Integrals at $d \approx 2$ dimensions and of the first terms of their expansion in $(d - 2)$, while the results of [144] give only two of the four Master Integrals at exactly $d = 2$ dimensions, but no other information on the remaining Master Integrals and their expansion in $(d - 2)$.

We introduce a family of particular polynomials in the scalar products of the vectors occurring in the Feynman integrals, dubbed *Schouten polynomials*, which have the property of vanishing at some fixed integer value of the dimension d . By using those polynomials one can introduce an *ad hoc* set of amplitudes, from which one can at least in principle extract an independent set of new amplitudes which vanish in a non trivial way (see below) at that value of d (say at $d = N$ for definiteness). If those new amplitudes are expressed in terms of the previously chosen set of Master Integrals, their vanishing gives a set of relations between the Master Integrals, valid at $d = N$, which we call *Schouten identities*. Alternatively, one can introduce a new set of Master Integrals including as new Master Integrals some of the independent amplitudes vanishing at $d = N$, write the system of differential equations satisfied by the new set of Master Integrals and expand them recursively in powers of $(d - N)$ around $d = N$. As some of the new Master Integrals vanish at $d = N$, the system of equations takes a simpler block structure.

The pattern is very general, and applies in principle to the integrals of any Feynman graph. We work out explicitly the case of the sunrise amplitudes at $d = 2$ with different masses, finding the existence of two independent Schouten identities, *i.e.* of two independent relations between the usual Master Integrals at $d = 2$, or, which is the same, we can introduce a new set of Master Integrals, consisting of two “conventional” Master Integrals (say the full scalar amplitude and another MI) and two new Master Integrals vanishing at $d = 2$. The system of differential equations satisfied by the new set of Master Integrals can then be expanded in powers of $(d - 2)$. At zeroth-order we find a two by two system for the two “conventional” MIs (the other two Master Integrals vanish), equivalent to the second-order equation found in [144],

while at first-order in $(d-2)$ we find in particular two relatively simple equations for the first terms of the expansion of the two new MIs, in which the zeroth-orders of the two “conventional” MIs appear as non homogeneous known terms.

One can move from $d \approx 2$ to the physically more interesting $d \approx 4$ case by means of the Tarasov’s shifting relations; it is found that for obtaining the zeroth-order term in $(d-4)$ of all the four MIs (of the old or of the new set) at $d \approx 4$ one needs, besides the zeroth-order term in $(d-2)$ of the two “old” MIs at $d \approx 2$, also the first term in $(d-2)$ of the new MIs.

The plan of the chapter is as follows: in sec. 2.2.5 we introduce the Schouten polynomials for an arbitrary number of dimensions, while their applications to Feynman Amplitudes is discussed in sec. 5.2. In sec. 5.3 we show how, by using the Schouten Identities, a new set of Master Integrals can be found, whose differential equations in $d = 2$ take an easier block form and can be therefore re-casted (see sec. 5.4) as a second-order differential equation for one of the Masters. In sec. 5.5 we show how the results at $d \approx 4$ can be recovered from those at $d \approx 2$ through Tarasov’s shifting relations. Finally, in sec. 5.6, which is somewhat pedagogical, we present a thorough treatment of the imaginary parts of the Master Integrals in $d = 2$ and $d = 4$ dimensions. Many lengthy formulas and some explicit derivations can be found in the Appendices.

5.2 The Schouten Identities for the Sunrise graph

We discuss in this Section the use of the Schouten polynomial $P_3(d; a, b, c)$ introduced in Section 2.2.5 in the case of the sunrise, the two-loop self-mass graph of Fig.(1).

The external momentum is p and the internal masses are m_1, m_2, m_3 . We use the Euclidean metric, so that p^2 is positive when spacelike; sometimes we will use also $s = W^2 = -p^2$, so that the sunrise amplitudes develop an imaginary part when $\sqrt{s} = W > (m_1 + m_2 + m_3)$, the threshold of the Feynman graph. We write the propagators as

$$\begin{aligned} D_1 &= q_1^2 + m_1^2, \\ D_2 &= q_2^2 + m_2^2, \\ D_3 &= (p - q_1 - q_2)^2 + m_3^2, \end{aligned} \tag{5.2.1}$$

and define the loop integration measure, in agreement with previous works, as:

$$\int \mathfrak{D}^d q = \frac{1}{C(d)} \int \frac{d^d q}{(2\pi)^{d-2}}, \tag{5.2.2}$$

with

$$C(d) = (4\pi)^{(4-d)/2} \Gamma\left(3 - \frac{d}{2}\right), \tag{5.2.3}$$

so that

$$C(2) = 4\pi \quad \text{and} \quad C(4) = 1 . \quad (5.2.4)$$

With that definition the Tadpole $T(d, m)$ reads

$$T(d; m) = \int \mathfrak{D}^d q \frac{1}{q^2 + m^2} = \frac{m^{d-2}}{(d-2)(d-4)} . \quad (5.2.5)$$

In what follows we will use the “double” tadpoles

$$T(d; m_1, m_2) = \int \mathfrak{D}^d q_1 \mathfrak{D}^d q_2 \frac{1}{D_1 D_2} , \quad (5.2.6)$$

together with the similarly defined $T(d; m_1, m_3)$, $T(d; m_2, m_3)$, and the four amplitudes

$$\begin{aligned} S(d; p^2) &= \int \mathfrak{D}^d q_1 \mathfrak{D}^d q_2 \frac{1}{D_1 D_2 D_3} , \\ S_1(d; p^2) &= -\frac{d}{dm_1^2} S(d; p^2) = \int \mathfrak{D}^d q_1 \mathfrak{D}^d q_2 \frac{1}{D_1^2 D_2 D_3} , \\ S_2(d; p^2) &= -\frac{d}{dm_2^2} S(d; p^2) = \int \mathfrak{D}^d q_1 \mathfrak{D}^d q_2 \frac{1}{D_1 D_2^2 D_3} , \\ S_3(d; p^2) &= -\frac{d}{dm_3^2} S(d; p^2) = \int \mathfrak{D}^d q_1 \mathfrak{D}^d q_2 \frac{1}{D_1 D_2 D_3^2} . \end{aligned} \quad (5.2.7)$$

All those amplitudes depend on the three masses m_1, m_2, m_3 , even if the masses are not written explicitly in the arguments for simplicity. The four amplitudes are equal, when multiplied by an overall constant factor $(2\pi)^4$, to the four MIs used in [128]. $S(d; p^2)$, in particular, is the full scalar amplitude already referred to previously. Those amplitudes were chosen in [128] as MIs for the sunrise problem, and in the following they will be sometimes referred to as the “conventional” MIs .

We can now introduce the *Schouten amplitudes* defined, for arbitrary d , as

$$Z(d; n_1, n_2, n_3, p^2) = \int \mathfrak{D}^d q_1 \mathfrak{D}^d q_2 \frac{P_3(d; p, q_1, q_2)}{D_1^{n_1} D_2^{n_2} D_3^{n_3}} , \quad (5.2.8)$$

where the n_i are positive integer numbers and $P_3(d; p, q_1, q_2)$ is the Schouten polynomial defined in Eq.(2.31). The convergence of the integrals, for a given value of d , depends of course on the powers n_i , as the Schouten polynomial in the numerator contributes always with four powers of the loop momenta q_1 and q_2 .

We are interested here in the $d = 2$ case. If the Schouten amplitude is convergent at $d = 2$, due to Eq.(2.32), it is also vanishing at $d = 2$, *i.e.* $Z(2; n_1, n_2, n_3, p^2) = 0$. Note that in the massive case all the integrals we are considering are *i.r.* finite, therefore the divergences can only be of *u.v.* nature.

As one can express any sunrise Feynman amplitude in terms of a valid set of MIs, we will write in the following a few Schouten amplitudes in terms of the “conventional” MIs given in Eq.s(5.2.7). A few explicit results are now listed:

$$\begin{aligned}
Z_1(d; p^2) &= Z(d; 1, 2, 2) \\
&= \frac{(d-1)}{12} [-(d-2)p^2 + (d-3)(-2m_1^2 + m_2^2 + m_3^2)] S(d; p^2) \\
&\quad - \frac{(d-1)}{6} (p^2 + m_1^2) m_1^2 S_1(d; p^2) \\
&\quad + \frac{(d-1)}{12} (p^2 - 3m_1^2 + m_2^2 + 3m_3^2) m_2^2 S_2(d; p^2) \\
&\quad + \frac{(d-1)}{12} (p^2 - 3m_1^2 + 3m_2^2 + m_3^2) m_3^2 S_3(d; p^2) \\
&\quad + \frac{(d-1)(d-2)}{24} [T(d; m_1, m_2) + T(d; m_1, m_3) - 2T(d; m_2, m_3)] , \quad (5.2.9)
\end{aligned}$$

$$\begin{aligned}
Z_2(d; p^2) &= Z(d; 2, 1, 2, p^2) \\
&= \frac{(d-1)}{12} [-(d-2)p^2 + (d-3)(m_1^2 - 2m_2^2 + m_3^2)] S(d; p^2) \\
&\quad + \frac{(d-1)}{12} (p^2 + m_1^2 - 3m_2^2 + 3m_3^2) m_1^2 S_1(d; p^2) \\
&\quad - \frac{(d-1)}{6} (p^2 + m_2^2) m_2^2 S_2(d; p^2) \\
&\quad + \frac{(d-1)}{12} (p^2 + 3m_1^2 - 3m_2^2 + m_3^2) m_3^2 S_3(d; p^2) \\
&\quad + \frac{(d-1)(d-2)}{24} [T(d; m_1, m_2) - 2T(d; m_1, m_3) + T(d; m_2, m_3)] , \quad (5.2.10)
\end{aligned}$$

$$\begin{aligned}
Z_3(d; p^2) &= Z(d; 2, 2, 1, p^2) \\
&= \frac{(d-1)}{12} [-(d-2)p^2 + (d-3)(m_1^2 + m_2^2 - 2m_3^2)] S(d; p^2) , \\
&\quad + \frac{(d-1)}{12} (p^2 + m_1^2 + 3m_2^2 - 3m_3^2) m_1^2 S_1(d; p^2) \\
&\quad + \frac{(d-1)}{12} (p^2 + 3m_1^2 + m_2^2 - 3m_3^2) m_2^2 S_2(d; p^2) \\
&\quad - \frac{(d-1)}{6} (p^2 + m_3^2) m_3^2 S_3(d; p^2) \\
&\quad + \frac{(d-1)(d-2)}{24} [-2T(d; m_1, m_2) + T(d; m_1, m_3) + T(d; m_2, m_3)] , \quad (5.2.11)
\end{aligned}$$

$$\begin{aligned}
Z(d; 2, 2, 2, p^2) = & -\frac{(d-1)(d-2)}{4} \\
& \times \left[(d-3)S(d; p^2) + m_1^2 S_1(d; p^2) + m_2^2 S_2(d; p^2) + m_3^2 S_3(d; p^2) \right] .
\end{aligned}
\tag{5.2.12}$$

Some comments are in order. Elementary power counting arguments give $N = 2(n_1 + n_2 + n_3)$ powers of the integration momenta in the denominator (independently of d) and, in $d = 2$ dimensions, all together eight powers in the numerator (see Eq.(5.2.8) for the definition of the integrals), so that the minimum value of N necessary to guarantee the convergence is $N = 10$. In the case of $Z(d; 2, 2, 2, p^2)$ of Eq.(5.2.12) $N = 12$, more than the minimum required value $N = 10$; therefore the integrals in the loop momenta q_1, q_2 do converge, so that the vanishing of $P_3(d; p, q_1, q_2)$ in the numerator at $d = 2$ (and, as a matter of fact at $d = 1$ as well) does imply the vanishing of the whole amplitude. The explicit result, Eq.(5.2.12), shows indeed that the amplitude vanishes at $d = 1$ and $d = 2$, but that is due to an overall factor $(d-1)(d-2)$, so that Eq.(5.2.12) does not give any useful information. This pattern – the vanishing at $d = 2$ of the amplitudes with $P_3(d; p, q_1, q_2)$ in the numerator and $N > 10$ due to the appearance of an overall factor $(d-2)$ – is of general nature, and showed up in all the cases which we were able to check (needless to say, the algebraic complications increase quickly with the powers of the denominators).

The $Z_i(d; p^2)$, Eq.s(5.2.9,5.2.10,5.2.11), are more interesting; in this case, $N = 10$, which is the minimum value needed to guarantee convergence in $d = 2$ dimensions, so that those amplitudes are expected to vanish at $d = 2$ (and therefore also at $d = 1$) as a consequence of the vanishing of $P_3(d; p, q_1, q_2)$ at $d = 1, d = 2$. The vanishing at $d = 1$ is trivially given by the overall factor $(d-1)$ (in $d = 1$ the minimum value of N to guarantee convergence is $N = 8$, while in the integrals we are now considering $N = 10$), but the vanishing at $d = 2$ is totally non trivial, providing new (and so far not known) relations between the four conventional MIs $S(d; p^2), S_i(d; p^2)$ at $d = 2$.

Any of the three amplitudes $Z_i(d; p^2)$ can obviously be obtained from the others by a suitable permutation of the three masses, as immediately seen from their explicit expression. When summing the three relations, one obtains

$$Z_1(d; p^2) + Z_2(d; p^2) + Z_3(d; p^2) = -\frac{(d-1)(d-2)}{4} p^2 S(d; p^2) , \tag{5.2.13}$$

showing that at $d = 2$ they are not independent from each other; indeed, if one takes as input $Z_2(2; p^2) = 0$ and $Z_3(2; p^2) = 0$, the previous equation gives $Z_1(2; p^2) = 0$, showing that the condition $Z_1(2; p^2) = 0$ depends on the other two. When written explicitly, the vanishing of $Z_2(2; p^2) = 0$ and $Z_3(2; p^2) = 0$ reads

$$\begin{aligned}
Z_2(2; p^2) &= -\frac{1}{12}(m_1^2 - 2m_2^2 + m_3^2)S(2; p^2) \\
&\quad + \frac{1}{12}(p^2 + m_1^2 - 3m_2^2 + 3m_3^2) m_1^2 S_1(2; p^2) \\
&\quad - \frac{1}{6}(p^2 + m_2^2) m_2^2 S_2(2; p^2) \\
&\quad + \frac{1}{12}(p^2 + 3m_1^2 - 3m_2^2 + m_3^2) m_3^2 S_3(2; p^2) \\
&\quad + \frac{1}{96} \ln \frac{m_2^2}{m_1 m_3} \\
&= 0 ,
\end{aligned} \tag{5.2.14}$$

$$\begin{aligned}
Z_3(2; p^2) &= -\frac{1}{12}(m_1^2 + m_2^2 - 2m_3^2)S(2; p^2) , \\
&\quad + \frac{1}{12}(p^2 + m_1^2 + 3m_2^2 - 3m_3^2) m_1^2 S_1(2; p^2) \\
&\quad + \frac{1}{12}(p^2 + 3m_1^2 + m_2^2 - 3m_3^2) m_2^2 S_2(2; p^2) \\
&\quad - \frac{1}{6}(p^2 + m_3^2) m_3^2 S_3(2; p^2) \\
&\quad + \frac{1}{96} \ln \frac{m_3^2}{m_1 m_2} \\
&= 0 .
\end{aligned} \tag{5.2.15}$$

The validity of identities Eq.s(5.2.14,5.2.15) in $d = 2$ has been checked with SecDec [51]. By using the above relations, which hold identically in p^2, m_1^2, m_2^2, m_3^2 , one can express two of the conventional MIs in terms of the other two, showing that, at $d = 2$, there are in fact only two independent MIs. As can be seen from Eq.s(5.2.14,5.2.15), the relations between the MIs are not trivial (in particular, none of the MIs vanishes at $d = 2$; according to the definition Eq.(5.2.7) for space-like p they are all positive definite).

5.3 A New Set of Master Integrals

We have seen in the previous Section that the “conventional” MIs in $d = 2$ dimensions satisfy two independent conditions, written explicitly in Eq.s(5.2.14,5.2.15), so that two of them can be expressed as a combination of the other two, which can be taken as independent. On the other hand, it is known that in the equal mass limit the Sunrise has two independent MIs (in any dimension, including $d = 2$) so that no other independent conditions can exist. It can therefore be convenient to introduce a new set of MIs, formed by two “conventional” MIs , say

$S(d; p^2)$, $S_1(d; p^2)$ of Eq.(5.2.7), and two Schouten amplitudes, say $Z_2(d; p^2)$, $Z_3(d; p^2)$ of Eq.s(5.2.10,5.2.11). The advantage of the choice is that two conditions at $d = 2$ take the simple form $Z_2(2; p^2) = 0$, $Z_3(2; p^2) = 0$. The actual choice of the new MIs satisfying the above criteria is of course not unique (a fully equivalent set could be for instance $S(d; p^2)$, $S_2(d; p^2)$, $Z_1(d; p^2)$, $Z_2(d; p^2)$ etc.).

In the new basis of MIs, the two discarded conventional MIs are expressed as

$$\begin{aligned}
P(p^2, m_1, m_2, m_3) m_2^2 S_2(d; p^2) = & \\
& \left\{ (m_1^2 - m_2^2) [(d-3)(m_1^2 + m_2^2 - m_3^2) - p^2] - (d-2)p^2(p^2 + m_3^2) \right\} S(d; p^2) \\
& + P(p^2, m_2, m_1, m_3) m_1^2 S_1(d; p^2) \\
& - \frac{8}{(d-1)} (p^2 + m_3^2) Z_2(d; p^2) \\
& - \frac{4}{(d-1)} (p^2 + 3m_1^2 - 3m_2^2 + m_3^2) Z_3(d; p^2) \\
& - (d-2) (m_1^2 - m_2^2) T(d; m_1, m_2) \\
& - \frac{(d-2)}{2} (p^2 - m_1^2 + m_2^2 + m_3^2) T(d; m_1, m_3) \\
& + \frac{(d-2)}{2} (p^2 + m_1^2 - m_2^2 + m_3^2) T(d; m_2, m_3) , \tag{5.3.1}
\end{aligned}$$

$$\begin{aligned}
P(p^2, m_1, m_2, m_3) m_3^2 S_3(d; p^2) = & \\
& \left\{ (m_1^2 - m_3^2) [(d-3)(m_1^2 - m_2^2 + m_3^2) - p^2] - (d-2)p^2(p^2 + m_2^2) \right\} S(d; p^2) \\
& + P(p^2, m_3, m_1, m_2) m_1^2 S_1(d; p^2) \\
& - \frac{4}{(d-1)} (p^2 + 3m_1^2 + m_2^2 - 3m_3^2) Z_2(d; p^2) \\
& - \frac{8}{(d-1)} (p^2 + m_2^2) Z_3(d; p^2) \\
& - \frac{(d-2)}{2} (p^2 - m_1^2 + m_2^2 + m_3^2) T(d; m_1, m_2) \\
& - (d-2) (m_1^2 - m_3^2) T(d; m_1, m_3) \\
& + \frac{(d-2)}{2} (p^2 + m_1^2 + m_2^2 - m_3^2) T(d; m_2, m_3) , \tag{5.3.2}
\end{aligned}$$

where $P(p^2, m_1, m_2, m_3)$ is the polynomial

$$\begin{aligned}
P(p^2, m_1, m_2, m_3) = & p^4 + 2(m_2^2 + m_3^2 - m_1^2)p^2 \\
& - 3m_1^4 + m_2^4 + m_3^4 + 2m_1^2m_2^2 + 2m_1^2m_3^2 - 2m_2^2m_3^2 . \tag{5.3.3}
\end{aligned}$$

Note that $P(p^2, m_1, m_2, m_3)$, which is symmetric in the last two arguments,

$$P(p^2, m_1, m_2, m_3) = P(p^2, m_1, m_3, m_2) , \tag{5.3.4}$$

occurs with different arguments in different places.

By substituting the above expressions in the differential equations for the conventional MIs as given, for instance, in Ref. [128], one obtains the new equations

$$\begin{aligned}
P(p^2, m_1, m_2, m_3) p^2 \frac{d}{dp^2} S(d; p^2) = & (p^2 + m_1^2) \left[(p^2 - m_1^2 + m_2^2 + m_3^2) \right. \\
& + (d-2)(p^2 + m_1^2 - m_2^2 - m_3^2) \left. \right] S(d; p^2) \\
& - Q(p^2, m_1, m_2, m_3) m_1^2 S_1(d; p^2) \\
& + \frac{4}{(d-1)} (3p^2 + 3m_1^2 + m_2^2 - m_3^2) Z_2(d; p^2) \\
& + \frac{4}{(d-1)} (3p^2 + 3m_1^2 - m_2^2 + m_3^2) Z_3(d; p^2) \\
& + \frac{(d-2)}{2} (p^2 + m_1^2 - m_2^2 + m_3^2) T(d; m_1, m_2) \\
& + \frac{(d-2)}{2} (p^2 + m_1^2 + m_2^2 - m_3^2) T(d; m_1, m_3) \\
& - (d-2) (p^2 + m_1^2) T(d; m_2, m_3) , \tag{5.3.5}
\end{aligned}$$

$$\begin{aligned}
D(p^2, m_1, m_2, m_3) P(p^2, m_1, m_2, m_3) p^2 \frac{d}{dp^2} S_1(d; p^2) = & \\
& \left[\frac{(d-2)^2}{2} (p^2 + m_1^2 - m_2^2 - m_3^2) P_{10}^{(2)}(p^2, m_1, m_2, m_3) \right. \\
& - (d-2) P_{10}^{(1)}(p^2, m_1, m_2, m_3) - P_{10}^{(0)}(p^2, m_3, m_1, m_2) \left. \right] S(d; p^2) \\
& + \left[\frac{(d-2)}{2} P_{11}^{(1)}(p^2, m_1, m_2, m_3) - P_{11}^{(0)}(p^2, m_1, m_2, m_3) \right] S_1(d; p^2) \\
& + \frac{4(d-3)}{(d-1)} \left[P_{12}^{(0)}(p^2, m_1, m_2, m_3) Z_2(d; p^2) + P_{12}^{(0)}(p^2, m_1, m_3, m_2) Z_3(d; p^2) \right] \\
& + \frac{(d-2)}{4} \left[\frac{(d-2)}{m_1^2} P_{14}^{(2)}(p^2, m_1, m_2, m_3) - 2 P_{14}^{(1)}(p^2, m_1, m_2, m_3) \right] T(d; m_1, m_2) \\
& + \frac{(d-2)}{4} \left[\frac{(d-2)}{m_1^2} P_{14}^{(2)}(p^2, m_1, m_3, m_2) - 2 P_{14}^{(1)}(p^2, m_1, m_3, m_2) \right] T(d; m_1, m_3) \\
& - \frac{(d-2)}{2} \left[(d-2) P_{10}^{(2)}(p^2, m_1, m_2, m_3) \right. \\
& \left. - \left(P_{14}^{(1)}(p^2, m_1, m_2, m_3) + P_{14}^{(1)}(p^2, m_1, m_3, m_2) \right) \right] T(d; m_2, m_3) , \tag{5.3.6}
\end{aligned}$$

$$\begin{aligned}
P(p^2, m_1, m_2, m_3) p^2 \frac{d}{dp^2} Z_2(d; p^2) = & p^2 \frac{(d-1)(d-2)}{8} \left[2 (m_1^2 - m_2^2) (p^2 + m_1^2 + m_2^2 - m_3^2) \right. \\
& + (d-2) (p^2 + m_1^2 - m_2^2 - m_3^2) (p^2 + m_1^2 - m_2^2 + m_3^2) \left. \right] S(d; p^2) \\
& - p^2 \frac{(d-1)(d-2)}{4} P(p^2, m_2, m_1, m_3) m_1^2 S_1(d; p^2)
\end{aligned}$$

$$\begin{aligned}
& + \frac{(d-2)}{2} P_{22}(p^2, m_1, m_2, m_3) Z_2(d; p^2) \\
& + p^2 (d-2) (p^2 + 3m_1^2 - 3m_2^2 + m_3^2) Z_3(d; p^2) \\
& + p^2 \frac{(d-1)(d-2)^2}{4} (m_1^2 - m_2^2) T(d; m_1, m_2) \\
& + p^2 \frac{(d-1)(d-2)^2}{8} (p^2 - m_1^2 + m_2^2 + m_3^2) T(d; m_1, m_3) \\
& - p^2 \frac{(d-1)(d-2)^2}{8} (p^2 + m_1^2 - m_2^2 + m_3^2) T(d; m_2, m_3) , \\
\end{aligned} \tag{5.3.7}$$

$$\begin{aligned}
P(p^2, m_1, m_2, m_3) p^2 \frac{d}{dp^2} Z_3(d; p^2) = & p^2 \frac{(d-1)(d-2)}{8} \left[2 (m_1^2 - m_3^2) (p^2 + m_1^2 - m_2^2 + m_3^2) \right. \\
& + (d-2) (p^2 + m_1^2 - m_2^2 - m_3^2) (p^2 + m_1^2 + m_2^2 - m_3^2) \left. \right] S(d; p^2) \\
& - p^2 \frac{(d-1)(d-2)}{4} P(p^2, m_3, m_1, m_2) m_1^2 S_1(d; p^2) \\
& + p^2 (d-2) (p^2 + 3m_1^2 + m_2^2 - 3m_3^2) Z_2(d; p^2) \\
& + \frac{(d-2)}{2} P_{22}(p^2, m_1, m_3, m_2) Z_3(d; p^2) \\
& + p^2 \frac{(d-1)(d-2)^2}{8} (p^2 - m_1^2 + m_2^2 + m_3^2) T(d; m_1, m_2) \\
& + p^2 \frac{(d-1)(d-2)^2}{4} (m_1^2 - m_3^2) T(d; m_1, m_3) \\
& - p^2 \frac{(d-1)(d-2)^2}{8} (p^2 + m_1^2 + m_2^2 - m_3^2) T(d; m_2, m_3) . \\
\end{aligned} \tag{5.3.8}$$

In the above equations,

$$\begin{aligned}
D(p^2, m_1, m_2, m_3) = & (p^2 + (m_1 + m_2 + m_3)^2)(p^2 + (m_1 - m_2 + m_3)^2) \\
& (p^2 + (m_1 + m_2 - m_3)^2)(p^2 + (m_1 - m_2 - m_3)^2) \\
\end{aligned} \tag{5.3.9}$$

is the product of all the threshold and pseudo-threshold factors already present in [128],

$$\begin{aligned}
Q(p^2, m_1, m_2, m_3) = & 3p^4 + 2p^2 (m_1^2 + m_2^2 + m_3^2) \\
& - (m_1 + m_2 + m_3)(m_1 - m_2 + m_3)(m_1 + m_2 - m_3)(m_1 - m_2 - m_3) , \\
\end{aligned} \tag{5.3.10}$$

while $P(p^2, m_1, m_2, m_3)$ is the polynomial previously defined in Eq.(5.3.3). Finally the $P_{ij}^{(n)}$ are also polynomials depending on p^2 and the masses; their explicit (and sometimes lengthy expression) is given in Appendix B.1. Note that a same polynomial can occur in different equations with a different permutation of the masses

within its arguments.

We want to stress here an important aspect of the last two equations, Eq.(5.3.7,5.3.8), namely the presence of an overall factor $(d-2)$ in the *r.h.s.*, which plays an important role in the expansion in powers of $(d-2)$ discussed in the next Subsection.

5.3.1 The expansion of the Equations around $d = 2$

Let us start off by expanding all MIs in powers of $(d-2)$ around $d = 2$,

$$\begin{aligned} S(d; p^2) &= S(2; p^2) + (d-2)S^{(1)}(2, p^2) + \dots \\ S_1(d; p^2) &= S_1(2; p^2) + (d-2)S_1^{(1)}(2, p^2) + \dots \\ Z_2(d; p^2) &= Z_2(2; p^2) + (d-2)Z_2^{(1)}(2, p^2) + \dots \\ Z_3(d; p^2) &= Z_3(2; p^2) + (d-2)Z_3^{(1)}(2, p^2) + \dots \end{aligned} \quad (5.3.11)$$

Due to the overall factor $(d-2)$ in the *r.h.s.*, at 0th order in $(d-2)$ the differential equations Eq.s(5.3.7,5.3.8) become

$$\begin{aligned} \frac{d}{dp^2} Z_2(2; p^2) &= 0 \\ \frac{d}{dp^2} Z_3(2; p^2) &= 0, \end{aligned} \quad (5.3.12)$$

showing that $Z_2(2; p^2), Z_3(2; p^2)$ must be constants. But we know from Eq.s(5.2.14), (5.2.15) the actual value of that constant, i.e. the two functions vanish identically, $Z_2(2; p^2) = 0, Z_3(2; p^2) = 0$, so that at 0th order in $(d-2)$ the differential equations Eq.(5.3.5), Eq.(5.3.6) for $S(2; p^2), S_1(2; p^2)$ become

$$\begin{aligned} P(p^2, m_1, m_2, m_3) p^2 \frac{d}{dp^2} S(2; p^2) &= (p^2 + m_1^2) (p^2 - m_1^2 + m_2^2 + m_3^2) S(2; p^2) \\ &\quad - Q(p^2, m_1, m_2, m_3) m_1^2 S_1(2; p^2) \\ &\quad + \frac{1}{8} \left[(p^2 + m_1^2) \ln \frac{m_1^2}{m_2 m_3} + (m_2^2 - m_3^2) \ln \frac{m_3}{m_2} \right], \end{aligned} \quad (5.3.13)$$

$$\begin{aligned} D(p^2, m_1, m_2, m_3) P(p^2, m_1, m_2, m_3) p^2 \frac{d}{dp^2} S_1(2; p^2) &= \\ &\quad - P_{10}^{(0)}(p^2, m_1, m_2, m_3) S(2, p^2) - P_{11}^{(0)}(p^2, m_1, m_2, m_3) S_1(2, p^2) \\ &\quad - \frac{1}{8} \left[P_{14}^{(1)}(p^2, m_1, m_2, m_3) \ln \frac{m_1}{m_3} + P_{14}^{(1)}(p^2, m_1, m_3, m_2) \ln \frac{m_1}{m_2} \right. \\ &\quad \left. - \frac{p^2}{m_1^2} P^2(p^2, m_1, m_2, m_3) \right], \end{aligned} \quad (5.3.14)$$

which are obviously completely decoupled from the (trivial) equations for $Z_2(2; p^2)$, $Z_3(2; p^2)$.

Going now one order higher in the expansion, one finds that the first-order terms in $(d - 2)$ of the $Z_i(d; p^2)$ satisfy the equations

$$\begin{aligned} P(p^2, m_1, m_2, m_3) \frac{d}{dp^2} Z_2^{(1)}(2; p^2) = & \frac{1}{4}(m_1^2 - m_2^2)(p^2 + m_1^2 + m_2^2 - m_3^2) S(2; p^2) \\ & - \frac{1}{4}P(p^2, m_2, m_1, m_3) m_1^2 S_1(2; p^2) \\ & + \frac{1}{32} \left[(p^2 + m_3^2) \ln \frac{m_1}{m_2} + (m_1^2 - m_2^2) \ln \frac{m_1 m_2}{m_3^2} \right], \end{aligned} \quad (5.3.15)$$

$$\begin{aligned} P(p^2, m_1, m_2, m_3) \frac{d}{dp^2} Z_3^{(1)}(2; p^2) = & \frac{1}{4}(m_1^2 - m_3^2)(p^2 + m_1^2 - m_2^2 + m_3^2) S(2; p^2) \\ & - \frac{1}{4}P(p^2, m_3, m_1, m_2) m_1^2 S_1(2; p^2) \\ & + \frac{1}{32} \left[(p^2 + m_2^2) \ln \frac{m_1}{m_3} + (m_1^2 - m_3^2) \ln \frac{m_1 m_3}{m_2^2} \right]. \end{aligned} \quad (5.3.16)$$

It is to be noted that $Z_2^{(1)}(2; p^2)$, $Z_3^{(1)}(2; p^2)$ do not appear in the *r.h.s.* of Eq.s(5.3.15), (5.3.16), which contains only $S(2; p^2)$ and $S_1(2; p^2)$, to be considered known once Eq.s(5.3.13), (5.3.14) for the 0th orders in $(d - 2)$ have been solved. Eq.s(5.3.15), (5.3.16), indeed, are absolutely trivial when considered as differential equations, as they contain only the derivatives of $Z_2^{(1)}(2; p^2)$, $Z_3^{(1)}(2; p^2)$, and can therefore be solved by a simple quadrature.

Knowing $Z_2^{(1)}(2; p^2)$, $Z_3^{(1)}(2; p^2)$, one can move to the differential equations for $S^{(1)}(2; p^2)$, $S_1^{(1)}(2; p^2)$ (which we don't write here for the sake of brevity); they involve $Z_2^{(1)}(2; p^2)$, $Z_3^{(1)}(2; p^2)$ as known inhomogeneous terms, and form again a closed set of two differential equations, decoupled from the equations for the other two MIs, as at 0th order in $(d - 2)$.

Thanks to the overall factor $(d - 2)$ in the *r.h.s.* of Eq.s(5.3.7, 5.3.8), the pattern – a quadrature for $Z_2^{(k)}(2; p^2)$, $Z_3^{(k)}(2; p^2)$ and a closed set of two differential equations for $S^{(k)}(2; p^2)$, $S_1^{(k)}(2; p^2)$ – is completely general, and can be iterated, at least in principle, up to any required order k in $(d - 2)$.

5.4 Second-order Differential Equation for $S(d; p^2)$

We go back now to the system of differential equations Eq.s(5.3.5, 5.3.6), for obtaining a second-order differential equation for $S(d; p^2)$. We can use Eq.(5.3.5) in order to express $S_1(d; p^2)$ in function of $S(d; p^2)$ and of its derivative, $dS(d; p^2)/dp^2$. By

substituting this expression into Eq.(5.3.6) we can then derive a second-order differential equation for $S(d; p^2)$ only, which however still contains $Z_2(d; p^2)$ and $Z_3(d; p^2)$ in the inhomogeneous part:

$$\begin{aligned}
0 = & A_1(p^2, m_1, m_2, m_3) \left(\frac{d}{dp^2} \right)^2 S(d; p^2) \\
& + \left[A_2^{(0)}(p^2, m_1, m_2, m_3) + (d-2) A_2^{(1)}(p^2, m_1, m_2, m_3) \right] \frac{d}{dp^2} S(d; p^2) \\
& + (d-3) \left[A_3^{(0)}(p^2, m_1, m_2, m_3) + (d-2) A_3^{(1)}(p^2, m_1, m_2, m_3) \right] S(d; p^2) \\
& + \frac{(d-3)}{(d-1)} \left[A_4(p^2, m_1, m_2, m_3) Z_2(d; p^2) + A_4(p^2, m_1, m_3, m_2) Z_3(d; p^2) \right] \\
& + (d-2) \left[A_5^{(1)}(p^2, m_1, m_2, m_3) + (d-2) A_5^{(2)}(p^2, m_1, m_2, m_3) \right] T(d; m_1, m_2) \\
& + (d-2) \left[A_5^{(1)}(p^2, m_1, m_3, m_2) + (d-2) A_5^{(2)}(p^2, m_1, m_3, m_2) \right] T(d; m_1, m_3) \\
& + (d-2) \left[A_5^{(1)}(p^2, m_2, m_3, m_1) + (d-2) A_5^{(2)}(p^2, m_2, m_3, m_1) \right] T(d; m_2, m_3), \quad (5.4.1)
\end{aligned}$$

where

$$A_1(p^2, m_1, m_2, m_3) = p^2 D(p^2, m_1^2, m_2^2, m_3^2) P(p^2, m_1, m_2, m_3),$$

with $D(p^2, m_1^2, m_2^2, m_3^2)$ and $P(p^2, m_1, m_2, m_3)$ being the usual polynomials defined by Eq.s(5.3.3, 5.3.9). The $A_j^{(n)}(p^2, m_1, m_2, m_3)$ are also polynomials which depend on the three masses and on p^2 , but *do not* depend on the dimensions d . Their explicit expressions, as usual quite lengthy, can be found in Appendix B.2.

The equation above is exact in d but contains, besides $S(d; p^2)$ and its derivatives, also $Z_2(d; p^2)$ and $Z_3(d; p^2)$ as inhomogeneous terms. Nevertheless, recalling once more that $Z_2(2; p^2) = Z_3(2; p^2) = 0$, we can expand Eq.(5.4.1) in powers of $(d-2)$ and obtain at leading order in $(d-2)$ a second-order differential equation for $S(2; p^2)$ only:

$$\begin{aligned}
& A_1(p^2, m_1, m_2, m_3) \left(\frac{d}{dp^2} \right)^2 S(2; p^2) + A_2^{(0)}(p^2, m_1, m_2, m_3) \left(\frac{d}{dp^2} \right) S(2; p^2) \\
& - A_3^{(0)}(p^2, m_1, m_2, m_3) S(2; p^2) + \frac{1}{4} \left[A_5^{(2)}(p^2, m_1, m_2, m_3) \right. \\
& + A_5^{(2)}(p^2, m_1, m_3, m_2) + A_5^{(2)}(p^2, m_2, m_3, m_1) \\
& \left. + A_5^{(1)}(p^2, m_1, m_2, m_3) \ln \left(\frac{m_1}{m_3} \right) + A_5^{(1)}(p^2, m_1, m_3, m_2) \ln \left(\frac{m_1}{m_2} \right) \right] = 0, \quad (5.4.2)
\end{aligned}$$

where we made use of the relation Eq.(B.2.8) of Appendix B.2. We compared Eq.(5.4.2) with the second-order differential equation derived in [144], finding perfect agreement. Eq.(5.4.2) has been solved in reference [79] in terms of one-dimensional integrals over elliptic integrals.

Upon inserting the result in Eq.(5.3.13) one can obtain $S_1(2; p^2)$ in terms of $S(2; p^2)$ and $dS(2; p^2)/dp^2$. Inserting then $S(2; p^2)$ and $S_1(2; p^2)$ in Eq.s(5.3.15, 5.3.16), one obtains by quadrature the first-order terms, $Z_2^{(1)}(2; p^2)$ and $Z_3^{(1)}(2; p^2)$, of the expansion in $(d - 2)$ of $Z_2(d; p^2)$ and $Z_3(d; p^2)$.

Having these results on hand, we can now consider the first-order in $(d - 2)$ of the Eq.(5.4.1), which is now a second-order differential equation for $S^{(1)}(2; p^2)$ only, with known inhomogeneous terms (namely $S(2; p^2)$, $Z_2^{(1)}(2; p^2)$ and $Z_3^{(1)}(2; p^2)$). Proceeding in this way, at least in principle, the whole procedure can be iterated up to any required order in $(d - 2)$.

5.5 Shifting relations from $d = 2$ to $d = 4$ dimensions

In the previous Sections we have shown how to use the Schouten identities for writing the differential equations for the MIs of the massive sunrise at $d = 2$ dimensions in block form, and outlined the procedure for obtaining iteratively all the coefficients of the expansion in $(d - 2)$ of the four MIs starting from a second-order differential equation for $S(2; p^2)$, the leading term of the expansion.

The physically interesting case corresponds however to the expansion of the MIs for $d \approx 4$; we have therefore to convert the information given by the expansion at $d \approx 2$ in useful information at $d \approx 4$.

As it is well known, quite in general one can relate any Feynman integral evaluated in d dimensions to the very same integral evaluated in $(d - 2)$ dimensions by means of the Tarasov's shifting relation [47]. This dimensional shift is achieved by acting on the Feynman integral with a suitable combination of derivatives with respect to the internal masses. In the case of the "conventional " MIs of the sunrise graph, as defined in Eq.(5.2.7), the shifting relations read:

$$\begin{aligned} S(d - 2; p^2) &= \frac{2^2}{(d - 6)} \Delta S(d; p^2), \\ S_i(d - 2; p^2) &= \frac{2^2}{(d - 6)} \Delta S_i(d; p^2), \quad i = 1, 2, 3, \end{aligned} \quad (5.5.1)$$

where the differential operator Δ takes the form:

$$\Delta = \frac{\partial}{\partial m_1^2} \frac{\partial}{\partial m_2^2} + \frac{\partial}{\partial m_1^2} \frac{\partial}{\partial m_3^2} + \frac{\partial}{\partial m_2^2} \frac{\partial}{\partial m_3^2}. \quad (5.5.2)$$

Carrying out the derivatives in the integral representation for the four MIs of Eq.(5.2.7), one obtains a combination of integrals which are still related to the sunrise graph.

They can be expressed in terms of the full set of MIs in d dimensions (by full set we mean the four MIs and the tadpoles); one obtains in that way a set of four equations which explicitly relate the four MIs of the sunrise graph evaluated in $(d - 2)$ dimensions to suitable combinations of the same integrals (and of the tadpoles) evaluated in d dimensions. In that *direct* form the shifting relations would be of no practical use in our case, as they might give the MIs at $(d - 2) \approx 2$ in terms of those (less known) at $d \approx 4$.

It is however straightforward to invert the system and, in this way, to obtain the *inverse* shifting relations, expressing the four MIs in $d + 2 \approx 4$ dimensions in function of those in $d \approx 2$ dimensions. In addition, we can also use Eq.s(5.3.1,5.3.2) for expressing $S_2(d; p^2)$ and $S_3(d; p^2)$, in terms of $S(d; p^2)$, $S_1(d; p^2)$ and $Z_2(d; p^2)$, $Z_3(d; p^2)$. As a result one arrives at expressing any of the four “conventional” MIs $S(d+2, p^2)$, $S_i(d+2; p^2)$, $i = 1, 2, 3$, as a linear combination (whose coefficients depend – and in a non trivial way – on d and the kinematical variables of the problem) of the “new” MIs $S(d; p^2)$, $S_1(d; p^2)$, $Z_2(d; p^2)$ and $Z_3(d; p^2)$ (and the tadpoles). Indicating for simplicity the four “conventional” MIs with $M_i(d)$ and with $N_j(d)$ the four “new” MIs and the tadpoles, and ignoring for ease of notation all the kinematical variables, the *inverse* shifting relations can be written as

$$M_i(d+2) = \sum_j C_{i,j}(d) N_j(d) . \quad (5.5.3)$$

Given a relation of the form

$$F(d+2) = G(d) ,$$

by expanding around $d = 2$ one has, quite in general

$$F(d+2) = \sum_{n=r}^p (d-2)^n F^{(n)}(4) ,$$

$$G(d) = \sum_{n=r}^p (d-2)^n G^{(n)}(2) ,$$

where r , the first value of the summation index, can be negative (as it is the case in a Laurent expansion), so that

$$F^{(n)}(4) = G^{(n)}(2) .$$

In the case of the *inverse* shift Eq.(5.5.3), one has that the coefficients of the expansion of the “conventional” MIs in $(d - 4)$ for $d \approx 4$ are completely determined by those of the expansion in $(d - 2)$ for $d \approx 2$ of the “new” MIs, discussed in the previous Sections, and of the tadpoles (expanding around $d = 2$ the two sides of Eq.(5.5.3) requires also the expansion of the coefficients $C_{i,j}(d)$, but that is not a problem once the *inverse* shift has been written down explicitly).

The explicit formulas of the *direct* or *inverse* shifting relations are easily obtained but very lengthy and we decided not to include them entirely here for the sake of

brevity. For what follows, it is sufficient to discuss only the general features of one of the *inverse* shifting relations, namely the relation expressing $S(d+2; p^2)$ in terms of $S(d; p^2)$, $S_1(d; p^2)$ and $Z_2(d; p^2)$, $Z_3(d; p^2)$. Keeping for simplicity only the leading term of the expansion in $(d-2)$ of the coefficients we find:

$$\begin{aligned}
S(d+2; p^2) = & \left[C(p^2, m_1, m_2, m_3) + \mathcal{O}(d-2) \right] S(d; p^2) \\
& + \left[C_1(p^2, m_1, m_2, m_3) + \mathcal{O}(d-2) \right] S_1(d; p^2) \\
& + \left[\frac{1}{d-2} C_2(p^2, m_1, m_2, m_3) + \mathcal{O}(1) \right] Z_2(d; p^2) \\
& + \left[\frac{1}{d-2} C_3(p^2, m_1, m_2, m_3) + \mathcal{O}(1) \right] Z_3(d; p^2) \\
& + \left[C_4^{(0)}(p^2, m_1, m_2, m_3) + \mathcal{O}(d-2) \right] T(d; m_1, m_2) \\
& + \left[C_5^{(0)}(p^2, m_1, m_2, m_3) + \mathcal{O}(d-2) \right] T(d; m_1, m_2) \\
& + \left[C_6^{(0)}(p^2, m_1, m_2, m_3) + \mathcal{O}(d-2) \right] T(d; m_1, m_2). \tag{5.5.4}
\end{aligned}$$

In the formula above the $C(p^2, m_1, m_2, m_3)$, $C_i(p^2, m_1, m_2, m_3)$, are ratios of suitable polynomials which, as usual, depend on p^2 and on the three masses but, most importantly, *do not* depend on the dimensions d . The explicit expressions for $C(p^2, m_1, m_2, m_3)$, $C_1(p^2, m_1, m_2, m_3)$, $C_2(p^2, m_1, m_2, m_3)$ and $C_3(p^2, m_1, m_2, m_3)$, which will also be used in the following, can be found in Appendix B.3, Eq.s(B.3.2-B.3.5). Note anyway that:

$$C_3(p^2, m_1, m_2, m_3) = C_2(p^2, m_1, m_3, m_2).$$

By writing the expansion of $S(d+2; p^2)$ at $d \approx 2$ as

$$S(d+2; p^2) = \sum_n S^{(n)}(4; p^2)(d-2)^n, \tag{5.5.5}$$

and then expanding Eq.(5.5.4) at $d \approx 2$, one recovers the expression of the coefficients $S^{(n)}(4; p^2)$ in terms of the coefficients of the expansion of the four MIs and the tadpoles in $(d-2)$.

A few observations are in order. Eq.(5.5.4) exhibits an explicit pole in $1/(d-2)$ only in the coefficients of $Z_2(d; p^2)$ and $Z_3(d; p^2)$; recalling once more that at $d=2$ both $Z_2(2; p^2)$ and $Z_3(2; p^2)$ are identically zero, see Eq.s(5.2.14,5.2.15), it is clear that these poles will not generate any singularity of $S(d; p^2)$ as $d \rightarrow 2$. On the other hand, the tadpoles in the *r.h.s.* of Eq.(5.5.4) do generate polar singularities of $S(d+2; p^2)$; recalling Eq.s(5.2.5,5.2.6) and by using the lengthy explicit form of the coefficients (which we did not write for brevity) one finds

$$\begin{aligned}
S^{(-2)}(4; p^2) &= -\frac{(m_1^2 + m_2^2 + m_3^2)}{8}, \\
S^{(-1)}(4; p^2) &= \frac{1}{32} \left[p^2 + 6(m_1^2 + m_2^2 + m_3^2) \right]
\end{aligned}$$

$$-\frac{1}{8} \left[m_1^2 \ln(m_1^2) + m_2^2 \ln(m_2^2) + m_3^2 \ln(m_3^2) \right], \quad (5.5.6)$$

formulas already known for a long time in the literature [128].

As a second observation, let us look at the zeroth-order term $S^{(0)}(4; p^2)$ of $S(d; p^2)$ in $(d-4)$, *i.e.* the zeroth-order term in $(d-2)$ of Eq.(5.5.4). We have already commented the apparent polar singularity $1/(d-2)$ in the coefficients of $Z_2(d; p^2)$ and $Z_3(d; p^2)$, actually absent because $Z_2(2; p^2)$ and $Z_3(2; p^2)$ are both vanishing. But due to the presence of the $1/(d-2)$ polar factor, in order to recover the zeroth-order term $S^{(0)}(4; p^2)$, one needs, besides $S(2; p^2)$, $S_1(2; p^2)$, also the first-order of the corresponding expansion of $Z_2(d; p^2)$ and $Z_3(d; p^2)$, namely $Z_2^{(1)}(2; p^2)$ and $Z_3^{(1)}(2; p^2)$ – obtained, in our approach, from the systematic expansion of the differential equations, see Eq.s(5.3.15, 5.3.16) or Section 5.4.

The complete expression of $S^{(0)}(4; p^2)$, which is rather cumbersome, is given by Eq.(B.3.1) of Appendix B.3.

5.6 The imaginary parts of the Master Integrals.

In this section, which is somewhat pedagogical, we discuss the relationship between the imaginary parts of the MIs at $d=2$ and $d=4$ dimensions, as a simple but explicit example of functions exhibiting the properties described in the previous sections.

At $d=2$ the Cutkosky-Veltman rule [98, 99] gives for $S(d; p^2)$, as defined by the first of Eq.s(5.2.7),

$$\frac{1}{\pi} \text{Im} S(2; -W^2) = N_2 \int_{b_2}^{b_3} db \frac{1}{\sqrt{R_4(b; b_1, b_2, b_3, b_4)}}, \quad (5.6.1)$$

where the following notations were introduced:

$$\begin{aligned} N_2 &= 1/2 \\ p^2 &= -W^2, \quad W \geq m_1 + m_2 + m_3, \\ (m_2 - m_3)^2 &= b_1 \leq (m_2 + m_3)^2 = b_2 \leq (W - m_1)^2 = b_3 \leq (W + m_1)^2 = b_4, \\ R_4(b; b_1, b_2, b_3, b_4) &= (b - b_1)(b - b_2)(b_3 - b)(b_4 - b). \end{aligned} \quad (5.6.2)$$

We have the relation

$$R_4(b; b_1, b_2, b_3, b_4) = R_2(b, m_2^2, m_3^2) R_2(W^2, b, m_1^2), \quad (5.6.3)$$

where

$$R_2(a, b, c) = a^2 + b^2 + c^2 - 2ab - 2ac - 2bc, \quad (5.6.4)$$

is the familiar invariant form appearing in the two-body phase space, showing that the system of the three particles, whose masses enter in the definition of $R_4(b; b_1, b_2, b_3, b_4)$,

can be considered as the merging of a two-body system of total energy \sqrt{b} and masses m_2, m_3 with a two-body system of total energy W and masses \sqrt{b}, m_1 . According to Eq.s(5.2.7), for $i=1,2,3$

$$\frac{1}{\pi} ImS_i(2; -W^2) = -\frac{d}{dm_i^2} \left(\frac{1}{\pi} ImS(2; -W^2) \right) ; \quad (5.6.5)$$

the integral representation Eq.(5.6.1), however, is of no use for obtaining $ImS_i(2; -W^2)$ through a direct differentiation (due to the appearance of end point singularities). It is more convenient to use Eq.(3.24), so that Eq.(5.6.1) becomes

$$\frac{1}{\pi} ImS(2; -W^2) = N_2 \frac{2}{\sqrt{(b_4 - b_2)(b_3 - b_1)}} K(w^2) , \quad (5.6.6)$$

where $K(w^2)$ is the complete elliptic integral of the first kind, Eq.(3.20), and

$$\begin{aligned} w^2 &= \frac{(b_4 - b_1)(b_3 - b_1)}{(b_4 - b_2)(b_3 - b_1)} \\ &= \frac{(W + m_1 + m_2 - m_3)(W + m_1 - m_2 + m_3)}{(W + m_1 + m_2 + m_3)(W + m_1 - m_2 - m_3)} \\ &\quad \times \frac{(W - m_1 + m_2 - m_3)(W - m_1 - m_2 + m_3)}{(W - m_1 + m_2 - m_3)(W - m_1 - m_2 + m_3)} . \end{aligned} \quad (5.6.7)$$

Let us observe, in passing, that, even if $ImS(2, -W^2)$ (and, more generally $S(d; p^2)$ as well) is obviously symmetric in the three masses m_1, m_2, m_3 , the symmetry is not explicitly shown by the integral representation Eq.(5.6.1), while the manifest symmetry is restored in Eq.s(5.6.6,5.6.7).

One can now use Eq.(5.6.6) to carry out the derivative with respect to the masses m_i^2 in Eq.(5.6.5); the result reads

$$\begin{aligned} \frac{1}{\pi} ImS_1(2; -W^2) &= N_2 \frac{1}{2m_1^2 \sqrt{(b_3 - b_1)(b_4 - b_2)}} \frac{1}{(b_3 - b_2)(b_4 - b_1)} \\ &\quad \times [4m_1(m_1 m_3^2 + m_1 m_2^2 - m_1^3 + 2m_2 m_3 W + m_1 W^2) K(w^2) \\ &\quad - P(-W^2, m_1, m_2, m_3) E(w^2)] , \end{aligned} \quad (5.6.8)$$

$$\begin{aligned} \frac{1}{\pi} ImS_2(2; -W^2) &= N_2 \frac{1}{2m_2^2 \sqrt{(b_3 - b_1)(b_4 - b_2)}} \frac{1}{(b_3 - b_2)(b_4 - b_1)} \\ &\quad \times [4m_2(m_2 m_3^2 + m_2 m_1^2 - m_2^3 + 2m_1 m_3 W + m_2 W^2) K(w^2) \\ &\quad - P(-W^2, m_2, m_1, m_3) E(w^2)] , \end{aligned} \quad (5.6.9)$$

$$\frac{1}{\pi} ImS_3(2; -W^2) = N_2 \frac{1}{2m_3^2 \sqrt{(b_3 - b_1)(b_4 - b_2)}} \frac{1}{(b_3 - b_2)(b_4 - b_1)}$$

$$\begin{aligned} & \times [4m_3(m_3m_1^2 + m_3m_2^2 - m_3^3 + 2m_2m_1W + m_3W^2) K(w^2) \\ & - P(-W^2, m_3, m_2, m_1) E(w^2)] , \end{aligned} \quad (5.6.10)$$

where w^2 is given by the first of Eq.s(5.6.7), $P(p^2, m_1, m_2, m_3)$ is the polynomial already introduced in Eq.(5.3.3), symmetric in the last two arguments, and $E(w^2)$ is the complete elliptic integral of the second kind, see Eq.(3.21).

Eq.s(5.6.6), (5.6.8), (5.6.9), (5.6.10) express the four quantities $ImS(2; -W^2)$, $ImS_i(2, -W^2)$, $i = 1, 2, 3$ in terms of just two functions, the elliptic integrals $K(w^2)$, $E(w^2)$; therefore, the four imaginary parts cannot be all linearly independent. It is indeed easy to check that they satisfy the two equations

$$\begin{aligned} & -\frac{1}{12}(m_1^2 - 2m_2^2 + m_3^2) ImS(2; -W^2) \\ & + \frac{1}{12}(-W^2 + m_1^2 - 3m_2^2 + 3m_3^2) m_1^2 ImS_1(2, -W^2) \\ & - \frac{1}{6}(-W^2 + m_2^2) m_2^2 ImS_2(2; -W^2) \\ & + \frac{1}{12}(-W^2 + 3m_1^2 - 3m_2^2 + m_3^2) m_3^2 ImS_3(2; -W^2) = 0 , \end{aligned}$$

$$\begin{aligned} & -\frac{1}{12}(m_1^2 + m_2^2 - 2m_3^2) ImS(2; -W^2) \\ & + \frac{1}{12}(-W^2 + m_1^2 + 3m_2^2 - 3m_3^2) m_1^2 ImS_1(2; -W^2) \\ & + \frac{1}{12}(-W^2 + 3m_1^2 + m_2^2 - 3m_3^2) m_2^2 ImS_2(2; -W^2) \\ & - \frac{1}{6}(-W^2 + m_3^2) m_3^2 ImS_3(2; -W^2) = 0 , \end{aligned}$$

which are nothing but the imaginary parts of $Z_2(2; -W^2)$, $Z_3(2; -W^2)$, Eq.s(5.2.14), (5.2.15).

As a further comment on the imaginary parts at $d = 2$, let us observe that they take a finite value at threshold, *i.e.* in the $W \rightarrow (m_1 + m_2 + m_3)$ limit. In that limit, indeed, $b_3 \rightarrow b_2 = (m_2 + m_3)^2$, and one finds

$$\begin{aligned} \int_{b_2}^{b_3} \frac{db}{\sqrt{R_4(b; b_1, b_2, b_3, b_4)}} & \rightarrow \frac{1}{\sqrt{(b_2 - b_1)(b_4 - b_2)}} \int_{b_2}^{b_3} \frac{db}{\sqrt{(b - b_2)(b_3 - b)}} \\ & = \frac{\pi}{\sqrt{(b_2 - b_1)(b_4 - b_2)}} , \end{aligned}$$

so that

$$\frac{1}{\pi} ImS(2; -W^2) \xrightarrow{W \rightarrow (m_1 + m_2 + m_3)} \frac{N_2}{4\sqrt{m_1 m_2 m_3 (m_1 + m_2 + m_3)}} . \quad (5.6.11)$$

The extension to the value at threshold of the $ImS_i(2, -W^2)$ is similar, even if requiring one more term in the expansion due to the presence of the denominator $1/(b_3 - b_2)$ in their definitions, Eq.s(5.6.8,5.6.9,5.6.10). The threshold values are

$$\begin{aligned}
& \frac{1}{\pi} ImS_1(2; -W^2) \xrightarrow{W \rightarrow (m_1+m_2+m_3)} \\
& \quad \frac{N_2}{32} \left(-\frac{3}{m_1} + \frac{1}{m_2} + \frac{1}{m_3} - \frac{1}{m_1+m_2+m_3} \right) \frac{1}{\sqrt{m_1 m_2 m_3 (m_1+m_2+m_3)}} , \\
& \frac{1}{\pi} ImS_2(2; -W^2) \xrightarrow{W \rightarrow (m_1+m_2+m_3)} \\
& \quad \frac{N_2}{32} \left(+\frac{1}{m_1} - \frac{3}{m_2} + \frac{1}{m_3} - \frac{1}{m_1+m_2+m_3} \right) \frac{1}{\sqrt{m_1 m_2 m_3 (m_1+m_2+m_3)}} , \\
& \frac{1}{\pi} ImS_3(2; -W^2) \xrightarrow{W \rightarrow (m_1+m_2+m_3)} \\
& \quad \frac{N_2}{32} \left(+\frac{1}{m_1} + \frac{1}{m_2} - \frac{3}{m_3} - \frac{1}{m_1+m_2+m_3} \right) \frac{1}{\sqrt{m_1 m_2 m_3 (m_1+m_2+m_3)}} .
\end{aligned} \tag{5.6.12}$$

At $d = 4$ the imaginary part of $S(d; p^2)$, by using the same notation as in Eq.(5.6.1), is given by

$$\frac{1}{\pi} ImS(4; -W^2) = N_4 \int_{b_2}^{b_3} db \frac{1}{b} \sqrt{R_4(b; b_1, b_2, b_3, b_4)} . \tag{5.6.13}$$

with

$$N_4 = \frac{1}{8W^2} . \tag{5.6.14}$$

At variance with the $d = 2$ case, the $ImS_i(4, -W^2)$ can be obtained at once by differentiating with respect to the masses the previous integral representation for $ImS(4; -W^2)$. The result can be most conveniently expressed in terms of the four (independent) integrals $I(-1, W)$, $I(0, W)$, $I(1, W)$, $I(2, W)$, defined (see Eq.(3.17) and Section 3.2.2 for more details and the relation to the standard complete elliptic integrals) through

$$I(n, W) = \int_{b_2}^{b_3} db b^n \frac{1}{\sqrt{R_4(b; b_1, b_2, b_3, b_4)}} . \tag{5.6.15}$$

An explicit calculation gives

$$\begin{aligned}
\frac{1}{\pi} ImS(4; -W^2) = N_4 & \left[b_1 b_2 b_3 b_4 I(-1, W) \right. \\
& \left. - \frac{3}{4} (b_2 b_3 b_4 + b_1 b_3 b_4 + b_1 b_2 b_4 + b_1 b_2 b_3) I(0, W) \right]
\end{aligned}$$

$$\begin{aligned}
& + \frac{1}{2}(b_3b_4 + b_2b_4 + b_2b_3 + b_1b_4 + b_1b_3 + b_1b_2) I(1, W) \\
& - \frac{1}{4}(b_1 + b_2 + b_3 + b_4) I(2, W) \Big] \tag{5.6.16}
\end{aligned}$$

$$\begin{aligned}
\frac{1}{\pi}ImS_1(4; -W^2) = N_4 & \Big[b_1b_2(-(b_4 - b_3)W + (b_4 + b_3)m_1) I(-1, W) \\
& + ((b_2 + b_1)(b_4 - b_3)W - (b_2b_4 + b_2b_3 + b_1b_4 + b_1b_3 + 2b_1b_2)m_1) I(0, W) \\
& + ((b_4 - b_3)W + (b_4 + b_3 + 2b_2 + 2b_1)m_1) I(1, W) \\
& - 2m_1 I(2, W) \Big] \tag{5.6.17}
\end{aligned}$$

$$\begin{aligned}
\frac{1}{\pi}ImS_2(4; -W^2) = N_4 & \Big[b_3b_4(-(b_2 - b_1)m_3 + (b_2 + b_1)m_2) I(-1, W) \\
& + (-(2b_3b_4 + b_2b_4 + b_2b_3 + b_1b_4 + b_1b_3)m_2 + (b_2 - b_1)(b_4 + b_3)m_3) I(0, W) \\
& + ((2b_4 + 2b_3 + b_2 + b_1)m_2 - (b_2 - b_1)m_3) I(1, W) \\
& - 2m_2 I(2, W) \Big] \tag{5.6.18}
\end{aligned}$$

$$\begin{aligned}
\frac{1}{\pi}ImS_3(4; -W^2) = N_4 & \Big[b_3b_4(-(b_2 - b_1)m_2 + (b_2 + b_1)m_3) I(-1, W) \\
& + (-(2b_3b_4 + b_2b_4 + b_2b_3 + b_1b_4 + b_1b_3)m_3 + (b_2 - b_1)(b_4 + b_3)m_2) I(0, W) \\
& + ((2b_4 + 2b_3 + b_2 + b_1)m_3 - (b_2 - b_1)m_2) I(1, W) \\
& - 2m_3 I(2, W) \Big] \tag{5.6.19}
\end{aligned}$$

Again at variance with the $d = 2$ case, the four imaginary parts are now combinations of four independent elliptic integrals, and therefore all independent of each other.

Having recalled the main features of the imaginary parts of the MIs at $d = 2$ and $d = 4$ dimensions, we can look at the way the Tarasov's shifting relations work in their case.

Let us start from the “direct” shift expressing the imaginary parts at $d = 2$ in terms of those at $d = 4$. The $d \rightarrow 4$ limit of the shifting relations is trivial, even if the relevant formulas are as usual rather lengthy. Keeping only the imaginary parts of the master integrals one finds for the MI $S(2, p^2)$, with $-p^2 = W^2 \geq (m_1 + m_2 + m_3)^2$

$$\begin{aligned}
\frac{1}{\pi}ImS(2, -W^2) = \tilde{A}(W, m_1, m_2, m_3) & \frac{1}{\pi}ImS(4, -W^2) \\
& + \tilde{B}(W, m_1, m_2, m_3)m_1 \frac{1}{\pi}ImS_1(4, -W^2) \\
& + \tilde{B}(W, m_2, m_3, m_1)m_2 \frac{1}{\pi}ImS_2(4, -W^2)
\end{aligned}$$

$$+ \tilde{B}(W, m_3, m_1, m_2) m_3 \frac{1}{\pi} \text{Im}S_3(4, -W^2) , \quad (5.6.20)$$

where

$$\begin{aligned} \tilde{A}(W, m_1, m_2, m_3) &= A(W, m_1, m_2, m_3) + A(W, m_1, -m_2, m_3) \\ &\quad + A(W, m_1, m_2, -m_3) + A(W, m_1, -m_2, -m_3) , \\ \tilde{B}(W, m_1, m_2, m_3) &= B(W, m_1, m_2, m_3) + B(W, m_1, -m_2, m_3) \\ &\quad + B(W, m_1, m_2, -m_3) + B(W, m_1, -m_2, -m_3) , \\ A(W, m_1, m_2, m_3) &= \frac{1}{2m_1 m_2 m_3} \frac{m_1 + m_2 + m_3}{W^2 - (m_1 + m_2 + m_3)^2} , \\ B(W, m_1, m_2, m_3) &= \frac{1}{2} (2m_1 + m_2 + m_3) A(W, m_1, m_2, m_3) . \end{aligned} \quad (5.6.21)$$

Eq.(5.6.20) is relatively simple, and, when substituting in it the explicit values of $\text{Im}S(4, -W^2)$ and $\text{Im}S_i(4, -W^2)$, as given by Eq.s(5.6.16–5.6.19), Eq.(5.6.1) is recovered. The same happens for $\text{Im}S_i(2, -W^2)$, $i = 1, 2, 3$ as well.

Conversely, one can look at the inverse formulas, giving the imaginary parts at $d + 2 \rightarrow 4$ in terms of the imaginary parts at $d \rightarrow 2$. For $\text{Im}S(4, -W^2)$, taking only the imaginary part at $d = 2$ of Eq.(5.5.4), one obtains:

$$\begin{aligned} \frac{1}{\pi} \text{Im}S(4, -W^2) &= C(-W^2, m_1, m_2, m_3) \frac{1}{\pi} \text{Im}S(2; -W^2) \\ &\quad + C_1(-W^2, m_1, m_2, m_3) \frac{1}{\pi} \text{Im}S_1(2; -W^2) \\ &\quad + C_2(-W^2, m_1, m_2, m_3) \frac{1}{\pi} \text{Im}Z_2^{(1)}(2; -W^2) \\ &\quad + C_3(-W^2, m_1, m_2, m_3) \frac{1}{\pi} \text{Im}Z_3^{(1)}(2; -W^2) , \end{aligned} \quad (5.6.22)$$

where the $C(-W^2, m_1, m_2, m_3)$, $C_i(-W^2, m_1, m_2, m_3)$ have been defined in the previous section, and their explicit expressions can be found in Appendix B.3 in Eq.s(B.3.2–B.3.5), $\text{Im}S(2; -W^2)$, $\text{Im}S_1(2; -W^2)$ are the imaginary parts of the corresponding Master Integrals at $d = 2$, while $\text{Im}Z_2^{(1)}(2; -W^2)$, $\text{Im}Z_3^{(1)}(2; -W^2)$ are the imaginary parts of the first term of the expansion in $(d - 2)$ of the corresponding functions, see Eq.s(5.3.11) (let us recall once more that according to Eq.s(5.2.14, 5.2.15) $Z_2(2; p^2)$, $Z_3(2; p^2)$ vanish identically). An equation similar to Eq.(5.6.22) holds for $\text{Im}S_1(4; -W^2)$; we do not write it explicitly for the sake of brevity.

The functions $\text{Im}S(4; -W^2)$, $\text{Im}S_1(4; -W^2)$ and $\text{Im}S(2; -W^2)$, $\text{Im}S_1(2; -W^2)$ are known, see Eq.s(5.6.16, 5.6.17) and Eq.s(5.6.6, 5.6.8); by combining Eq.(5.6.22) and the similar (not written) equation for $\text{Im}S_1(4; -W^2)$, one can obtain the explicit values of $\text{Im}Z_2^{(1)}(2; -W^2)$, $\text{Im}Z_3^{(1)}(2; -W^2)$. One finds

$$\frac{1}{\pi} \text{Im}Z_2^{(1)}(2; -W^2) = \frac{N_2}{16} \left[(W^2 - m_3^2 + m_2^2 - m_1^2) I(0, W) + I(1, W) \right]$$

$$- (m_3^2 - m_2^2)(W^2 - m_1^2)I(-1, W) \Big] , \quad (5.6.23)$$

$$\begin{aligned} \frac{1}{\pi} \text{Im} Z_3^{(1)}(2; -W^2) &= \frac{N_2}{16} \Big[(W^2 + m_3^2 - m_2^2 - m_1^2)I(0, W) + I(1, W) \\ &\quad + (m_3^2 - m_2^2)(W^2 - m_1^2)I(-1, W) \Big] , \end{aligned} \quad (5.6.24)$$

From the previous equations and the same procedure giving Eq.s(5.6.11,5.6.12) we obtain in particular the values at threshold

$$\begin{aligned} \frac{1}{\pi} \text{Im} Z_2^{(1)}(2; -W^2) &\xrightarrow{W \rightarrow (m_1+m_2+m_3)} \frac{N_2}{16} \sqrt{\frac{m_2(m_1 + m_2 + m_3)}{m_1 m_3}} \\ \frac{1}{\pi} \text{Im} Z_3^{(1)}(2; -W^2) &\xrightarrow{W \rightarrow (m_1+m_2+m_3)} \frac{N_2}{16} \sqrt{\frac{m_3(m_1 + m_2 + m_3)}{m_1 m_2}} . \end{aligned} \quad (5.6.25)$$

$\text{Im} Z_2^{(1)}(2; -W^2)$ can also be evaluated solving, by quadrature, the imaginary part of the differential equation Eq.(5.3.15), *i.e.* by evaluating

$$\text{Im} Z_2^{(1)}(2; -W^2) = C + \int^{-W^2} dp^2 \text{Im} \left(\frac{d}{dp^2} Z_2^{(1)}(2; p^2) \right) ,$$

where C is an integration constant and $dZ_2^{(1)}(2; p^2)/dp^2$ is obtained from Eq.(5.3.15) itself. The constant C can be fixed, *a posteriori*, by requiring that the imaginary parts of the “conventional” MI vanish at threshold in $d = 4$ dimensions, a condition which leads again to Eq.s(5.6.25).

After many algebraic simplifications, one obtains for $\text{Im} Z_2^{(1)}(2; -W^2)$

$$\begin{aligned} \frac{1}{\pi} \text{Im} Z_2^{(1)}(2; -W^2) &= \frac{N_2}{16} \sqrt{\frac{m_2(m_1 + m_2 + m_3)}{m_1 m_3}} \\ &\quad + \frac{1}{64} \int_{(m_1+m_2+m_3)^2}^{W^2} ds \Big[\tilde{F}(s, m_1, m_2, m_3) I(0, s) \\ &\quad - \tilde{G}(s, m_1, m_2, m_3) I(1, s) \\ &\quad + \tilde{H}(s, m_1, m_2, m_3) I(2, s) \Big] . \end{aligned} \quad (5.6.26)$$

where the three quantities $\tilde{F}, \tilde{G}, \tilde{H}$ are all expressed in terms of the corresponding functions F, G, H by the relation

$$\begin{aligned} \tilde{F}(s, m_1, m_2, m_3) &= F(s, m_1, m_2, m_3) + F(s, m_1, -m_2, m_3) \\ &\quad + F(s, m_1, m_2, -m_3) + F(s, m_1, -m_2, -m_3) , \end{aligned}$$

and the explicit expressions of those functions are

$$\begin{aligned} F(s, m_1, m_2, m_3) &= \frac{(m_2 + m_3)^2}{m_1 m_3} \frac{2m_1^2 + m_2^2 + m_3^2 + 2m_1 m_2 + 2m_1 m_3}{s - (m_1 + m_2 + m_3)^2}, \\ G(s, m_1, m_2, m_3) &= 2 \frac{m_1^2 + m_2^2 + m_3^2 + m_1 m_2 + m_1 m_3 + m_2 m_3}{m_1 m_3 [s - (m_1 + m_2 + m_3)^2]}, \\ H(s, m_1, m_2, m_3) &= \frac{1}{m_1 m_3 [s - (m_1 + m_2 + m_3)^2]}. \end{aligned}$$

To carry out the integration, we use the integral representations Eq.(3.18) for the elliptic integrals $I(n, s)$ and exchange the order of integration according to

$$\begin{aligned} \int_{(m_1+m_2+m_3)^2}^{W^2} ds \int_{(m_2+m_3)^2}^{(\sqrt{s}-m_1)^2} \frac{db}{\sqrt{R_4(b; b_1, b_2, b_3, b_4)}} = \\ \int_{(m_2+m_3)^2}^{(W-m_1)^2} \frac{db}{\sqrt{R_2(b, m_2^2, m_3^2)}} \int_{(\sqrt{b}+m_1)^2}^{W^2} \frac{ds}{\sqrt{R_2(s, b, m_1^2)}}, \end{aligned}$$

where Eq.(5.6.3) was used. The s integration is then elementary, giving only logarithms of suitable arguments and new square roots quadratic in b ; a subsequent integration by parts in b removes those logarithms with some of the accompanying square roots, and the result is Eq.(5.6.23), as expected.

The same applies also for $ImZ_3^{(1)}(2; -W^2)$, whose value is obtained by simply exchanging m_2 and m_3 in Eq.(5.6.23).

5.7 Conclusions

In this chapter we showed how the newly introduced Schouten identities (see Section 2.2.5) can be applied to the case of the massive two-loop sunrise graph with different masses, finding that in $d = 2$ dimensions only two of the four Master Integrals (MIs) are actually independent, so that the other two can be expressed as suitable linear combinations of the latter.

In the general case of arbitrary dimension d and different masses, the four MIs are known to fulfil a system of four first-order coupled differential equations in the external momentum transfer. The system can equivalently be re-phrased as a fourth-order differential equation for one of the MIs only.

Using these relations we introduced a new set of four independent MIs, valid for any number of dimensions d , whose property is that two of the newly defined integrals vanish identically in $d = 2$. The new system of differential equations for this set of MIs takes then a simpler block form when expanded in $(d - 2)$.

Starting from this system, one can derive a second-order differential equation, *exact in d* , for the full scalar amplitude, which still contains the two integrals, whose

value is zero at $d = 2$, as inhomogeneous terms. We verified that the zeroth-order of our equation corresponds to the equation derived in [144]. Our equations, once expanded in powers of $(d - 2)$, can be used, together with the linear equations for the remaining three MIs, for evaluating recursively, at least in principle, all four MIs, up to any order in $(d - 2)$.

We then worked out explicitly the Tarasov's shifting relations needed to recover the physically more relevant value of the four MIs expanded in $(d - 4)$ at $d \approx 4$ starting from the expansion in $(d - 2)$ at $d \approx 2$ worked out in our approach.

As an example of this procedure we discussed the relationship between the *imaginary parts* of the four MIs in $d = 2$ and $d = 4$. The latter can be computed using the Cutkosky-Veltman rule. We showed how in $d = 2$ the imaginary parts of the four MIs can be written in terms of two independent functions only, namely the complete elliptic integrals of the first and of the second kind. The same is not true in $d = 4$ dimensions, where four independent elliptic integrals are needed in order to represent the four imaginary parts. We then showed how the Tarasov's shift formulas relate the imaginary parts in $d = 2$ and $d = 4$ dimensions. Finally, we gave an explicit example of how the differential equations for the imaginary parts of the master integrals can be integrated by quadrature.

Chapter 6

Two-loop QCD Amplitudes for $q\bar{q} \rightarrow Z\gamma/W\gamma$

The material presented in this chapter is the result of an original research done in collaboration with T. Gehrmann, and it is entirely based on the paper [32]. The same techniques described here have been used for the computation of the two-loop QCD helicity amplitudes for $gg \rightarrow Z^0\gamma$ and $gg \rightarrow Z^0g$ [125], in collaboration with T. Gehrmann and E. Weihs.

6.1 Introduction

Pair production of electroweak gauge bosons (γ, W^\pm, Z^0) offers a wide spectrum of observables, which allow to test the theory of the electroweak interaction, to probe the Higgs mechanism of electroweak symmetry breaking and to search for physics beyond the standard model. While photons are directly observed in the detector, the massive W and Z bosons are identified from their leptonic decay modes.

The standard model predicts specific values and structures for the couplings among the electroweak gauge bosons: W^\pm , Z^0 and γ . Physics effects beyond the standard model could modify these gauge boson self-couplings [145–147]. Observations of such anomalous couplings may help to constrain new theory models and could provide indirect evidence for new physics effects at energy scales above the nominal collision energy. The couplings of the massive W^\pm, Z^0 bosons to the photon are determined at hadron colliders by measuring $W^\pm\gamma$ and $Z^0\gamma$ production cross sections and comparing them to theoretical predictions. Measurements have been carried out at Tevatron [148–153], and first results from the LHC are already becoming available [154, 155]. The accuracy of the coupling determination is potentially limited by both the experimental accuracy and by uncertainties inherent to the theoretical prediction.

At present, $W^\pm\gamma$ and $Z^0\gamma$ production at hadron colliders is described theoretically to next-to-leading order (NLO) in QCD [111–114, 147] and to NLO in the electroweak

theory [117], while recently, thanks also to the results described in this chapter, the full NNLO calculation for $Z^0\gamma$ production has become available [122]. With increasing order in perturbative QCD, new production channels (with new combinations of parton distributions) for vector boson pairs start contributing; the complete spectrum of partonic channels is only present from next-to-next-to-leading order (NNLO) onwards. Moreover, the inclusion of NNLO corrections to gauge boson pair production will lower the inherent theoretical uncertainty of the prediction (usually quantified by variation of the renormalisation and factorisation scales) and allow for a fully consistent inclusion of NNLO parton distribution functions.

The calculation of gauge boson pair production at NNLO requires three types of ingredients: the two-loop partonic $2 \rightarrow 2$ matrix elements for the production of the gauge boson pair under consideration, the one-loop partonic $2 \rightarrow 3$ matrix elements for the production of the gauge boson pair in association with an extra parton and the tree-level $2 \rightarrow 4$ matrix elements involving two extra partons. The latter two contributions are equally contributing to the NLO corrections for the production of a vector boson pair with an extra jet, which have been computed for $\gamma\gamma j$ [156], $V\gamma j$ [157, 158] and VVj [159–163] already some time ago. At NNLO, the contributions from both these channels will contain infrared singularities from one or two final state partons becoming soft or collinear. These singularities cancel only when combined with the infrared-singular two-loop contributions, such that a method is needed for their extraction from the real radiation processes. Several methods have been applied successfully in NNLO calculations of exclusive observables in the recent past: sector decomposition [22, 23, 50, 164–167], q_T -subtraction [25] and antenna subtraction [26, 27, 168–172]. It should be noted that the q_T -subtraction method is restricted to observables that are described by non-QCD processes at leading order, which is the case for vector boson pair production. The first calculations of NNLO corrections to vector boson pair production processes ($pp \rightarrow \gamma\gamma$, $pp \rightarrow Z^0\gamma$, $pp \rightarrow Z^0Z^0$) have been performed using this method [110, 121, 122].

In this chapter we will describe in detail the calculation of the two-loop corrections to the helicity amplitudes for the production of a massive vector boson and a photon $q\bar{q} \rightarrow W^\pm\gamma$ and $q\bar{q} \rightarrow Z^0\gamma$, which were a crucial ingredient to the NNLO corrections to $Z^0\gamma$ [122]. The calculation follows closely the techniques that were employed in the calculation of two-loop corrections to the $\gamma^* \rightarrow q\bar{q}g$ matrix elements [33, 173].

This chapter is structured as follows: in Section 6.2, we fix the notation and discuss the basic helicity structure of the process under consideration. The calculation of the two-loop amplitudes is described in Section 6.3, and the results are discussed in Section 6.4. The two-loop helicity amplitudes are obtained in a closed analytic form, which is however too large to be quoted here explicitly. Computer algebra files containing the results with the submission of the original paper [32]. We performed several non-trivial checks on the results, which are described in Section 6.5. We conclude with an outlook in Section 6.6.

6.2 Kinematics and basic helicity structure

The production of a massive vector boson and a photon in quark-antiquark annihilation is related by crossing to the decay of the vector boson into a quark-antiquark-photon final state, which has the same kinematics as three-jet-production ($3j$) in e^+e^- annihilation. Technically, the calculation of QCD corrections to the $q\bar{q} \rightarrow V\gamma$ amplitudes is thus similar to previous calculations for the helicity amplitudes for $3j$ -production, which have been derived to two-loop accuracy in QCD [33].

Including the leptonic decay of the vector boson, the partonic subprocesses yielding $V\gamma$ final states are:

$$\begin{aligned} q(p_2) + \bar{q}(p_1) &\rightarrow \gamma(-p_3) + Z^0(q) \rightarrow \gamma(-p_3) + l^+(p_5) + l^-(p_6) , \\ q(p_2) + \bar{q}'(p_1) &\rightarrow \gamma(-p_3) + W^-(q) \rightarrow \gamma(-p_3) + \bar{\nu}(p_5) + l^-(p_6) , \\ q(p_2) + \bar{q}'(p_1) &\rightarrow \gamma(-p_3) + W^+(q) \rightarrow \gamma(-p_3) + l^+(p_5) + \nu(p_6) . \end{aligned}$$

The Z^0 -boson process implicitly includes also a contribution from an off-shell photon γ^* . In the most general case where two quarks of two different flavours appear, to fix the conventions, we will refer from now on to p_1 as the momentum of the anti-quark \bar{q}' and as p_2 to the momentum of the quark q . The momentum of the vector boson is given by

$$q^\mu = p_5^\mu + p_6^\mu . \quad (6.2.1)$$

It is convenient to define the invariants

$$s_{12} = (p_1 + p_2)^2 , \quad s_{13} = (p_1 + p_3)^2 , \quad s_{23} = (p_2 + p_3)^2 , \quad (6.2.2)$$

which fulfil

$$q^2 = (p_1 + p_2 + p_3)^2 = s_{12} + s_{13} + s_{23} \equiv s_{123} , \quad (6.2.3)$$

as well as the dimensionless invariants

$$x = s_{12}/s_{123} , \quad y = s_{13}/s_{123} , \quad z = s_{23}/s_{123} , \quad (6.2.4)$$

which satisfy $x + y + z = 1$.

In $3j$ -production, q^2 is time-like (hence positive) and all the s_{ij} are also positive, which implies that x, y, z all lie in the interval $[0; 1]$, with the above constraint $x + y + z = 1$. For the $V\gamma$ production, q^2 remains time-like, but only s_{12} is positive:

$$q^2 > 0 , \quad s_{12} > 0 , \quad s_{13} < 0 , \quad s_{23} < 0 , \quad (6.2.5)$$

or, equivalently,

$$x > 0 , \quad y < 0 , \quad z < 0 . \quad (6.2.6)$$

It was shown in [174] that the kinematical situation of this configuration can be expressed by introducing new dimensionless variables

$$u = -\frac{s_{13}}{s_{12}} = -\frac{y}{x} , \quad v = \frac{q^2}{s_{12}} = \frac{1}{x} , \quad (6.2.7)$$

which fulfil

$$0 \leq u \leq v, \quad 0 \leq v \leq 1.$$

The helicity amplitudes for $q\bar{q} \rightarrow V\gamma$ can be expressed as a product of a partonic current S_μ and a leptonic current L_μ :

$$A(p_5, p_6; p_1, p_3, p_2) = L^\mu(p_5; p_6) S_\mu(p_1; p_3; p_2). \quad (6.2.8)$$

Only the partonic current receives contributions from QCD radiative corrections, and it can be perturbatively decomposed as:

$$\begin{aligned} S_\mu(p_1; p_3; p_2) = \sqrt{4\pi\alpha} \left(S_\mu^{(0)}(p_1; p_3; p_2) + \left(\frac{\alpha_s}{2\pi} \right) S_\mu^{(1)}(p_1; p_3; p_2) \right. \\ \left. + \left(\frac{\alpha_s}{2\pi} \right)^2 S_\mu^{(2)}(p_1; p_3; p_2) + \mathcal{O}(\alpha_s^3) \right). \end{aligned} \quad (6.2.9)$$

It is a colour-singlet. The vector boson decay to a lepton-antilepton pair is described by a leptonic current. To be as general as possible, we consider only the basic amplitude structure in the partonic and leptonic current, and include charges and coupling factors related to the massive vector boson only when assembling the final results. We have extracted a factor $e = \sqrt{4\pi\alpha}$ for the photon coupling in the partonic current, such that all the quark charges will be expressed in units of e .

As discussed in Section 2.1.1, the most general structure of the partonic current can be derived from symmetry considerations:

$$\begin{aligned} S_\mu(p_1; p_3; p_2) = A_{11} T_{11\mu} + A_{12} T_{12\mu} + A_{13} T_{13\mu} \\ + A_{21} T_{21\mu} + A_{22} T_{22\mu} + A_{23} T_{23\mu} \\ + B T_\mu, \end{aligned} \quad (6.2.10)$$

where $T_{ij\mu}$ and T_μ are the following tensor structures:

$$\begin{aligned} T_{1j\mu} &= \bar{v}(p_1) \left[\not{p}_3 \epsilon_3 \cdot p_1 p_{j\mu} - \frac{s_{13}}{2} \epsilon_3 p_{j\mu} + \frac{s_{j4}}{4} \epsilon_3 \not{p}_3 \gamma_\mu \right] u(p_2), \\ T_{2j\mu} &= \bar{v}(p_1) \left[\not{p}_3 \epsilon_3 \cdot p_2 p_{j\mu} - \frac{s_{23}}{2} \epsilon_3 p_{j\mu} + \frac{s_{j4}}{4} \gamma_\mu \not{p}_3 \epsilon_3 \right] u(p_2), \\ T_\mu &= \bar{v}(p_1) \left[s_{23} \left(\gamma_\mu \epsilon_3 \cdot p_1 + \frac{1}{2} \epsilon_3 \not{p}_3 \gamma_\mu \right) - s_{13} \left(\gamma_\mu \epsilon_3 \cdot p_2 + \frac{1}{2} \gamma_\mu \not{p}_3 \epsilon_3 \right) \right] u(p_2), \end{aligned} \quad (6.2.11)$$

where we defined:

$$s_{14} = s_{12} + s_{13}, \quad s_{24} = s_{12} + s_{23}, \quad s_{34} = s_{13} + s_{23}.$$

The tensor coefficients A_{ij} and B can be determined by appropriate projectors, applied to the Feynman-diagrammatic expression of the amplitude. Projections on the diagrams are performed in dimensional regularisation in $d = 4 - 2\epsilon$ dimensions. The projectors can be found in [174].

Each of the unrenormalised coefficients A_{ij} and B has a perturbative expansion of the form

$$\begin{aligned} A_{ij}^{\text{un}} &= \sqrt{4\pi\alpha} \left[A_{ij}^{(0),\text{un}} + \left(\frac{\alpha_s}{2\pi}\right) A_{ij}^{(1),\text{un}} + \left(\frac{\alpha_s}{2\pi}\right)^2 A_{ij}^{(2),\text{un}} + \mathcal{O}(\alpha_s^3) \right], \\ B^{\text{un}} &= \sqrt{4\pi\alpha} \left[B^{(0),\text{un}} + \left(\frac{\alpha_s}{2\pi}\right) B^{(1),\text{un}} + \left(\frac{\alpha_s}{2\pi}\right)^2 B^{(2),\text{un}} + \mathcal{O}(\alpha_s^3) \right], \end{aligned} \quad (6.2.12)$$

where the dependence on $(s_{13}, s_{23}, s_{123})$ is implicit.

By fixing the helicities of the partons, the partonic current can be cast in the usual spinor helicity notation [175]. All helicity configurations can be obtained from the amplitude

$$\begin{aligned} S_R^\mu(p_1^-; p_3^+; p_2^+) &= \frac{1}{\sqrt{2}} \langle 12 \rangle [13]^2 (p_{1\mu} A_{11} + p_{2\mu} A_{12} + p_{3\mu} A_{13}) - \frac{1}{\sqrt{2}} \frac{\langle 12 \rangle [13]}{\langle 23 \rangle} [1 | \gamma_\mu | 2 \rangle s_{23} B \\ &+ \frac{1}{\sqrt{2}} [13] [3 | \gamma_\mu | 2 \rangle \left[s_{23} B + \frac{1}{2} ((A_{11} + A_{12}) s_{12} + (A_{11} + A_{13}) s_{13} + (A_{12} + A_{13}) s_{23}) \right] \end{aligned} \quad (6.2.13)$$

by charge and parity conversion. For $\bar{q}'(p_1)$, $q(p_2)$ incoming, the above amplitude corresponds to a right-handed current. Notice that (6.2.13) has been obtained assuming that the momentum of the photon is $-p_3$. We have:

$$\begin{aligned} S_L^\mu(p_1^+; p_3^-; p_2^-) &= [S_R^\mu(p_1^-; p_3^+; p_2^+)]^*, \\ S_L^\mu(p_1^+; p_3^+; p_2^-) &= -S_R^\mu(p_2^-; p_3^+; p_1^+), \\ S_R^\mu(p_1^-; p_3^-; p_2^+) &= [-S_R^\mu(p_2^-; p_3^+; p_1^+)]^*. \end{aligned} \quad (6.2.14)$$

It is also straightforward to include the spin-correlations with the leptonic decay products by contracting the partonic current with the leptonic current L_μ for fixed helicities of the final state leptons. Consider the decay of the vector boson V into two leptons:

$$V(q) \longrightarrow l^+(p_5) + l^-(p_6).$$

The purely vectorial tree-level leptonic current reads:

$$L^\mu(p_5, p_6) = \bar{u}(p_6) \gamma^\mu v(p_5), \quad (6.2.15)$$

where in the case of an outgoing lepton-antilepton pair $L_\mu(p_5^-, p_6^+)$ corresponds to a right handed current, and $L_\mu(p_5^+, p_6^-)$ to a left-handed current. We find straightforwardly:

$$L_R^\mu(p_5^-, p_6^+) = [6 | \gamma^\mu | 5 \rangle, \quad L_L^\mu(p_5^+, p_6^-) = [5 | \gamma^\mu | 6 \rangle = [L_R^\mu(p_5^-, p_6^+)]^*. \quad (6.2.16)$$

In order to write down the lepton-parton contraction it is convenient to introduce the set of helicity coefficients defined in [33]:

$$\alpha(u, v) = \frac{s_{13}s_{23}}{4} (2B + A_{12} - A_{11}), \quad (6.2.17)$$

$$\beta(u, v) = \frac{s_{13}}{4} \left(2s_{23}B + 2(s_{12} + s_{13})A_{11} + s_{23}(A_{12} + A_{13}) \right), \quad (6.2.18)$$

$$\gamma(u, v) = \frac{s_{13}s_{23}}{4} (A_{11} - A_{13}), \quad (6.2.19)$$

$$\delta(u, v) = -\frac{s_{12}s_{13}}{4} A_{11}, \quad (6.2.20)$$

which, from their definition in terms of the coefficients A_{ij} and B , respect the relation

$$\alpha(u, v) - \beta(u, v) - \gamma(u, v) - \frac{2s_{123}}{s_{12}}\delta(u, v) = 0. \quad (6.2.21)$$

The relations above can be inverted for A_{11} , $A_{12} + 2B$ and A_{13} , and in these variables the contracted amplitude assumes a particularly simple form. We take the contraction of the right-handed quark current with positive photon helicity, and the right-handed leptonic current, as basic object from which all other helicity configurations are obtained:

$$\begin{aligned} A_{RR}^+(p_5, p_6; p_1, p_3, p_2) &= L_R^\mu(p_5^-; p_6^+) S_{R,\mu}(p_1^-; p_3^+; p_2^+) \\ &= -2\sqrt{2} \left[\frac{\langle 25 \rangle \langle 12 \rangle [16]}{\langle 13 \rangle \langle 23 \rangle} \alpha(u, v) - \frac{\langle 25 \rangle [36]}{\langle 13 \rangle} \beta(u, v) + \frac{\langle 15 \rangle [13] [36]}{\langle 13 \rangle [23]} \gamma(u, v) \right]. \end{aligned} \quad (6.2.22)$$

The unrenormalised helicity amplitude coefficients α , β and γ are vectors in colour space and have perturbative expansions:

$$\Omega^{\text{un}} = \sqrt{4\pi\alpha} \delta_{ij} \left[\Omega^{(0),\text{un}} + \left(\frac{\alpha_s}{2\pi} \right) \Omega^{(1),\text{un}} + \left(\frac{\alpha_s}{2\pi} \right)^2 \Omega^{(2),\text{un}} + \mathcal{O}(\alpha_s^3) \right], \quad (6.2.23)$$

for $\Omega = \alpha, \beta, \gamma$. The dependence on (u, v) is again implicit.

From $A_{RR}^+(p_5, p_6; p_1, p_3, p_2)$, all other helicity amplitudes can be obtained by parity and charge conjugation. Axial contributions from the weak gauge boson couplings can be accounted for in a straightforward manner, by simply reweighting the different right-handed and left-handed helicity amplitudes with appropriate weights.

The eight possible helicity configurations are obtained from A_{RR}^+ as follows:

$$\begin{aligned} L_R^\mu(p_5^-; p_6^+) S_{R,\mu}(p_1^-; p_3^+; p_2^+) &= A_{RR}^+(p_5, p_6; p_1, p_3, p_2), \\ L_R^\mu(p_5^-; p_6^+) S_{R,\mu}(p_1^-; p_3^-; p_2^+) &= A_{RR}^-(p_5, p_6; p_1, p_3, p_2) = [-A_{RR}^+(p_6, p_5; p_2, p_3, p_1)]^*, \\ L_R^\mu(p_5^-; p_6^+) S_{L,\mu}(p_1^+; p_3^+; p_2^-) &= A_{RL}^+(p_5, p_6; p_1, p_3, p_2) = -A_{RR}^+(p_5, p_6; p_2, p_3, p_1), \\ L_R^\mu(p_5^-; p_6^+) S_{L,\mu}(p_1^+; p_3^-; p_2^-) &= A_{RL}^-(p_5, p_6; p_1, p_3, p_2) = [A_{RR}^+(p_6, p_5; p_1, p_3, p_2)]^*, \end{aligned} \quad (6.2.24)$$

$$\begin{aligned} L_L^\mu(p_5^+; p_6^-) S_{R,\mu}(p_1^-; p_3^+; p_2^+) &= A_{LR}^+(p_5, p_6; p_1, p_3, p_2) = A_{RR}^+(p_6, p_5; p_1, p_3, p_2), \\ L_L^\mu(p_5^+; p_6^-) S_{R,\mu}(p_1^-; p_3^-; p_2^+) &= A_{LR}^-(p_5, p_6; p_1, p_3, p_2) = [-A_{RR}^+(p_5, p_6; p_2, p_3, p_1)]^*, \\ L_L^\mu(p_5^+; p_6^-) S_{L,\mu}(p_1^+; p_3^+; p_2^-) &= A_{LL}^+(p_5, p_6; p_1, p_3, p_2) = -A_{RR}^+(p_6, p_5; p_2, p_3, p_1), \end{aligned}$$

$$L_L^\mu(p_5^+; p_6^-) S_{L\mu}(p_1^+; p_3^-; p_2^-) = A_{LL}^-(p_5, p_6; p_1, p_3, p_2) = [A_{RR}^+(p_5, p_6; p_1, p_3, p_2)]^*. \quad (6.2.25)$$

The general form of the gauge boson coupling to fermions is:

$$\mathcal{V}_\mu^{V, f_1 f_2} = -i e \Gamma_\mu^{V, f_1 f_2} \quad \text{with} \quad e = \sqrt{4\pi\alpha}, \quad (6.2.26)$$

whose explicit form depends on the gauge boson, on the type of fermions, and on their helicities:

$$\Gamma_\mu^{V, f_1 f_2} = L_{f_1 f_2}^V \gamma_\mu \left(\frac{1 - \gamma_5}{2} \right) + R_{f_1 f_2}^V \gamma_\mu \left(\frac{1 + \gamma_5}{2} \right). \quad (6.2.27)$$

The left- and right-handed couplings are identical for a pure vector interaction, and are in general different if vector and axial-vector interactions contribute. Their values for a photon are

$$L_{f_1 f_2}^\gamma = R_{f_1 f_2}^\gamma = -e_{f_1} \delta_{f_1 f_2}, \quad (6.2.28)$$

while for a Z boson

$$L_{f_1 f_2}^Z = \frac{I_3^{f_1} - \sin^2 \theta_w e_{f_1}}{\sin \theta_w \cos \theta_w} \delta_{f_1 f_2}, \quad R_{f_1 f_2}^Z = -\frac{\sin \theta_w e_{f_1}}{\cos \theta_w} \delta_{f_1 f_2}, \quad (6.2.29)$$

and finally for a W^\pm

$$L_{f_1 f_2}^W = \frac{1}{\sqrt{2} \sin \theta_w}, \quad R_{f_1 f_2}^W = 0. \quad (6.2.30)$$

The charges e_i are measured in units of the fundamental electric charge $e > 0$.

The vector boson propagator can be written as:

$$P_{\mu\nu}^V(q, \xi) = \frac{i \Delta_{\mu\nu}^V(q, \xi)}{D_V(q)}, \quad (6.2.31)$$

where $\Delta_{\mu\nu}^V(q, \xi)$ and $D_V(q)$ are, respectively, the numerator and the denominator in the R_ξ gauge:

$$\Delta_{\mu\nu}^V(q, \xi) = \left(-g_{\mu\nu} + (1 - \xi) \frac{q_\mu q_\nu}{q^2 - \xi M_V^2} \right), \quad (6.2.32)$$

$$D_{Z, W^\pm}(q) = (q^2 - M_V^2 + i\Gamma_V M_V), \quad (6.2.33)$$

$$D_\gamma(q) = q^2. \quad (6.2.34)$$

In the narrow-width approximation we can simplify expression (6.2.33) to

$$D_{Z, W^\pm}(q) \approx i\Gamma_V M_V \quad \text{and} \quad q^2 = M_V^2, \quad (6.2.35)$$

where M_V is the mass of the vector boson, while Γ_V is its decay width.

Since we do not consider any electroweak corrections, the vector boson V is always coupled to a fermion line and this allows us to neglect the R_ξ dependence (or equivalently to put $\xi = 1$). With this notation we obtain for the different choices of $V = (\gamma^*, Z, W^\pm)$, and helicity combinations (with the obvious notation $p_{ij} = p_i + p_j$):

$$\mathcal{M}_V(p_5^-, p_6^+; p_1^-, p_3^+, p_2^+) = -i(4\pi\alpha) \frac{R_{q_1q_2}^V R_{f_5f_6}^V}{D_V(p_{56})} A_{RR}^+(p_5, p_6; p_1, p_3, p_2), \quad (6.2.36)$$

$$\mathcal{M}_V(p_5^-, p_6^+; p_1^+, p_3^-, p_2^-) = -i(4\pi\alpha) \frac{L_{q_1q_2}^V R_{f_5f_6}^V}{D_V(p_{56})} [A_{RR}^+(p_6, p_5; p_1, p_3, p_2)]^*, \quad (6.2.37)$$

$$\mathcal{M}_V(p_5^-, p_6^+; p_1^+, p_3^+, p_2^-) = -i(4\pi\alpha) \frac{L_{q_1q_2}^V R_{f_5f_6}^V}{D_V(p_{56})} [-A_{RR}^+(p_5, p_6; p_2, p_3, p_1)], \quad (6.2.38)$$

$$\mathcal{M}_V(p_5^-, p_6^+; p_1^-, p_3^-, p_2^+) = -i(4\pi\alpha) \frac{R_{q_1q_2}^V R_{f_5f_6}^V}{D_V(p_{56})} [-A_{RR}^+(p_6, p_5; p_2, p_3, p_1)]^*. \quad (6.2.39)$$

The corresponding amplitudes for left-handed leptonic current can be obtained simply interchanging $p_5 \leftrightarrow p_6$ and $R_{f_5f_6}^V \rightarrow L_{f_5f_6}^V$.

6.3 Outline of the calculation

The two-loop corrections to the coefficients Ω for $W^\pm\gamma$ and $Z^0\gamma$ production can be evaluated through a calculation of the relevant Feynman diagrams. The diagrams which contribute at the two-loop level can be organised in different classes, some of which are present in both $V = Z^0, W^\pm$ cases, while others contribute only to one of the two processes.

To identify the different classes of diagrams, it is useful to start with the tree-level. We can define three classes of processes, each represented by a single diagram:

1. We call $I_1^{(0)}$ the contribution from diagram (1) in Figure 6.1, where the photon is attached on the quark q' . The charge factor of this diagram is $e_{q'}$.
2. We refer as $I_2^{(0)}$ to the contribution from diagram (2) in Figure 6.1, where the photon is attached on the quark q . The charge factor of this diagram is e_q .
3. $I_3^{(0)}$ is finally the contribution from diagram (3) in Figure 6.1, where an off-shell W^* radiates the final state. The charge factor of this diagram is unity.

The e_i are measured in units of e , so that $e_{q'} - e_q = 1$.

One can compute the $\Omega_j^{(0)}$ through the use of the projectors defined above, and once the three different contributions are known one can reconstruct the correct values for the helicity coefficients as:

$$\Omega_{W^\pm}^{(0)} = U_{qq'} \left(e_{q'} \Omega_1^{(0)} + e_q \Omega_2^{(0)} + \Omega_3^{(0)} \right) = U_{qq'} \left[e_{q'} \left(\Omega_1^{(0)} + \Omega_2^{(0)} \right) + \Omega_3^{(0)} - \Omega_2^{(0)} \right], \quad (6.3.1)$$

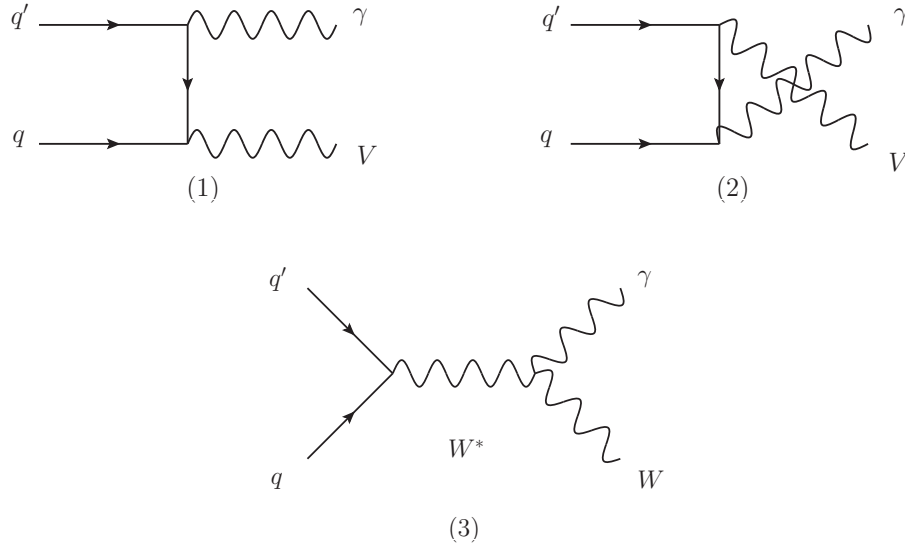


Figure 6.1: Abelian and non-abelian tree-level contribution.

$$\Omega_{Z,\gamma^*}^{(0)} = e_q \left(\Omega_1^{(0)} + \Omega_2^{(0)} \right), \quad (6.3.2)$$

where U_{ij} are the CKM matrix elements. To simplify the expression above, we made use of the fact that the Z^0 boson does not couple to the photon, and that in this case there is no flavour change, i.e. $e_{q'} = e_q$.

At leading order, the d -dimensional expressions for the coefficients read:

$$\begin{aligned} \alpha_1^{(0)} &= \frac{d-4}{4(d-3)} \left(2 + \frac{v}{u} - \frac{1}{u} \right), & \alpha_2^{(0)} &= -\frac{d-4}{4(d-3)} \left(2 + \frac{v}{u} - \frac{1}{u} \right) + 1, \\ \alpha_3^{(0)} &= -\frac{d-4}{4(d-3)} \left(2 + \frac{v}{u} - \frac{1}{u} \right) + 1 - \frac{u}{1-v}. \end{aligned} \quad (6.3.3)$$

$$\begin{aligned} \beta_1^{(0)} &= \frac{d-4}{4(d-3)} \left(1 - \frac{1}{u} \right) + 1, & \beta_2^{(0)} &= -\frac{d-4}{4(d-3)} \left(1 - \frac{1}{u} \right), \\ \beta_3^{(0)} &= -\frac{d-4}{4(d-3)} \left(1 - \frac{1}{u} \right) - \frac{u}{1-v}. \end{aligned} \quad (6.3.4)$$

$$\begin{aligned} \gamma_1^{(0)} &= -\frac{d-4}{4(d-3)} \left(1 + \frac{v}{u} \right), & \gamma_2^{(0)} &= \frac{d-4}{4(d-3)} \left(1 + \frac{v}{u} \right), \\ \gamma_3^{(0)} &= \frac{d-4}{4(d-3)} \left(1 + \frac{v}{u} \right). \end{aligned} \quad (6.3.5)$$

Using (6.3.1) and (6.3.2) we find

$$\alpha_W^{(0)} = U_{qq'} \left(e_{q'} - \frac{u}{1-v} \right), \quad \beta_W^{(0)} = U_{qq'} \left(e_{q'} - \frac{u}{1-v} \right), \quad \gamma_W^{(0)} = 0, \quad (6.3.6)$$

$$\alpha_{Z,\gamma^*}^{(0)} = e_q, \quad \beta_{Z,\gamma^*}^{(0)} = e_q, \quad \gamma_{Z,\gamma^*}^{(0)} = 0. \quad (6.3.7)$$

At one-loop, the same classification of contributions applies: $I_1^{(1)}, I_2^{(1)}, I_3^{(1)}$. A further type of diagrams, with both the photon and the gauge boson which couple to a closed quark loop, is zero due to colour conservation. At two loops, besides $I_1^{(2)}, I_2^{(2)}, I_3^{(2)}$, three further classes of diagrams appear:

1. $I_4^{(2)}$ are the diagrams where both γ and V couple to the same fermion loop, as depicted for example in Figure 6.2, diagram (4).

This contribution is denoted by $N_{F,V}$ and is proportional to the charge weighted sum of the quark flavours. In case of a γ^* exchange we find

$$N_{F,\gamma} = \frac{\sum_{q'} e_{q'}^2}{e_q}. \quad (6.3.8)$$

Considering Z -interactions, the same class of diagrams yields not only a contribution from the vector component of the Z , which for the right-handed quark amplitude is given by

$$N_{F,Z} = \frac{\sum_{q'} (L_{q'q'}^Z + R_{q'q'}^Z) e_{q'}}{2R_{qq}^Z}, \quad (6.3.9)$$

but also a contribution involving the axial couplings of the Z . This contribution vanishes identically for $Z^0\gamma$ production, already before summing over the quark flavours inside the loop. In the case of W^\pm exchange charge conservation ensures that

$$N_{F,W^\pm} = 0. \quad (6.3.10)$$

2. $I_5^{(2)}$ are the diagrams where the photon couples alone to a fermion loop, while V couples to the fermion line, as depicted in Figure 6.2, diagram (5). This class of diagrams has to sum to zero due to Furry's theorem.
3. $I_6^{(2)}$ are finally the diagrams where V couples alone to a fermion loop, while γ couples to the fermion line, as depicted in Figure 6.2, diagram (6). These diagrams give both a vector and an axial contribution, where the vector contribution is again zero due to Furry's theorem, while the axial contribution is zero in the framework of massless QCD [176].

We explicitly evaluated the contributions from classes $I_5^{(2)}, I_6^{(2)}$, and their vanishing provides a check on our calculation.

The classes $I_j^{(2)}$, $j = 1, 6$ exhaust all the possible two-loop QCD diagrams which can contribute to the production of a pair $V\gamma$, whatever is the identity of the vector boson V .

When computing the helicity amplitudes, one can evaluate the contributions from

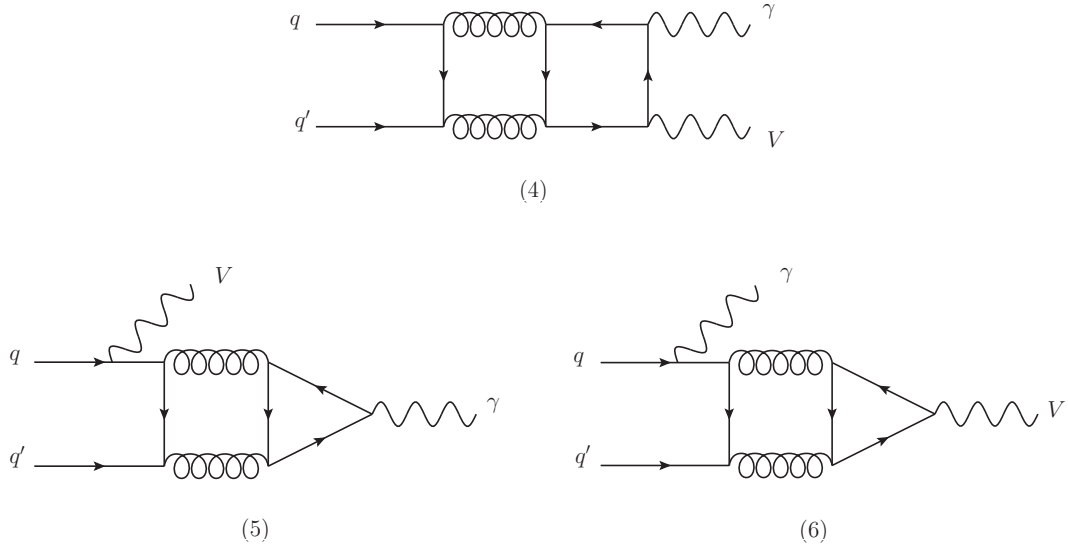


Figure 6.2: Examples of two-loop diagrams in the classes $I_4^{(2)}$, $I_5^{(2)}$ and $I_6^{(2)}$.

these six classes of diagrams independently, without keeping track of the axial current contributions, thus considering the vector boson V as an off-shell purely vector particle. Once the $I_j^{(2)}$ are known, as for the tree-level case, one can reconstruct the proper amplitudes for $V = Z^0, W^\pm$ summing these six contributions up, multiplied by appropriate weights.

The calculation proceeds as follows. The 143 two-loop diagrams belonging to the classes $j = (1, 2, 4, 5, 6)$ are produced using QGRAF [34] while, on the other hand, we did not need to evaluate explicitly the diagrams in class $I_3^{(2)}$, since they only account for the QCD corrections of the quark form factor, which is known up to three loops in the literature [177–180].

The tensor coefficients are then evaluated analytically diagram by diagram applying the projectors defined in [176]. As a result, one obtains the tensor coefficients in terms of thousands of planar and non-planar two-loop scalar integrals, which can be easily classified in two auxiliary topologies, one planar and the other non-planar [173]. Through the usual IBP identities [38, 39] one can reduce independently all the integrals belonging to these two auxiliary topologies to a small set of master integrals. This reduction is performed using the Laporta algorithm [43], implemented in the Reduze code [46]. All the masters for such topologies are known [59, 84] as series in the parameter $\epsilon = (4 - d)/2$, through a systematic approach based on the differential equation method [35]. The masters are expressed as Laurent expansion in ϵ , with coefficients containing harmonic polylogarithms (HPLs, [58]) and two-dimensional harmonic polylogarithms (2dHPLs, [59, 84]). Numerical implementations of these functions are available [66, 67]. For all the intermediate algebraic manipulations we

have made extensive use of FORM [132].

The two-loop unrenormalised helicity coefficients $\Omega^{(2),\text{un}}$ can then be evaluated as linear combination of the tensor coefficients, and in particular they can be evaluated separately for every class of diagrams:

$$\Omega_j^{(2),\text{un}}, \quad \text{with } j = 1, 6. \quad (6.3.11)$$

As for the tree level case, it is trivial to reconstruct the amplitudes for the processes considered as linear combinations of these six amplitudes.

We start considering the case where $V = W^\pm$. The W boson couples only to left-handed fermions and charge conservation implies that $N_{F,W} = 0$. The amplitudes for $W^\pm\gamma$ production at two loops thus receive contributions only from three of the six classes of diagrams above, i.e.:

$$\begin{aligned} \Omega_{W^\pm}^{(2),\text{un}} &= U_{qq'} \left(e_{q'} \Omega_1^{(2),\text{un}} + e_q \Omega_2^{(2),\text{un}} + \Omega_3^{(2),\text{un}} \right) \\ &= U_{qq'} \left[e_{q'} \left(\Omega_1^{(2),\text{un}} + \Omega_2^{(2),\text{un}} \right) + \Omega_3^{(2),\text{un}} - \Omega_2^{(2),\text{un}} \right]. \end{aligned} \quad (6.3.12)$$

As for the tree level, U_{ij} are the CKM matrix elements.

For the $V = Z^0, \gamma^*$ case, $I_3^{(n)} = 0$ at all orders, since the Z^0 and γ^* are electrically neutral, while $I_4^{(2)}$ is non-vanishing since charge conservation does not forbid such diagrams anymore.

$$\Omega_V^{(2),\text{un}} = e_q \left(\Omega_1^{(2),\text{un}} + \Omega_2^{(2),\text{un}} \right) + N_{F,V} \Omega_4^{(2),\text{un}}, \quad (6.3.13)$$

for $V = (Z^0, \gamma^*)$.

6.4 Two-loop helicity amplitudes

Renormalisation of ultraviolet divergences is performed in the $\overline{\text{MS}}$ scheme by replacing the bare coupling α_0 with the renormalised coupling $\alpha_s \equiv \alpha_s(\mu^2)$, evaluated at the renormalisation scale μ^2 . Since the tree amplitudes are of $\mathcal{O}(\alpha_s^0)$, we only need the one loop relation between the bare and renormalised couplings:

$$\alpha_0 \mu_0^{2\epsilon} S_\epsilon = \alpha_s \mu^{2\epsilon} \left[1 - \frac{\beta_0}{\epsilon} \left(\frac{\alpha_s}{2\pi} \right) + \mathcal{O}(\alpha_s^2) \right], \quad (6.4.1)$$

where

$$S_\epsilon = (4\pi)^\epsilon e^{-\epsilon\gamma} \quad \text{with Euler constant } \gamma = 0.5772 \dots$$

and μ_0^2 is the mass parameter introduced in dimensional regularisation to maintain a dimensionless coupling in the bare QCD Lagrangian density. β_0 is the first coefficient of the QCD β -function:

$$\beta_0 = \frac{11C_A - 4T_R N_F}{6}, \quad (6.4.2)$$

with the QCD colour factors

$$C_A = N, \quad C_F = \frac{N^2 - 1}{2N}, \quad T_R = \frac{1}{2}. \quad (6.4.3)$$

The renormalisation is performed at fixed scale $\mu^2 = q^2$. The renormalised helicity coefficients read:

$$\begin{aligned} \Omega^{(0)} &= \Omega^{(0),\text{un}}, \\ \Omega^{(1)} &= S_\epsilon^{-1} \Omega^{(1),\text{un}}, \\ \Omega^{(2)} &= S_\epsilon^{-2} \Omega^{(2),\text{un}} - \frac{\beta_0}{\epsilon} S_\epsilon^{-1} \Omega^{(1),\text{un}}. \end{aligned} \quad (6.4.4)$$

The full scale dependence of the coefficients can be recovered from the renormalisation group. It reads:

$$\begin{aligned} \Omega(\mu^2, \alpha_s(\mu^2)) &= \sqrt{4\pi\alpha} \delta_{ij} \left[\Omega^{(0)} + \left(\frac{\alpha_s(\mu^2)}{2\pi} \right) \Omega^{(1)} \right. \\ &\quad \left. + \left(\frac{\alpha_s(\mu^2)}{2\pi} \right)^2 \left(\Omega^{(2)} + \beta_0 \Omega^{(1)} \ln \left(\frac{\mu^2}{q^2} \right) \right) + \mathcal{O}(\alpha_s^3) \right], \end{aligned} \quad (6.4.5)$$

After performing ultraviolet renormalisation, the amplitudes still contain singularities, which are of infrared origin and will be analytically cancelled by those occurring in radiative processes of the same order. Catani [181] has shown how to organise the infrared pole structure of the one- and two-loop contributions renormalised in the $\overline{\text{MS}}$ -scheme in terms of the tree and renormalised one-loop amplitudes. The same procedure applies to the tensor coefficients. Their pole structure can be separated off as follows:

$$\begin{aligned} \Omega^{(1)} &= \mathbf{I}^{(1)}(\epsilon) \Omega^{(0)} + \Omega^{(1),\text{finite}}, \\ \Omega^{(2)} &= \left(-\frac{1}{2} \mathbf{I}^{(1)}(\epsilon) \mathbf{I}^{(1)}(\epsilon) - \frac{\beta_0}{\epsilon} \mathbf{I}^{(1)}(\epsilon) + e^{-\epsilon\gamma} \frac{\Gamma(1-2\epsilon)}{\Gamma(1-\epsilon)} \left(\frac{\beta_0}{\epsilon} + K \right) \mathbf{I}^{(1)}(2\epsilon) \right. \\ &\quad \left. + \mathbf{H}^{(2)}(\epsilon) \right) \Omega^{(0)} + \mathbf{I}^{(1)}(\epsilon) \Omega^{(1)} + \Omega^{(2),\text{finite}}, \end{aligned} \quad (6.4.6)$$

where the constant K is

$$K = \left(\frac{67}{18} - \frac{\pi^2}{6} \right) C_A - \frac{10}{9} T_R N_F. \quad (6.4.7)$$

In our case, there is only a quark–antiquark pair present in the initial state, so that $\mathbf{I}^{(1)}(\epsilon)$ is given by,

$$\mathbf{I}^{(1)}(\epsilon) = -\frac{e^{\epsilon\gamma}}{2\Gamma(1-\epsilon)} \left[\frac{N^2 - 1}{2N} \left(\frac{2}{\epsilon^2} + \frac{3}{\epsilon} \right) \mathbf{S}_{12} \right], \quad (6.4.8)$$

where, since we have set $\mu^2 = s_{12}^2$:

$$S_{12} = \left(-\frac{\mu^2}{s_{12}} \right)^\epsilon = (x)^{-\epsilon} (-1 - i0)^{-\epsilon}. \quad (6.4.9)$$

Note that on expanding S_{12} , imaginary parts are generated, the sign of which is fixed by the small imaginary part $+i0$ of s_{12} . The hard radiation constant is a scalar in colour space:

$$\mathbf{H}^{(2)}(\epsilon) = \frac{e^{\epsilon\gamma}}{4\epsilon\Gamma(1-\epsilon)} H^{(2)}. \quad (6.4.10)$$

with

$$H^{(2)} = 2H_q^{(2)} \quad (6.4.11)$$

where in the $\overline{\text{MS}}$ scheme

$$\begin{aligned} H_q^{(2)} = (N^2 - 1) & \left[\left(\frac{7}{4}\zeta_3 + \frac{409}{864} - \frac{11\pi^2}{96} \right) N^2 + \left(\frac{3}{2}\zeta_3 + \frac{3}{32} - \frac{\pi^2}{8} \right) \frac{1}{N^2} \right. \\ & \left. + \left(\frac{\pi^2}{48} - \frac{25}{216} \right) \frac{N_F}{N} \right]. \end{aligned} \quad (6.4.12)$$

For the infrared factorisation of the two-loop results, the renormalised next-to-leading order helicity amplitude coefficients are needed through to $\mathcal{O}(\epsilon^2)$. Their decomposition in colour structures is straightforward:

$$\Omega_j^{(1),\text{finite}}(u, v) = C_F a_\Omega^{(j)}(u, v). \quad (6.4.13)$$

The expansion of the coefficients through to ϵ^2 yields HPLs and 2dHPLs up to weight 4. The explicit expressions are of considerable size, such that we only quote the ϵ^0 -terms in the appendix. To this order, the coefficients had been derived previously [182, 183] in terms of logarithms and dilogarithms. The expressions through to $\mathcal{O}(\epsilon^2)$ in FORM format are appended to the arXiv submission of [32].

The finite two-loop remainder is obtained by subtracting the predicted infrared structure (expanded through to $\mathcal{O}(\epsilon^0)$) from the renormalised helicity coefficient. We further decompose the finite remainder according to the colour structures as follows:

$$\begin{aligned} \Omega_j^{(2),\text{finite}}(u, v) = (N^2 - 1) & \left(A_\Omega^{(j)}(u, v) + \frac{1}{N^2} B_\Omega^{(j)}(u, v) \right) + C_F N_F C_\Omega^{(j)}(u, v) \\ & + C_F N_{F,V} D_\Omega^{(j)}(u, v), \end{aligned} \quad (6.4.14)$$

where the last term, as discussed above, is generated by graphs where the virtual gauge boson does not couple directly to the final-state quarks, and is different from zero only for the $V = Z, \gamma^*$ case.

The helicity coefficients contain HPLs and 2dHPLs up to weight 4. The size of each helicity coefficient is comparable to the size of the helicity-averaged tree times two-loop matrix element for $3j$ production quoted in [173], and we decided not to include them here explicitly. The complete set of coefficients in FORM format is attached to the arXiv submission [32].

6.5 Checks on the result

Several non-trivial checks were applied to validate our results:

1. All seven tensor coefficients in (6.2.10) were computed. We validated that they fulfil the following relations, which follow from the symmetry properties of the tensor under an interchange $p_1 \leftrightarrow p_2$:

$$\begin{aligned} A_{21}(s_{13}, s_{23}, s_{123}) &= -A_{12}(s_{23}, s_{13}, s_{123}), \\ A_{22}(s_{13}, s_{23}, s_{123}) &= -A_{11}(s_{23}, s_{13}, s_{123}), \\ A_{23}(s_{13}, s_{23}, s_{123}) &= -A_{13}(s_{23}, s_{13}, s_{123}), \\ B(s_{13}, s_{23}, s_{123}) &= B(s_{23}, s_{13}, s_{123}). \end{aligned} \quad (6.5.1)$$

2. We computed explicitly the helicity coefficients for all the diagrams in classes $I_5^{(2)}$ and $I_6^{(2)}$, which should yield a vanishing contribution due to Furry's theorem. Each diagram gives a non-vanishing contribution, a full cancellation is obtained only in the sum of all diagrams.
3. The IR singularity structure of our result agrees with the prediction of the Catani formula [181].
4. We compared the helicity coefficients $\Omega_Z^{(2)}$ for $q\bar{q} \rightarrow Z\gamma$, with those for $\gamma^* \rightarrow q\bar{q}g$ [33]. As explained in [32, 33], the unrenormalised two-loop Ω_{3j} coefficients can be decomposed according to their colour structure as:

$$\begin{aligned} \Omega_{3j}^{(2,\text{un})}(u, v) &= N^2 A_\Omega^{(3j,\text{un})}(u, v) + B_\Omega^{(3j,\text{un})}(u, v) + \frac{1}{N^2} C_\Omega^{(3j,\text{un})}(u, v) \\ &+ N N_F D_\Omega^{(3j,\text{un})}(u, v) + \frac{N_F}{N} E_\Omega^{(3j,\text{un})}(u, v) + N_F^2 F_\Omega^{(3j,\text{un})}(u, v) \\ &+ N_{F,V} \left(\frac{4}{N} - N \right) G_\Omega^{(3j,\text{un})}(u, v). \end{aligned} \quad (6.5.2)$$

We checked that in the decay kinematical configuration $Z \rightarrow q\bar{q}\gamma$, prior to UV renormalisation and IR subtraction, the following identities are fulfilled

$$\begin{aligned} B_\Omega^{(Z,\text{un})}(y, z) &= - C_\Omega^{(3j,\text{un})}(y, z), \\ C_\Omega^{(Z,\text{un})}(y, z) &= - 2 E_\Omega^{(3j,\text{un})}(y, z), \\ D_\Omega^{(Z,\text{un})}(y, z) &= - 4 G_\Omega^{(3j,\text{un})}(y, z), \end{aligned} \quad (6.5.3)$$

which follow from the structure of the underlying two-loop diagrams. UV renormalisation and IR subtraction of the $Z \rightarrow q\bar{q}\gamma$ and $Z \rightarrow q\bar{q}g$ amplitudes differ. However, two of the above relations are unaffected by renormalisation and retain the same IR structure, such that we obtain:

$$\begin{aligned} B_\Omega^{(Z,\text{finite})}(u, v) &= - C_\Omega^{(3j,\text{finite})}(u, v), \\ D_\Omega^{(Z,\text{finite})}(u, v) &= - 4 G_\Omega^{(3j,\text{finite})}(u, v), \end{aligned} \quad (6.5.4)$$

which also remain true after analytic continuation.

6.6 Conclusions and Outlook

In this chapter we discussed the derivation of the two-loop corrections to the helicity amplitudes for the processes $q\bar{q} \rightarrow W^\pm\gamma$ and $q\bar{q} \rightarrow Z^0\gamma$. Our calculation was performed in dimensional regularisation by applying d -dimensional projection operators to the most general tensor structure of the amplitude. Our results are expressed in terms of dimensionless helicity coefficients, which multiply the basic tree-level amplitudes, expressed in four-dimensional spinors. By applying Catani's infrared factorisation formula, we extract the finite parts of the helicity coefficients, which are independent on the precise scheme used to define the helicity amplitudes. We provide compact analytic expressions for the two-loop helicity coefficients in terms of HPLs and 2dHPLs.

The study of $V\gamma$ production provides a direct access to the photonic couplings of the weak gauge bosons and is a crucial test of the structure of the electroweak theory at high energies. The amplitudes derived here have been recently used, in combination with the amplitudes relevant to $V\gamma j$ production at NLO [157, 158], for the computation of the NNLO corrections to $Z\gamma$ production at hadron colliders [122]. Since the leading order contribution to this process does not contain any QCD partons in the final state, the well-established q_T subtraction method [25] has been used for this calculation. As an almost straightforward extension of this, the NNLO corrections to $W^\pm\gamma$ production at hadron collider are being computed exploiting the same techniques.

Chapter 7

ZZ production at hadron colliders in NNLO QCD

The material presented in this last chapter is based on the results obtained together with F. Cascioli, T. Gehrmann, M. Grazzini, S. Kallweit, P. Maierhöfer, A. von Manteuffel, S. Pozzorini, D. Rathlev, and E. Weihs, and has appeared for the first time in [110].

The production of vector-boson pairs is a crucial process for physics studies within and beyond the Standard Model (SM). In particular the production of Z -boson pairs is an irreducible background for Higgs boson production and new-physics searches. Various measurements of ZZ hadroproduction have been carried out at the Tevatron and the LHC (for some recent results see Refs. [184–189]).

The theoretical efforts for a precise prediction of ZZ production in the Standard Model started more than 20 years ago, with the first NLO QCD calculations [190,191] with stable Z bosons. The leptonic decays of the Z bosons were then added, initially neglecting spin correlations in the virtual contributions [192]. The computation of the relevant one-loop helicity amplitudes [114] allowed complete NLO calculations [147,193] including spin correlations and off-shell effects. The loop-induced gluon fusion contribution, which is formally next-to-next-to-leading order (NNLO), has been computed in Refs. [194,195]. The corresponding leptonic decays have been included in Refs. [196–198]. Since the gluon-induced contribution is enhanced by the gluon luminosity, it is often assumed to provide the bulk of the NNLO corrections. NLO predictions for ZZ production including the gluon-induced contribution, the leptonic decay with spin correlations and off-shell effects have been presented in Ref. [199]. The NLO QCD corrections to on-shell $ZZ + \text{jet}$ production have been discussed in Refs. [162,200], and the electroweak (EW) corrections to ZZ production have been computed in Ref. [119].

In this chapter we report on the first calculation of the inclusive production of on-shell ZZ pairs at hadron colliders in NNLO QCD. The NNLO computation requires the evaluation of the tree-level scattering amplitudes with two additional (un-

resolved) partons, of the one-loop amplitudes with one additional parton, and of the one-loop-squared and two-loop corrections to the Born subprocess $q\bar{q} \rightarrow ZZ$. All the relevant tree and one-loop matrix elements are automatically generated with OPENLOOPS [201], which implements a fast numerical recursion for the calculation of NLO scattering amplitudes within the SM. For the numerically stable evaluation of tensor integrals we rely on the COLLIER library [202], which is based on the Denner–Dittmaier reduction techniques [203, 204] and the scalar integrals of [205]. The loop-induced gluon fusion contribution is also obtained with OPENLOOPS, including five light-quark flavours and massive top-quark loops. The SM Higgs boson contribution is also considered. Following the recent computation of the relevant two-loop master integrals [86, 89–91] the last missing contribution, the genuine two-loop correction to the ZZ amplitude, has been computed by some of us, and will be reported elsewhere. In the two-loop correction, contributions involving a top-quark loop are neglected. For the numerical evaluation of the multiple polylogarithms in the two-loop expressions we employ the implementation [68] in the GiNAC [134] library.

The implementation of the various scattering amplitudes in a complete NNLO calculation is a highly non-trivial task due to the presence of infrared (IR) singularities at intermediate stages of the calculation that prevent a straightforward application of numerical techniques. To handle and cancel these singularities at NNLO we employ the q_T subtraction method [25]. This approach applies to the production of a colourless high-mass system F in generic hadron collisions and has been used for the computation of NNLO corrections to several hadronic processes [25, 121, 122, 206, 207]. According to the q_T subtraction method [25], the $pp \rightarrow F + X$ cross section at NNLO can be written as

$$d\sigma_{NNLO}^F = \mathcal{H}_{NNLO}^F \otimes d\sigma_{LO}^F + \left[d\sigma_{NLO}^{F+\text{jet}} - d\sigma_{NLO}^{CT} \right] , \quad (7.0.1)$$

where $d\sigma_{NLO}^{F+\text{jet}}$ is the cross section for the inclusive production of the system F plus one jet at NLO accuracy, and can be evaluated with any available version of the NLO subtraction formalism. When the transverse momentum q_T of the colourless system F is non-vanishing, $d\sigma_{NLO}^{F+\text{jet}}$ is the sole contribution to the NNLO cross section. The IR subtraction counterterm $d\sigma_{NLO}^{CT}$ in Eq. (7.0.1) has the purpose of cancelling the singularity developed by $d\sigma_{NLO}^{F+\text{jet}}$ as $q_T \rightarrow 0$ and is obtained from the resummation of the logarithmically-enhanced contributions to q_T distributions [208]. The function \mathcal{H}_{NNLO}^F , which also compensates for the subtraction of $d\sigma_{NLO}^{CT}$, corresponds to the NNLO truncation of the process-dependent perturbative function

$$\mathcal{H}^F = 1 + \frac{\alpha_S}{\pi} \mathcal{H}^{F(1)} + \left(\frac{\alpha_S}{\pi} \right)^2 \mathcal{H}^{F(2)} + \dots . \quad (7.0.2)$$

The NLO calculation of $d\sigma^F$ requires the knowledge of $\mathcal{H}^{F(1)}$, and the NNLO calculation also requires $\mathcal{H}^{F(2)}$.

The general structure of $\mathcal{H}^{F(1)}$ is known [209]: $\mathcal{H}^{F(1)}$ is obtained from the process-dependent scattering amplitudes by using a process-independent relation. Exploiting

the explicit results of $\mathcal{H}^{F(2)}$ for Higgs [210] and vector-boson [211] production, the process-independent relation of Ref. [209] has been extended to the calculation of the NNLO coefficient $\mathcal{H}^{F(2)}$ [212]. Such results have been confirmed with a fully independent calculation of the relevant coefficients in the framework of Soft-Collinear Effective Theory (SCET) [213, 214]. We have performed our NNLO calculation for ZZ production according to Eq. (7.0.1), starting from a computation of the $d\sigma_{NLO}^{ZZ+jet}$ cross section with the dipole-subtraction method [19, 215]. The numerical calculation employs the generic Monte Carlo program that was developed for Ref. [122]. Although the q_T subtraction method and our implementation are suitable to perform a fully exclusive computation of ZZ production including the leptonic decays and the corresponding spin correlations, here we restrict ourselves to the inclusive production of on-shell Z bosons.

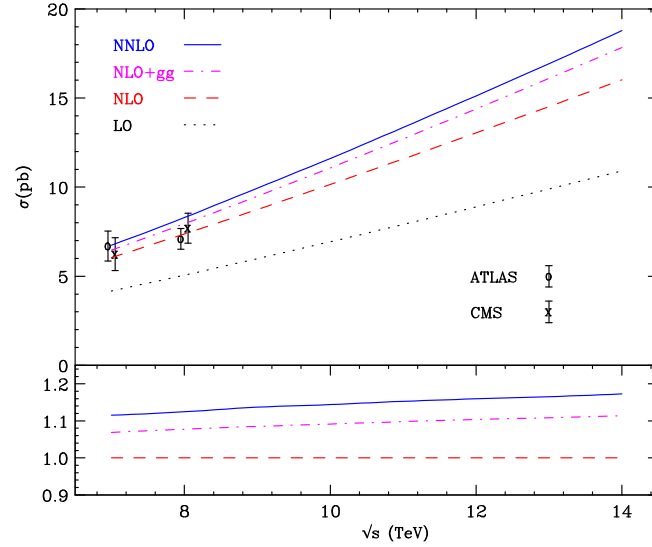


Figure 7.1: ZZ cross section at LO (dots), NLO (dashes), NLO+gg (dot dashes) and NNLO (solid) as a function of \sqrt{s} . The ATLAS and CMS experimental results at $\sqrt{s} = 7$ TeV and $\sqrt{s} = 8$ TeV are also shown for comparison [186–189]. The lower panel shows the NNLO and NLO+gg results normalised to the NLO prediction.

We consider pp collisions with \sqrt{s} ranging from 7 to 14 TeV. As for the EW couplings, we use the so-called G_μ scheme, where the input parameters are G_F , m_W , m_Z . In particular we use the values $G_F = 1.16639 \times 10^{-5} \text{ GeV}^{-2}$, $m_W = 80.399 \text{ GeV}$, $m_Z = 91.1876 \text{ GeV}$. The top mass $m_t = 173.2 \text{ GeV}$ and the Higgs mass $m_H = 125 \text{ GeV}$ only enter through the loop-induced gluon fusion contribution¹. We use the MSTW 2008 [216] sets of parton distributions, with densities and α_s evaluated at each corresponding order (i.e., we use $(n+1)$ -loop α_s at $N^n\text{LO}$, with $n = 0, 1, 2$), and

¹Since we consider the production of on-shell Z bosons, the Higgs contribution is strongly suppressed, and provides only about 1% to the loop-induced $gg \rightarrow ZZ$ cross section.

we consider $N_f = 5$ massless quark flavours. The default renormalisation (μ_R) and factorisation (μ_F) scales are set to $\mu_R = \mu_F = m_Z$.

The corresponding LO, NLO and NNLO cross sections as a function of \sqrt{s} are reported in Fig. 1. For comparison, we also show the NLO result supplemented with the loop-induced gluon fusion contribution (“NLO+gg”) computed with NNLO PDFs. The lower panel in Fig. 1 shows the NNLO and NLO+gg predictions normalised to the NLO result. The NLO corrections increase the LO result by about 45%. The impact of NNLO corrections with respect to the NLO result ranges from 11% ($\sqrt{s} = 7$ TeV) to 17% ($\sqrt{s} = 14$ TeV). Using NNLO PDFs throughout, the gluon fusion contribution provides between 58% and 62% of the full NNLO correction.

The theoretical predictions can be compared to the ATLAS and CMS measurements [186–189] carried out at $\sqrt{s} = 7$ TeV and $\sqrt{s} = 8$ TeV, which are also shown in the plot. We see that the experimental uncertainties are still relatively large and that the ATLAS and CMS results are compatible with both the NLO and NNLO predictions. The only exception is the ATLAS measurement at $\sqrt{s} = 8$ TeV [188], which seems to prefer a lower cross section. The comparison between our predictions and the experimental results, however, should be interpreted with care. First, we point out that the LHC experiments obtain their ZZ production cross section from four-lepton production using an interval in dilepton invariant masses around the Z boson mass, thus not including some contribution from far off-shell Z bosons. Then, EW corrections are not included in our calculation, and are expected to provide a negative contribution to the inclusive cross section [119].

In Table 1 we report the LO, NLO and NNLO cross sections and scale uncertainties, evaluated by varying μ_R and μ_F simultaneously and independently in the range $0.5m_Z < \mu_R, \mu_F < 2m_Z$ with the constraint $0.5 < \mu_F/\mu_R < 2$. From Table 1 we see that the scale uncertainties are about $\pm 3\%$ at NLO and remain of the same order at NNLO. We also see that the NLO scale uncertainty does not cover the NNLO effect. This is not unexpected since the gluon fusion channel, which provides a rather large contribution, opens up only at NNLO.

We have reported here on the first calculation of the inclusive cross section for the production of on-shell ZZ pairs at the LHC up to NNLO in QCD perturbation theory. The NNLO corrections increase the NLO result by an amount varying from 11% to 17% as \sqrt{s} ranges from 7 to 14 TeV. The loop-induced gluon fusion contribution provides more than half of the complete NNLO effect. Our calculation of the total cross section is based on the two-loop matrix element for $q\bar{q} \rightarrow ZZ$ for on-shell Z bosons.

\sqrt{s} (TeV)	σ_{LO} (pb)	σ_{NLO} (pb)	σ_{NNLO} (pb)
7	$4.167^{+0.7\%}_{-1.6\%}$	$6.044^{+2.8\%}_{-2.2\%}$	$6.735^{+2.9\%}_{-2.3\%}$
8	$5.060^{+1.6\%}_{-2.7\%}$	$7.369^{+2.8\%}_{-2.3\%}$	$8.284^{+3.0\%}_{-2.3\%}$
9	$5.981^{+2.4\%}_{-3.5\%}$	$8.735^{+2.9\%}_{-2.3\%}$	$9.931^{+3.1\%}_{-2.4\%}$
10	$6.927^{+3.1\%}_{-4.3\%}$	$10.14^{+2.9\%}_{-2.3\%}$	$11.60^{+3.2\%}_{-2.4\%}$
11	$7.895^{+3.8\%}_{-5.0\%}$	$11.57^{+3.0\%}_{-2.4\%}$	$13.34^{+3.2\%}_{-2.4\%}$
12	$8.882^{+4.3\%}_{-5.6\%}$	$13.03^{+3.0\%}_{-2.4\%}$	$15.10^{+3.2\%}_{-2.4\%}$
13	$9.887^{+4.9\%}_{-6.1\%}$	$14.51^{+3.0\%}_{-2.4\%}$	$16.91^{+3.2\%}_{-2.4\%}$
14	$10.91^{+5.4\%}_{-6.7\%}$	$16.01^{+3.0\%}_{-2.4\%}$	$18.77^{+3.2\%}_{-2.4\%}$

Table 7.1: Inclusive cross section for ZZ production at the LHC at LO, NLO and NNLO with $\mu_F = \mu_R = m_Z$. The uncertainties are obtained by varying the renormalisation and factorisation scales in the range $0.5m_Z < \mu_R, \mu_F < 2m_Z$ with the constraint $0.5 < \mu_F/\mu_R < 2$.

Conclusions

The apparently endless number of discoveries of the past century have changed completely our conception of the physical world, regarding both its content and the forces that determine its evolution. Special relativity on one side and quantum mechanics on the other have demolished the foundations of newtonian physics, starting from the nature of space and time, all the way to basic concepts like the distinction between particles and waves, or the deterministic evolution of a physical system. If these two breakthroughs have opened new scenarios which were entirely unimaginable before, it was the attempt of combining them which triggered a real “earthquake” in theoretical physics. Special relativity unifies the two apparently different concepts of *matter* and *energy*, unveiling how they must be nothing but two manifestations of the very same thing. It is however its interplay with quantum mechanics to unhinge something even more fundamental. Let us consider a particle with mass m , momentum p and total energy E . In special relativity every particle must fulfil the so-called on-shell condition $E^2 = p^2 + m^2$. When quantum mechanics comes into play though, this fundamental relation, which is equivalent to the requirement of positivity of the kinetic energy, does not always turn out to be true. Particles which do not fulfil the on-shell relation are called *virtual particles*.

One can intuitively imagine that if there exist particles which can elude this fundamental requirement, then nothing can prevent them from being, at least in principle, produced everywhere in arbitrary amounts. In quantum field theory virtual particles do not exist as free states, while their exchanges are responsible for the interactions among “real” particles. For the same reasoning above, once virtual particles are allowed to be exchanged, there is no reason why these exchanges should be limited in number. The possibility of creating such an enormous “jungle” of virtual particles has to be somehow accounted for, and we can therefore expect the mathematical structure of quantum field theory to be extremely complicated. We can intuitively imagine that the more virtual particles are created, the lower must be the probability for this event to happen, and this is entailed by the perturbative expansion in Feynman diagrams. The more intermediate virtual states we produce, the more loops we can draw in a diagram, the higher will be its order in perturbation theory.

Feynman diagrams have been for a long time, and remain to a large extent still today, our main “access point” to quantum field theory, since the complexity of the

theory prevents us from performing any exact computation. Even on the perturbative level, nonetheless, computing higher orders corrections is all but trivial, and in the second half of the past century a lot of progress has been made in gaining a deeper insight in the mathematical and physical properties of Feynman diagrams. This is important from two different perspectives. On one side, the computation of Feynman diagrams is the principal way we have to extract phenomenologically relevant predictions from the theory, and therefore to compare them with experimental results. On the other, the mathematical structures that appear at the perturbative level can give a hint of the properties of the exact theory as well, and the hope is that while “digging” deeper in this direction (which remains often the only practicable) a more general grasp on the whole theory can be gained.

Not long time ago we assisted to the so-called *NLO revolution*. The shared efforts in the computation of first order corrections gave the possibility to realise that a very general structure underlies NLO calculations, rather independently of the process and even of the theory considered. Having this general pattern at disposal allowed to write automated codes which can, at least in principle, compute the NLO corrections to any process. This has conceptually solved the problem of computing first order corrections, provided obviously that enough computational resources are at disposal.

On the contrary, second order corrections appeared soon rather more complicated, mainly because of the interplay between the more involved structure of the two-loop virtual amplitudes, together with the difficulty of building up flexible and efficient subtraction schemes to consistently account for the cancellation of the IR poles between virtual and real corrections. The main focus of this thesis has been on the developments of new mathematical tools which can address the first of these two issues, namely the computation of multiloop virtual corrections.

The techniques described in this thesis have a quite short history and most of them are undergoing a profound development as this thesis is being completed. The method of differential equations for master integrals in particular, together with a much deeper insight on the mathematical properties of the special functions which appear in the computation of Feynman diagrams, set off a real “explosion” of new computations, at least as far as two-loop corrections to $2 \rightarrow 2$ processes are concerned. This, supplemented by the concurrent development of efficient NNLO subtraction schemes, made many new NNLO computations for diverse processes relevant for LHC phenomenology possible. An important role among such processes is indeed played by the production of pairs of electroweak vector bosons in hadronic collisions, as this provides a large number of observables which allow to test with high precision the electroweak sector of the Standard Model.

In this thesis we reported on the results we have obtained in particular in the computation of two-loop virtual corrections to vector boson pair production. We made use of the differential equations method in order to compute the full set of two-loop master integrals required for the second-order QCD corrections to the production of two massive vector bosons with equal masses [86, 90]. In order to complete this calculation we employed recently introduced ideas for the choice of a canonical basis

for the master integrals [105]. We have then used these master integrals for the first computation of the NNLO corrections to the fully-inclusive total cross-section for on-shell ZZ production at hadron colliders [110]. A full account of these results can be found respectively in chapters 4 and 7 of this thesis. Note moreover that the same set of integrals can be used to compute the NNLO corrections to the production of two on-shell W bosons. This calculation is currently ongoing. Still concerning vector boson pair production, we have employed the set of four-point master integrals with one off-shell external leg, which have been known for a long time in the literature [59, 84], in order to compute the two-loop QCD helicity amplitudes for $Z\gamma$ and $W\gamma$ production. An account of these results is provided in chapter 6. Our amplitudes have been recently used for the full NNLO QCD corrections to $Z\gamma$ production at hadron colliders [122]. In this context we note also that the very same techniques can be employed for the NNLO corrections to $W\gamma$ production.

Finally, in parallel to our work on vector boson pair production, we have carried out a thorough study of the master integrals of the two-loop massive sunrise graph [37], see chapter 5. This has required the introduction of a new class of identities for master integrals, valid for integer numbers of the space-time dimensions, which have been dubbed Schouten identities. The application of the latter to more involved cases is currently under study. Note also that the sunrise graph constitutes still today the bottleneck for most two-loop computations involving massive internal particles, in particular in the electroweak sector of the standard model.

We believe that the techniques which have been used and, in part also developed and refined within this thesis, could constitute a contribution towards the automation of NNLO calculations in the near future.

In conclusion, after the recent discovery of a Higgs-like particle at the LHC, we are finally close to having enough statistics for precision measurements of the Higgs quantum numbers and of its couplings to fermions and gauge bosons. This, together with the precise theoretical predictions which have been obtained also thanks to the work carried out here, might ultimately help clarify the real nature of the electroweak symmetry breaking mechanism in the standard model of particle physics, and possibly open new scenarios for alternative models.

Acknowledgements

And we are finally close to the end. Getting to write the acknowledgements for my PhD thesis! I must admit that although I have been craving for this moment for a long time, now that this moment is here, I cannot hide a good amount of melancholy. This thesis closes a period of almost four years of my life which has enriched me unexpectedly much, from many different points of view. Unexpectedly because before moving to Zurich it was even hard to imagine the experiences that I would make and, more than anything else, the things that I would learn. And none of this would have been possible without the people who, in one way or another, have crossed my path during these years. So even if this will remain just a piece of paper that not so many people will want to read from the beginning to the end, I feel the need of thanking those that, each one in his or her own way, have been part of this journey. First of all, I need to thank Thomas Gehrmann, my supervisor, because it is only thanks to him and to the trust he decided to put in me that this journey has started. I must thank him for his time and his helpfulness throughout these years. But more than anything else, I want to thank him for having been at the same time a firm guide, and also for having always given me the space to “experiment” in many different directions, even if this sometimes brought me distant from our original projects. My gratitude goes also to all the people I had the pleasure to work with during these years. To my collaborator and friend Erich Weihs, who accepted to embark with me on a long, challenging (and sometimes frustrating!) project. Working with you has made it possible to see the end of it! Thank you for your patience! To Andreas von Manteuffel, whose deep understanding of multiloop Feynman integrals and of programming always makes me feel a little bit “stupid”, but it is as well a great motivation to go further and learn as much as I can. To Pierpaolo Mastrolia, for having shared with me very interesting projects and ideas. A very special thank you goes then to my first teacher and mentor, Ettore Remiddi. It was his passion for physics that brought me ultimately here, let alone his continuous encouragement and his precious suggestions. Thank you for teaching me something new every time that we meet. I must also thank all members of the institute of theoretical physics of the University of Zurich (now officially the “Physik-Institut”), because they made this institute one of the best environments where I could hope to spend the years of my PhD. I am especially grateful to Regina and Esther, because

without their kindness and helpfulness we would have all been lost. Special thanks go also to Mark and Elena, for having read parts of my thesis and having given me many useful suggestions.

But in spite of all this, I must say that, luckily, my life here was not only confined to the physics institute. My heartfelt gratitude goes to Benoit, Daniela, Davide, Fabio, Andrea and Sandra, and to the “new entries” Elena and Valentina, who have been my family in Zurich. In particular, thanks to Fabio, Davide and Valentina, for having been perfect flatmates and great friends. A huge thank you goes also to Marcos, Anastasiya and Mirjam, because the only way learning German could be so much fun was with you guys! Thanks for your friendship, your support, your patience and for the motivation, not only with German!! Also, I will never be able to thank enough Andrea (Gosty), Antonietta, Antonio, Isabel and Giuseppe, who have been there for me always, without having ever expected anything in return. Thank you, because without you I don’t know where I would be!! I can also not avoid to thank my longtime friends Mauro and Mariangela, which even from very far away, have always had time for me. Finally, thanks to all my family, grazie ai miei genitori che mi hanno supportato sempre, alle mie sorelle, Angela e Francesca, e a Luigi e Vittoria, perché una famiglia così non avrei potuto trovarla da nessun'altra parte! Last but not least, I would like to thank Marco, because although since a long time we went our separate ways, I know that if I could get here where I am now, this is also thanks to you.

Appendices

Appendix A

The canonical basis for $q\bar{q} \rightarrow VV$

As a result of the algorithm described in section 3.3.3 we find the following canonical basis. We recall here that the basis in mathematica format can be found attached to the arXiv submission of [90].

$$\begin{aligned}
m_1 &= \epsilon^2 \frac{m^2(1+x)^2}{x} f_1^{A38}, \quad m_2 = \epsilon^2 m^2 f_2^{A134}, \quad m_3 = \epsilon^2 m^2 z f_3^{A148}, \\
m_4 &= \epsilon^2 \frac{m^2(1+x^2-xz)}{x} f_4^{\bar{A}148}, \quad m_5 = \epsilon^2 \frac{m^4(1+x)^4}{x^2} f_5^{A99}, \quad m_6 = \epsilon^2 \frac{m^4(1+x)^2}{x} f_6^{A195}, \\
m_7 &= \epsilon^2 m^4 f_7^{A387}, \quad m_8 = -\epsilon^2 m^4 z f_8^{A394}, \quad m_9 = -\epsilon^2 \frac{m^4(1+x^2-xz)}{x} f_9^{\bar{A}394}, \quad m_{10} = \epsilon^2 m^4 z^2 f_{10}^{A408}, \\
m_{11} &= \epsilon^2 \frac{m^4(1+x^2-xz)^2}{x^2} f_{11}^{\bar{A}408}, \quad m_{12} = \epsilon^2 m^4 f_{12}^{A418}, \quad m_{13} = -\epsilon^3 \frac{m^2(1+x)^2}{x} f_{13}^{A53}, \\
m_{14} &= \epsilon^3 m^2(1+z) f_{14}^{A142}, \quad m_{15} = \epsilon^3 \frac{m^2(1+x+x^2-xz)}{x} f_{15}^{\bar{A}142}, \quad m_{16} = -\epsilon^3 m^2(1+z) f_{16}^{A149}, \\
m_{17} &= -\epsilon^3 \frac{m^2(1+x+x^2-xz)}{x} f_{17}^{\bar{A}149}, \quad m_{18} = \epsilon^3 \frac{m^2(1-x^2)}{x} f_{19}^{A166}, \\
m_{19} &= \epsilon^2 \left[(1-2\epsilon)(1-3\epsilon) f_{18}^{A166} + \frac{m^2(1+x)^2}{2x} f_1^{A38} \right] - \epsilon^3 \frac{m^2(1+x)}{x} f_{19}^{A166}, \\
m_{20} &= \epsilon^3 \frac{m^2(1-x^2)}{x} f_{21}^{A198}, \quad m_{21} = \epsilon^2 [(1-2\epsilon)(1-3\epsilon) f_{20}^{A198} - m^2 f_2^{A134}] - \epsilon^3 \frac{m^2(1-2x^2)}{x} f_{21}^{A198}, \\
m_{22} &= \epsilon^3 \frac{m^4(1-x)(1+x)^3}{x^2} f_{22}^{A227}, \quad m_{23} = \epsilon^3 \frac{m^4(1-x^2)}{x} f_{23}^{A419}, \quad m_{24} = \epsilon^4 \frac{m^2(1-x^2)}{x} f_{24}^{A199}, \\
m_{25} &= \epsilon^4 m^2(1+z) f_{25}^{A398}, \quad m_{26} = \epsilon^4 \frac{m^2(1+x+x^2-xz)}{x} f_{26}^{\bar{A}398}, \quad m_{27} = \epsilon^4 \frac{m^2(1-x^2)}{x} f_{27}^{A422}, \\
m_{28} &= \epsilon^3 \frac{m^4 z(1+x)^2}{x} f_{28}^{A174}, \quad m_{29} = \epsilon^3(1-2\epsilon) \frac{m^2(1-x^2)}{x} f_{29}^{A181}, \quad m_{30} = \epsilon^3 \frac{m^4 z(1+x)^2}{x} f_{30}^{A181}, \\
m_{31} &= \epsilon^3(1-2\epsilon) \frac{m^2(1-x^2)}{x} f_{31}^{\bar{A}181}, \quad m_{32} = \epsilon^3 \frac{m^4(1+x)^2(1+x^2-xz)}{x^2} f_{32}^{\bar{A}181}, \\
m_{33} &= \epsilon^4 \frac{m^2(1+x+x^2-xz)}{x} f_{33}^{A182}, \quad m_{34} = \epsilon^3 m^4(1+z) f_{34}^{A182}, \quad m_{35} = \epsilon^4 m^2(1+z) f_{35}^{\bar{A}182},
\end{aligned}$$

$$\begin{aligned}
m_{36} &= \epsilon^3 \frac{m^4(1+x+x^2-xz)}{x} f_{36}^{\bar{A}182}, \quad m_{37} = \epsilon^3 \frac{m^4 z(1+x)^2}{x} f_{37}^{A214}, \\
m_{38} &= \epsilon^3 \frac{m^4(1+x)^2(1+x^2-xz)}{x^2} f_{38}^{\bar{A}214}, \quad m_{39} = \epsilon^3 \frac{m^6 z(1+x)^2}{x} f_{39}^{A427}, \\
m_{40} &= \epsilon^4 \frac{m^4(1+z)(1+x)^2}{x} f_{40}^{A215}, \quad m_{41} = \epsilon^4 \frac{m^4(1+x+x^2-xz)(1+x)^2}{x^2} f_{41}^{\bar{A}215}, \\
m_{42} &= \epsilon^4 \frac{m^4(z(1+x+x^2)-x)}{x} f_{42}^{A430}, \quad m_{43} = \epsilon^4 \frac{m^6 z(1+x)^4}{x^2} f_{43}^{A247}, \\
m_{44} &= -\epsilon^2 \frac{m^2(1+x)^2}{2xz} f_1^{A38} + \epsilon^2 \frac{5m^2}{2z} f_2^{A134} + \epsilon^2 \frac{9m^2}{2} f_3^{A148} + \epsilon^3 \frac{6m^2(1+z)}{z} f_{16}^{A149} \\
&\quad + \epsilon^2 \frac{4(1-2\epsilon)(1-3\epsilon)}{z} f_{18}^{A166} - \epsilon^3 \frac{2m^2(1+x)^2}{xz} f_{19}^{A166} + \epsilon^3 \frac{2m^4(1+x)^2}{x} f_{30}^{A181} \\
&\quad + \epsilon^4 \frac{6m^2(1+x+x^2-xz)}{xz} f_{33}^{A182} + \epsilon^3 \frac{4m^4(1+z)}{z} f_{34}^{A182} + \epsilon^4 \frac{m^4(1+x)^4}{x^2} f_{44}^{A247}, \\
m_{45} &= \epsilon^4 \frac{m^4(1-x)(1+x)^3}{x^2} f_{45}^{A247}, \quad m_{46} = \epsilon^4 \frac{m^6 z^2(1+x)^2}{x} f_{46}^{A446}, \\
m_{47} &= \epsilon^4 m^4 z \left(\frac{(1+x)^2}{x} f_{42}^{A430} + (1+z) f_{47}^{A446} \right), \quad m_{48} = \epsilon^3 \frac{m^4(x-z)(1-xz)}{x} f_{48}^{B174}, \\
m_{49} &= \epsilon^3 \frac{m^4(x-z)(1-xz)}{x} f_{49}^{\bar{B}174}, \quad m_{50} = \epsilon^4 \frac{m^2(1+x)^2}{x} f_{50}^{B182}, \quad m_{51} = \epsilon^4 \frac{m^2(1-x^2)}{x} f_{51}^{B213}, \\
m_{52} &= \epsilon^3 \frac{m^4(1+x+x^2-xz)}{x} f_{52}^{B213}, \quad m_{53} = \epsilon^3 m^4(1+z) f_{53}^{B213}, \quad m_{54} = \epsilon^3 \frac{m^4(x-z)(1-xz)}{x} f_{54}^{B213}, \\
m_{55} &= \epsilon^3 \frac{m^6(x-z)(1-xz)}{x} f_{55}^{B249}, \quad m_{56} = \epsilon^4 \frac{m^4(1+z)(1+x^2-xz)}{x} f_{56}^{B215}, \\
m_{57} &= \epsilon^4 \frac{m^4 z(1+x+x^2-xz)}{x} f_{57}^{\bar{B}215}, \quad m_{58} = \epsilon^4 \frac{m^6(x-z)(1-xz)(1+x^2-xz)}{x^2} f_{58}^{B247}, \\
m_{59} &= -\epsilon^2 \frac{3m^2(1+x+x^2-xz)}{2(x-z)(1-xz)} f_2^{A134} - \epsilon^2 \frac{3m^2 z(1+x+x^2-xz)}{4(x-z)(1-xz)} f_3^{A148} \\
&\quad - \epsilon^2 \frac{3m^2(1+x^2-xz)(1+x+x^2-xz)}{4x(x-z)(1-xz)} f_4^{\bar{A}148} - \epsilon^3 \frac{m^4(1+x+x^2-xz)}{x} f_{49}^{\bar{B}174} \\
&\quad + \epsilon^4 \frac{3m^2(1+x)^2(1+x+x^2-xz)}{x(x-z)(1-xz)} f_{50}^{B182} + \epsilon^4 \frac{m^4(1+x^2-xz)(1+x+x^2-xz)}{x^2} f_{59}^{B247}, \\
m_{60} &= \epsilon^4 \frac{m^4(1-x^2)^2}{x^2} f_{60}^{C231}, \quad m_{61} = \epsilon^4 m^4(1+z)^2 f_{61}^{C252}, \quad m_{62} = \epsilon^4 \frac{m^4(1+x)^4}{x^2} f_{62}^{C318}, \\
m_{63} &= \epsilon^4 \frac{m^4(1+x)^2}{x} f_{63}^{C126}, \quad m_{64} = \epsilon^4 m^2(1+z) [f_{64}^{C126} - f_{33}^{A182}], \quad m_{65} = \epsilon^4 \frac{m^4(1+x)^2}{x} f_{65}^{C207}, \\
m_{66} &= +\epsilon^2 \frac{m^2(1+x)^2}{4x(1+z)} [f_2^{A134} + z f_3^{A148}] + \epsilon^3 \frac{m^2(1+x)^2}{x} f_{16}^{A149} - \epsilon^4 \frac{m^4(1+x)^2(1+x^2-xz)}{x^2} f_{65}^{C207} \\
&\quad + \epsilon^4 \frac{m^2(1+x+x^2-xz)}{x} f_{66}^{C207}, \\
m_{67} &= +\epsilon^2 \frac{m^2(1+x)^2}{4(1+x+x^2-xz)} \left[f_2^{A134} + \frac{(1+x^2-xz)}{x} f_4^{\bar{A}148} \right] + \epsilon^3 \frac{m^2(1+x)^2}{x} [f_{17}^{\bar{A}149} + \epsilon f_{33}^{A182}]
\end{aligned}$$

$$\begin{aligned}
& -\epsilon^4 m^2(1+z) [f_{51}^{B213} + f_{66}^{C207} - f_{67}^{C207}] , \\
m_{68} = & +\epsilon^4 \frac{m^2(1-x^2)}{x} [f_{68}^{C207} - f_{33}^{A182}] , \\
m_{69} = & +\epsilon^4 \frac{m^4(1-x^2)(1+z)}{x} f_{65}^{C207} - \epsilon^4 \frac{m^4(1-x^2)(1+x)}{x^2} f_{60}^{C231} \\
& - \epsilon^4 \frac{m^4(1-x^2)(1+x)^2}{x^2} [f_{41}^{\bar{A}215} - f_{70}^{C239}] , \\
m_{70} = & +\epsilon^4 m^4(1+x)(1+z) f_{65}^{C207} + \epsilon^4 \frac{m^4(1+x)^2(1-xz)}{2x^2} [f_{60}^{C231} - 2f_{70}^{C239}] \\
& + \epsilon^4 \frac{m^6(1+x)^2(1-xz)(x-z)}{2x^2} f_{69}^{C239} - \epsilon^4 \frac{m^4(1+x)^3}{x} f_{41}^{\bar{A}215} , \\
m_{71} = & +\epsilon^4 m^4(1+z) [f_{42}^{A430} + z f_{72}^{C254}] + \epsilon^2 \frac{3m^2 z(1+x)^2}{2(1-xz)(x-z)} f_2^{A134} + \epsilon^2 \frac{3m^2 z^2(1+x)^2}{4(1-xz)(x-z)} f_3^{A148} \\
& + \epsilon^3 \frac{m^4 z(1+x)^2}{x} [f_{48}^{B174} + \epsilon f_{65}^{C207}] + \epsilon^2 \frac{3m^2 z(1+x)^2(1+x^2-xz)}{4(1-xz)(x-z)x} f_4^{\bar{A}148} \\
& - \epsilon^4 \frac{3m^2 z(1+x)^4}{x(1-xz)(x-z)} f_{50}^{B182} , \\
m_{72} = & -\epsilon^4 \frac{m^4(1-xz)(x-z)}{x(1+z)} [f_{42}^{A430} + z f_{72}^{C254}] - \epsilon^3 \frac{2m^2 z(1+x)^2}{(1+z)x} [f_{14}^{A142} + f_{16}^{A149} - f_{17}^{\bar{A}149}] \\
& - \epsilon^4 \frac{2m^2 z(1+x)^2}{(1+z)x} [f_{25}^{A398} - f_{35}^{\bar{A}182} + f_{51}^{B213} - f_{64}^{C126} + f_{66}^{C207} - f_{67}^{C207}] - \epsilon^2 \frac{3m^2 z^2(1+x)^2}{2(1+z)^2 x} f_3^{A148} \\
& - \epsilon^3 \frac{m^4 z(1+x)^2}{(1+z)x} [f_{34}^{A182} - f_{53}^{B213}] - \epsilon^4 \frac{m^4 z(1+x)^2}{2x} f_{61}^{C252} \\
& - \epsilon^2 \frac{m^2 z(1+x)^2(3+2x-4xz+3x^2)}{2(1+z)^2(1+x+x^2-xz)x} f_2^{A134} \\
& + \epsilon^4 \frac{m^6 z(1+x)^2(1-xz)(x-z)}{2(1+z)x^2} f_{71}^{C254} + \epsilon^2 \frac{m^2 z(1+x)^2(1+x^2-xz)}{2x(1+z)(1+x+x^2-xz)} f_4^{\bar{A}148} \\
& + \epsilon^4 \frac{m^4(1+x)^2(-z+3x+2xz+xz^2-x^2z)}{2(1+z)x^2} [f_{63}^{C126} - f_{65}^{C207}] , \\
m_{73} = & -\epsilon^4 \frac{m^4(1+x)^2 z}{x} [f_{63}^{C126} - f_{74}^{C382}] + \epsilon^2 \frac{m^2(1+x)^2(1+x^2)}{4(1+x^2-xz)x} [f_1^{A38} + 4\epsilon f_{19}^{A166}] \\
& - \epsilon^3 \frac{m^4(1+x)^2(1+x^2)}{x^2} f_{32}^{\bar{A}181} - (1-2\epsilon)(1-3\epsilon)\epsilon^2 \frac{2(1+x^2)}{(1+x^2-xz)} f_{18}^{A166} \\
& - \epsilon^2 \frac{5m^2(1+x^2)}{4(1+x^2-xz)} f_2^{A134} - \epsilon^2 \frac{9m^2(1+x^2)}{4x} f_4^{\bar{A}148} \\
& - \epsilon^3 \frac{m^2(1+x^2)(1+x+x^2-xz)}{(1+x^2-xz)x} [3f_{17}^{\bar{A}149} + 2m^2 f_{36}^{\bar{A}182}] - \epsilon^4 \frac{3m^2(1+x^2)(1+z)}{(1+x^2-xz)} f_{35}^{\bar{A}182} , \\
m_{74} = & -\epsilon^4 \frac{m^4(1+x)^2(1-2xz+x^2)}{x^2} f_{63}^{C126} + \epsilon^4 \frac{m^6(1+x)^4(1+x^2-xz)}{x^3} f_{73}^{C382} \\
& - \epsilon^3 \frac{m^4(1+x)^2(1+x^2)}{x^2} [2f_{30}^{A181} - f_{32}^{\bar{A}181} + \epsilon f_{74}^{C382}] \\
& + \epsilon^2 \frac{m^2(1+x)^2(1+x^2)(2-3xz+2x^2)}{4(1+x^2-xz)x^2 z} [f_1^{A38} + 4\epsilon f_{19}^{A166}]
\end{aligned}$$

$$\begin{aligned}
& -\epsilon^2 \frac{9(1+x^2)m^2}{4x} \left[2f_3^{A148} - f_4^{\bar{A}148} \right] - (1-2\epsilon)(1-3\epsilon)\epsilon^2 \frac{2(1+x^2)(2-3xz+2x^2)}{(1+x^2-xz)xz} f_{18}^{A166} \\
& -\epsilon^2 \frac{5(1+x^2)(2-3xz+2x^2)m^2}{4(1+x^2-xz)xz} f_2^{A134} - \epsilon^4 \frac{6(1+x^2)(1+x+x^2-xz)m^2}{x^2z} f_{33}^{A182} \\
& + \epsilon^3 \frac{(1+x^2)(1+x+x^2-xz)m^2}{(1+x^2-xz)x} \left[3f_{17}^{\bar{A}149} + 2m^2 f_{36}^{\bar{A}182} \right] \\
& - \epsilon^3 \frac{(1+x^2)(1+z)m^2}{xz} \left[6f_{16}^{A149} + 4m^2 f_{34}^{A182} \right] + \epsilon^4 \frac{3(1+x^2)(1+z)m^2}{(1+x^2-xz)} f_{35}^{\bar{A}182}, \\
\\
m_{75} = & -\epsilon^2 \frac{3m^2z}{4(1+x)} f_3^{A148} + \epsilon^2 \frac{3m^2(2+x+xz+2x^2-x^2z+x^3)}{4(1-2\epsilon)(1+x)x} f_4^{\bar{A}148} \\
& + \epsilon^2 \frac{m^2(1+x+4xz+x^2-x^2z+x^3)}{4(1-2\epsilon)(1+x)(1+x^2-xz)} f_2^{A134} - \epsilon^3 \frac{(7+7x+3xz+3x^2-3x^2z+3x^3)}{(1+x)(1+x^2-xz)} f_{18}^{A166} \\
& + \epsilon^2 \frac{(1+x+xz+x^2-x^2z+x^3)}{(1+x)(1+x^2-xz)} f_{18}^{A166} - \epsilon^4 \frac{3m^2(1+x+x^2-xz)}{(1+x)x} f_{33}^{A182} \\
& + \epsilon^3 \frac{m^4(1+x+x^2-xz)(3+x+xz+3x^2-x^2z+x^3)}{2(1-2\epsilon)(1+x)(1+x^2-xz)x} f_{36}^{\bar{A}182} \\
& + \epsilon^3 \frac{3m^2(1+x+x^2-xz)(1+x+xz+x^2-x^2z+x^3)}{2(1-2\epsilon)(1+x)(1+x^2-xz)x} f_{17}^{\bar{A}149} - \epsilon^4 \frac{m^2(1-x^2)}{x} f_{75}^{C382} \\
& - \epsilon^3 \frac{m^4(1+z)}{(1+x)} f_{34}^{A182} + \epsilon^4 \frac{12}{(1+x^2-xz)} f_{18}^{A166} + \epsilon^4 \frac{2m^2(1+x)}{(1-2\epsilon)x} f_{13}^{A53} - \epsilon^3 \frac{9m^2}{2(1-2\epsilon)x} f_4^{\bar{A}148} \\
& - \epsilon^4 \frac{m^4(1+x)z}{x} f_{74}^{C382} + \epsilon^3 \frac{m^2(1+x)(2+x-xz+x^2)}{2(1-2\epsilon)(1+x^2-xz)x} f_1^{A38} \\
& + \epsilon^3 \frac{m^4(1+x)(1+x+xz+x^2-x^2z+x^3)}{2(1-2\epsilon)x^2} f_{32}^{\bar{A}181} - \epsilon^4 \frac{6m^2(1+x+x^2-xz)}{(1-2\epsilon)(1+x^2-xz)x} f_{17}^{\bar{A}149} \\
& - \epsilon^4 \frac{4m^4(1+x+x^2-xz)}{(1-2\epsilon)(1+x^2-xz)x} f_{36}^{\bar{A}182} - \epsilon^2 \frac{m^2(1+x)(1+x+x^2-x^2z+x^3)}{4(1-2\epsilon)(1+x^2-xz)x} f_1^{A38} \\
& + \epsilon^4 \frac{m^4(1+x)(1+z)}{x} f_{63}^{C126} - \epsilon^3 \frac{m^2(1+x)^2}{2(1-2\epsilon)x} f_{13}^{A53} + \epsilon^4 \frac{2m^2(1+x)^2}{(1-2\epsilon)(1+x^2-xz)x} f_{19}^{A166} \\
& - \epsilon^4 \frac{2m^4(1+x)^2}{(1-2\epsilon)x^2} f_{32}^{\bar{A}181} + \epsilon^4 \frac{m^4(1+x)^3}{2x^2} f_{62}^{C318} - \epsilon^3 \frac{m^2(1+x)(1+x^2)}{(1-2\epsilon)(1+x^2-xz)x} f_{19}^{A166} \\
& - \epsilon^5 \frac{2m^2(1+3x+2xz+x^3z-x^4)}{(1-2\epsilon)(1+x^2-xz)x} f_{35}^{\bar{A}182} + \epsilon^4 \frac{3m^2(1+x^2)(1+z)}{(1-2\epsilon)(1+x)(1+x^2-xz)} f_{35}^{\bar{A}182} \\
& - \epsilon^3 \frac{m^2(2+5x+3xz-3x^2)}{2(1-2\epsilon)(1+x)(1+x^2-xz)} f_2^{A134}.
\end{aligned}$$

We remark here that even if the formulas look in some cases rather cumbersome, they are always at most linear combinations of the starting basis f_j with rational coefficients. Obviously, choosing differently this starting basis can simplify or even complicate substantially these relations. On the other hand the main point of the derivation given in Section 3.3.3 is to show how, starting from a basis whose differential equations fulfil some initial requirements, a canonical basis (if it exists) MI can be built in an almost algorithmic way.

Appendix B

The two-loop massive sunrise

B.1 The first-order differential equations

In this appendix we give the explicit expressions for the polynomials appearing in the first-order differential equations in section 5.3. All polynomials are functions of p^2 and of the three masses m_1, m_2, m_3 , while they do not depend on the dimensions d .

$$\begin{aligned}
P_{10}^{(0)}(p^2, m_1, m_2, m_3) = & -m_1^2(m_1 + m_2 + m_3)(m_1 - m_2 + m_3)(m_1 + m_2 - m_3)(m_1 - m_2 - m_3) \\
& \times (m_1^2 - m_2^2 - m_3^2)^2 \\
& + p^2 (m_1^8 + 4m_2^2m_1^6 - 14m_2^4m_1^4 + 12m_2^6m_1^2 - 3m_2^8 + 4m_3^2m_1^6 + 4m_3^2m_2^4m_1^2 \\
& - 8m_3^2m_2^6 - 14m_3^4m_1^4 + 4m_3^4m_2^2m_1^2 + 22m_3^4m_2^4 + 12m_3^6m_1^2 - 8m_3^6m_2^2 - 3m_3^8) \\
& + p^4 (10m_1^6 - 4m_2^2m_1^4 + 2m_2^4m_1^2 - 8m_2^6 - 4m_3^2m_1^4 + 16m_3^2m_2^4 + 2m_3^4m_1^2 \\
& + 16m_3^4m_2^2 - 8m_3^6) \\
& + p^6 (14m_1^4 - 4m_2^2m_1^2 - 6m_2^4 - 4m_3^2m_1^2 + 24m_3^2m_2^2 - 6m_3^4) \\
& + 7p^8 m_1^2 + p^{10}, \tag{B.1.1}
\end{aligned}$$

$$\begin{aligned}
P_{10}^{(1)}(p^2, m_1, m_2, m_3) = & (m_1 + m_2 + m_3)(m_1 - m_2 + m_3)(m_1 + m_2 - m_3)(m_1 - m_2 - m_3) \\
& \times (m_1^2 - m_2^2 - m_3^2) (7m_1^4 - 6m_2^2m_1^2 - m_2^4 - 6m_3^2m_1^2 + 2m_3^2m_2^2 - m_3^4) \\
& + p^2 (11m_1^8 - 48m_2^2m_1^6 + 78m_2^4m_1^4 - 56m_2^6m_1^2 + 15m_2^8 - 48m_3^2m_1^6 \\
& + 68m_3^2m_2^2m_1^4 - 40m_3^2m_2^4m_1^2 + 20m_3^2m_2^6 + 78m_3^4m_1^4 - 40m_3^4m_2^2m_1^2 \\
& - 70m_3^4m_2^4 - 56m_3^6m_1^2 + 20m_3^6m_2^2 + 15m_3^8) \\
& + p^4 (-2m_1^6 - 14m_2^2m_1^4 + 2m_2^4m_1^2 + 14m_2^6 - 14m_3^2m_1^4 + 60m_3^2m_2^2m_1^2 \\
& - 62m_3^2m_2^4 + 2m_3^4m_1^2 - 62m_3^4m_2^2 + 14m_3^6) \\
& - 2p^6 (m_1^2 - m_2^2 - 3m_3^2) (m_1^2 - 3m_2^2 - m_3^2) + p^8 (11m_1^2 + m_2^2 + m_3^2) \\
& + 7p^{10}, \tag{B.1.2}
\end{aligned}$$

$$P_{10}^{(2)}(p^2, m_1, m_2, m_3) = (m_1 + m_2 + m_3)(m_1 - m_2 + m_3)(m_1 + m_2 - m_3)(m_1 - m_2 - m_3)$$

$$\begin{aligned}
& \times (5m_1^4 - 4m_2^2m_1^2 - m_2^4 - 4m_3^2m_1^2 + 2m_3^2m_2^2 - m_3^4) \\
& + p^2 (8m_1^6 - 18m_2^2m_1^4 + 20m_2^4m_1^2 - 10m_2^6 - 18m_3^2m_1^4 + 24m_3^2m_2^2m_1^2 \\
& + 10m_3^2m_2^4 + 20m_3^4m_1^2 + 10m_3^4m_2^2 - 10m_3^6) \\
& + p^4 (10m_1^4 + 6m_2^2m_1^2 - 8m_2^4 + 6m_3^2m_1^2 + 48m_3^2m_2^2 - 8m_3^4) \\
& + p^6 (16m_1^2 + 10m_2^2 + 10m_3^2) + 9p^8, \tag{B.1.3}
\end{aligned}$$

$$\begin{aligned}
P_{11}^{(0)}(p^2, m_1, m_2, m_3) &= (m_1 + m_2 + m_3)^2(m_1 - m_2 + m_3)^2(m_1 + m_2 - m_3)^2(m_1 - m_2 - m_3)^2 \\
& \times (m_1^2 - m_2^2 - m_3^2) m_1^2 \\
& + p^2 (-6m_1^{10} + m_2^2m_1^8 + 32m_2^4m_1^6 - 42m_2^6m_1^4 + 14m_2^8m_1^2 + m_2^{10} + m_3^2m_1^8 \\
& - 64m_3^2m_2^2m_1^6 + 26m_3^2m_2^4m_1^4 + 40m_3^2m_2^6m_1^2 - 3m_3^2m_2^8 + 32m_3^4m_1^6 \\
& + 26m_3^4m_2^2m_1^4 - 108m_3^4m_2^4m_1^2 + 2m_3^4m_2^6 - 42m_3^6m_1^4 + 40m_3^6m_2^2m_1^2 \\
& + 2m_3^6m_2^4 + 14m_3^8m_1^2 - 3m_3^8m_2^2 + m_3^{10}) \\
& + p^4 (-33m_1^8 + 6m_2^2m_1^6 - 20m_2^4m_1^4 + 42m_2^6m_1^2 + 5m_2^8 + 6m_3^2m_1^6 \\
& - 24m_3^2m_2^2m_1^4 - 26m_3^2m_2^4m_1^2 - 4m_3^2m_2^6 - 20m_3^4m_1^4 - 26m_3^4m_2^2m_1^2 \\
& - 2m_3^4m_2^4 + 42m_3^6m_1^2 - 4m_3^6m_2^2 + 5m_3^8) \\
& + p^6 (-52m_1^6 - 6m_2^2m_1^4 + 32m_2^4m_1^2 + 10m_2^6 - 6m_3^2m_1^4 - 64m_3^2m_2^2m_1^2 \\
& + 6m_3^2m_2^4 + 32m_3^4m_1^2 + 6m_3^4m_2^2 + 10m_3^6) \\
& + p^8 (-33m_1^4 - m_2^2m_1^2 + 10m_2^4 - m_3^2m_1^2 + 12m_3^2m_2^2 + 10m_3^4) \\
& + p^{10} (-6m_1^2 + 5m_2^2 + 5m_3^2) + p^{12}, \tag{B.1.4}
\end{aligned}$$

$$\begin{aligned}
P_{11}^{(1)}(p^2, m_1, m_2, m_3) &= (m_1 + m_2 + m_3)^2(m_1 - m_2 + m_3)^2(m_1 + m_2 - m_3)^2(m_1 - m_2 - m_3)^2 \\
& \times (5m_1^4 - 4m_2^2m_1^2 - m_2^4 - 4m_3^2m_1^2 + 2m_3^2m_2^2 - m_3^4) \\
& + p^2 (2m_1^{10} - 28m_2^2m_1^8 + 76m_2^4m_1^6 - 80m_2^6m_1^4 + 34m_2^8m_1^2 \\
& - 4m_2^{10} - 28m_3^2m_1^8 + 40m_3^2m_2^2m_1^6 - 48m_3^2m_2^4m_1^4 + 24m_3^2m_2^6m_1^2 \\
& + 12m_3^2m_2^8 + 76m_3^4m_1^6 - 48m_3^4m_2^2m_1^4 - 116m_3^4m_2^4m_1^2 - 8m_3^4m_2^6 \\
& - 80m_3^6m_1^4 + 24m_3^6m_2^2m_1^2 - 8m_3^6m_2^4 + 34m_3^8m_1^2 + 12m_3^8m_2^2 - 4m_3^{10}) \\
& + p^4 (-41m_1^8 - 42m_2^4m_1^4 + 88m_2^6m_1^2 - 5m_2^8 + 52m_3^2m_2^2m_1^4 - 152m_3^2m_2^4m_1^2 \\
& + 4m_3^2m_2^6 - 42m_3^4m_1^4 - 152m_3^4m_2^2m_1^2 + 2m_3^4m_2^4 + 88m_3^6m_1^2 + 4m_3^6m_2^2 - 5m_3^8) \\
& + p^6 (-84m_1^6 - 8m_2^2m_1^4 + 60m_2^4m_1^2 - 8m_2^6m_1^4 - 184m_3^2m_2^2m_1^2 + 60m_3^4m_1^2) \\
& + p^8 (-61m_1^4 - 8m_2^2m_1^2 + 5m_2^4 - 8m_3^2m_1^2 + 6m_3^2m_2^2 + 5m_3^4) \\
& + p^{10} (-14m_1^2 + 4m_2^2 + 4m_3^2) + p^{12}, \tag{B.1.5}
\end{aligned}$$

$$\begin{aligned}
P_{12}^{(0)}(p^2, m_1, m_2, m_3) &= (m_1 + m_2 + m_3)(m_1 - m_2 + m_3)(m_1 + m_2 - m_3)(m_1 - m_2 - m_3) \\
& \times (m_1^2 - m_2^2 - m_3^2) (3m_1^2 + m_2^2 - m_3^2) \\
& + p^2 (18m_1^6 + 2m_2^2m_1^4 - 10m_2^4m_1^2 - 10m_2^6 - 32m_3^2m_1^4 + 24m_3^2m_2^2m_1^2 \\
& + 40m_3^2m_2^4 + 34m_3^4m_1^2 - 10m_3^4m_2^2 - 20m_3^6)
\end{aligned}$$

$$\begin{aligned}
 &+ p^4 (36m_1^4 - 12m_2^2m_1^2 - 8m_2^4 + 6m_3^2m_1^2 + 66m_3^2m_2^2 - 34m_3^4) \\
 &+ p^6 (30m_1^2 + 10m_2^2 - 4m_3^2) + 9p^8,
 \end{aligned} \tag{B.1.6}$$

$$\begin{aligned}
 P_{14}^{(1)}(p^2, m_1, m_2, m_3) &= (m_1 + m_2 + m_3)(m_1 - m_2 + m_3)(m_1 + m_2 - m_3)(m_1 - m_2 - m_3) \\
 &\times (m_1^2 - m_2^2 - m_3^2)(m_1^2 - m_2^2 + m_3^2) \\
 &+ p^2 (6m_1^6 - 22m_2^2m_1^4 + 26m_2^4m_1^2 - 10m_2^6 + 12m_3^2m_1^4 + 8m_3^2m_2^2m_1^2 \\
 &- 20m_3^2m_2^4 - 18m_3^4m_1^2 + 30m_3^4m_2^2) \\
 &+ p^4 (12m_1^4 + 8m_2^2m_1^2 - 20m_2^4 - 10m_3^2m_1^2 + 22m_3^2m_2^2 + 6m_3^4) \\
 &+ p^6 (10m_1^2 - 6m_2^2 + 8m_3^2) + 3p^8,
 \end{aligned} \tag{B.1.7}$$

$$\begin{aligned}
 P_{14}^{(2)}(p^2, m_1, m_2, m_3) &= (m_1 + m_2 + m_3)(m_1 - m_2 + m_3)(m_1 + m_2 - m_3)(m_1 - m_2 - m_3) \\
 &\times (m_1^2 - m_2^2 + m_3^2)(5m_1^4 - 4m_2^2m_1^2 - m_2^4 - 4m_3^2m_1^2 + 2m_3^2m_2^2 - m_3^4) \\
 &+ p^2 (m_1^2 - m_2^2 + m_3^2)(17m_1^6 - 31m_2^2m_1^4 + 19m_2^4m_1^2 - 5m_2^6 - 29m_3^2m_1^4 \\
 &+ 46m_3^2m_2^2m_1^2 + 7m_3^2m_2^4 + 15m_3^4m_1^2 + m_3^4m_2^2 - 3m_3^6) \\
 &+ p^4 (22m_1^6 + 14m_2^2m_1^4 - 46m_2^4m_1^2 + 10m_2^6 - 42m_3^2m_1^4 + 72m_3^2m_2^2m_1^2 \\
 &- 6m_3^2m_2^4 + 38m_3^4m_1^2 - 2m_3^4m_2^2 - 2m_3^6) \\
 &+ p^6 (14m_1^4 - 16m_2^2m_1^2 + 10m_2^4 + 28m_3^2m_1^2 + 4m_3^2m_2^2 + 2m_3^4) \\
 &+ p^8 (5m_1^2 + 5m_2^2 + 3m_3^2) + p^{10},
 \end{aligned} \tag{B.1.8}$$

$$\begin{aligned}
 P_{22}(p^2, m_1, m_2, m_3) &= 3m_1^4 - 2m_2^2m_1^2 - m_2^4 - 2m_3^2m_1^2 + 2m_3^2m_2^2 - m_3^4 \\
 &+ 2p^2 (m_1^2 - m_2^2 + m_3^2) + 3p^4,
 \end{aligned} \tag{B.1.9}$$

The polynomials defined above fulfil, among the others, the relation:

$$\begin{aligned}
 &P_{14}^{(2)}(p^2, m_1, m_2, m_3) + P_{14}^{(2)}(p^2, m_1, m_3, m_2) \\
 &- 2m_1^2P_{10}^{(2)}(p^2, m_1, m_2, m_3) - 2p^2P^2(p^2, m_1, m_2, m_3) = 0,
 \end{aligned} \tag{B.1.10}$$

where note that the polynomial $P(p^2, m_1, m_2, m_3)$, defined in Eq.(5.3.3), appears squared.

B.2 The second-order differential equation

In this second appendix we give the explicit expressions of the polynomials that appear in the second-order differential equation derived in section 5.4. Also in this case, they are functions of p^2 and of the three masses m_1 , m_2 and m_3 , but they do not depend on the dimensions d .

$$A_2^{(0)}(p^2, m_1, m_2, m_3) = -(m_1 - m_2 - m_3)^3(m_1 - m_2 + m_3)^3(m_1 + m_2 - m_3)^3(m_1 + m_2 + m_3)^3$$

$$\begin{aligned}
& -8p^2(m_1 - m_2 - m_3)(m_1 - m_2 + m_3)(m_1 + m_2 - m_3)(m_1 + m_2 + m_3) \\
& \times (m_1^6 - m_2^2 m_1^4 - m_2^4 m_1^2 + m_2^6 - m_3^2 m_1^4 + 10m_3^2 m_2^2 m_1^2 \\
& - m_3^2 m_2^4 - m_3^4 m_1^2 - m_3^4 m_2^2 + m_3^6) \\
& - p^4 (13m_1^8 - 36m_2^2 m_1^6 + 46m_2^4 m_1^4 - 36m_2^6 m_1^2 + 13m_2^8 - 36m_3^2 m_1^6 \\
& - 124m_3^2 m_2^2 m_1^4 - 124m_3^2 m_2^4 m_1^2 - 36m_3^2 m_2^6 + 46m_3^4 m_1^4 - 124m_3^4 m_2^2 m_1^2 \\
& + 46m_3^4 m_2^4 - 36m_3^6 m_1^2 - 36m_3^6 m_2^2 + 13m_3^8) \\
& + 8p^6 (m_1^2 + m_2^2 + m_3^2) (m_1^4 + 6m_2^2 m_1^2 + m_2^4 + 6m_3^2 m_1^2 + 6m_3^2 m_2^2 + m_3^4) \\
& + p^8 (37m_1^4 + 70m_2^2 m_1^2 + 37m_2^4 + 70m_3^2 m_1^2 + 70m_3^2 m_2^2 + 37m_3^4) \\
& + 32p^{10} (m_1^2 + m_2^2 + m_3^2) + 9p^{12}
\end{aligned} \tag{B.2.1}$$

$$\begin{aligned}
A_2^{(1)}(p^2, m_1, m_2, m_3) = & -\frac{1}{2} (m_1 - m_2 - m_3)^3 (m_1 - m_2 + m_3)^3 (m_1 + m_2 - m_3)^3 (m_1 + m_2 + m_3)^3 \\
& + p^2 (m_1 - m_2 - m_3)(m_1 - m_2 + m_3)(m_1 + m_2 - m_3)(m_1 + m_2 + m_3) \\
& \times (5m_1^6 - 5m_2^2 m_1^4 - 5m_2^4 m_1^2 + 5m_2^6 - 5m_3^2 m_1^4 + 2m_3^2 m_2^2 m_1^2 \\
& - 5m_3^2 m_2^4 - 5m_3^4 m_1^2 - 5m_3^4 m_2^2 + 5m_3^6) \\
& + \frac{1}{2} p^4 (41m_1^8 - 84m_2^2 m_1^6 + 86m_2^4 m_1^4 - 84m_2^6 m_1^2 + 41m_2^8 - 84m_3^2 m_1^6 \\
& + 52m_3^2 m_2^2 m_1^4 + 52m_3^2 m_2^4 m_1^2 - 84m_3^2 m_2^6 + 86m_3^4 m_1^4 + 52m_3^4 m_2^2 m_1^2 \\
& + 86m_3^4 m_2^4 - 84m_3^6 m_1^2 - 84m_3^6 m_2^2 + 41m_3^8) \\
& + 2p^6 (11m_1^6 - 19m_2^2 m_1^4 - 19m_2^4 m_1^2 + 11m_2^6 - 19m_3^2 m_1^4 + 54m_3^2 m_2^2 m_1^2 \\
& - 19m_3^2 m_2^4 - 19m_3^4 m_1^2 - 19m_3^4 m_2^2 + 11m_3^6) \\
& + \frac{1}{2} p^8 (m_1^4 - 50m_2^2 m_1^2 + m_2^4 - 50m_3^2 m_1^2 - 50m_3^2 m_2^2 + m_3^4) \\
& - 11p^{10} (m_1^2 + m_2^2 + m_3^2) - \frac{9}{2} p^{12}
\end{aligned} \tag{B.2.2}$$

$$\begin{aligned}
A_3^{(0)}(p^2, m_1, m_2, m_3) = & (m_1 - m_2 - m_3)(m_1 - m_2 + m_3)(m_1 + m_2 - m_3)(m_1 + m_2 + m_3) \\
& \times (m_1^6 - m_2^2 m_1^4 - m_2^4 m_1^2 + m_2^6 - m_3^2 m_1^4 \\
& + 6m_3^2 m_2^2 m_1^2 - m_3^2 m_2^4 - m_3^4 m_1^2 - m_3^4 m_2^2 + m_3^6) \\
& + p^2 (5m_1^8 - 8m_2^2 m_1^6 + 6m_2^4 m_1^4 - 8m_2^6 m_1^2 + 5m_2^8 - 8m_3^2 m_1^6 \\
& - 8m_3^2 m_2^2 m_1^4 - 8m_3^2 m_2^4 m_1^2 - 8m_3^2 m_2^6 + 6m_3^4 m_1^4 - 8m_3^4 m_2^2 m_1^2 \\
& + 6m_3^4 m_2^4 - 8m_3^6 m_1^2 - 8m_3^6 m_2^2 + 5m_3^8) \\
& + 2p^4 (3m_1^6 - 7m_2^2 m_1^4 - 7m_2^4 m_1^2 + 3m_2^6 - 7m_3^2 m_1^4 \\
& - 7m_3^2 m_2^4 - 7m_3^4 m_1^2 - 7m_3^4 m_2^2 + 3m_3^6) \\
& - 2p^6 (m_1^4 + 8m_2^2 m_1^2 + m_2^4 + 8m_3^2 m_1^2 + 8m_3^2 m_2^2 + m_3^4) \\
& - 7p^8 (m_1^2 + m_2^2 + m_3^2) - 3p^{10}
\end{aligned} \tag{B.2.3}$$

$$\begin{aligned}
A_3^{(1)}(p^2, m_1, m_2, m_3) = & -\frac{1}{2} (m_1 - m_2 - m_3)(m_1 - m_2 + m_3)(m_1 + m_2 - m_3)(m_1 + m_2 + m_3) \\
& \times (m_1^2 - m_2^2 - m_3^2) (m_1^2 - m_2^2 + m_3^2) (m_1^2 + m_2^2 - m_3^2)
\end{aligned}$$

$$\begin{aligned}
 & -\frac{1}{2}p^2 (17m_1^8 - 32m_2^2m_1^6 + 18m_2^4m_1^4 - 8m_2^6m_1^2 + 5m_2^8 - 32m_3^2m_1^6 \\
 & + 20m_3^2m_2^2m_1^4 + 8m_3^2m_2^4m_1^2 + 4m_3^2m_2^6 + 18m_3^4m_1^4 + 8m_3^4m_2^2m_1^2 \\
 & - 18m_3^4m_2^4 - 8m_3^6m_1^2 + 4m_3^6m_2^2 + 5m_3^8) \\
 & - p^4 (21m_1^6 - 31m_2^2m_1^4 + 7m_2^4m_1^2 + 3m_2^6 - 31m_3^2m_1^4 + 30m_3^2m_2^2m_1^2 \\
 & - 3m_3^2m_2^4 + 7m_3^4m_1^2 - 3m_3^4m_2^2 + 3m_3^6) \\
 & - p^6 (17m_1^4 - 20m_2^2m_1^2 - m_2^4 - 20m_3^2m_1^2 + 22m_3^2m_2^2 - m_3^4) \\
 & - \frac{1}{2}p^8 (5m_1^2 - 7m_2^2 - 7m_3^2) + \frac{3}{2}p^{10}
 \end{aligned} \tag{B.2.4}$$

$$\begin{aligned}
 A_4(p^2, m_1, m_2, m_3) = & - (m_1^2 - m_2^2) \left[\right. \\
 & 24(m_1 - m_2 - m_3)(m_1 - m_2 + m_3)(m_1 + m_2 - m_3)(m_1 + m_2 + m_3) \\
 & \times (m_1^2 + m_2^2 - m_3^2) \\
 & + 8p^2 (9m_1^4 - 10m_2^2m_1^2 + 9m_2^4 - 14m_3^2m_1^2 - 14m_3^2m_2^2 + 5m_3^4) \\
 & \left. + 24p^4 (3m_1^2 + 3m_2^2 - 7m_3^2) + 24p^6 \right]
 \end{aligned} \tag{B.2.5}$$

$$\begin{aligned}
 A_5^{(1)}(p^2, m_1, m_2, m_3) = & (m_1 - m_2 - m_3)(m_1 - m_2 + m_3)(m_1 + m_2 - m_3)(m_1 + m_2 + m_3) \\
 & \times (m_1^4 - 2m_2^2m_1^2 + m_2^4 + m_3^2m_1^2 + m_3^2m_2^2 - 2m_3^4) \\
 & + p^2 (3m_1^6 - 3m_2^2m_1^4 - 3m_2^4m_1^2 + 3m_2^6 - 8m_3^2m_1^4 - 8m_3^2m_2^4 \\
 & + 11m_3^4m_1^2 + 11m_3^4m_2^2 - 6m_3^6) \\
 & + p^4 (3m_1^4 - 14m_2^2m_1^2 + 3m_2^4 + 7m_3^2m_1^2 + 7m_3^2m_2^2 - 6m_3^4) \\
 & + p^6 (m_1^2 + m_2^2 - 2m_3^2)
 \end{aligned} \tag{B.2.6}$$

$$\begin{aligned}
 A_5^{(2)}(p^2, m_1, m_2, m_3) = & -\frac{1}{2} (m_1 - m_2 - m_3)(m_1 - m_2 + m_3)(m_1 + m_2 - m_3)(m_1 + m_2 + m_3) \\
 & \times (m_1^2 - m_2^2 - m_3^2) (m_1^2 - m_2^2 + m_3^2) \\
 & - p^2 (3m_1^6 - 3m_2^2m_1^4 - 3m_2^4m_1^2 + 3m_2^6 - 2m_3^2m_1^4 + 4m_3^2m_2^2m_1^2 \\
 & - 2m_3^2m_2^4 + 7m_3^4m_1^2 + 7m_3^4m_2^2 - 8m_3^6) \\
 & - p^4 (6m_1^4 - 12m_2^2m_1^2 + 6m_2^4 + 11m_3^2m_1^2 + 11m_3^2m_2^2 - 13m_3^4) \\
 & - p^6 (5m_1^2 + 5m_2^2 - 4m_3^2) - \frac{3}{2}p^8
 \end{aligned} \tag{B.2.7}$$

Note that, in order to derive Eq.(5.4.2), we made use of the following relation:

$$A_5^{(1)}(p^2, m_1, m_2, m_3) + A_5^{(1)}(p^2, m_1, m_3, m_2) + A_5^{(1)}(p^2, m_2, m_3, m_1) = 0. \tag{B.2.8}$$

B.3 Tarasov's shift

In this Appendix we enclose the explicit formula for the order zero of the Tarasov's shift, Eq.(5.5.4) discussed in section 5.5, which relates the zeroth-order of the full

scalar amplitude, evaluated in $d = 4$ dimensions, to a linear combination of the four new MIs evaluate in $d = 2$ dimensions, namely $S(2; p^2)$, $S_1(2; p^2)$, $Z_2^{(1)}(2; p^2)$ and $Z_3^{(1)}(2; p^2)$.

$$\begin{aligned}
S^{(0)}(4; p^2) = & -\frac{1}{128} [13p^2 + 24(m_1^2 + m_2^2 + m_3^2)] \\
& + \frac{1}{8} \left[(m_1^2 - m_2^2 - m_3^2) \ln(m_3) \ln(m_2) - (m_1^2 - m_2^2 + m_3^2) \ln(m_3) \ln(m_1) \right. \\
& - (m_1^2 + m_2^2 - m_3^2) \ln(m_2) \ln(m_1) - \ln(m_3)^2 m_3^2 - \ln(m_2)^2 m_2^2 - \ln(m_1)^2 m_1^2 \Big] \\
& + \frac{1}{96 p^2} \left\{ \left[2p^4 + 6(4m_1^2 + m_2^2 + m_3^2)p^2 \right. \right. \\
& + (2m_1^4 - 6m_2^2 m_1^2 - m_2^4 - 6m_3^2 m_1^2 + 12m_3^2 m_2^2 - m_3^4) \Big] \ln(m_1) \\
& + \left[2p^4 + 6(m_1^2 + 4m_2^2 + m_3^2)p^2 \right. \\
& - (m_1^4 + 6m_2^2 m_1^2 - 2m_2^4 - 12m_3^2 m_1^2 + 6m_3^2 m_2^2 + m_3^4) \Big] \ln(m_2) \\
& + \left[2p^4 + 6(m_1^2 + m_2^2 + 4m_3^2)p^2 \right. \\
& - (m_1^4 - 12m_2^2 m_1^2 + m_2^4 + 6m_3^2 m_1^2 + 6m_3^2 m_2^2 - 2m_3^4) \Big] \ln(m_3) \Big\} \\
& - \frac{1}{96 p^2 P(p^2, m_1, m_2, m_3)} \left\{ \left[2p^8 - 2(2m_1^2 - 5m_2^2 - 5m_3^2)p^6 \right. \right. \\
& + (26m_1^4 - 56m_2^2 m_1^2 + 13m_2^4 - 56m_3^2 m_1^2 + 32m_3^2 m_2^2 + 13m_3^4)p^4 \\
& + 2(16m_1^6 - 25m_2^2 m_1^4 - 17m_2^4 m_1^2 + 2m_2^6 - 25m_3^2 m_1^4 + 8m_3^2 m_2^4 \\
& - 17m_3^4 m_1^2 + 8m_3^4 m_2^2 + 2m_3^6)p^2 \\
& + (16m_2^2 m_1^6 - 13m_2^4 m_1^4 - 2m_2^6 m_1^2 - m_2^8 + 16m_3^2 m_1^6 - 100m_3^2 m_2^2 m_1^4 + 22m_3^2 m_2^4 m_1^2 \\
& + 14m_3^2 m_2^6 - 13m_3^4 m_1^4 + 22m_3^4 m_2^2 m_1^2 - 26m_3^4 m_2^4 - 2m_3^6 m_1^2 + 14m_3^6 m_2^2 - m_3^8) \Big] \ln(m_1) \\
& - \left[p^8 - 2(m_1^2 - 7m_2^2 + 2m_3^2)p^6 \right. \\
& + (13m_1^4 - 22m_2^2 m_1^2 + 26m_2^4 - 34m_3^2 m_1^2 + 16m_3^2 m_2^2 - 13m_3^4)p^4 \\
& + 2(8m_1^6 - 50m_2^2 m_1^4 + 11m_2^4 m_1^2 + 7m_2^6 + 25m_3^2 m_1^4 - 8m_3^2 m_2^4 \\
& - 28m_3^4 m_1^2 + 16m_3^4 m_2^2 - 5m_3^6)p^2 \\
& + (-16m_2^2 m_1^6 + 13m_2^4 m_1^4 + 2m_2^6 m_1^2 + m_2^8 + 32m_3^2 m_1^6 - 50m_3^2 m_2^2 m_1^4 - 34m_3^2 m_2^4 m_1^2 \\
& + 4m_3^2 m_2^6 - 26m_3^4 m_1^4 + 56m_3^4 m_2^2 m_1^2 - 13m_3^4 m_2^4 - 4m_3^6 m_1^2 + 10m_3^6 m_2^2 - 2m_3^8) \Big] \ln(m_2) \\
& - \left[p^8 - 2(m_1^2 + 2m_2^2 - 7m_3^2)p^6 \right. \\
& + (13m_1^4 - 34m_2^2 m_1^2 - 13m_2^4 - 22m_3^2 m_1^2 + 16m_3^2 m_2^2 + 26m_3^4)p^4 \\
& + 2(8m_1^6 + 25m_2^2 m_1^4 - 28m_2^4 m_1^2 - 5m_2^6 - 50m_3^2 m_1^4 + 16m_3^2 m_2^4 \\
& + 11m_3^4 m_1^2 - 8m_3^4 m_2^2 + 7m_3^6)p^2 \\
& - (-32m_2^2 m_1^6 + 26m_2^4 m_1^4 + 4m_2^6 m_1^2 + 2m_2^8 + 16m_3^2 m_1^6 + 50m_3^2 m_2^2 m_1^4 - 56m_3^2 m_2^4 m_1^2 \\
& - 10m_3^2 m_2^6 - 13m_3^4 m_1^4 + 34m_3^4 m_2^2 m_1^2 + 13m_3^4 m_2^4 - 2m_3^6 m_1^2 - 4m_3^6 m_2^2 - m_3^8) \Big] \ln(m_3) \Big\} \\
& - \frac{1}{4 p^2 P(p^2, m_1, m_2, m_3)} \left\{ (3m_1^2 - 2m_2^2 - 2m_3^2)p^8 \right.
\end{aligned}$$

$$\begin{aligned}
& + 2(2m_2^2m_1^2 - m_2^4 + 2m_3^2m_1^2 - 8m_3^2m_2^2 - m_3^4)p^6 \\
& - 2(5m_1^6 - 8m_2^2m_1^4 + 8m_2^4m_1^2 - m_2^6 - 8m_3^2m_1^4 \\
& + 2m_3^2m_2^2m_1^2 + 5m_3^2m_2^4 + 8m_3^4m_1^2 + 5m_3^4m_2^2 - m_3^6)p^4 \\
& - 2(4m_1^8 - 6m_2^2m_1^6 + 3m_2^4m_1^4 - m_2^8 - 6m_3^2m_1^6 + 8m_3^2m_2^4m_1^2 \\
& + 6m_3^2m_2^6 + 3m_3^4m_1^4 + 8m_3^4m_2^2m_1^2 - 10m_3^4m_2^4 + 6m_3^6m_2^2 - m_3^8)p^2 \\
& - (m_1 - m_2 - m_3)(m_1 - m_2 + m_3)(m_1 + m_2 - m_3)(m_1 + m_2 + m_3) \\
& \times (m_1^2 - m_2^2 - m_3^2)(m_1^2 + m_2^2 + m_3^2)m_1^2 \Big\} S^{(0)}(2; p^2) \\
& + \frac{D(p^2, m_1, m_2, m_3)}{4p^2 P(p^2, m_1, m_2, m_3)} [p^2 - (m_1^2 + m_2^2 + m_3^2)] S_1^{(0)}(2; p^2) m_1^2 \\
& - \frac{4}{p^2} \Big\{ (p^2 + m_3^2)(m_1^2 - m_2^2) Z_2^{(1)}(2; p^2) + (p^2 + m_2^2)(m_1^2 - m_3^2) Z_3^{(1)}(2; p^2) \Big\}, \quad (\text{B.3.1})
\end{aligned}$$

where $P(p^2, m_1, m_2, m_3)$ and $D(p^2, m_1, m_2, m_3)$ are the usual polynomials defined in Eq.(5.3.3) and Eq.(5.3.9). In particular, from this equation we can read off the explicit values of the functions $C(p^2, m_1, m_2, m_3)$, $C_1(p^2, m_1, m_2, m_3)$, $C_2(p^2, m_1, m_2, m_3)$ and $C_3(p^2, m_1, m_2, m_3)$ introduced in Eq.s(5.5.4, 5.6.22):

$$\begin{aligned}
C(p^2, m_1, m_2, m_3) = & -\frac{1}{4p^2 P(p^2, m_1, m_2, m_3)} \Big[(3m_1^2 - 2m_2^2 - 2m_3^2)p^8 \\
& + 2(2m_2^2m_1^2 - m_2^4 + 2m_3^2m_1^2 - 8m_3^2m_2^2 - m_3^4)p^6 \\
& - 2(5m_1^6 - 8m_2^2m_1^4 + 8m_2^4m_1^2 - m_2^6 - 8m_3^2m_1^4 \\
& + 2m_3^2m_2^2m_1^2 + 5m_3^2m_2^4 + 8m_3^4m_1^2 + 5m_3^4m_2^2 - m_3^6)p^4 \\
& - 2(4m_1^8 - 6m_2^2m_1^6 + 3m_2^4m_1^4 - m_2^8 - 6m_3^2m_1^6 + 8m_3^2m_2^4m_1^2 \\
& + 6m_3^2m_2^6 + 3m_3^4m_1^4 + 8m_3^4m_2^2m_1^2 - 10m_3^4m_2^4 + 6m_3^6m_2^2 - m_3^8)p^2 \\
& - (m_1 - m_2 - m_3)(m_1 - m_2 + m_3)(m_1 + m_2 - m_3)(m_1 + m_2 + m_3) \\
& \times (m_1^2 - m_2^2 - m_3^2)(m_1^2 + m_2^2 + m_3^2)m_1^2 \Big], \quad (\text{B.3.2})
\end{aligned}$$

$$C_1(p^2, m_1, m_2, m_3) = \frac{m_1^2 D(p^2, m_1, m_2, m_3)}{4p^2 P(p^2, m_1, m_2, m_3)} [p^2 - (m_1^2 + m_2^2 + m_3^2)], \quad (\text{B.3.3})$$

$$C_2(p^2, m_1, m_2, m_3) = -\frac{4}{p^2} (p^2 + m_3^2)(m_1^2 - m_2^2), \quad (\text{B.3.4})$$

$$C_3(p^2, m_1, m_2, m_3) = -\frac{4}{p^2} (p^2 + m_2^2)(m_1^2 - m_3^2). \quad (\text{B.3.5})$$

Bibliography

- [1] J. D. Bjorken and S. D. Drell, *Relativistic quantum fields*, McGraw-Hill College (1965).
- [2] M. E. Peskin and D. V. Schroeder, *An Introduction to quantum field theory*, Westview Press (1995).
- [3] M. Srednicki, *Quantum field theory*, Cambridge University Press (2007).
- [4] **ATLAS** Collaboration, G. Aad et al., *Observation of a new particle in the search for the Standard Model Higgs boson with the ATLAS detector at the LHC*, *Phys.Lett.* **B716** (2012) 1–29, [[arXiv:1207.7214](#)].
- [5] **CMS** Collaboration, S. Chatrchyan et al., *Observation of a new boson at a mass of 125 GeV with the CMS experiment at the LHC*, *Phys.Lett.* **B716** (2012) 30–61, [[arXiv:1207.7235](#)].
- [6] R. K. Ellis, W. J. Stirling, and B. Webber, *QCD and collider physics*, *Camb.Monogr.Part.Phys.Nucl.Phys.Cosmol.* **8** (1996).
- [7] G. Dissertori, I. Knowles, and M. Schmelling, *Quantum Chromodynamics, High energy experiments and theory*, *International Series of Monographs on Physics*, Oxford University press **115** (2003).
- [8] G. 't Hooft and M. Veltman, *Regularization and Renormalization of Gauge Fields*, *Nucl.Phys.* **B44** (1972) 189–213.
- [9] G. Cicuti and E. Montaldi, *Analytic renormalization via continuous space dimension*, *Lett.Nuovo Cim.* **4** (1972) 329–332.
- [10] C. Bollini and J. Giambiagi, *Dimensional Renormalization: The Number of Dimensions as a Regularizing Parameter*, *Nuovo Cim.* **B12** (1972) 20–25.
- [11] D. J. Gross and F. Wilczek, *Ultraviolet Behavior of Nonabelian Gauge Theories*, *Phys.Rev.Lett.* **30** (1973) 1343–1346.
- [12] D. J. Gross and F. Wilczek, *Asymptotically Free Gauge Theories. 1*, *Phys.Rev.* **D8** (1973) 3633–3652.

- [13] D. J. Gross and F. Wilczek, *Asymptotically Free Gauge Theories. 2.*, *Phys.Rev.* **D9** (1974) 980–993.
- [14] H. D. Politzer, *Reliable Perturbative Results for Strong Interactions?*, *Phys.Rev.Lett.* **30** (1973) 1346–1349.
- [15] H. D. Politzer, *Asymptotic Freedom: An Approach to Strong Interactions*, *Phys.Rept.* **14** (1974) 129–180.
- [16] T. Kinoshita, *Mass singularities of Feynman amplitudes*, *J.Math.Phys.* **3** (1962) 650–677.
- [17] T. Lee and M. Nauenberg, *Degenerate Systems and Mass Singularities*, *Phys.Rev.* **133** (1964) B1549–B1562.
- [18] S. Frixione, Z. Kunszt, and A. Signer, *Three jet cross-sections to next-to-leading order*, *Nucl.Phys.* **B467** (1996) 399–442, [[hep-ph/9512328](#)].
- [19] S. Catani and M. Seymour, *A General algorithm for calculating jet cross-sections in NLO QCD*, *Nucl.Phys.* **B485** (1997) 291–419, [[hep-ph/9605323](#)].
- [20] G. Heinrich, *A numerical method for NNLO calculations*, *Nucl.Phys.Proc.Suppl.* **116** (2003) 368–372, [[hep-ph/0211144](#)].
- [21] A. Gehrmann-De Ridder, T. Gehrmann, and G. Heinrich, *Four particle phase space integrals in massless QCD*, *Nucl.Phys.* **B682** (2004) 265–288, [[hep-ph/0311276](#)].
- [22] C. Anastasiou, K. Melnikov, and F. Petriello, *A new method for real radiation at NNLO*, *Phys.Rev.* **D69** (2004) 076010, [[hep-ph/0311311](#)].
- [23] T. Binoth and G. Heinrich, *Numerical evaluation of phase space integrals by sector decomposition*, *Nucl.Phys.* **B693** (2004) 134–148, [[hep-ph/0402265](#)].
- [24] C. Anastasiou, K. Melnikov, and F. Petriello, *Real radiation at NNLO: $e^+ e^- \rightarrow 2$ jets through $O(\alpha^2(s))$* , *Phys.Rev.Lett.* **93** (2004) 032002, [[hep-ph/0402280](#)].
- [25] S. Catani and M. Grazzini, *An NNLO subtraction formalism in hadron collisions and its application to Higgs boson production at the LHC*, *Phys.Rev.Lett.* **98** (2007) 222002, [[hep-ph/0703012](#)].
- [26] A. Gehrmann-De Ridder, T. Gehrmann, and E. N. Glover, *Antenna subtraction at NNLO*, *JHEP* **0509** (2005) 056, [[hep-ph/0505111](#)].
- [27] A. Daleo, T. Gehrmann, and D. Maitre, *Antenna subtraction with hadronic initial states*, *JHEP* **0704** (2007) 016, [[hep-ph/0612257](#)].

- [28] J. Currie, E. Glover, and S. Wells, *Infrared Structure at NNLO Using Antenna Subtraction*, *JHEP* **1304** (2013) 066, [[arXiv:1301.4693](#)].
- [29] C. Anastasiou, C. Duhr, F. Dulat, F. Herzog, and B. Mistlberger, *Real-virtual contributions to the inclusive Higgs cross-section at N^3LO* , *JHEP* **1312** (2013) 088, [[arXiv:1311.1425](#)].
- [30] C. Anastasiou, C. Duhr, F. Dulat, E. Furlan, T. Gehrmann, et al., *Higgs boson gluon-fusion production at threshold in N^3LO QCD*, [arXiv:1403.4616](#).
- [31] K.-T. Chen, *Iterated path integrals*, *Bull.Am.Math.Soc.* **83** (1977) 831–879.
- [32] T. Gehrmann and L. Tancredi, *Two-loop QCD helicity amplitudes for $q\bar{q} \rightarrow W^\pm\gamma$ and $q\bar{q} \rightarrow Z^0\gamma$* , *JHEP* **1202** (2012) 004, [[arXiv:1112.1531](#)].
- [33] L. Garland, T. Gehrmann, E. N. Glover, A. Koukoutsakis, and E. Remiddi, *Two loop QCD helicity amplitudes for $e^+e^- \rightarrow$ three jets*, *Nucl.Phys.* **B642** (2002) 227–262, [[hep-ph/0206067](#)].
- [34] P. Nogueira, *Automatic Feynman graph generation*, *J.Comput.Phys.* **105** (1993) 279–289.
- [35] T. Gehrmann and E. Remiddi, *Differential equations for two loop four point functions*, *Nucl.Phys.* **B580** (2000) 485–518, [[hep-ph/9912329](#)].
- [36] M. Argeri and P. Mastrolia, *Feynman Diagrams and Differential Equations*, *Int.J.Mod.Phys.* **A22** (2007) 4375–4436, [[arXiv:0707.4037](#)].
- [37] E. Remiddi and L. Tancredi, *Schouten identities for Feynman graph amplitudes; the Master Integrals for the two-loop massive sunrise graph*, [arXiv:1311.3342](#).
- [38] F. Tkachov, *A Theorem on Analytical Calculability of Four Loop Renormalization Group Functions*, *Phys.Lett.* **B100** (1981) 65–68.
- [39] K. Chetyrkin and F. Tkachov, *Integration by Parts: The Algorithm to Calculate beta Functions in 4 Loops*, *Nucl.Phys.* **B192** (1981) 159–204.
- [40] S. Laporta and E. Remiddi, *The Analytical value of the electron ($g-2$) at order α^3 in QED*, *Phys.Lett.* **B379** (1996) 283–291, [[hep-ph/9602417](#)].
- [41] R. Lee, *Group structure of the integration-by-part identities and its application to the reduction of multiloop integrals*, *JHEP* **0807** (2008) 031, [[arXiv:0804.3008](#)].
- [42] A. von Manteuffel and C. Studerus, *Reduze 2 - Distributed Feynman Integral Reduction*, [arXiv:1201.4330](#).

- [43] S. Laporta, *High precision calculation of multiloop Feynman integrals by difference equations*, *Int.J.Mod.Phys.* **A15** (2000) 5087–5159, [[hep-ph/0102033](#)].
- [44] C. Anastasiou and A. Lazopoulos, *Automatic integral reduction for higher order perturbative calculations*, *JHEP* **0407** (2004) 046, [[hep-ph/0404258](#)].
- [45] A. Smirnov, *Algorithm FIRE – Feynman Integral REduction*, *JHEP* **0810** (2008) 107, [[arXiv:0807.3243](#)].
- [46] C. Studerus, *Reduze-Feynman Integral Reduction in C++*, *Comput.Phys.Commun.* **181** (2010) 1293–1300, [[arXiv:0912.2546](#)].
- [47] O. Tarasov, *Connection between Feynman integrals having different values of the space-time dimension*, *Phys.Rev.* **D54** (1996) 6479–6490, [[hep-th/9606018](#)].
- [48] R. Lee, *Space-time dimensionality D as complex variable: Calculating loop integrals using dimensional recurrence relation and analytical properties with respect to D* , *Nucl.Phys.* **B830** (2010) 474–492, [[arXiv:0911.0252](#)].
- [49] A. Smirnov and M. Tentyukov, *Feynman Integral Evaluation by a Sector decomposition Approach (FIESTA)*, *Comput.Phys.Commun.* **180** (2009) 735–746, [[arXiv:0807.4129](#)].
- [50] J. Carter and G. Heinrich, *SecDec: A general program for sector decomposition*, *Comput.Phys.Commun.* **182** (2011) 1566–1581, [[arXiv:1011.5493](#)].
- [51] S. Borowka, J. Carter, and G. Heinrich, *Numerical Evaluation of Multi-Loop Integrals for Arbitrary Kinematics with SecDec 2.0*, *Comput.Phys.Commun.* **184** (2013) 396–408, [[arXiv:1204.4152](#)].
- [52] M. Czakon, P. Fiedler, and A. Mitov, *Total Top-Quark Pair-Production Cross Section at Hadron Colliders Through $O(\epsilon \pm \frac{4}{5})$* , *Phys.Rev.Lett.* **110** (2013), no. 25 252004, [[arXiv:1303.6254](#)].
- [53] J. Tausk, *Nonplanar massless two loop Feynman diagrams with four on-shell legs*, *Phys.Lett.* **B469** (1999) 225–234, [[hep-ph/9909506](#)].
- [54] C. Anastasiou, T. Gehrmann, C. Oleari, E. Remiddi, and J. Tausk, *The Tensor reduction and master integrals of the two loop massless crossed box with lightlike legs*, *Nucl.Phys.* **B580** (2000) 577–601, [[hep-ph/0003261](#)].
- [55] E. E. Kummer, *Über die Transcendenten, welche aus wiederholten Integrationen rationaler Formeln entstehen*, *J. reine ang. Mathematik* **21** (1840) 74–90; 193–225; 328–371.

- [56] A. Goncharov, *Multiple polylogarithms and mixed Tate motives*, [math/0103059](#).
- [57] N. Nielsen, *Der Eulersche Dilogarithmus und seine Verallgemeinerungen*, *Nova Acta Leopoldina, Abh. der Kaiserlich Leopoldinisch-Carolinischen Deutschen Akad. der Naturforsch* **90** (1909) 121–212.
- [58] E. Remiddi and J. Vermaseren, *Harmonic polylogarithms*, *Int.J.Mod.Phys.* **A15** (2000) 725–754, [[hep-ph/9905237](#)].
- [59] T. Gehrmann and E. Remiddi, *Two loop master integrals for $\gamma^* \rightarrow 3$ jets: The Planar topologies*, *Nucl.Phys.* **B601** (2001) 248–286, [[hep-ph/0008287](#)].
- [60] D. Zagier, *Polylogarithms, Dedekind zeta functions and the algebraic K-theory of fields*, in *Arithmetic Algebraic Geometry* (J. G.v.d.Geer, F.Oort, ed.), vol. Prog. Math. 89, pp. 391–430., Birkhäuser, 1991.
- [61] A. B. Goncharov, *Geometry of configurations, polylogarithms, and motivic cohomology*, *Adv. Math.* **114** (1995), no. 2 197–318.
- [62] A. Goncharov, *Galois symmetries of fundamental groupoids and noncommutative geometry*, *Duke Math.J.* **128** (2005) 209, [[math/0208144](#)].
- [63] A. B. Goncharov, M. Spradlin, C. Vergu, and A. Volovich, *Classical Polylogarithms for Amplitudes and Wilson Loops*, *Phys.Rev.Lett.* **105** (2010) 151605, [[arXiv:1006.5703](#)].
- [64] C. Duhr, H. Gangl, and J. R. Rhodes, *From polygons and symbols to polylogarithmic functions*, *JHEP* **1210** (2012) 075, [[arXiv:1110.0458](#)].
- [65] C. Duhr, *Hopf algebras, coproducts and symbols: an application to Higgs boson amplitudes*, *JHEP* **1208** (2012) 043, [[arXiv:1203.0454](#)].
- [66] T. Gehrmann and E. Remiddi, *Numerical evaluation of harmonic polylogarithms*, *Comput.Phys.Commun.* **141** (2001) 296–312, [[hep-ph/0107173](#)].
- [67] T. Gehrmann and E. Remiddi, *Numerical evaluation of two-dimensional harmonic polylogarithms*, *Comput.Phys.Commun.* **144** (2002) 200–223, [[hep-ph/0111255](#)].
- [68] J. Vollinga and S. Weinzierl, *Numerical evaluation of multiple polylogarithms*, *Comput.Phys.Commun.* **167** (2005) 177, [[hep-ph/0410259](#)].
- [69] D. Maitre, *HPL, a mathematica implementation of the harmonic polylogarithms*, *Comput.Phys.Commun.* **174** (2006) 222–240, [[hep-ph/0507152](#)].

- [70] D. Maitre, *Extension of HPL to complex arguments*, *Comput.Phys.Commun.* **183** (2012) 846, [[hep-ph/0703052](#)].
- [71] S. Buehler and C. Duhr, *CHAPLIN - Complex Harmonic Polylogarithms in Fortran*, [arXiv:1106.5739](#).
- [72] D. Kreimer, *The Master two loop two point function: The General case*, *Phys.Lett.* **B273** (1991) 277–281.
- [73] F. A. Berends, M. Buza, M. Bohm, and R. Scharf, *Closed expressions for specific massive multiloop selfenergy integrals*, *Z.Phys.* **C63** (1994) 227–234.
- [74] F. A. Berends and J. Tausk, *On the numerical evaluation of scalar two loop selfenergy diagrams*, *Nucl.Phys.* **B421** (1994) 456–470.
- [75] S. Bauberger, M. Bohm, G. Weiglein, F. A. Berends, and M. Buza, *Calculation of two loop selfenergies in the electroweak standard model*, *Nucl.Phys.Proc.Suppl.* **37B** (1994) 95–114, [[hep-ph/9406404](#)].
- [76] S. Bauberger, F. A. Berends, M. Bohm, and M. Buza, *Analytical and numerical methods for massive two loop selfenergy diagrams*, *Nucl.Phys.* **B434** (1995) 383–407, [[hep-ph/9409388](#)].
- [77] S. Laporta and E. Remiddi, *Analytic treatment of the two loop equal mass sunrise graph*, *Nucl.Phys.* **B704** (2005) 349–386, [[hep-ph/0406160](#)].
- [78] O. Tarasov, *Hypergeometric representation of the two-loop equal mass sunrise diagram*, *Phys.Lett.* **B638** (2006) 195–201, [[hep-ph/0603227](#)].
- [79] L. Adams, C. Bogner, and S. Weinzierl, *The two-loop sunrise graph with arbitrary masses*, [arXiv:1302.7004](#).
- [80] S. Bloch and P. Vanhove, *The elliptic dilogarithm for the sunset graph*, [arXiv:1309.5865](#).
- [81] L. Adams, C. Bogner, and S. Weinzierl, *The two-loop sunrise graph with arbitrary masses in terms of elliptic dilogarithms*, [arXiv:1405.5640](#).
- [82] U. Aglietti, R. Bonciani, L. Grassi, and E. Remiddi, *The Two loop crossed ladder vertex diagram with two massive exchanges*, *Nucl.Phys.* **B789** (2008) 45–83, [[arXiv:0705.2616](#)].
- [83] A. Jonqui re, *Note sur la s rie $\sum_{n=1}^{\infty} \frac{x^n}{n^s}$* , *Bulletin de la Soci t  Math matique de France* **17** (1889) 142–152.
- [84] T. Gehrmann and E. Remiddi, *Two loop master integrals for $\gamma^* \rightarrow 3$ jets: The Nonplanar topologies*, *Nucl.Phys.* **B601** (2001) 287–317, [[hep-ph/0101124](#)].

- [85] F. Chavez and C. Duhr, *Three-mass triangle integrals and single-valued polylogarithms*, *JHEP* **1211** (2012) 114, [[arXiv:1209.2722](#)].
- [86] T. Gehrmann, L. Tancredi, and E. Weihs, *Two-loop master integrals for $q\bar{q} \rightarrow VV$: the planar topologies*, *JHEP* **1308** (2013) 070, [[arXiv:1306.6344](#)].
- [87] A. von Manteuffel and C. Studerus, *Massive planar and non-planar double box integrals for light N_f contributions to $gg \rightarrow tt$* , [arXiv:1306.3504](#).
- [88] J. M. Henn and V. A. Smirnov, *Analytic results for two-loop master integrals for Bhabha scattering I*, *JHEP* **1311** (2013) 041, [[arXiv:1307.4083](#)].
- [89] J. M. Henn, K. Melnikov, and V. A. Smirnov, *Two-loop planar master integrals for the production of off-shell vector bosons in hadron collisions*, [arXiv:1402.7078](#).
- [90] T. Gehrmann, A. von Manteuffel, L. Tancredi, and E. Weihs, *The Two-Loop Master Integrals for $q\bar{q} \rightarrow VV$* , [arXiv:1404.4853](#).
- [91] F. Caola, J. M. Henn, K. Melnikov, and V. A. Smirnov, *Non-planar master integrals for the production of two off-shell vector bosons in collisions of massless partons*, [arXiv:1404.5590](#).
- [92] R. Barbieri, J. Mignaco, and E. Remiddi, *Electron form factors up to fourth order. 2.*, *Nuovo Cim.* **A11** (1972) 865–916.
- [93] V. A. Smirnov, *Analytical result for dimensionally regularized massless on shell double box*, *Phys.Lett.* **B460** (1999) 397–404, [[hep-ph/9905323](#)].
- [94] F. Brown, *The Massless higher-loop two-point function*, *Commun.Math.Phys.* **287** (2009) 925–958, [[arXiv:0804.1660](#)].
- [95] E. Panzer, *Algorithms for the symbolic integration of hyperlogarithms with applications to Feynman integrals*, [arXiv:1403.3385](#).
- [96] E. Remiddi, *Dispersion Relations for Feynman Graphs*, *Helv.Phys.Acta* **54** (1982) 364.
- [97] S. Laporta and E. Remiddi, *Progress in the analytical evaluation of the electron ($g-2$) in QED: The Scalar part of the triple cross graphs*, *Phys.Lett.* **B356** (1995) 390–397.
- [98] R. Cutkosky, *Singularities and discontinuities of Feynman amplitudes*, *J.Math.Phys.* **1** (1960) 429–433.
- [99] M. Veltman, *Unitarity and causality in a renormalizable field theory with unstable particles*, *Physica* **29** (1963) 186–207.

- [100] A. Kotikov, *Differential equations method: New technique for massive Feynman diagrams calculation*, *Phys.Lett.* **B254** (1991) 158–164.
- [101] E. Remiddi, *Differential equations for Feynman graph amplitudes*, *Nuovo Cim.* **A110** (1997) 1435–1452, [[hep-th/9711188](#)].
- [102] R. Bonciani, P. Mastrolia, and E. Remiddi, *Vertex diagrams for the QED form-factors at the two loop level*, *Nucl.Phys.* **B661** (2003) 289–343, [[hep-ph/0301170](#)].
- [103] R. Bonciani, A. Ferroglia, P. Mastrolia, E. Remiddi, and J. van der Bij, *Planar box diagram for the $N_F = 1$ two loop QED virtual corrections to Bhabha scattering*, *Nucl.Phys.* **B681** (2004) 261–291, [[hep-ph/0310333](#)].
- [104] R. Bonciani, A. Ferroglia, T. Gehrmann, and C. Studerus, *Two-Loop Planar Corrections to Heavy-Quark Pair Production in the Quark-Antiquark Channel*, *JHEP* **0908** (2009) 067, [[arXiv:0906.3671](#)].
- [105] J. M. Henn, *Multiloop integrals in dimensional regularization made simple*, [arXiv:1304.1806](#).
- [106] M. Argeri, S. Di Vita, P. Mastrolia, E. Mirabella, J. Schlenk, et al., *Magnus and Dyson Series for Master Integrals*, *JHEP* **1403** (2014) 082, [[arXiv:1401.2979](#)].
- [107] M. Beneke and V. A. Smirnov, *Asymptotic expansion of Feynman integrals near threshold*, *Nucl.Phys.* **B522** (1998) 321–344, [[hep-ph/9711391](#)].
- [108] V. A. Smirnov, *Applied asymptotic expansions in momenta and masses*, *Springer Tracts Mod.Phys.* **177** (2002) 1–262.
- [109] V. A. Smirnov, *Analytic tools for Feynman integrals*, *Springer Tracts Mod.Phys.* **250** (2012) 1–296.
- [110] F. Cascioli, T. Gehrmann, M. Grazzini, S. Kallweit, P. Maierhoefer, et al., *ZZ production at hadron colliders in NNLO QCD*, [arXiv:1405.2219](#).
- [111] J. Ohnemus, *Order α_s calculations of hadronic $W^\pm\gamma$ and $Z\gamma$ production*, *Phys.Rev.* **D47** (1993) 940–955.
- [112] U. Baur, T. Han, and J. Ohnemus, *QCD corrections to hadronic $W\gamma$ production with nonstandard $WW\gamma$ couplings*, *Phys.Rev.* **D48** (1993) 5140–5161, [[hep-ph/9305314](#)].
- [113] U. Baur, T. Han, and J. Ohnemus, *QCD corrections and anomalous couplings in $Z\gamma$ production at hadron colliders*, *Phys.Rev.* **D57** (1998) 2823–2836, [[hep-ph/9710416](#)].

- [114] L. J. Dixon, Z. Kunszt, and A. Signer, *Helicity amplitudes for $O(\alpha_s)$ production of W^+W^- , $W^\pm Z$, ZZ , $W^\pm\gamma$, or $Z\gamma$ pairs at hadron colliders*, *Nucl.Phys.* **B531** (1998) 3–23, [[hep-ph/9803250](#)].
- [115] E. Accomando, A. Denner, and A. Kaiser, *Logarithmic electroweak corrections to gauge-boson pair production at the LHC*, *Nucl.Phys.* **B706** (2005) 325–371, [[hep-ph/0409247](#)].
- [116] E. Accomando and A. Kaiser, *Electroweak corrections and anomalous triple gauge-boson couplings in W^+W^- and $W^\pm Z$ production at the LHC*, *Phys.Rev.* **D73** (2006) 093006, [[hep-ph/0511088](#)].
- [117] E. Accomando, A. Denner, and C. Meier, *Electroweak corrections to $W\gamma$ and $Z\gamma$ production at the LHC*, *Eur.Phys.J.* **C47** (2006) 125–146, [[hep-ph/0509234](#)].
- [118] J. Baglio, L. D. Ninh, and M. M. Weber, *Massive gauge boson pair production at the LHC: a next-to-leading order story*, *Phys.Rev.* **D88** (2013) 113005, [[arXiv:1307.4331](#)].
- [119] A. Bierweiler, T. Kasprzik, and J. H. Kühn, *Vector-boson pair production at the LHC to $\mathcal{O}(\alpha^3)$ accuracy*, [arXiv:1305.5402](#).
- [120] M. Billoni, S. Dittmaier, B. Jäger, and C. Speckner, *Next-to-leading order electroweak corrections to $pp \rightarrow W+W^- \rightarrow 4$ leptons at the LHC in double-pole approximation*, *JHEP* **1312** (2013) 043, [[arXiv:1310.1564](#)].
- [121] S. Catani, L. Cieri, D. de Florian, G. Ferrera, and M. Grazzini, *Diphoton production at hadron colliders: a fully-differential QCD calculation at NNLO*, *Phys.Rev.Lett.* **108** (2012) 072001, [[arXiv:1110.2375](#)].
- [122] M. Grazzini, S. Kallweit, D. Rathlev, and A. Torre, *$Z\gamma$ production at hadron colliders in NNLO QCD*, *Phys.Lett.* **B731** (2014) 204, [[arXiv:1309.7000](#)].
- [123] Z. Bern, A. De Freitas, and L. J. Dixon, *Two loop amplitudes for gluon fusion into two photons*, *JHEP* **0109** (2001) 037, [[hep-ph/0109078](#)].
- [124] C. Anastasiou, E. N. Glover, and M. Tejeda-Yeomans, *Two loop QED and QCD corrections to massless fermion boson scattering*, *Nucl.Phys.* **B629** (2002) 255–289, [[hep-ph/0201274](#)].
- [125] T. Gehrmann, L. Tancredi, and E. Weihs, *Two-loop QCD helicity amplitudes for $gg \rightarrow Zg$ and $gg \rightarrow Z\gamma$* , *JHEP* **1304** (2013) 101, [[arXiv:1302.2630](#)].
- [126] G. Chachamis, M. Czakon, and D. Eiras, *W Pair Production at the LHC. I. Two-loop Corrections in the High Energy Limit*, *JHEP* **0812** (2008) 003, [[arXiv:0802.4028](#)].

- [127] T. Birthwright, E. Glover, and P. Marquard, *Master integrals for massless two-loop vertex diagrams with three offshell legs*, *JHEP* **0409** (2004) 042, [[hep-ph/0407343](#)].
- [128] M. Caffo, H. Czyz, S. Laporta, and E. Remiddi, *The Master differential equations for the two loop sunrise selfmass amplitudes*, *Nuovo Cim.* **A111** (1998) 365–389, [[hep-th/9805118](#)].
- [129] S. Caron-Huot and J. M. Henn, *Iterative structure of finite loop integrals*, [arXiv:1404.2922](#).
- [130] C. Anastasiou, C. Duhr, F. Dulat, and B. Mistlberger, *Soft triple-real radiation for Higgs production at N^3LO* , [arXiv:1302.4379](#).
- [131] R. Bonciani, A. Ferroglia, T. Gehrmann, A. von Manteuffel, and C. Studerus, *Light-quark two-loop corrections to heavy-quark pair production in the gluon fusion channel*, *JHEP* **1312** (2013) 038, [[arXiv:1309.4450](#)].
- [132] J. Vermaseren, *New features of FORM*, [math-ph/0010025](#).
- [133] W. Research, *Mathematica*. Wolfram Reserach, Champaign, Illinois, USA, 8.0 ed., 2010.
- [134] C. W. Bauer, A. Frink, and R. Kreckel, *Introduction to the GiNaC framework for symbolic computation within the C++ programming language*, [cs/0004015](#).
- [135] R. Lewis, *Computer Algebra System Fermat*. <http://www.bway.net/~lewis>.
- [136] A. von Manteuffel, R. M. Schabinger, and H. X. Zhu, *The Complete Two-Loop Integrated Jet Thrust Distribution In Soft-Collinear Effective Theory*, *JHEP* **1403** (2014) 139, [[arXiv:1309.3560](#)].
- [137] W. van Neerven, *Dimensional Regularization of Mass and Infrared Singularities in Two Loop On-shell Vertex Functions*, *Nucl.Phys.* **B268** (1986) 453.
- [138] A. von Manteuffel, *a Mathematica package for multiple polylogarithms*.
- [139] E. Weihs, *a Mathematica package for multiple polylogarithms*.
- [140] S. Borowka and G. Heinrich, *Massive non-planar two-loop four-point integrals with SecDec 2.1*, [arXiv:1303.1157](#).
- [141] O. Tarasov, *Generalized recurrence relations for two loop propagator integrals with arbitrary masses*, *Nucl.Phys.* **B502** (1997) 455–482, [[hep-ph/9703319](#)].

- [142] M. Caffo, H. Czyz, M. Gunia, and E. Remiddi, *BOKASUN: A Fast and precise numerical program to calculate the Master Integrals of the two-loop sunrise diagrams*, *Comput.Phys.Commun.* **180** (2009) 427–430, [[arXiv:0807.1959](#)].
- [143] S. Pozzorini and E. Remiddi, *Precise numerical evaluation of the two loop sunrise graph master integrals in the equal mass case*, *Comput.Phys.Commun.* **175** (2006) 381–387, [[hep-ph/0505041](#)].
- [144] S. Mueller-Stach, S. Weinzierl, and R. Zayadeh, *A Second-Order Differential Equation for the Two-Loop Sunrise Graph with Arbitrary Masses*, *Commun.Num.Theor.Phys.* **6** (2012) 203–222, [[arXiv:1112.4360](#)].
- [145] U. Baur and E. L. Berger, *Probing the $WW\gamma$ Vertex at the Tevatron Collider*, *Phys.Rev.* **D41** (1990) 1476.
- [146] U. Baur and E. L. Berger, *Probing the weak boson sector in $Z\gamma$ production at hadron colliders*, *Phys.Rev.* **D47** (1993) 4889–4904.
- [147] L. J. Dixon, Z. Kunszt, and A. Signer, *Vector boson pair production in hadronic collisions at order α_s : Lepton correlations and anomalous couplings*, *Phys.Rev.* **D60** (1999) 114037, [[hep-ph/9907305](#)].
- [148] **CDF** Collaboration, D. Acosta et al., *Measurement of $W\gamma$ and $Z\gamma$ production in $p\bar{p}$ collisions at $\sqrt{s} = 1.96$ TeV*, *Phys.Rev.Lett.* **94** (2005) 041803, [[hep-ex/0410008](#)].
- [149] **D0** Collaboration, V. Abazov et al., *Measurement of the $p - \bar{p} \rightarrow W\gamma + X$ cross section at $\sqrt{s} = 1.96$ -TeV and $WW\gamma$ anomalous coupling limits*, *Phys.Rev.* **D71** (2005) 091108, [[hep-ex/0503048](#)].
- [150] **D0** Collaboration, V. Abazov et al., *$Z\gamma$ production and limits on anomalous $ZZ\gamma$ and $Z\gamma\gamma$ couplings in $p\bar{p}$ collisions at $\sqrt{s} = 1.96$ - TeV*, *Phys.Lett.* **B653** (2007) 378–386, [[arXiv:0705.1550](#)].
- [151] **D0** Collaboration, V. Abazov et al., *First study of the radiation-amplitude zero in $W\gamma$ production and limits on anomalous $WW\gamma$ couplings at $\sqrt{s} = 1.96$ - TeV*, *Phys.Rev.Lett.* **100** (2008) 241805, [[arXiv:0803.0030](#)].
- [152] **D0** Collaboration, V. Abazov et al., *Measurement of the Z gamma $\rightarrow \nu\bar{\nu}$ anti-nu gamma cross section and limits on anomalous ZZ gamma and Z gamma gamma couplings in p anti- p collisions at $s^{*(1/2)} = 1.96$ -TeV*, *Phys.Rev.Lett.* **102** (2009) 201802, [[arXiv:0902.2157](#)].
- [153] **CDF** Collaboration, T. Aaltonen et al., *Measurement of Z gamma Production in $p\bar{p}$ Collisions at $\sqrt{s} = 1.96$ TeV*, *Phys.Rev.* **D82** (2010) 031103, [[arXiv:1004.1140](#)].

- [154] **CMS** Collaboration, S. Chatrchyan et al., *Measurement of $W\gamma$ and $Z\gamma$ production in pp collisions at $\sqrt{s} = 7$ TeV*, *Phys.Lett.* **B701** (2011) 535–555, [[arXiv:1105.2758](#)].
- [155] **ATLAS** Collaboration, G. Aad et al., *Measurement of $W\gamma$ and $Z\gamma$ production in proton-proton collisions at $\sqrt{s} = 7$ TeV with the ATLAS Detector*, *JHEP* **1109** (2011) 072, [[arXiv:1106.1592](#)].
- [156] V. Del Duca, F. Maltoni, Z. Nagy, and Z. Trocsanyi, *QCD radiative corrections to prompt diphoton production in association with a jet at hadron colliders*, *JHEP* **0304** (2003) 059, [[hep-ph/0303012](#)].
- [157] F. Campanario, C. Englert, M. Spannowsky, and D. Zeppenfeld, *NLO-QCD corrections to $W\gamma j$ production*, *Europhys.Lett.* **88** (2009) 11001, [[arXiv:0908.1638](#)].
- [158] F. Campanario, C. Englert, and M. Spannowsky, *Precise predictions for (non-standard) $W\gamma + \text{jet}$ production*, *Phys.Rev.* **D83** (2011) 074009, [[arXiv:1010.1291](#)].
- [159] S. Dittmaier, S. Kallweit, and P. Uwer, *NLO QCD corrections to $WW + \text{jet}$ production at hadron colliders*, *Phys.Rev.Lett.* **100** (2008) 062003, [[arXiv:0710.1577](#)].
- [160] S. Dittmaier, S. Kallweit, and P. Uwer, *NLO QCD corrections to $pp/p\bar{p} \rightarrow WW + \text{jet} + X$ including leptonic W -boson decays*, *Nucl.Phys.* **B826** (2010) 18–70, [[arXiv:0908.4124](#)].
- [161] J. M. Campbell, R. K. Ellis, and G. Zanderighi, *Next-to-leading order predictions for $WW + 1 \text{ jet}$ distributions at the LHC*, *JHEP* **0712** (2007) 056, [[arXiv:0710.1832](#)].
- [162] T. Binoth, T. Gleisberg, S. Karg, N. Kauer, and G. Sanguinetti, *NLO QCD corrections to $ZZ + \text{jet}$ production at hadron colliders*, *Phys.Lett.* **B683** (2010) 154–159, [[arXiv:0911.3181](#)].
- [163] F. Campanario, C. Englert, S. Kallweit, M. Spannowsky, and D. Zeppenfeld, *NLO QCD corrections to $WZ + \text{jet}$ production with leptonic decays*, *JHEP* **1007** (2010) 076, [[arXiv:1006.0390](#)].
- [164] T. Binoth and G. Heinrich, *An automatized algorithm to compute infrared divergent multiloop integrals*, *Nucl.Phys.* **B585** (2000) 741–759, [[hep-ph/0004013](#)].
- [165] G. Heinrich, *Sector Decomposition*, *Int.J.Mod.Phys.* **A23** (2008) 1457–1486, [[arXiv:0803.4177](#)].

- [166] C. Anastasiou, F. Herzog, and A. Lazopoulos, *On the factorization of overlapping singularities at NNLO*, *JHEP* **1103** (2011) 038, [[arXiv:1011.4867](#)].
- [167] C. Anastasiou, F. Herzog, and A. Lazopoulos, *The fully differential decay rate of a Higgs boson to bottom-quarks at NNLO in QCD*, *JHEP* **1203** (2012) 035, [[arXiv:1110.2368](#)].
- [168] A. Gehrmann-De Ridder, T. Gehrmann, E. Glover, and G. Heinrich, *Infrared structure of $e^+ e^- \rightarrow 3$ jets at NNLO*, *JHEP* **0711** (2007) 058, [[arXiv:0710.0346](#)].
- [169] A. Daleo, A. Gehrmann-De Ridder, T. Gehrmann, and G. Luisoni, *Antenna subtraction at NNLO with hadronic initial states: initial-final configurations*, *JHEP* **1001** (2010) 118, [[arXiv:0912.0374](#)].
- [170] R. Boughezal, A. Gehrmann-De Ridder, and M. Ritzmann, *Antenna subtraction at NNLO with hadronic initial states: double real radiation for initial-initial configurations with two quark flavours*, *JHEP* **1102** (2011) 098, [[arXiv:1011.6631](#)].
- [171] T. Gehrmann and P. F. Monni, *Antenna subtraction at NNLO with hadronic initial states: real-virtual initial-initial configurations*, *JHEP* **1112** (2011) 049, [[arXiv:1107.4037](#)].
- [172] E. Nigel Glover and J. Pires, *Antenna subtraction for gluon scattering at NNLO*, *JHEP* **1006** (2010) 096, [[arXiv:1003.2824](#)].
- [173] L. Garland, T. Gehrmann, E. N. Glover, A. Koukoutsakis, and E. Remiddi, *The Two loop QCD matrix element for $e^+ e^- \rightarrow 3$ jets*, *Nucl.Phys.* **B627** (2002) 107–188, [[hep-ph/0112081](#)].
- [174] T. Gehrmann and E. Remiddi, *Analytic continuation of massless two loop four point functions*, *Nucl.Phys.* **B640** (2002) 379–411, [[hep-ph/0207020](#)].
- [175] L. J. Dixon, *Calculating scattering amplitudes efficiently*, [hep-ph/9601359](#).
- [176] T. Gehrmann, M. Jaquier, E. Glover, and A. Koukoutsakis, *Two-Loop QCD Corrections to the Helicity Amplitudes for $H \rightarrow 3$ partons*, *JHEP* **1202** (2012) 056, [[arXiv:1112.3554](#)].
- [177] S. Moch, J. Vermaseren, and A. Vogt, *Three-loop results for quark and gluon form-factors*, *Phys.Lett.* **B625** (2005) 245–252, [[hep-ph/0508055](#)].
- [178] P. Baikov, K. Chetyrkin, A. Smirnov, V. Smirnov, and M. Steinhauser, *Quark and gluon form factors to three loops*, *Phys.Rev.Lett.* **102** (2009) 212002, [[arXiv:0902.3519](#)].

- [179] R. Lee, A. Smirnov, and V. Smirnov, *Analytic Results for Massless Three-Loop Form Factors*, *JHEP* **1004** (2010) 020, [[arXiv:1001.2887](#)].
- [180] T. Gehrmann, E. Glover, T. Huber, N. Ikizlerli, and C. Studerus, *Calculation of the quark and gluon form factors to three loops in QCD*, *JHEP* **1006** (2010) 094, [[arXiv:1004.3653](#)].
- [181] S. Catani, *The Singular behavior of QCD amplitudes at two loop order*, *Phys.Lett.* **B427** (1998) 161–171, [[hep-ph/9802439](#)].
- [182] R. K. Ellis, D. Ross, and A. Terrano, *The Perturbative Calculation of Jet Structure in $e^+ e^-$ Annihilation*, *Nucl.Phys.* **B178** (1981) 421.
- [183] W. Giele and E. N. Glover, *Higher order corrections to jet cross-sections in $e^+ e^-$ annihilation*, *Phys.Rev.* **D46** (1992) 1980–2010.
- [184] **CDF** Collaboration, T. Aaltonen et al., *Measurement of ZZ production in leptonic final states at \sqrt{s} of 1.96 TeV at CDF*, *Phys.Rev.Lett.* **108** (2012) 101801, [[arXiv:1112.2978](#)].
- [185] **D0** Collaboration, V. M. Abazov et al., *A measurement of the WZ and ZZ production cross sections using leptonic final states in 8.6 fb^{-1} of $p\bar{p}$ collisions*, *Phys.Rev.* **D85** (2012) 112005, [[arXiv:1201.5652](#)].
- [186] **ATLAS** Collaboration, G. Aad et al., *Measurement of ZZ production in pp collisions at $\sqrt{s} = 7 \text{ TeV}$ and limits on anomalous ZZZ and $ZZ\gamma$ couplings with the ATLAS detector*, *JHEP* **1303** (2013) 128, [[arXiv:1211.6096](#)].
- [187] **CMS** Collaboration, S. Chatrchyan et al., *Measurement of the ZZ production cross section and search for anomalous couplings in $2 \text{ l}2\text{l}'$ final states in pp collisions at $\sqrt{s} = 7 \text{ TeV}$* , *JHEP* **1301** (2013) 063, [[arXiv:1211.4890](#)].
- [188] **ATLAS** Collaboration, *ATLAS-CONF-2013-020*.
- [189] **CMS** Collaboration, *CMS-PAS-SMP-13-005*.
- [190] J. Ohnemus and J. Owens, *An Order α_s calculation of hadronic ZZ production*, *Phys.Rev.* **D43** (1991) 3626–3639.
- [191] B. Mele, P. Nason, and G. Ridolfi, *QCD radiative corrections to Z boson pair production in hadronic collisions*, *Nucl.Phys.* **B357** (1991) 409–438.
- [192] J. Ohnemus, *Hadronic ZZ, W^-W^+ , and $W^\pm Z$ production with QCD corrections and leptonic decays*, *Phys.Rev.* **D50** (1994) 1931–1945, [[hep-ph/9403331](#)].
- [193] J. M. Campbell and R. K. Ellis, *An Update on vector boson pair production at hadron colliders*, *Phys.Rev.* **D60** (1999) 113006, [[hep-ph/9905386](#)].

- [194] E. N. Glover and J. van der Bij, *Z BOSON PAIR PRODUCTION VIA GLUON FUSION*, *Nucl.Phys.* **B321** (1989) 561.
- [195] D. A. Dicus, C. Kao, and W. Repko, *Gluon Production of Gauge Bosons*, *Phys.Rev.* **D36** (1987) 1570.
- [196] T. Matsuura and J. van der Bij, *Characteristics of leptonic signals for Z boson pairs at hadron colliders*, *Z.Phys.* **C51** (1991) 259–266.
- [197] C. Zecher, T. Matsuura, and J. van der Bij, *Leptonic signals from off-shell Z boson pairs at hadron colliders*, *Z.Phys.* **C64** (1994) 219–226, [[hep-ph/9404295](#)].
- [198] T. Binoth, N. Kauer, and P. Mertsch, *Gluon-induced QCD corrections to $pp \rightarrow ZZ \rightarrow l \text{ anti-}l \text{ } l\text{-prime anti-}l\text{-prime}$* , [arXiv:0807.0024](#).
- [199] J. M. Campbell, R. K. Ellis, and C. Williams, *Vector boson pair production at the LHC*, *JHEP* **1107** (2011) 018, [[arXiv:1105.0020](#)].
- [200] **SM and NLO Multileg Working Group** Collaboration, J. Andersen et al., *The SM and NLO Multileg Working Group: Summary report*, [arXiv:1003.1241](#).
- [201] F. Cascioli, P. Maierhofer, and S. Pozzorini, *Scattering Amplitudes with Open Loops*, *Phys.Rev.Lett.* **108** (2012) 111601, [[arXiv:1111.5206](#)].
- [202] A. Denner, S. Dittmaier, and L. Hofer, *In preparation*.
- [203] A. Denner and S. Dittmaier, *Reduction of one loop tensor five point integrals*, *Nucl.Phys.* **B658** (2003) 175–202, [[hep-ph/0212259](#)].
- [204] A. Denner and S. Dittmaier, *Reduction schemes for one-loop tensor integrals*, *Nucl.Phys.* **B734** (2006) 62–115, [[hep-ph/0509141](#)].
- [205] A. Denner and S. Dittmaier, *Scalar one-loop 4-point integrals*, *Nucl.Phys.* **B844** (2011) 199–242, [[arXiv:1005.2076](#)].
- [206] S. Catani, L. Cieri, G. Ferrera, D. de Florian, and M. Grazzini, *Vector boson production at hadron colliders: a fully exclusive QCD calculation at NNLO*, *Phys.Rev.Lett.* **103** (2009) 082001, [[arXiv:0903.2120](#)].
- [207] G. Ferrera, M. Grazzini, and F. Tramontano, *Associated WH production at hadron colliders: a fully exclusive QCD calculation at NNLO*, *Phys.Rev.Lett.* **107** (2011) 152003, [[arXiv:1107.1164](#)].
- [208] G. Bozzi, S. Catani, D. de Florian, and M. Grazzini, *Transverse-momentum resummation and the spectrum of the Higgs boson at the LHC*, *Nucl.Phys.* **B737** (2006) 73–120, [[hep-ph/0508068](#)].

- [209] D. de Florian and M. Grazzini, *The Structure of large logarithmic corrections at small transverse momentum in hadronic collisions*, *Nucl.Phys.* **B616** (2001) 247–285, [[hep-ph/0108273](#)].
- [210] S. Catani and M. Grazzini, *Higgs Boson Production at Hadron Colliders: Hard-Collinear Coefficients at the NNLO*, *Eur.Phys.J.* **C72** (2012) 2013, [[arXiv:1106.4652](#)].
- [211] S. Catani, L. Cieri, D. de Florian, G. Ferrera, and M. Grazzini, *Vector boson production at hadron colliders: hard-collinear coefficients at the NNLO*, *Eur.Phys.J.* **C72** (2012) 2195, [[arXiv:1209.0158](#)].
- [212] S. Catani, L. Cieri, D. de Florian, G. Ferrera, and M. Grazzini, *Universality of transverse-momentum resummation and hard factors at the NNLO*, *Nucl.Phys.* **B881** (2014) 414–443, [[arXiv:1311.1654](#)].
- [213] T. Gehrmann, T. Lubbert, and L. L. Yang, *Transverse parton distribution functions at next-to-next-to-leading order: the quark-to-quark case*, *Phys.Rev.Lett.* **109** (2012) 242003, [[arXiv:1209.0682](#)].
- [214] T. Gehrmann, T. Luebbert, and L. L. Yang, *Calculation of the transverse parton distribution functions at next-to-next-to-leading order*, [arXiv:1403.6451](#).
- [215] S. Catani and M. Seymour, *The Dipole formalism for the calculation of QCD jet cross-sections at next-to-leading order*, *Phys.Lett.* **B378** (1996) 287–301, [[hep-ph/9602277](#)].
- [216] A. Martin, W. Stirling, R. Thorne, and G. Watt, *Parton distributions for the LHC*, *Eur.Phys.J.* **C63** (2009) 189–285, [[arXiv:0901.0002](#)].